Durham E-Theses

Theoretical aspects of structure bonding and reactivity of some unsaturated organic systems;

Ian William Scanlan

How to cite:

Use policy

UNIVERSITY OF DURHAM

A Thesis Entitled

THEORETICAL ASPECTS OF STRUCTURE, BONDING AND

REACTIVITY OF SOME UNSATURATED ORGANIC SYSTEMS

Submitted by

Ian William Scanlan, B.Sc.

(Grey College)

A candidate for the Degree of Doctor of Philosophy

1974

TO MY PARENTS

AND IN MEMORY OF IAN RITCHIE

MEMORANDUM

The work described in this thesis was carried out at the University of Durham between October 1971 and April 1974. It has not been submitted for any other degree and is the original work of the author except where acknowledged by reference.

Part of the work in this thesis has formed the subject matter of the whole, or part, of the following publications:

1. Ab Initio Calculations on Some Aspects of Structure, Bonding and Reactivity of Pyridine, Phosphabenzene, and Arsabenzene, D.T. Clark, I.W. Scanlan, J.C.S. Faraday II (in press).

2. Structure and Bonding in Diazocyclopentadiene and some of its Core and Valence Ionized States, D.T. Clark, D.B. Adams, I.W. Scanlan and I.S. Woolsey, Chem. Phys. Lett., 1974, 25, 263.

3. Non Empirical LCAO SCF MO Investigations of Electronic Reorganizations Accompanying Core Ionizations, D.T. Clark, I.W. Scanlan and J. Müller, Theoret. chim. Acta., (submitted for publication).

4. Photoelectron Spectra of Phosphabenzene, Arsabenzene and Stibabenzene, C. Baitch, E. Heilbronner, V. Hornung, A.J. Ashe III, D.T. Clark, D. Kilcast, I.W. Scanlan, U.T. Cobley, J. Amer. Chem. Soc., 1973, 95, 928.

SUMMARY

Theoretical aspects of structure, bonding and reactivity of a number of interesting unsaturated organic systems have been investigated within the Hartree-Fock formalism and a number of most useful interpretative techniques developed. Studies of a number of three-membered-rings are highlighted by the thiirenes where the thermodynamic stability is increased by the out-of-plane substitution at the heteroatom. The similarity in electronic structure of these thiirenes and their ring-opened dimethyl analogues is also discussed. Extensive studies however on the 6a-thiathiophthenes indicate the requirement for a delocalised description of the bonding and the use of ESCA, but not UPS, is indicated as a valuable tool in these investigations. The theoretical interpretation of these spectroscopic techniques is further investigated in pyridine, phosphabenzene and arsabenzene together with the ground state properties of these molecules. The effect of change in size and electronegativity of the heteroatom is seen to account for the variation in electronic structure but the necessity for inclusion of electronic relaxation energy considerations concomitant with core ionization is shown in making assignments from UPS from Koopman's Theorem.

Extensive (semi-empirical) and restrictive (non-empirical) studies of prototype radical-olefin reactions in the gas phase show that though the T/S occurs early on the PE surface, models based on both reactant and product electronic structure can account for the propensity for the reaction. A rationalisation based on the UHF procedure is advocated and is shown, even in its simplest form, to account for the vast majority of experimental observations.

ABBREVIATIONS

AO	Atomic Orbital
ATT	Attractive
BE	Binding Energy
ESCA	Electron Spectroscopy for Chemical Application (also known as X-ray Photoelectron Spectroscopy XPS)
eV	Electron volt
h	Planck's constant
h	Planck's constant divided by 2π
HO	Highest Occupied
IP	Ionization Potential
KE	Kinetic Energy
KIN	Kinetic
LCAO	Linear Combination of Atomic Orbitals
LU	Lowest Unoccupied
MO	Molecular Orbital
PBO	Partition Bond Overlap
PE	Potential Energy
REP	Repulsive
RHF	Spin Restricted Hartree-Fock
SCF	Self Consistent Field
SO	Single Occupied
SU	Single Unoccupied
UHF	Spin Unrestricted Hartree-Fock
UPS	Ultraviolet Photoelectron Spectroscopy
VB	Valence Bond

CONTENTS

APPENDIX: Co-ordinates

             Basis Sets

             Thermochemical Data

             Programs Employed

REFERENCES:

Simple Ψ man met a π man . . . .

Said that Ψ man to that π man . . .

(Traditional)

CHAPTER I.

The Wave Function – A General Introduction

Introduction

Organic Chemistry is an experimental science. Theoretical Organic Chemistry is concerned with the interpretation, rationalisation and extrapolation of data arising from such investigations. This may be approached in two distinct ways depending in general if the analysis is performed by the experimentalist or the theoretician.

The experimentalist would in general consider the electronic structure of a molecule in terms of a localised framework of σ bonds with, as needed, a delocalised π electron system and lone pairs. Nonconjugated functions are considered as their separate parts and the orbitals so derived confer on that group its characteristic chemical and physical properties. Intuitive ideas derived from previous experimental work are then employed and the familiar 'curly arrow' technique results.

There are two main disadvantages of this approach. Firstly the non-quantitative aspects render rationalisations susceptible to a certain degree of doubt. Secondly the inference of electronic structural information from experimental data is not always straightforward and can be misleading. Reference need only to be made to the relative acidities of acetic and fluoracetic acids and the basicities of the methylated amines where the previously accepted arguments based on inductive effects have proved to be incorrect.

The alternative approach has its origins in the development of Quantum Theory. A mathematical description of the electrons and the nuclei in the molecule generates a delocalised series of orbitals. These are usually produced by the molecular orbital (MO) and valence bond (VB) methods. In MO theory the electrons occupy molecular orbitals; in VB theory they occupy atomic orbitals with spins coupled in such a way as to

describe localised electron pairs. High speed computers and efficient

programming has now placed the second, more quantitative methods at the

disposal of the chemist. Though gross properties of a molecule may be

readily obtained (e.g. the total energy of a particular conformer) it is

the bonding and reactivity which are usually of interest. Methods and

techniques which provide a more chemical and/or more readily understandable

description will be discussed in the next chapter along with a discussion

of some fundamental concepts and ideas which apply to this work. In this

chapter though is outlined the MO theory which has been used in this work

together with the practicalities of the approach.

1)   The Schrodinger Equation and its Solution.

   a)   Quantum Mechanical Background.

        Any given system may be described by a suitable mathematical

expression. A composite of nuclei and electrons can be represented by a

function which only depends upon the time, the spatial and spin

co-ordinate of these particles. Such a function, which describes the

electronic structure of an atom, ion or molecule, is known as the

wavefunction.

        Any measurable property of this system may be symbolised by a

dynamic operator $(\hat{A})$. If this operates upon a wavefunction such that

the resultant is simply a multiple of the original function:

$$\hat{A}\Psi = A\Psi \qquad (1)$$

then Ψ is termed an eigenfunction of A with eigenvalue A. The case of

particular interest is where A is the operator which represents the

formalisation of the energy of the system. This leads to the Schrodinger

equation[2]

$$\hat{H}\Psi = E\Psi \qquad (2)$$

where H is the Hamiltonian (total energy operator) of the system and E is the eigenvalue corresponding to the total energy. As time-independent equations will only be of concern in this work Ψ is taken as describing the spatial and spin co-ordinates only. The wavefunction is taken to be normalised:

$$\int \Psi^*\Psi dq_1 dq_2 \cdots \cdots dq_{3N} = 1$$

and time independent. The physical interpretation of the N particles of the system is that they have a probability $\Psi^*\Psi$ of being in volume elements in space with coordinates q_1, q_2, $\ldots q_{3N}$ to $q_1 + dq_1$, $\ldots$ which are independent of time. Further for observable A, whose operator $\hat{A}$ commutes with H:

$$A = \int \Psi^*\hat{A}\Psi d\tau \qquad (3)$$

In the particular case where $\hat{A}$ is H

$$E = \int \Psi^*\hat{H}\Psi d\tau \qquad (4)$$

which is an alternative form of (2). In order to obtain Ψ and hence E then the solution to equation (2) is required.

The Hamiltonian (H) possesses the Hermitian property i.e. in matrix form its transpose is its conjugate.

$$H^* = H^+ \text{ and } (H^+)^* = H \qquad (5)$$

when H^* is the conjugate and H^+ the transpose of H.

For a system of nuclei $(\mu, \nu \cdots)$ and electrons $(i, j \ldots)$ with coordinates and masses (Q, M) and (q, m) respectively the total spin free non-relativistic Hamiltonian operator is given by

$$H(Q,q) = -\sum_{\mu} \frac{\hbar^2}{2M_\mu} \nabla^2_\mu - \sum_i \frac{\hbar^2}{2m_i} \nabla^2_i \qquad (6)$$
$$+ V_{ne}(Q,q) + V_{nn}(Q) + V_{ee}(q)$$

The first two terms account for the kinetic energy of the system. The potential energy is given by the last three terms where

$$V_{ne}(Q,q) = \sum_{\mu} \sum_{i} \frac{Z_{\mu}e^2}{r_{\mu i}} \quad V_{nn}(Q) = \sum_{\mu < \nu} \frac{Z_{\mu}Z_{\nu}}{r_{\mu\nu}} \quad V_{ee}(q) = \sum_{i < j} \frac{e^2}{r_{ij}} \tag{7}$$

The total wavefunction is assumed to be separable into its electronic and nuclear parts according to the Born-Oppenheimer approximation.[3]

$$\Psi(Q,q) = \Psi_n(Q)\Psi_e(Q,q) \tag{8}$$

The electronic wavefunction is then defined by

$$He(Q,q)\Psi_e(Q,q) = E_e(Q)\Psi_e(Q,q) \tag{9}$$

where

$$He(Q,q) = H(Q,q) + \sum_{\mu} \frac{\hbar^2}{2M\mu} \nabla_{\mu}^2 - V_{nn} \tag{10}$$

and the nuclear wavefunction by

$$[Hn(Q) + E_e(Q)]\Psi_n(Q) = E\Psi_n(Q) \tag{11}$$

with Hn defined analogously to He.

($\Psi_n(Q)$ may be further separated into the translational, vibrational and rotational components).

The electronic wavefunction is solved for fixed positions of the nuclei using equation (9) and generates the total electronic energy of the system.   The total energy is then given by:-

$$E = E_e(Q) + E_n \tag{12}$$

where E_n = V_{nn} + contributions from translation, vibration and rotation. This will include the zero point energies of the system which are usually small however compared with $E_e(Q)$ and V_{nn}.

The approximation is valid provided that the electronic energy is a slowly varying function of the nuclear co-ordinates.   This is justified

by examination of the expansion of equation (2) with the approximation:

$$[He(Q,q) + Hn(Q)]\psi_n(Q)\psi_e(Q,q) = E\psi_e(Q,q)\psi_n(Q) \tag{13}$$

Expanding the Hamiltonian in its two parts

$$He(Q,q)\psi_n(Q)\psi_e(Q,q) = \psi_n(Q)E_e(Q)\psi_e(Q,q) \tag{14}$$

$$Hn(Q)\psi_n(Q)\psi_e(Q,q) = -\sum_\mu \frac{\hbar^2}{2M\mu} \nabla^2_\mu \psi_n(Q)\psi_e(Q,q) = -\sum_\mu \frac{\hbar^2}{2M\mu} \psi_n(Q)\nabla^2_\mu \psi_e(Q,q)$$

$$+ \psi_e(Q,q)\nabla^2_\mu \psi_n(Q) + 2\nabla_\mu \psi_n \psi_e \tag{15}$$

substituting for He in (13)

$$[E_e(Q) + H_n(Q)]\psi_n(Q)\psi_e(Q,q) = E\psi_e(Q,q)\psi_n(Q) \tag{16}$$

This will produce (11) if, and only if, the terms in $\nabla^2_\mu \psi_e(Q,q)$

and $\nabla_\mu(Q,q)$ from (15) can be neglected.

The electronic wavefunction (4) as defined by (9) has been taken

to be real. A further fundamental property is that eigenfunctions

corresponding to different eigenvalues of the same Hamiltonian are

orthogonal i.e.

$$\int \varphi_i \varphi_j d\tau = \delta_{ij} \tag{17}$$

$$\delta_{ij} = 0 \text{ if } i \neq j \quad \delta_{ii} = 1$$

The electronic Hamiltonian may be written as

$$He = \sum_i - \tfrac{1}{2}\nabla^2_i - \sum_\mu \sum_i \frac{Z_\mu}{r_{\mu i}} + \sum_{i<j} \frac{1}{r_{ij}} \tag{18}$$

where for convenience the expression is in atomic units. This system

of units leads to a considerable simplification in the form of the

equations, viz:

Length:- The Bohr radius of the hydrogen atom as

$$a_0 = h^2/4 \text{ me} = 0.529167 \times 10^{-8} \text{ cm.}$$

$$= 0.529167 \text{ Å.}$$

Mass:- The mass of an electron

$$m = 9.0191 \times 10^{-18} \text{ gm.}$$

Energy:- Often referred to in Hartrees is the energy of interaction

$$E = e^2/a_0 = 27.2107 \text{ eV.}$$

of two unit charges separated by one Bohr radius

b) <u>Solution for Atoms and Molecules.</u>

The Schrodinger equation may be solved for the simplest of all atoms, the hydrogen atom. The method employs separation of the three co-ordinate variables of the electron, represented in spherical polar co-ordinates, in both the wavefunction and Hamiltonian with solution of the resultant equations

$$\varphi(r,\theta,\phi) = R(r)T(\theta)S(\phi) \tag{19}$$

$$\frac{\partial r^2}{\partial r} \frac{\partial R(r)}{\partial r} - \frac{M^2 R(r)}{2mr^2} - \frac{R(r)}{r} = ER(r) \tag{20}$$

where M is given by

$$\frac{1}{\sin\theta} \frac{\partial}{\partial\theta} \sin\theta \frac{\partial}{\partial\theta} T(\theta)S(\phi) + \frac{M_z^2}{\sin\theta} T(\theta)S(\phi) = M^2 T(\theta)S(\phi) \tag{21}$$

and M_z by

$$\frac{-ih\partial}{\partial\phi} S(\phi) = M_z S(\phi) \tag{22}$$

$$Y_{1m}(\theta,\phi) = T(\theta)S(\phi) \tag{23}$$

This separation is obtained by employing operators which commute with the Hamiltonian and with each other. These operators reduce in classical mechanics to the constants of the motion. As a rule there are only five such variables, the three translational modes and the total and one component of the angular momentum. These five constants of the motion enable therefore only an analytical solution for at most two particles.

Solution of the three eigenvalue equations leads to the introduction of three constants, respectively the principal ($n \geqslant 1$), azimuthal ($0 < 1 < n$) and the magnetic ($-1 \leqslant m \leqslant 1$) quantum numbers.

The 1 & m quantum numbers describe the angular features of the quantum shell n and are absorbed in the spherical harmonic function $Y_{1m}(\theta,\phi)$

There is also a fourth quantum number $(m_s = \pm \frac{1}{2})$ which is an eigenvalue of one component of the spin angular momenta and describes the spin property of the electron. Since a one electron Hamiltonian contains only spatial co-ordinates it must commute with the spin operators S^2 and S_z : it follows then that the spin orbital may be represented as the product of a spin function α $(m_s = +\frac{1}{2})$ or β $(m_s = -\frac{1}{2})$ and a spatial orbital. The resultant is known as a spin orbital $\emptyset$.

$$\emptyset_i(1) = \omega_i(1)\alpha \text{ or } \varphi_i(1)\beta \tag{24}$$

with

$$\int \alpha\beta d\sigma = 0 \tag{25}$$

$$\int \alpha\alpha d\sigma = \int \beta\beta d\sigma = 1$$

For each spatial orbital two spin orbitals are constructed.

The application of quantum theory to chemical problems requires an alternative procedure. This was developed initially by Hartree[4] in the late 1920's and modified shortly after by Fock[5]. (Hartree-Fock Method) and splits many electron problems into a series of one electron equations. The electronic Hamiltonian for a system of nuclei and electrons may be written.

$$H = \sum_i - \frac{\nabla_i^2}{2} - \sum_i \sum_m \frac{z_m}{r_{im}} - \sum_{i<j} \frac{1}{r_{ij}} \tag{26}$$

The third term, which represents the electron - electron interaction, is replaced in the Hartree scheme by an average of the repulsion between electrons i and the other electrons in the atom. A series of one electron Hamiltonians may therefore be set up

$$H_i = -\frac{1}{2}\nabla_i^2 - \sum_m \frac{z_n}{r_{im}} + \sum_j (\frac{1}{r_{ij}})\text{av. over } j \tag{27}$$

where

$$H_H = \sum_i H_i - \sum_{i<j}\sum(\frac{1}{r_{ij}})\text{av. over } i \text{ and } j \tag{28}$$

The problem is then reduced to a set of independent equations.

Each H_i commutes with each other and the total Hartree Hamiltonian H_H .

The total wavefunction may therefore be separated in terms of one electron functions which are then expanded as in the two particle case and solved analytically

$$\Psi = \prod_i \phi_i(i) \tag{29}$$

$$\phi_i = Y_{1m}(\theta,\phi)R(r) \tag{30}$$

There are two inherent drawbacks to this approach. Firstly the probability of finding electron i in a region of space $d\tau_i$ $(\Psi^2 d\tau_i)$ is independent of the instantaneous position of the other electrons. The energy associated with this correlation is neglected. The second problem lies in the fact that energies produced by this equation are too low. The cause of this is that the wavefunction as defined by equations 27 - 29 is not antisymmetrical as required by the Pauli Principle. Exchange of any two electrons is required to change the sign of the expression. This is readily produced by replacing equations (29) by a matrix formalism.

$$\Psi = \sqrt{\frac{1}{N!}} \; \begin{vmatrix} \phi_1(1)\phi_1(2)\cdots & \phi_1(n) \\ \phi_2(1)\phi_2(2)\cdots & \phi_2(n) \\ \phi_n(1)\phi_n(2)\cdots & \phi_n(n) \end{vmatrix} \tag{31}$$

where $\sqrt{\frac{1}{N!}}$ is a normalising constant, or

$$\Psi = |\phi_1(1)\phi_2(2) \qquad \phi_n(n)| \tag{32}$$

as a shortened form of (31) with only the diagonal terms represented explicitly[6] . The inherent properties of a matrix concerning exchange of rows will account for the Pauli exclusion principle. The solution employing equation (31) was first introduced by Fock and the treatment is therefore referred to as the Hartree-Fock method.

c). Hartree-Fock Method.

The Hamiltonian operator is written as the sum of one electron (H_i) and two electron terms ($1/r_{ij}$)

$$H = \sum_i H_i + \sum_{i<j}\sum \frac{1}{r_{ij}} \tag{33}$$

and the energy evaluated from equation (4). If the one electron term is considered first, H_i is a function of the co-ordinates of electron i only. Thus for an orthogonalised wavefunction an integral of the form:-

$$\iint \cdots \emptyset_a(1)\emptyset_b(2)\cdots H_i \cdots \emptyset_k(n)\emptyset_l(n)\cdots d\tau_1\cdots d\tau_m$$

will give only diagonal terms involving the orbital associated with electron i from a consideration of the orthogonality of $\emptyset_a$. Thus

$$\iint \varphi(\sum_i H_i)\varphi d\tau d\sigma = N!\sum_m E_m \tag{34}$$

$$E_m = \int \varphi_m(i)H_i\varphi_m(i)d\tau_i \tag{35}$$

The two electron term involving electrons i and j in the expansion will be non-vanishing again unless all the spin orbitals excluding those involving electrons i and j are identical. Two types of terms then remain.

a) Electron i associated with spin orbital $\emptyset_m$ in both determinants and similarly electron j with $\emptyset_n$. This represents a coulomb repulsion between electron i and j

$$J_{mn} = \iint \varphi_m^2(i)\frac{1}{r_{ij}}\varphi_n^2(j)d\tau_i d\tau_j \tag{36}$$

where the spin part has been factored out.

b) Electron i associated with spin orbital $\emptyset_m$ in one determinant and $\emptyset_n$ in the other with the converse for electron j. This represents an exchange interaction of the two electrons.

$$K_{mn} = \iint \varphi_m(i)\varphi_n(i)\frac{1}{r_{ij}}\varphi_m(j)\varphi_n(j)d\tau_i d\tau_j \tag{37}$$

With consideration of the spin property as shown

$$\iint \varphi \frac{1}{r_{ij}}\varphi d\tau = N!(\sum_m\sum_n J_{mn} - \sum_m^\uparrow\sum_n^\uparrow K_{mn}) \tag{38}$$

and hence

$$E = \sum_m E_m + \sum_{m<n} \sum J_{mn} - \overset{\uparrow\uparrow}{\sum_{m<n} \sum} K_{mn} \tag{39}$$

This energy differs from the Hartree energy in the last term.
This is a direct consequence of the Pauli principal in that repulsion
between electron i, j of the same spin will be reduced by an amount K_{ij}
because of the reduced probability of these electrons ever being very
close together. Further as the form of K_{ij} involves overlap of orbitals
some allowance for correlation (exchange correlation) is made. The
mutual coulomb repulsion of all pairs of electrons (coulomb correlation)
is however still neglected.

The energy ϵ of an orbital is given by

$$\epsilon_m = E_m + \sum_n J_{mn} - \sum_n K_{mn} \tag{40}$$

and the one electron Hamiltonian will be of the form

$$H_i = -\tfrac{1}{2}\nabla_i^2 - \sum_m Z_m/r_{im} + V_i \tag{41}$$

where V_i is a common potential function for all the electrons, including
i. The set of 1 electron Schrodinger equations may be solved for atoms
with the assumption that the overall electron distribution is spherically
symmetrical and the eigenfunctions are generated in numerical form as
opposed to analytical functions of the co-ordinates. Though approximate
analytical wavefunctions have been employed for atoms in extending to
molecular systems further criteria are required.

d) The Variation Theorem and Roothaan's Method

The perfect single determinental wavefunction for the closed shell molecule in its ground state gives an expectation value for the energy corresponding to the Hartree-Fock limit. It is apparent however that some criterion is required in order to gauge the accuracy of the Slater determinant and how close to physical reality is the description of the system. Such a criterion is provided by the variation principle.

The variation theorem states that given any approximate wavefunction which satisfies the boundary conditions of the problem, the expectation value for the energy calculated from this function will always be higher than the true ground state energy E_o of the normalised wavefunction φ_o.

$$\int \varphi H \varphi = E \geqslant E_o \tag{42}$$

The wavefunction in Roothaan's proceedure [7] is expanded as the Slater determinant of one electron molecular orbitals which are then in turn expanded as a linear combination of atomic orbitals (LCAO). All the electrons of the molecule are then represented by LCAO MO'S as given by

$$\varphi_i = \sum_p c_{ip} \chi_p \tag{43}$$

with

$$\int \chi_p^* \chi_q d\tau = S_{pq} \tag{44}$$

The c_{ip}'s are taken as the variational coefficients to be determined to produce the minimum energy.

The orthogonality constant on the wavefunction is given by equation (17) and the variational constraint is then

$$\int (\delta \varphi_i^*) \varphi_j d\tau + \int \delta \varphi_j \varphi_i^* d\tau = 0 \tag{45}$$

Roothaan applied this variational criterion to the solution of equation (42). Re-writing equation (39) in the more convenient matrix form

$$E = 2 \text{tr.} \underline{RH} + \text{tr.} \underline{RG}[R] \tag{46}$$

where

$$R_{ab} = \sum_i C_{ia} C_{ib} \tag{47}$$

$$H_{ab} = \int \chi_a^* H_1 \chi_b d\tau \tag{48}$$

$$\underline{G}[R] = 2\underline{J}[R] - \underline{K}[R] \tag{49}$$

$$J_{ab} = \sum_{c,d} \iint R_{cd} \chi_a(1)\chi_b(1) {}^1/r_{12} \chi_c(2)\chi_d(2) d\tau_1 d\tau_2 \tag{50}$$

$$K_{ab} = \sum_{cd} \iint R_{cd} \chi_a(1)\chi_c(1) {}^1/r_{12}\chi_b(2)\chi_d(2) d\tau_1 d\tau_2 \tag{51}$$

and $\underline{M}$ is the matrix of the elements M_{ab} with $\underline{M}_i$ the column vector $\sum_k M_{ik}$

The problem of minimising E in equation (46) may then be solved by the method of Lagrangian Multipliers. When each MO φ_i is varied by an infinitesimal amount $\delta\varphi_i$ the variation of the energy becomes

$$\delta E = 2\sum_i \delta H_i + \sum_{ij}(2\delta J_{ij} - \delta K_{ij}) \tag{52}$$

Expansion of (52) and utilising the hermitian properties of $\hat{J}i$, $\hat{K}i$, $\hat{H}i$ where

$$\hat{J}_i(1)\varphi(1) = (\int \varphi_i^2(2) {}^1/r_{12} d\tau_2)\varphi(1) \tag{53}$$

$$\hat{K}_i(1)\varphi(1) = (\int \varphi_i(2)\varphi(2) {}^1/r_{12} d\varphi_2)\varphi_i(1) \tag{54}$$

$$\hat{H}_i = \int \varphi_i^* H\varphi_i d\tau \tag{55}$$

gives:-

$$\delta E = 2\sum_i(\delta\underline{c}_i^*)^\dagger \underline{F}\underline{c}_i + 2\sum_i(\delta\underline{c}_i^\dagger)\underline{F}^*\underline{c}_i^* \tag{56}$$

with $\underline{F}$ defined in an analogous manner to (49)

$$\underline{F} = \underline{H} + \sum_j(2\underline{J}_j - \underline{K}_j) \tag{57}$$

With the lagrangian multipliers in conjunction with (45) and combining with (56) and (44)

$$\delta E' = 0 = 2\sum_i(\delta\underline{c}_i^*)^\dagger(\underline{F}\underline{c}_i - \sum_j \underline{S}\underline{c}_j \epsilon_{ji})$$
$$+ 2\sum_i(\delta\underline{c}_i^\dagger)(\underline{F}^*\underline{c}_i^* - \sum_j \underline{S}^*\underline{c}_j^* \epsilon_{ij}) \tag{58}$$

whence

$$\underline{F}\underline{c}_i = \sum_j \underline{S}\underline{c}_j \epsilon_{ji} \qquad \underline{F}^*\underline{c}_i^* = \sum_j \underline{S}^*\underline{c}_j^* \epsilon_{ij} \tag{59}$$

The matrix of lagrangian multipliers is thus Hermitian and the two

equations are equivalent.

F is termed the Hartree-Fock Hamiltonian operator though equation 59 is now generally known as the Roothaan equation. These are cubic in the coefficients; the F matrix is itself a quadratic function of the ϵ_{ji}, and the equation has to be solved by an iterative process.

$$F_{ij} = H_{ij} + G_{ij}[R] \tag{60}$$

Since the matrix of ϵ_{ji} is hermitian there will be a unitary transform which will convert 59 into a diagonal matrix with real diagonal elements Ei. Then

$$\underline{Fc_i} = \epsilon_i \underline{Sc_i} \tag{61}$$

$$|\underline{F} - \epsilon \underline{S}|\underline{c} = 0 \tag{62}$$

The Roothaan procedure is an extension, using LCAO MO's, of the original approach of Fock. By an analogous procedure the molecular basis may be retained and equations 61 and 57 may be re-written.

$$\underline{F}\varphi = \varphi\underline{\epsilon} \tag{63}$$

$$\underline{F}\varphi_i = \sum_j \epsilon_{ij}\varphi_j \tag{64}$$

The solutions to equation 63 will be numerous. Since they can be transformed from one into another by appropriate unitary transformation there is no loss in generality if a particular form is chosen. There are two unitary transformations which are of importance in interpreting the wavefunction. Firstly the production of the diagonal matrix of the lagrangian multipliers gives the so called 'best' MO'S which satisfy the equation

$$\underline{F}\varphi_i = \epsilon_i\varphi_i \tag{65}$$

or in the LCAO approximation equation (61).

Each molecular orbital (i) is then delocalised over all the atomic

orbitals. Further the eigenvalue ϵ_i as will be shown later relates to the energy of a particular orbital. This is of considerable importance in photoelectron spectroscopy where ionization occurs of a core (ESCA)[8] or valence (UPS)[9] electron, the energy required being approximated as the negative of the orbital energy via Koopmans' theorem[10].

This diagonal matrix produces a delocalised description of the bonding of each molecular orbital. It is often useful however to generate by means of a unitary transformation a set of localised SCF orbitals i.e. produce a set of orbitals which relates to chemical ideas concerning electron pair bonds etc. This may be achieved by minimising the sum of the exchange integrals K_{ij} where i and j go over the occupied SCF orbitals. In the limit, if a unitary transform could be found which made all these integrals zero, then the antisymmetric wavefunction would reduce to a single product. Edmiston & Ruedenberg provided a simple prescription for minimising the sum of K_{ij} by performing rotations of each pair of SCF orbitals i and j. The integrals are now, however, over a molecular basis and for large basis sets the construction of SCF orbitals is quite time consuming. An alternative proposed by Boys[12] maximises the product of the distances between the centroids of charge of the various orbitals and require only the one electron dipole moment operator. Though not so fundamental, the latter approach approximates the first quite adequately for the valance shell orbitals

e). Wavefunctions for Open Shells.

It is not possible in general to express the Hartree-Fock wavefunction for an open shell atom or molecule as a single determinant. Symmetry determined linear combination of derterminants may be taken and the orbitals

varied to produce the lowest energy. This procedure developed by

Nesbet[13] has proved in general very effective. The concern in this

thesis will be with half-closed shell species, i.e. the open shell

consists of one single occupied molecular orbital. Roothaans' equation

may then be extended in an analogous manner to that outlined for closed

shell wavefunctions with incorporation via coupling operators of the

diagonal elements involving the open shell orbital[14].

The solutions to Roothaans' equations do give occasional problems

with the relative ordering in energies of the highest occupied closed

shell orbitals and the open shell orbital, particularly if an aufbau

technique is employed. An interesting and alternative technique, which

embodies Roothaans' method and has been employed in this thesis, was

proposed by Hillier and Saunders[15]. They considered the conditions for

a stationary energy. A general Hamiltonian over a molecular basis with

m_1 doubly occupied, m_2 single occupied and m_3 virtual MO'S is written as

$$\underline{H}^{MO} = \begin{vmatrix} T_1^{\dagger}H_D T_1 & T_1^{\dagger}H_3 T_2 & T_1^{\dagger}H_1 T_3 \\ T_2^{\dagger}H_3 T_1 & T_2^{\dagger}H_5 T_2 & T_2^{\dagger}H_2 T_3 \\ T_3^{\dagger}H_1 T_1 & T_3^{\dagger}H_2 T_2 & T_3^{\dagger}H_V T_3 \end{vmatrix} \tag{66}$$

where T_1, T_2, T_3 are $n \times m_1$, $n \times m_2$ and $n \times m_3$ matrices of the molecular

orbital coefficients.

$$T_1^{\dagger} = \sum_i^{m_1} \underline{c}_i \tag{67}$$

$$H_x = F + 2J[R_1] + J[R_2] - K[R_1] \pm {}^n/2 K[R_2] \tag{68}$$

The value n is varied to give half integral changes in the matrices

H_x, $x = 1$, 5 and H_d, H_s, H_v are particular matrices for the doubly and

singly occupied and virtual orbitals Hamiltonian H_x. The necessary

condition for a stationary state is then given by

$$T_1^{\dagger}H_1 T_3 = 0; \quad T_2^{\dagger}H_2 T_3 = 0; \quad T_1^{\dagger}H_3 T_2 = 0 \tag{69}$$

coupled with the orthogonality of the orbitals. The solution to the

variational problem will not always give the required configuration. Iterating with this more general procedure does give more control over the form of the generated wavefunction as will be discussed later.

The major difference between these two methods is when the state studied is degenerate (F^2P with the configuration $1s^2, 2s^2, 2p_x^2, 2p_y^2, 2p_z^1$) The procedure of Roothaan will describe the set of degenerate total wavefunctions (x,y,z indistinguishable) while the method of Hillier & Saunders gives just one component of this energy. An alternative (the OCBSE method), as proposed by Hunt, Dunning and Goddard[16] has also been employed quite widely and derives essentially from Roothaan's procedure.

The single determinantal restricted HF procedure cannot account however for spin densities. In the unrestricted HF method[17] determinants constructed from the α and β spin density matrices are separately diagonalised. The F matrices are now of the form

$$\underline{F}^\alpha = \underline{H} + \underline{J}[R^\alpha] + \underline{J}[R^\beta] + \underline{K}[R^\alpha]; \quad \underline{F}^\beta = \underline{H} + \underline{J}[R^\alpha] + J[R^\beta] + K[R^\beta] \qquad (70)$$

Unfortunately the wavefunction derived from 70 is not generally an eigenfunction of the total spin operator $\hat{S}^2$,

$$S^2 \varphi = s(s+1)\hbar\varphi \qquad (71)$$

contaminants from excited doublets, quartets, octets etc., being mixed into the ground state doublet[18]. Normally however this mixing is small and values close to .75$\hbar$ are obtained as the eigenvalue of a doublet state[19].

2)   Practical Considerations.

The formulation of the theory of Hartree, Fock and Roothaan as outlined above, in theory enables quite detailed studies to be made of systems of chemical interest.   The implementation has however only been possible quite recently.   This is due to the considerable computing power required for their solutions.   The problem then becomes not one of chemistry or quantum theory but more of computer technology in both programming (softwear) and machines (hardwear).

This section considers the practicalities of the basic theory, in general within the LCAO approach, and indicates some of the problems which are encountered with their solutions.

a) Basis Functions and Basis Sets.

Within the LCAO approach

$$\varphi_1 = \sum_j c_{1j} \chi_j \qquad (72)$$

the atomic orbitals χ_j have in particular been represented either by one or more (χ_{ij}) Slater type functions (e^{-Zr}) or gaussian type functions $(e^{-\alpha r^2})$.

Slater Type Orbital   Gaussian Type Orbital
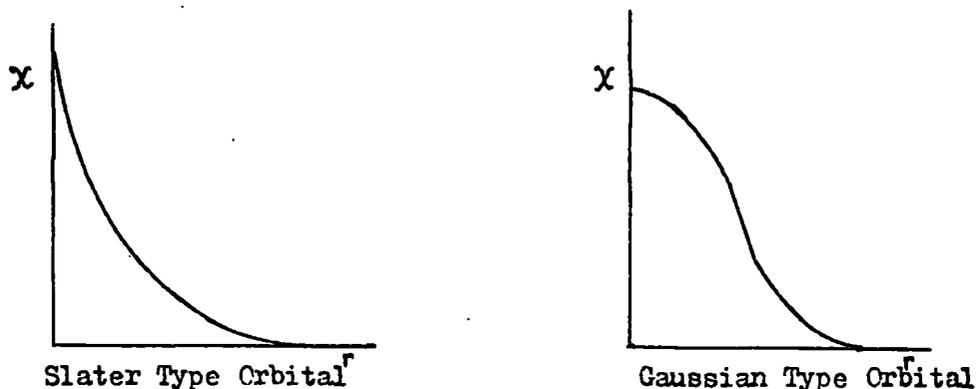
Figure 1.1.

i)   Slater Function.

$$\chi_{ij}(r,\theta,\emptyset) = N r^{n-1} e^{-Zr} Y_{1m}(\theta,\emptyset) \qquad (73)$$

Where N is a normalising factor, n is the principal quantum number and Z the orbital exponent. Together Slater and Zener[22] produced optimised values of Z representing the potential of an electron in that particular orbital. The functions are not orthogonal for different n but this defficiency may be accounted for by taking appropriate linear combinations. They have been employed quite widely in empirical work as they represent to a good approximation the H.F. atomic orbitals. In non-empirical work they have been generally superseded by the gaussian expansion due to difficulties associated with the evaluation of the large number of three and four centre two electron integrals, though research is still being channelled into them and has proved useful in linear systems. They are also employed in cases where larger numbers of these integrals are not required to be computed i.e. for atoms and in semi-empirical work.

ii) Gaussian Function.

The use of gaussian functions was first suggested by Boys. They have the form

$$\chi_{ij} = N x^p y^q z^s e^{-\alpha r^2}$$

$$\chi_{ij} = N Y_{1m}(\theta, \emptyset) r^n e^{-\alpha r^2} \tag{74}$$

depending on the representation of the angular dependence. Their use considerably simplifies the solution of the multicentre integrals since the product of two gaussians sited at different centres is another gaussian function positioned on the line joining the two original centres. Thus for example, integrals of the form

$$\int \chi_{ij}(g)_a \chi_{ij}(g)_b {}^1/r_{12} \chi_{ij}(g)_c \chi_{ij}(g)_d d\tau \tag{75}$$

with $\chi_{ij}(g)_a$ a gaussian type function centred on a are simplified to the form

$$\int f_1(g) e^{1/r_{12}} f_2(g) f d\tau \tag{76}$$

where $f_1(g)$ is another gaussian. The equations of Boys and co-workers have been accompanied by that of Shavitt[23] who has given a general description on the properties and use of gaussian function and integrals involving them. Their main practical disadvantage is that as $r \to 0$ (the cusp region) the function has the wrong properties (Fig.1).

iii) <u>Basis Size</u>

Each atomic orbital may be expressed either singly or as a sum of the above two classes of function. Further a decision has to be made 'a priori' as to which atomic orbitals will contribute to the electronic structure. A range from a minimal basis with a single function for each occupied atomic orbital to an extended basis with more than one function for each occupied atomic orbital and additions from other atomic orbitals may be considered. As a rule of thumb the time required for solution of the Hartree-Fock equations varies as n^{3-4} i.e. doubling the size of the basis will increase the time required for solution by a factor of 10. For this reason a suitable choice must be made of functions to provide a sufficiently accurate wavefunction with a minimal basis size.

There is a second consideration in that a balanced basis set should be chosen. with each atom in the molecule having its atomic orbital represented to a similar accuracy. Further, this is linked closely with the number of electrons in the valence shell as has been shown by Jansen and Ross[24]. (For a calculation then on LiF a considerably larger basis will be required for the F ao's as opposed to those of F).

iv) <u>Minimal Basis Sets.</u>

With this basis each atomic orbital which is considered to be occupied is represented by a single function, usually a Slater function with a suitable choice of exponent. Though the Slater-Zener exponents are in general sufficient, more quantitive values are now available from atomic set calculations by Clementi and Raimondi.[25] These 'best atom exponents' are then used for the basis functions in a molecular environment.

There are two inherent drawbacks with a minimal Slater basis notwithstanding their inherent approximate form. Firstly the molecular environment will often be drastically different from that of the free atom. In general this is neglected: optimisation of the exponent in the molecular environment is not usually computationally feasible For hydrogen however the field of the other nuclei will cause a contraction of the unshielded 1s orbital and the exponent is generally increased from $J = 1.0$ to $J = 1.2$. Secondly the integral evaluation is difficult.

The latter problem has been resolved by the work of Foster & Boys[26] and Pople and co-workers, the latter expanding each Slater type orbital as a sum of n gaussians (STO-nG)[27]. The coefficients and exponents of the gaussians are optimised and fixed for a unit Slater exponent. The Slater exponent is then chosen and the gaussian exponents scaled accordingly. Stewart has also considered expansions of the Hartree-Fock functions themselves in terms of a sum of a gaussian[28]. These procedures have proved to be conceptually simple and computationally easy to apply and are one of the major lines of approach taken in ab initio studies. The wavefunction produced is in the majority of molecules quite adequate though the energies are some way from the Hartree-Fock limit due to the poor description of the cusp region.

v). <u>Split Valence Basis Sets.</u>

The descriptive power of the wavefunction is considerably enhanced by employing two sets of functions for each valence atomic orbital. The choice of exponent is then less critical as radial relaxation of the orbitals to the molecular environment may occur. The STO-nG basis has been extended to great effect to give a STO-n1G basis, the valence atomic orbitals being described by a variable combination of n and 1 gaussians. The STO 4-31G [29] basis has been shown to be for hydrocarbon studies of sufficient accuracy to account for the majority of topics of interest for these species.

vi) <u>Double Zeta Basis Sets.</u>

Following from the above the core orbitals are now described as a variable combination of two functions. There is little variation in the overall electron distribution in this step but a considerable improvement in the total energy results. Atomic H.F. calculations with optimal exponents give with this basis near H.F. total energies as has been shown by Clementi[30-33]. It is important though to distinguish the fact that here the improvement in energy is due to an improved description of the actual cusp region: there is no appreciable change in optimised core exponent in the atomic or molecular situation.

vii) <u>Contracted Basis Sets.</u>

The STO-nG basis is one example of a contracted basis. There has been considerable effort employed in producing basis sets via the alternative route; from optimised contracted combinations of gaussian functions[34-38]. Regions in space (the cusp, core and valence atomic regions) are then distinguished by observation of the exponents and the gaussians accordingly grouped. Within each group the optimised

coefficients are then renormalised and taken as the weighting factors for each gaussian.

The major advantage occurring from such a procedure is in the SCF stage of the calculation. Cycling times vary approximately as the fourth power of the basis set size. Any reduction in this will thus produce much faster processing with a similar reduction in required backing store. Though contraction reduces the flexibility of the basis suitable combinations of functions as proposed by Dunning[36] reduces the iteration time with only slight loss in accuracy. The objective is then to retain maximum flexibility in the valence region but only allow any function to vary freely if it contributes strongly to more than one atomic orbital in the atom.

viii)   Polarisation Functions.

The LCAO approach is an approximation. One of its major failings is in describing the electronic structure in situations where bond cycles are much less than $90°$ i.e. combinations from two orthogonal p hybrids cannot provide a good description in the region between them. Inclusion of d and in some cases f type functions will provide a better description with their different angular dependencies and produce polarisation of the electronic distribution to these regions[39,40]. A secondary factor as outlined by Nesbet is that they also provide an added flexibility to the chosen basis.

1x)   Non L.C.A.O. Basis Sets

There is no inherent reason why the basis set should comprise functions centred on the constituent atoms in the molecule. Frost[41] and latterly Christoffersen[42] have proceeded to define a basis in terms of floating spherical gaussian functions (FSGO)

$$\chi_i = N\left[\exp(-(r-Ri)^2/\rho_i^2)\right] \qquad \bullet \qquad (77)$$

Both the radii (ρ_i) and the position (Ri) are minimised with respect to the total energy of the system. The major advantages are that fundamental units may be constructed and described by a suitable combination of gaussians which is much less than that required in the LCAO technique (for a n electron system $\frac{1}{2}$n basis functions may be used). The procedure lends itself then to the study of quite large molecules though the results are not directly related to quantitative ideas concerning bonding.

An intermediate approach developed independently by Preuss[43] and Whitten[44] employs spherical gaussians to represent the angular dependencies $T_{ln}(\theta,\phi)$ by taking the desired linear combination. These are referred to as lobe function. For example, a p type gaussian lobe function can be expressed as

$$\chi_i = N \exp(-\alpha(r-R_o\bar{\gamma})^2] - \exp[-\alpha(r+R_o\bar{\gamma})^2] \qquad (78)$$

where $\bar{\gamma}$ is a unit vector and R_o is a constant defining the distance from the origin. This is usually taken as a nuclear co-ordinate. The extra variable R_o may be linked with the exponent α ($R_o = C^{-\frac{1}{2}}$)and with a suitable value of C (~ 0.03) the results of LCAO and gaussian lobe calculations with the same exponents are closely similar.

b).Integral Evaluation

The total number of two electrons integrals which are in principle required to be calculated for a basis of n functions is given by the following equation

$$n/4(n + 1) \ (n/2(n + 1) + 1)$$

For a basis of 9 functions 1035 two electron integrals are required; 23 functions require 38,226 such integrals. Thus clearly other factors which will include storage and labelling of the functions will be of importance beside the formulation of reliable algorithms. Efficient

computing facilities are therefore essential for both evaluation and handling of data.

The computation of a particular integral is performed over the basis of uncontracted primitive functions. If these primitives are then required to be contracted they are stored in this form. The algorithms for this stage are not greatly different from those of Boys[21] and Shavitt[23]. The major problem and an area of immense research has been in efficient data handling and the reduction of unnecessary calculation by using any symmetry properties of the integrals to reduce the number required to be calculated. The formulation of an algorithm though for the latter does not necessarily produce any increased efficiency. There will be a finite time required to generate lists of redundant integrals and their associated parent, which, unless efficient data handling is employed, will negate the total saving by reduction of the number of two electron integrals.

These two philosophies have led to two classes of non-empirical programs. The polyatom system of Harrison[45] produced a list of integral labels that had no integrals in it that were zero by symmetry, and group together those integrals that were equal to within a sign, so that only one member of the group needed evaluation (i.e. a non-redundant list). The alternative approach the IBMOL programs of Clementi et al[33,46] considered all the integrals evaluated each separately. The list routine of Polyatom depended approximately on the third or fourth power of the number of basis functions whether or not zero or redundant integrals were present. In general POLYATOM was preferable for systems of high symmetry whilst IBMOL developed along low symmetry lines. More recently Hillier and Saunders[47] have produced the ATMOL series of programs whose integral routines, based on the POLYATOM system, are at present vastly superior to either method. The efficiency is derived in the main by better utilisation

of core by employing fast efficiently organised backing stores. Symmetry routines are thus quite advantageous.

In studies of organic compounds there are certain to be redundancies between calculations, thus the two centre integrals involving C-C and C=C will be recomputed in each calculation. Whitman and Eilers[48] have recently investigated this transferability between calculations with the establishment of libraries of HF matrix elements. For a given molecule the simulated Fock matrix is formed, the new overlap matrix calculated and one cycle of Roothaan's procedure generates the solution to equation (62). Total and orbital energies are reported in excellent agreement with a full calculation. It is probable that similar approaches to this will provide a means of investigating very large systems.

c). SCF Methods.

The aim of this stage is to reduce the matrix of lagrangian multipliers to diagonal form such that the eigenvectors defined from this matrix are self consistent:- a second cycle of diagonalisation will produce deviations in the elements less than a certain predetermined threshold. There are two parts in each cycle.

1). Formation of the Fock matrix, n^4 dependence ~70%

2). Diagonalisation n^3 depending ~30%

It is thus important that the backing store of integrals should be on a fast random access device i.e. disc as opposed to tapes.

The method of Roothaan[7] is suitable for the majority of calculations. After formation of the Fock matrix it is brought to diagonal form. Given the eigenvalue problem

$$\underline{H}_o \underline{C}_o = \underline{E}_o \underline{C}_o \tag{79}$$

a new matrix, $\underline{H}_1$, is formed where $\underline{H}_1 = \underline{P}^{-1} \underline{H}_o \underline{P}$ using a matrix $\underline{P}_1$ which introduces a zero off-diagonal element in $\underline{H}_1$. Further matrices $\underline{H}_2 \ \underline{H}_3$

are defined from the previous $\underline{H}$ matrix until the off-diagonal elements are less than a predetermined threshold. The final matrix $\underline{H}_r$ will be given by

$$\underline{H}_r = \underline{P_r}^\dagger \underline{P}_{r-1}^\dagger \ldots \underline{P}_{-1}^\dagger \underline{H}_0 \underline{P}_1 \ldots \underline{P}_{r-1} \underline{P}_r \qquad (80)$$

and the eigenvectors

$$\underline{C}_0 = \underline{P}_1 \quad \underline{P}_{r-1} \underline{P}_r \underline{C}_r \qquad (81)$$

To eliminate the element r,s of $\underline{H}$ ($r \neq s$) angular rotation elements of π are taken. The convergence between iterations may be accelerated by use of Aitken's procedure which relies on the geometric progression of the error in the coefficients.

Aitken:
$$x_i = x_i^{r+1} - \frac{(x_i^{r+1} - x_i)^2}{x_i^{r+2} - 2x_i^r + x_i^{r-1}} \qquad (82)$$

There are two improvements which may be made to reduce the computation time.

a). Reduction in the time required for formation of the F matrix. This reduces to more efficient storage of the two electron integrals. A most efficient method derives from Yoshimine[49] with the introduction of J and K supermatrices.

$$J (IJ, KL) = (ij, kl)$$

$$K (IJ, KL)/2 = ((ik,jl) + (il,jk))/4$$

For each set of indices i, j, k, l the non zero elements $P = J - K/2$ and $\frac{1}{2}K$ are stored in a sequential file along with their associated pair indices IJ,KL which are then separated into integral types and ordered A recent modification by Raffenetti[50] claims an improvement of a factor of 3 on conventional random integral retrieval process or a factor of 2 on total processing time.

b) A more direct approach is to reduce the number of iterations. The steepest descents method of McWeeny[51] though a more reliable iterative procedure does not always ensure a practical rate of convergence. The

method of Hunt et al with the orthogonality constrained basis set expansion (OCBSE)[16] claims a marked improvement. From a consideration of the convergence criteria Hillier – Saunders produced a new variant of the set equations[15]. The Roothaan-Hartree-Fock Hamiltonian is generated in the usual manner. This is then subjected to the transform:

$$\underline{H}^{MO} = \underline{C}^{\dagger}\underline{H}^{ao}\underline{C} \tag{83}$$

where the columns of $\underline{C}$ contain the coefficient of the trial molecular orbitals. This matrix is then diagonalised. The power of this procedure is however that as $\underline{C}$ tends to self consistency the matrix H^{mo} becomes diagonal. From equation (62)

$$\underline{FC} = \underline{SC\epsilon}$$

Considering the element $F'_{\mu\nu}$

$$F'_{\mu\nu} = (\underline{C}^{\dagger}\underline{FC})_{\mu\nu} \tag{84}$$

$$= \sum_{l}\sum_{m}\sum_{n} c_{l\mu} S_{lm} c_{mn} \epsilon_{n\nu} \tag{85}$$

$$= \sum_{l}\sum_{m} c_{l\mu} c_{m\nu} \epsilon_{\nu\nu} S_{lm} \tag{86}$$

$$= \varphi_{\mu}\varphi_{\nu} \epsilon_{\nu\nu} \tag{87}$$

From diagonalisation of $\underline{F}$ the resultant eigenvector array defines molecular orbitals as a linear combination of the trial molecular orbitals. The matrix of coefficients is then given by

$$\underline{C}^{r+1} = \underline{C}^{r}\underline{T} \tag{88}$$

The method is readily applicable to open shell calculations where the F matrix is split according to the three types of orbitals (singly, doubly occupied and virtual). By suitable choice of the diagonal Hamiltonians the wavefunction may be generated with certain physical properties e.g. Koopmans' theorem may be applied.

3)   Computer Programs for Non Empirical Calculation

   a) Programming Philosophies.

   There has been an immense dedication of time and effort into the
production of efficient routines and the lines of approach have been mainly
reflected in the IBMOL and POLYATOM programs.   From previous studies a few
desirable feature, as far as practical use of the programs are discernable.
These include:

1)   General applicability to all molecular systems.   As programs are
generally composed in FORTRAN dynamic programming is not available.   Thus
program for different size basis needs to be available.

2)   The machine dependence should be a minimum.   This must however be
weighted against machine language programming which is of high efficiency.
Further by low level programming, core space and data handling may be
optimised, desirable in a multiprogramming environment.   Use of peripheral
work stations has been used to circumvent this problem.

3)   Ease of data handling.   Standard libraries of basis set data kept in
store, may be called to generate input files.   This is particularly useful
for contracted basis where the number of primitives may be large (>200)
A check procedure in this context is also desirable.

4).   Conveyence guarantee.   Indiscriminate use of SCF packages may lead to
solutions of the eigenvalue problem which do not represent the ground state
wavefunction.   A set of readily applicable but still adaptable proceedures
is thus required to generate the required converging situation.

5).   Adaptability.   Addition, deletions or correction of groups of atoms
or/and basis functions will greatly reduce the two electron calculation.
Only those integrals involving alteration to the basis need then to be
recalculated.

6). Suitability to a Multiprogramming environment. This is of paramount importance and embodies many of the above points. In this context the program should be able to run with an optimum core requirement, dependent upon the system on which it is implemented, and in stages, i.e. the program must be restartable. This also implies that the program should be segmented into integral, SCF and wavefunction analysis components.

The majority of the nonempirical LCAO MO SCF calculations presented in this work have been performed with the IBMOL5[52] and ATMOL2[47] group of programs[53]. These were in the main implemented on the Rutherford High Energy Physics Laboratory IBM 370/195 computer. The latter program was also implemented on the ATLAS ICL 1906A and Cambridge 370/165 computers. Some of the standard work in second chapter employed the ALCHEMY[54] program, again implemented on the IBM 370/195 and this will be briefly discussed first.

b) ALCHEMY

This program devised by Yoshimine and Maclean, performs calculations with a basis set of Slater function for linear molecules only. It is written in FORTRAN and is relatively simple and flexible in format but requires a large amount of core($>$500K). The one centre integrals are calculated analytically and the others numerically. Extensive file handling is employed with fast backing store. The program generates at convergence the eigenvectors, eigenvalues and the orbital populations.

A typical calculation for FCCH gave the following cpu's for the three main steps for a starting set of eigenvalues from CNDO/2 analysis.

Calculation.	Time(sec.)	
2 - electron	575	(Basis set of 34
1 - electron	56	Slater Functions)
SCF	137	
Total	768	

c).<u>IBMOL 5</u>

The most recent of IBM production programs of Clementi et al, it is designed for large basis set calculations of low symmetry. With many of the design philosophies of ALCHEMY it is deficient in that it requires a large amount of user generated data in its standard form. The data required for the integrals section of the program includes the nuclear co-ordinates and charges for each centre, the basis function type $(s, p_x, d_{xx}$ etc.) and exponent. This basis may then be successfully contracted to produce functions of the same type, hybrids on the same centre and finally symmetry adapted functions which will depend upon the type of molecule. This latter step has the advantage of blocking the F matrix in diagonal form whence a reduction in the SCF stage results. It however imposes a severe restriction if at a later stage these symmetry integrals are required for a calculation with the molecule in a different symmetry (e.g. localised hole states, ionised states etc.)

The SCF data is presented in NAMELIST form. Starting vectors are usually presented from a CNDO/2 calculation. Facilities exist for deleting (but not adding) functions and for the recomputation of integrals involved when centres or basis are moved. Though the integral and SCF programs are packaged as a whole the analysis programs are separate. These employ punched card copies of the vectors from the parent program. In this work analysis of the wave function was performed with previously available programs which were extensively modified and extended to provide a compatable system. For a typical calculation on thiirene-1,1 dioxide with a symmetry split contracted basis of 69 functions of 104 primitives the cpu's are shown below.

Calculation.	cpu(sec.)
2 electron	2777
1 electron	3
SCF	241
Total	3021

d). ATMOL

The ATMOL series of programs were devised by Hillier and Saunders in the late 1960's as extensions to the polyatom system. With additions to this series and adaptions for convenient usage they provide an extremely efficient package for the solution and analysis of the wave equation. They require comparatively little main core; typically 210K on an IBM370/195.

The basic algorithms have been mentioned above. File handling is facilitated by means of extensive blocking of a fixed length data set. Basis functions may be altered, added or deleted and the user has the capability for full control over his data handling. Input requirement is a minimum for the integrals; a library of contracted functions being employed. Local symmetry is employed to reduce the labour and the integrals are stored with their associated ideas. Starting vectors may be generated either internally, externally or semi-externally by supplying diagonal elements of a starting F matrix which is then diagonalised to produce the eigenvectors. Convergence parameters are flexible and with the LOCK directive the aufbau ordering may be overridden to generate states of a required electronic configuration. Both a modified RHF and a UHF procedure are available for open shell calculations. A Mulliken population, localised orbital and density contour procedure are now available to augment the parent program.

Typical program times for a calculation on dimethyl sulphone (117 primitive gaussians contracted to a basis of 78 functions) are shown below.

Calculation.	cpu(sec.)
2 electron	1098
1 electron	10
SCF	1310
Total	2418

The flexibility of the latter program in particular renders it suitable for operation from a small work station (comprising a minimum of line printer, card reader and preferably a small core) linked to the main computer by means of GPO lines. Remote access to the IBM370/195 was employed via an IBM1130 and a GEC2050 system.

4) Semi-Empirical LCAO MO SCF Calculations.

Though ab initio studies are now possible for quite large species e.g. the guanine-cytosive pair [55], they are still quite computationally expensive. One of the main obstacles in ab initio calculations is the very large number of three and four centre integrals. A number of semi-empirical all valence electron methods based on approximation or neglect of these terms have been developed, mainly with a basis set of Slater functions. This results in a considerable (10^2) saving in cpu. Two levels of approach will be outlined below, the NDDO and CNDO schemes.

a).NDDO. Neglect of Diatomic Differential Overlap.

The approximations involved in this method are:-

i) The core levels are treated as an unpolarizable core.

ii) A minimal basis of the valence electrons is taken.

iii) Diatomic differential overlap is neglected.

$$S_{ij} = \int \chi_i \chi_j d\tau = 0 \qquad (89)$$

if the orbitals χ_i and χ_j are not on the same atom. Further

$$\iint \chi_i(1)\chi_k(2)\frac{1}{r_{12}}\chi_j(1)\chi_l(2)d\tau_1 d\tau_2 = 0 \qquad (90)$$

unless χ_i and χ_j are atomic orbitals belonging to the same atom (A) and χ_i and χ_j are atomic orbitals belonging to the same atom (A or B). Though the approximations here are quite drastic, all 3-4 centre integrals are neglected, there still remains the problem of too many integrals and further

simplifications with heed to the invariance requirement of the orbitals are required.

b). CNDO/INDO   Complete or Intermediate Neglect of Differential Overlap[56]

The spatial and hybridisation requirement of the basis may be shown by considering the integral

$$\iint \chi_s(1)\chi_p(2) \frac{1}{r_{12}} \chi_j(1)\chi_p(2) \, d\tau_1 d\tau_2 \tag{91}$$

The p orbitals p_x, p_y, p_z are three-fold degenerate, hence if

$$X = \frac{1}{2}(px' + py') \tag{92}$$

$$<ss/\chi\chi> = \frac{1}{2}<ss/x'x'> + 2<ss/x'y'> + <ss/y'y'> \tag{93}$$

For this to be so it is convenient to take[57]

$$<ss/\chi\chi> = <ss/x'x'> = <ss/y'y'> \quad <ss/x'y'> = 0 \tag{94}$$

Pople further neglected in the CNDO form the one centre interactions involving differential overlap.   Writing the electron interaction integrals

$$\iint \chi_A^2(1)\frac{1}{r_{12}} \chi_B^2(2) \, d\tau_1 d\tau_2 \tag{95}$$

as Γ_{AB} the Fock matrix elements F_{ij} become

$$F_{ii} = H_{ii} + (P_{AA} - \tfrac{1}{2}P_{ii})\Gamma_{AA} + \sum_{B\neq A} P_{BB}\Gamma_{AB} \tag{96}$$

$$F_{ij} = H_{ij} - \tfrac{1}{2}P_{ij}\Gamma_{AB}$$

where χ_i is centred on atom A, χ_j on atom B and P_{ij} is an element of the density matrix

$$P_{ij} = 2\sum_m^{occ} C_{mi}C_{mj} \tag{97}$$

The core matrix may be separated into two components,

$$H_{ii} = U_{ii} + \sum_{B\neq A} V_{AB} \tag{98}$$

and therefore equation (96) may be written

$$F_{ii} = U_{ii} + (P_{AA} - \tfrac{1}{2}P_{ii})\Gamma_{AA} + \sum_{B\neq A}(P_{BB}\Gamma_{AB} - V_{AB}) \tag{99}$$

In this form certain one centre exchange integrals of the form $(2s2p_x, 2s2p_x)$ are neglected and thus the qualitative effects of Hund's rule are inapplicable.   For radicals Pople developed a UHF INDO program

which retained only the rotational invariance. The matrix elements are

$$F_{ii}^{\alpha} = U_{ii} + \sum_{k,1}^{A} P_{k1}(ii/k1) - P_{k1}^{\alpha}(ik/i1) + \sum_{B \neq A} (P_{BB}\Gamma_{AB}-V_{AB}) \quad (i \text{ on atom A}) \quad (100)$$

$$F_{ij}^{\alpha} = U_{ij} + \sum_{k,1}^{A} (P_{k1}(ij/k1) - P_{k1}^{\alpha}(ik/j1)) \quad (i \neq j \text{ on A}) \quad F_{ij}^{\alpha} = H_{ij} - P_{ij}^{\alpha}\Gamma_{AB}$$

The F_{ij}^{β} element for electrons of opposite spins have the same form. The individual integrals are then estimated from non-empirical and spectral data as outlined below.

One-Centre Integrals : At the CNDO Level Γ_{AA} is approximated by the analytical value of the electrostatic repulsion energy of two electrons in a Slater s orbital[58]. The INDO formula expresses these in terms of Slater Condon F^k and G^k factors[59] , thus for example

$$<ss/ss> = <ss/xx> = F^o = \Gamma_{AA} \quad (101)$$
$$<sx/sx> = \frac{1}{3}G'$$
$$<ss/yy> = F^o - \frac{2}{25}F^2$$

Except for F^o, semi-empirical best fits to atomic spectra are taken. U_{ii} can similarly be estimated from spectroscopic data. At the CNDO/2 level

$$U_{ii} = -\frac{1}{2}(I_i+A_i) - (Z_A - \frac{1}{2})\Gamma_{AA} \quad (102)$$

where I_i is the ionization potential and $-A_i = U_{ii} + Z_a\Gamma_{aa}$ is the electron affinity. Similar results in terms of F^k and G^k factors are obtained in the INDO scheme.

Two-Centre Two Electron Integrals. This is the most difficult problem encountered in the design of semi-empirical quantum mechanical methods. In the limit of $R \rightarrow 0$ the integral should reduce to the one centre integral and towards e^2/r at large distances. These have been calculated as the two centre coulomb integral[60]

$$\Gamma_{AB} = \iint \chi_{SA}^2(1) \, ^1/r_{12} \chi_{SB}^2 d\tau_1 d\tau_2 \quad (103)$$

Formula for their evaluation have been listed by Roothaan[61]

Coulomb Penetration Integrals V_{AB} Attempts to estimate this

resulted in failures to predict bond lengths and bond energies for diatomic

molecules.   Since overlap neglects to introduce errors, similar (but

opposite in sign) neglect of penetration was argued where

$$V_{AB} = Z_B \Gamma_{AB}$$
(104)

Two Centre One Electron Integrals H_{ij} (Resonance Integrals).

This may be interpreted physically as the energy of an electron

occupying the overlap cloud between orbitals i and j in the field of the

core and remaining electrons

$$H_{ij} = \beta_{AB}^{o} S_{ij}$$
(105)

To retain rotational invariance β_{AB}^{o} should be characteristic of

χ_i and χ_j but independent of their positions in space.   Pople suggested

an averaging

$$\beta_{AB}^{o} = \tfrac{1}{2}(\beta_A^o + \beta_B^o)$$
(106)

where β_A^o and β_B^o are adjusted to give the best fit between CNDO and

LCAO SCF calculated charges[58,60,62].   The total energies are estimated

from the electronic energy and core repulsion energy (CR)

$$CR_{AB} = \frac{Z_A Z_B}{R_{AB}}$$
(107)

where Z_A Z_B are the effective core charges.

The CNDO/INDO calculations reported in this work were carried out

with a modified version of the standard package CNINDO[63].   This performs

CNDO calculations on molecules containing the atom hydrogen to chlorine

and INDO calculations up to fluorine.   Variable convergence and

redimensioning to allow calculations on molecules containing up to 120 basis

functions was performed together with an option for deletion of $3d$ atomic

orbitals from the basis of second row elements.

A version of the program was also developed for minimisation of geometries. The majority of the cpu is employed in the diagonalisation procedure. Generation of a sufficiently accurate set of starting vectors will thus reduce the number of cycles. Subtle changes in an initial molecular geometry will not greatly effect the final eigenvalue matrix from one calculation to the next. A procedure was therefore implemented whereby starting vectors for a new geometry were obtained from the final vectors of the previous geometry. A comprehensive geometry program was directly linked with the modified CNINDO package and three suitable changes in an angle or bond length taken. The minimum was found by expressing the energies as a second order expansion of the co-ordinate(i.e. an harmonic oscillator function). The saving in labour was better than a factor of x3 i.e. if several slight changes in geometry were to be performed the method was comparable for optimisation of one variable with an initial calculation with the variable fixed. Alternative techniques and programs are now also available for the direct minimisation of geometry by differentiation of the F matrix with respect to co-ordinates[64,65].

5). Limitations of Hartree-Fock Calculations.

With a sufficiently large basis set and computing power it is possible to approach the Hartree-Fock limit. The majority of calculations reported here are some way from this. However, a wealth of information is now available which indicates that with a suitably chosen basis the errors introduced are quite small[66]. Indeed for isodesmic processes i.e. those in which bond types and numbers of electron pairs remain constant in going from reactants to products, Pople and co-workers have shown that even a minimal STO-3G basis may be adequate[67,68]. There are, however, certain limitations inherent in the Hartree-Fock description of molecular electron structure.

a).<u>Relatavistic Correction</u>: The Virial theorem (V = 2T where V is the potential energy and T the kinetic energy) may be used as a test of the wavefunction. A consequence of the theorem is that an electron in a region of high potential will have a large kinetic energy and hence relatavistic effects will be increasingly important for core electrons. For the lighter elements, though the correction is not negligible in absolute terms, variations are insignificant.

b) <u>Correlation Energy.</u>

This is a more serious problem.   The H.F. wavefunction is generated from a set of one electron orbitals i.e. each electron experiences an average field of the nuclei and other electrons.   Thus no account is taken explicitly of the instantaneous correlations of electronic motion. Lowdin[69] has expressed this in terms of differences in expectation values between exact and   HF Hamiltonians

$$E_{MECE} = E_{Exact} - E_{HF} \tag{108}$$

where E_{MECE} is the molecular extra correlation energy.

Various methods have been developed for estimating E_{CORR}within the the LCAO MO formalisation.   The approximation that the total correlation may be split into a sum from each electron pair has found widespread use [70,71]

$$E_{corr} = \sum_{ij} \epsilon_{ij} \tag{109}$$

where ϵ_{ij} is the pair correlation between electron i and j.   For atoms this approaches closely the true energy, for molecules alternative methods are required.

The correlation energy may be separated into inter-and intra-atomic components

$$E_{corr} = E_{AA} + E_{AB} \tag{110}$$

The latter (E_{AA}) will give rise to the larger energies and attempts have been made to estimate it. Hollister and Sinanoglu[71] employed a pair correlation method whereby the pair energies are weighted by pair populations, usually obtained from a Mulliken population analysis.

$$E_{AA} = \sum_i \epsilon_{ii} \tfrac{1}{2} \rho_i + \sum_{i<j} \epsilon_{ij}\rho_i\rho_j \qquad (111)$$

where the first term allows for self-orbital correlation with atomic population ρ_i and the second for interorbital correlation. This method has been applied by Snyder and Basch[66] for the calculation of thermodynamic data. Despite their larger absolute magnitude, changes in E_{AB} were reported, similar and in an opposite sense to E_{AA} for a series of isodesmic reactions. An independent study by Pamuk[72] has also reported estimates of pair energies which are similar to those of Snyder and Basch. Snyder has also applied transferability of bonds and lone pairs to calculating the correlation energy associated with these paired electrons[73] (Table 1.1.). This has proved qualitatively successful in a number of reactions but lacks in its formalisation more than a qualitative relationship with the molecules under consideration.

c). Configuration Interaction.

The single determinant (Ψ_o) may be improved by the introduction of linearly varied determinants representing excited state, computed by considering the virtual orbitals, thus the improved configuration interaction (CI) wavefunction [74] Ψ is given by

$$\Psi = a\Psi_0 + b\Psi_1 + c\Psi_2 + \ldots \qquad (112)$$

A variant on this is to allow each of the Ψ_i to vary simultaneously.[75] This is difficult to implement for complex systems. The more basic CI is relatively simple to apply though at a quite considerable cost if a large number of configurations are chosen.

Figure 1.2.
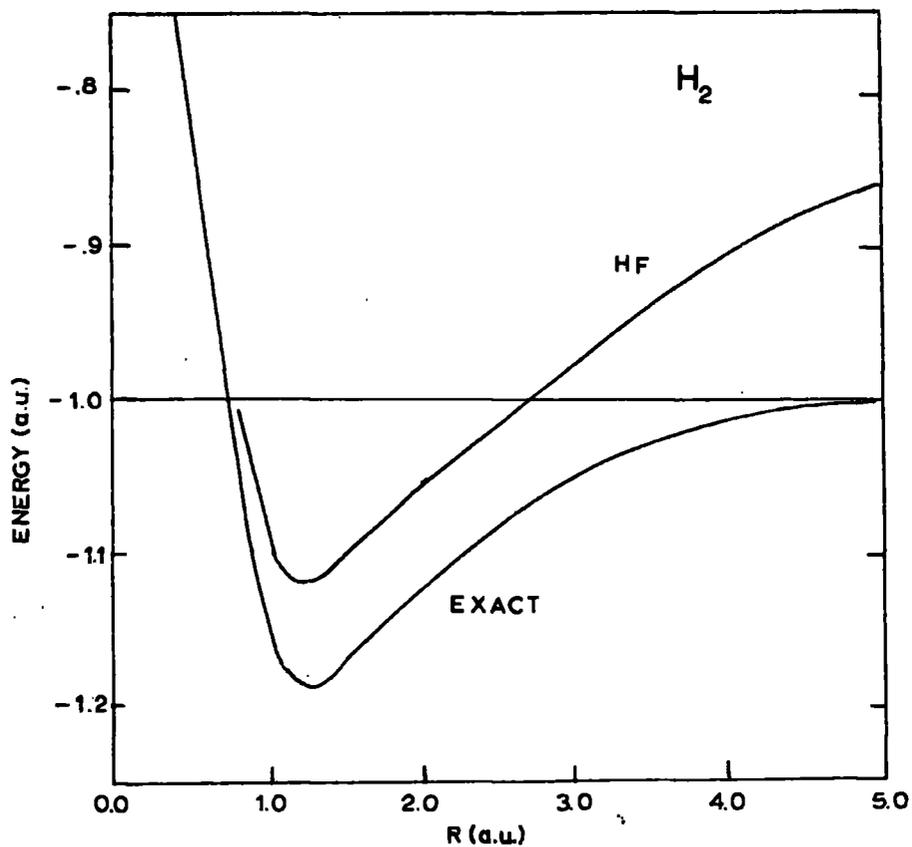
Table 1.1

Pair Correlation Energies for 1st row atoms.

Pair	au	eV
1s – 1s	– .0409	– 1.113
1s – 2s	– .0027	– 0.073
1s – 2p	– .0027	– 0.073
bond–bond	– .0407	– 1.110
bond–bond*	– .0118	– 0.321
lone pair	– .0257	– 0.699
lone pair–lone pair*	–.0358	– 0.974
lone pair–bond	– .0301	– 0.819

* For separate bond / lone pair.

The most important defect of the Hartree-Fock treatment is in
describing bond breaking. As is shown in Fig.1.2 the asymptotic
behaviour of the Hartree-Fock energy is incorrect for the bond breaking
in H_2 or F_2 . This arises from spurious ionic terms. The two curves
are approximately parallel to one another up to $\sim 2.5\text{Å}$ a distance
corresponding to $\sim$ twice the H-H bond length. Thus geometries and
short range potential surfaces are likely to be reasonably described by
a single determinant wavefunction though atomisation energies will not be.

d) Non LCAO-MO Techniques.

Finally in this chapter mention is made of the valence bond method.
Whereas the MO-method either generates the wrong asymptotic form in bond
cleavage $(RHF)^7$ or the incorrect spin state $(UHF)^{17}$ the valence bond
method can generate the correct form in both. The approach however has
practical as well as computational drawbacks. Goddard and Ladner[77] have
recently formulated a 'generalised' V.B. method where one orbital is still
employed per electron but the equations are converted to solution in the
HF manner.

CHAPTER II.

Theoretical Methods.

INTRODUCTION

In this chapter are discussed some practical applications of the theory outlined in the previous chapter. Firstly, some chemically interesting properties which may be obtained directly from the wavefunction are considered. This is then extended to a consideration of the more dynamic aspects of electron distribution in which some fundamental topics of great chemical importance are examined. Finally, a recent inovation in the spectroscopic field, ESCA (Electron Spectroscopy for Chemical Application) is discussed.

1) Analyis of the Wave Function

a) Eigenvalues and Eigenvectors.

For each molecular orbital, the eigenvalue and eigenvectors may be obtained directly from the self-consistent wavefunction. The eigenvalue, referred to as the orbital energy, reflects the energy of that orbital which is composed from the basis set of atomic orbitals weighted by their coefficients, the eigenvectors describing the spatial properties of the orbital. The orbital energy also represents to a good approximation the ionisation energy for this orbital for closed shell molecules. The total energy for an n electron system is from equation 1.39.

$$E = \sum_{i}^{n/2} 2H_{ii} + {}_{i}\sum_{j}(2J_{ij} - K_{ij}) \tag{1}$$

Consider ionisation from orbital k. Then the total energy is given by the equation.

$$E' = \sum_{i \neq k} 2H_{ii} + \sum_{i \neq k} \sum_{j \neq k}(2J_{ij} - K_{ij}) + J_{kk} + H_{kk} + \sum_{i \neq k}(2J_{ij} - K_{ij}) \tag{2}$$

with allowance made for the unpaired electron in orbital k. The ionisation energy is then given by

$$E - E' = H_{kk} - \sum_{i \neq k}(2J_{ik} - K_{ik}) + J_{kk} \tag{3}$$

which is of the same form as equation 1.40. This is Koopmans' theorem[10]

$$IP \sim \epsilon_i \tag{4}$$

Implicit in this is that E' is calculated from the wavefunction of the ground state i.e. there is no reorganisation of the remaining electrons upon ionisation.

b). <u>Population Analysis</u>

Since organic chemists like to be able to talk in terms of a charge distribution in a molecule (i.e. to assign a specific charge to each atom in a molecule) use is often made of a Mulliken population analysis[78]. The population q_μ of an orbital μ is defined as

$$q_\mu = P_{\mu\mu} + \sum_{\nu(\neq\mu)} P_{\mu\nu} S_{\mu\nu} \qquad (5)$$

$$P_{\mu\nu} = \sum_i^{occup} N_i C_{\mu i} C_{\nu i} \qquad (6)$$

with N_i electrons in each molecular orbital. Similarly the overlap population is defined as

$$q_{AB} = \sum_{\mu A} \sum_{\nu B} P_{\mu\nu} S_{\mu\nu} \qquad (7)$$

where now μ and ν are on atoms A and B respectively. This definition has been widely adopted and is employed in this work. There are however, a number of weaknesses[79]. Notable amongst these is the equal apportioning of electron density between two atoms in defining the charge at a centre (e.g. in a polar band) and the possibility of an atom having a negative electronic population, for a given molecular orbital, when the cross terms in equation 5 are sufficiently large and negative. Other definitions due to Lowdin[80] define the charges in terms of a set orthogonalized atomic orbitals or divide the overlap terms in a manner which preserves the calculated electronic moment of the molecular orbital. A fundamental spatial integration procedure has also been proposed by Politzer and Harris[81]. This is similar in concept to the proposal by Richards of employing a specific radius for a particular atom with integration overlap over this sphere[82]. An alternative method for measuring the bonding between two atoms in approximate MO theory is the partitioned bond overlap.[83]

$$PBO = \sum_{\mu A} \sum_{\nu B} P_{\mu\nu}^{CNDO} S_{\mu\nu} \qquad (8)$$

This is equivalent to equation 7 except in so far as no overlap is explicitly allowed in CNDO and INDO methods in defining $P_{\mu\nu}$. The density matrix corresponds however to the Lowdin basis detailed above. Though the Mulliken approximation has its deficiences used with discrimination it gives a good indication of the charge. It should be stressed though that the chemists intuitive idea of charge is in fact a measure of the potential at that atom since he is generally concerned with the tending of electrons to migrate to or from that centre. This will be discussed later (section 3).

c). Density Contours.

A fundamental and most useful method of presenting the wavefunction is by the use of density contour maps. In this approach the electronic density at a point in space $\tilde{r}$ is evaluated.

$$\rho(\tilde{r}) = \sum_i \sum_j |c_{ij} X_j|^2 \qquad (9)$$

A grid of densities is usually produced and from these contours built up by employing an interpolation procedure to generate further densities as required. The forms of these contours are not particularly basis set dependent though polarization functions are generally preferred in augmenting the basis providing a greater flexibility[84]. Of particular value in illustrating features of chemical interest are density difference maps.

$$\delta(\tilde{r}) = \rho_2(\tilde{r}) - \rho_1(\tilde{r}) \qquad (10)$$

For example, bonding features are shown when ρ_2 and ρ_1 are the molecular and juxtaposed atomic densities respectively.

d) Spins.

Within the RHF formalisation for a single occupied MO the spin density of orbital X_μ is given by

$$s = c_{i\mu}^2 + \sum_j c_{i\mu} c_{i\nu} S_{\mu\nu} \qquad (11)$$

In the UHF scheme, independent total α and β spin densities are obtained and the unpaired spin density is then:

$$S_\mu = S_\mu{}^\alpha - S_\mu{}^\beta \qquad (12)$$

The inherent problem as mentioned in the previous chapter is that now the wavefunction is no longer an eigenfunction of $\widehat{S}^2$ but contains contaminants of higher multiplicity. To obtain a pure doublet state either a projection operator can be employed or the contaminating states may be annihilated. It is usual to annihilate in this case the quartet contaminant and make the assumption that the higher states may be neglected[85].

e) Other Properties

Expectation values may be derived for the estimation of many other properties which find use mainly in spectroscopy; thus the polarisability and electric moments may be calculated. Of these only the dipole moment will be referred to in this work.

2). Theoretical Concepts.

From the considerable research activity of the past few years quite detailed analysis have been developed for the interpretation of many of the theoretical facets of organic chemistry. This has included substantial studies of substituent effects and charge distributions, thermochemical and conformational studies and the charting of potential energy surfaces. Introduced here are some of these and other concepts which have been important in this work.

a) The Role of d Functions.

There has been a great deal of confusion in the literature concerning the physical role of d functions from quantum mechanical studies. This has mainly revolved around gaussian basis set studies of phosphorus and

and sulphur compounds with a minimal basis and a set of added d

functions. The latter was usually composed by reducing the set of six

d functions $(d_{xy}, d_{xz}, d_{yz}, d_x{}^2, d_y{}^2, d_z{}^2$) to the set of 5 d ao

functions $(d_{xy}, d_{xz}, d_{yz}, d_{x^2-y^2}, d_{3z^2-r^2})$ and symmetric function $(d_{x^2+y^2+z^2})$

Addition of the set of 5 d functions to the minimal basis invariably

produced a considerable lowering in energy with large d orbital

populations. It was indicated by Clark[86] that the significance of such

an addition could be tested by consideration of addition of the symmetric

d function (henceforth referred to as $d(s)$). Studies of thiophene

and a number of organo-sulphur compounds[86] revealed that the bonding

could be described invariably without resort to inclusion of d functions.

This technique is computationally very attractive and has proved adequate

in examining their role as is shown in later chapters.

It is important to distinguish that the general features of

structure and bonding can be adequately described in for example

hydrocarbons with an sp basis.

For small ring species where bond angles are $< 109^\circ$ finer details

of the electronic structure become evident where the addition of d

functions would be expected to aid the movement of charge into the regions

between the ring atoms. An examination made of the relative energies of

a model system, bridged and classical vinyl cation, as a function of basis

is shown in Table 2.1. together with the geometry employed[87]. The

addition of 5 d type functions to the 6-31G and 6-1,1,1,1G basis sets

(formed from the 6-31G) results in a relative decrease in energy of the

bridged structure by 9.0 and 8.9 kcals mole^{-1} respectively. There is thus

only a very small augmenting effect to the sp basis and shows unambiguously

the polarising nature of these functions. Further addition of the $d(s)$

Table 2.1. Absolute Energies of Vinyl Cation and Bridged Protonated Acetylene(au.)

Structure	6-31 + P	6-31 + 5D	6-31+5D+P	6-1111+P	6-1111+5D+P	6-1111+6D+P	Gaussian Basis Set
Vinyl Cation	-77.03229	-77.044645	-77.053363	-77.052565	-77.072737	-77.072776	-76.9988
Bridge protonated	-77.009686	-77.028383	-77.045104	-77.030625	-77.064953	-77.064993	-76.9644
$E(Kcal.mole^{-1})$	14.17	10.19	5.17	13.77	4.88	4.88	21.59

(Structural diagrams: bridged structure with 183.0°, H 1.301, H 1.214 1.065; vinyl cation structure with H 121.1°, 1.253 1.068, 1.083)
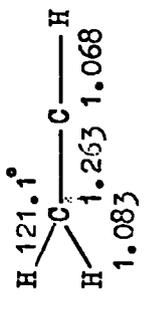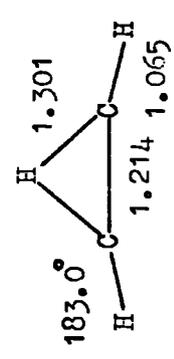
Table 2.2 Mulliken Population Analysis of some Substituted Acetylenes. σ/π

X		X	C	H	X	C	C	H	πDensity on CCH	Total Polarization in CCH
H	$\sigma\sigma$	0.816	4.183	0.816	0.063	1.937	1.937	0.063	(0)	(0)
	σ	0.803	4.197	0.803	0.103	1.897	1.897	0.103	(0)	(0)
F	$\sigma\sigma$	5.474	3.603	0.812	3.811	2.185	1.950	0.053	0.251	0.271
	σ	5.335	3.727	0.810	3.568	2.322	2.003	0.106	0.534	0.531
Cl	$\sigma\sigma$	9.080	3.931	0.816	7.827	2.147	1.962	0.062	0.234	0.236
	σ	9.028	4.004	0.809	7.787	2.116	1.975	0.125	0.319	0.319
CN	$\sigma\sigma$	9.036	3.918	0.848	4.062	2.075	1.816	0.046	0.001	0.276
	σ	9.004	3.997	0.788	4.000	2.051	1.855	0.094	0.062	0.205

Figure 2.1. Density Difference Map (d in – d out) Bridge Protonated Acetylene(– indicates loss in e density)
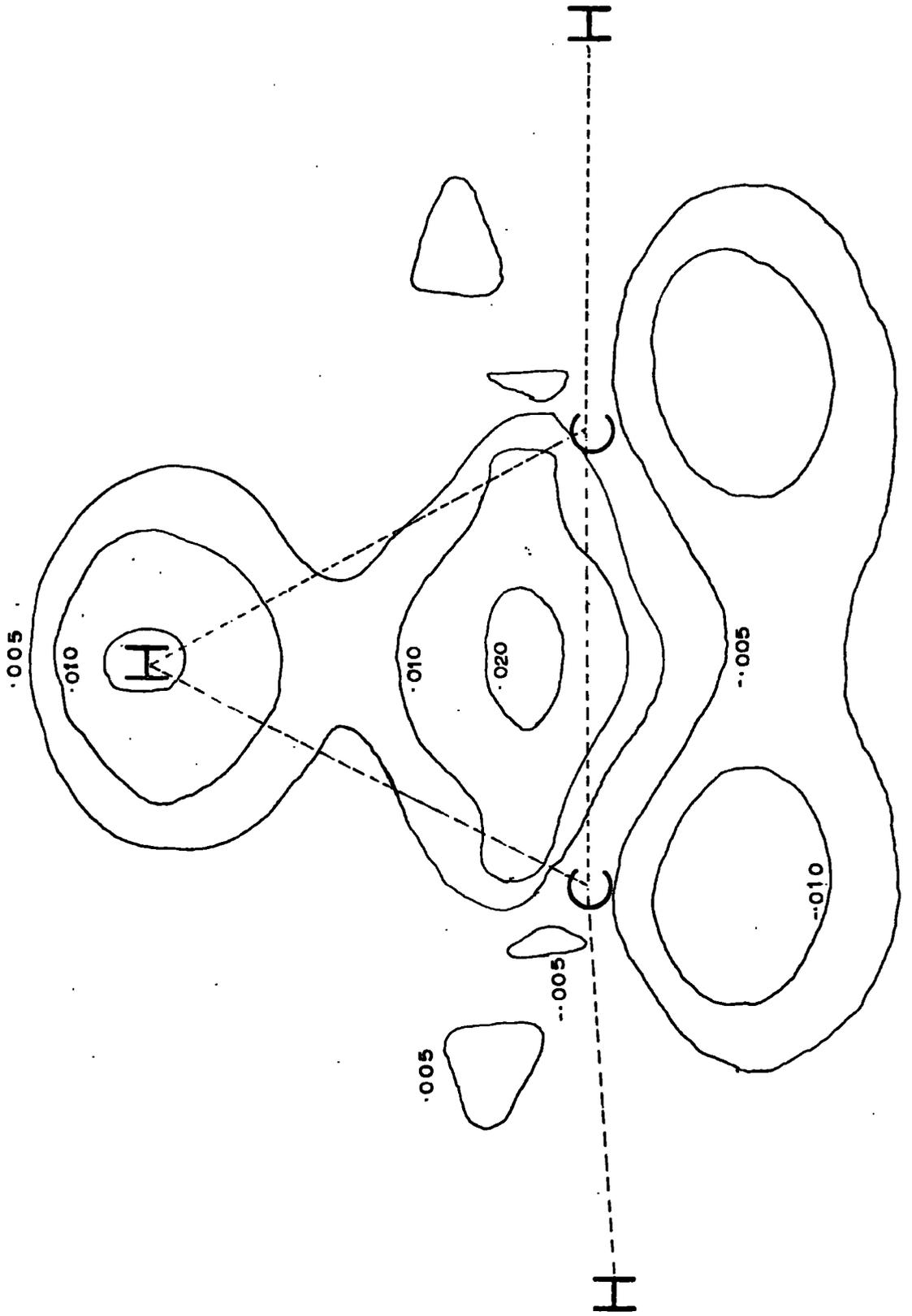
function to the basis causes no appreciable change in energies. It is also interesting to note that addition of p functions at hydrogen causes a relative lowering in energy of the bridged species of 5 kcals mole^{-1}. Thus in these geometrically constrained systems these polarization functions are of considerable importance. This movement of density is further highlighted by a density difference plot with and without the d basis (Fig.2.1.). Pople has investigated a number of ring and open systems with a similar basis with a view to studying thermochemical properties with similar conclusion[87,88]. It is important to note though that while d orbitals will cause preferential lowering in the energy of bridged species in such compounds they are of negligible importance in the bonding scheme, they merely serve to polarise the electron density defined by the sp basis.

b). Polarization.

The phenomena of electron polarization embodies a great wealth of chemical data. The base strengths of ammonia and methylamine, both in the gas phase and in solution, are known experimentally to be in the order $CH_3NH_2 > NH_3$ and from this it has been inferred that the methyl group is an electron donor. This concept pervades the whole of physical organic chemistry. Recent theoretical work has shown however that this is an artifact of interpreting solution data from arguments based on an isolated molecule. In fact the isolated molecule calculations show that the methyl group is a greater electron attractor and indicates that the CH_3 group provides a structure which may be much more effectively polarized by an adjacent cationic centre.

Polarization within a molecule has been demonstrated for a wide variety of unsaturated species. The π electron distribution in for

example fluorobenzene shows an alternation in the π electron distribution[85].

Total π   Inductive Polarization.
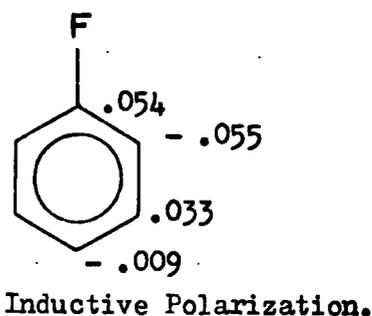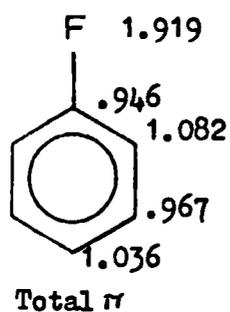
This alternating polarization of π charge in the ring parallels the expected mesomeric resonance conformers
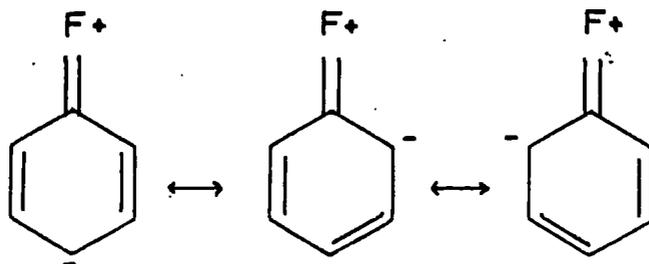
Though this is conceptionally a convenient approach it considerably overestimates the importance of such tautomers. For example, whilst the π donation from fluorine is ~0.08e the total polarization of the benzene ring is 0.320e; only 25% is actually caused by the donation of π charge, the inductive effect of the F on the ring being as shown above. A more striking result is obtained from a similar calculation on toluene[90].

Me   Me
.965   .035
1.027   - .024
.988   .012
1.014   - .011
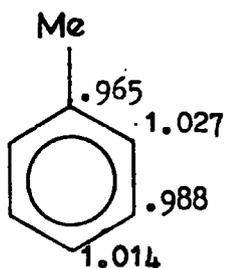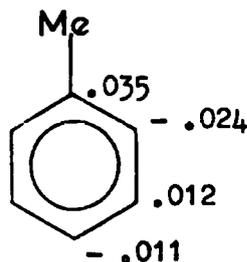
Total.π   Inductive Polarization.

The π charge on the ring is now 0.009e whilst the polarization
in the ring is 0.118e. Thus for tautomeric representations of the
electronic structure internal polarizations within the ring are of
more importance.

c)   σ/π Separability

Although in a planar unsaturated molecule the σ and π systems
are orthogonal by symmetry, mutual polarization of the charge clouds
will arise since the off-diagonal elements of the Fock matrix depend
upon the detailed desciption of the overall electron distribution.
It is a gross approximation therefore to treat the σ and π systems
separately as is implicit in the Huckel formalism for example[91].
The interaction between the σ and π systems is most readily
appreciated by considering a simple example such as ethylene. In
this particular case the total σ and π valence electron density has
been mapped in a plane through the carbon and at right angles to the
molecular plane. The results are shown in Fig.2.2. As can be seen
there is spatial overlap and hence considerable interaction between the

Figure 2.2. Total σ (....) and π (——) Density in plane through C – C Ir to molecular plane(contours 0.02,0.04,0.07e)
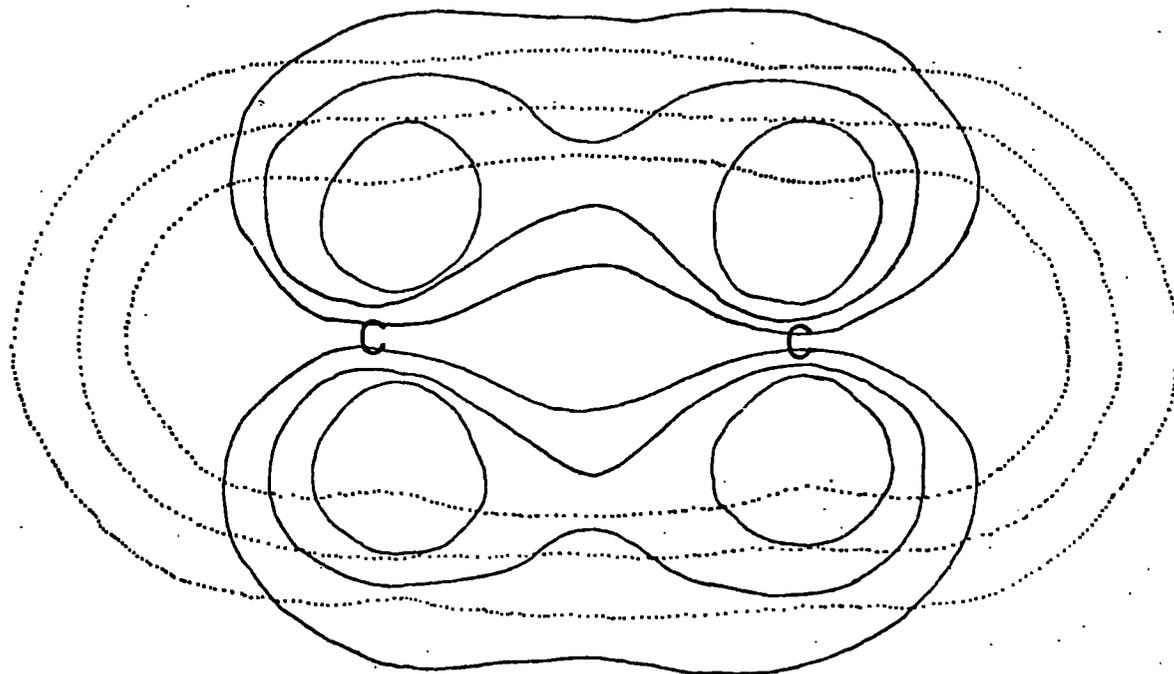
Figure 2.3. Orbital Interaction Diagram of p Orbital at Trigonal Carbon with pseudo π Orbital of Methyl Group.
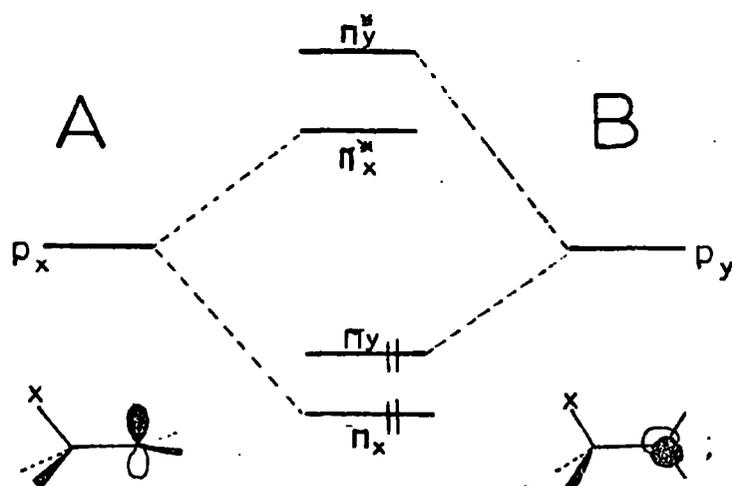
σ and π electrons. At large distances from the molecular plane however the π density is seen to be predominant. Initial interaction of the C — C electrons with bridging or attacking species may thus still be rationalised to a good first approximation by consideration of electrons alone.

Within molecules the σ/π separability concept is still extremely useful. To illustrate this, table 2.2. shows some results from single and double zeta Slater basis set calculations with polarization functions added, of some substitued acetylenes. The calculations were performed using the ALCHEMY program with standard geometries[92] or those minimised by Yoshimine and Maclean[93]. Exponents for the single and double zeta calculations are shown in the appendix.

Considering firstly the double zeta data from the first three acetylenes the effect of F and Cl replacement of H is seen to result in σ electron drift towards the halogen. Consistent with this is a drift of π electrons in the opposite direction. From the π population in Table 2.2. considerable π donation from F and Cl is seen which accounts for the majority of the change in the atomic π populations. Inductive polarization in the π fragment is small; thus though σ/π separation is not strictly valid a consideration along these lines serves to rationalise the problem. The electron distribution in the cyanide analog is markedly different. There is now no net drift of π electron density to the CCH fragment but a π electron polarization amounting to some .276e. The π electron polarization in the CN fragment towards C^+-N^- will be mainly responsible for this.

With the single zeta basis the qualitative agreement with the above is good but quantitatively the values are probably exaggerated.

For cyanoacetylene, though some π donation is now indicated the polarization is of comparable importance. It should be appreciated that replacement of H by either F or Cl in acetylene will also result in differences in the size of the π cloud around each carbon atom. Indeed calculation of $<1/r>$ for the π orbitals of the C-X carbon (X = F 0.981, X = Cl 1.208 au) and C-H carbon (X = F 0.802, X = Cl 0.946 au) in XCCH indicate the considerable orbital contraction at the site of substitution in accord with simple inductive considerations.

d). Hyperconjugation : Orbital Interaction.

The lone pair or 'localised' bond description is preferred by the chemist in discussing electronic structure. Interactions between these orbitals can occur to varying degrees through space or through bonds as has been collectively illustrated by Hoffmann[94]. A further type of interaction, which is of most importance in charged species is hyperconjugation[95].

An orbital scheme which includes this can be used to rationlise the conformations observed in substituted ethyl cations and anions ($XCH_2 - CH_2 \pm$) and is shown schematically in Figure 2.3. In the cation the unoccupied π orbital of the trigonal CH_2 group (p_x or p_y) will interact with either of the pseudo π orbitals of the CH_2X group depending on the conformer. The degenerate π_x, π_y orbitals of CH_2X when X = H will be split with π_x and π_x^* to lower energy if X is more electronegative than H. In the case of X = F interaction B is from first order perturbation considerations greater ($\propto 1/\Delta E$) and the

eclipsed conformer is predicted to be more stable in accord with a wealth of available data. Similar arguments may be applied for the anion. With the mixing of orbitals charge redistribution between the two interacting localised orbitals is implied. Further discussion is deferred until Chapter 6 however, where several rotational barriers have been computed for a number of substituted ethyl radicals in addition to the ions.

Hyperconjugation as discussed above is quite specific. The 'classical' representation by structures:

$$CH_2F - CH_2+ \qquad H+ \ FCH = CH_2 \qquad F+ \ CH_2 = CH_2$$

on the other hand is intuitively quite simple but less specific. In neutral molecules the hyperconjugation interaction will be much weaker. From a study by Pople of some methyl substituted toluenes[90] there is little conjugation as measured by the total π density in the ring, polarization of the ring π system being far greater as discussed above (Table 2.3.).

e) <u>Point Charge Model.</u>

The detailed theoretical study of the energetics and stereochemistry of organic reactions is usually accomplished either by eliminating certain degrees of freedom which can reasonably be assumed to remain constant throughout the course of the reaction or by investigating certain defined regions of the PE surface with a fuller optimisation of geometry. For systems involving abnormally long bond lengths however, electron correlation is of considerable importance and thus bond breaking cannot be handled within the Hartree-Fock formalisation. Such a situation is the approach of an electrophile.

Table 2.3.

Relative Hyperconjugated and Inductive Polarization in some Substituted Toluenes ($C_6H_5CH_2X$) in their most stable conformers.

X =	H	CH_3	NH_2	OH	F
Ring electronic Charge density.	6.008	6.007	6.009	6.007	6.004
Total polarization	0.088	0.037	0.079	0.039	0.052

Values taken from ref. 90.

Table 2.4.

Core Binding Energies of Protonated Acetylene(employing 6-31G basis).

Hole Centre	Koopmans'(eV)	Hole State(eV)	Relaxtion Energy(eV)
	316.40	304.65	11.75
	313.92	301.69	12.23
	315.38	303.20	12.18
*CH_4	304.49	292.23	12.26
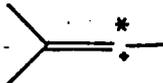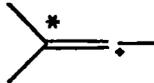
Relaxtion Energy = Koopmans' − Hole State.

For the simplest electrophile (H+) an attractive alternative is to accept that at long range a unit charge may be taken to represent H+. Then the potential of this charge at points in space (r_i) is calculated by evaluation of

$$V(r_i) = -\int \frac{\rho(1)}{r_{1i}} + \sum_{\alpha} \frac{Z_{\alpha}}{r_{\alpha i}} \qquad (13)$$

and plotting energy contours from which the potential energy surface may be deduced. This method due to Scrocco[97] has received some success in investigations of three membered ring heterocycles. No relaxtion of the molecular wavefunction is allowed however. This may be taken into account by performing a new SCF calculation after recomputation of the one electron integrals in the field of both the nuclear charges of the substrate and the point charge[98]. The necessary calculations are computationally inexpensive and trial molecular orbitals from the ground state calculation may be employed as a good initial set of coefficients. The validity of this method is restricted to the initial long range interactions and has been employed in Chapter V to investigate a number of properties of the pyridine molecule.

3)   Electron Spectroscopy for Chemical Application (ESCA)

The technique of Electron Spectroscopy is a relatively new tool for the study of chemical systems.   This can be classified into low energy (UPS) photoelectron stuies[9] when the valence levels are studied and high energy (ESCA) studies of the core (inner) electrons[8].   An incident beam of X-rays with energy $h\nu$ impinges on the sample to be studied and an electron is ejected with energy E_{KIN} according to the equation

$$BE = h\nu - E_{KIN} - E_R \qquad\qquad (14)$$

where BE is the binding energy and E_R the recoil energy of the sample which is negligible except for the light elements.   In UPS studies the incident beam is usually provided by a He discharge ($\sim 21.7eV$) Either Mg $K\alpha_{1,2}$ (1253.7) or Al $K\alpha_{1,2}$ (1486.6) photons can be used as the X-ray source in ESCA.   The emitted photoelectron has an energy related to the orbital from which it is derived.   For ESCA studies this allows qualitative elemental analysis and by consideration of intensities quantitive data may be obtained.

The major advantages of the techniques are that they are non-destructive and require relatively small amounts of sample (nominally 1mgm solid, .5cc gas STP).   For ESCA studies solids, liquids and gasses may be analysed but for UPS the sample is normally handled in the gas phase though it may be studied as a condensed film.   The techniques have high sensitivity (fraction of a monolayer) and can be applied in principle to the study of virtually all elements.   The main relevance to this work is that the theory is directly related to the electronic structure of a molecule, and can be adequately handled within the body of theory so far presented.

a).Practical Details.

This section will be mainly confined to the ESCA techniques for which some experimental studies have been performed. For core ionisation the resultant species with one electronless is defined as being in the hole state $(A^+)^*$. Electronic relaxtion of the remaining electrons to this state may occur by two processes.

1) X-ray emission where the primary vacancy is filled[8]

$$(A^+)^* \longrightarrow A^+ + h\nu$$

2) Auger Process[99]

$$(A^+)^* \longrightarrow A^{++} + e$$

Here the primary vacancy (in for example the K shell) is filled by an electron (e.g.L) concurrent with emission of another (e.g.M) electron. This is a KLM Auger Process. Among the manifold of processes which may result from the primary perturbation is that the valence electrons may be excited (shake up) or emitted (shake off)[100,101]. The energy for this will be taken up as loss in the K.E. of the core photoelectron to give a satellite of the parent peak. Whereas in ESCA the inherent line width of the high energy sources of radiation together with the short lifetime of the highly excited hole state combine to give rather broad spectra the low energy U.V. spectra with the much longer lifetime of the hole states can give detail concerning the vibrational fine structure. In practice the binding energy for metals are measured with reference to the Fermi level[8] defined as

$$\int_0^{E_f} N(E) \, dE = N \quad \text{where} \quad N(E) = Z(E)F(E)$$

where F(E) is the probability of a Fermi particle being in state E

with a density of states Z(E) . For an insulator the definition of

the Fermi level is less clear cut. If the mobility of the electrons

in the core hole species of the material however are the same as the

bulk then the Fermi level will be located mid-way between the valence

and conduction bond. However in ESCA if a sufficiently large number

of charge carriers are available then the sample will be in electric

contact with the spectrometer (viz: they both have the same Fermi

level). The binding energy is then given from Fig.2.4. by

$$BE = h\gamma - \phi_{sp} - KE \qquad (15)$$

and obviates any knowledge of the sample work function. Sample

charging at the surface though may occur however and can be of the

order of 1-2eV but since all photoelectrons will be so effected an

internal reference can usually be taken for this. For gaseous samples

the binding energies as measured differ from solid phase measurements

due to the charge in reference level and then

$$BE = h\nu - KE \qquad (16)$$

b). Theoretical Interpretation.

Though absolute determination of binding energies and their

correlation with theoretical models is useful for both core and valence

ionisation it is more often shifts in energies which are of most

interest for the core levels. Certain approximations which are valid

for core level shifts do not apply in absolute determination of valence

level ionisations.

Figure 2.4

BINDING ENERGY REFERENCE LEVEL in SOLIDS

$$BE = h\nu - \emptyset_{sp} - KE \quad (\emptyset \text{ is the work function})$$
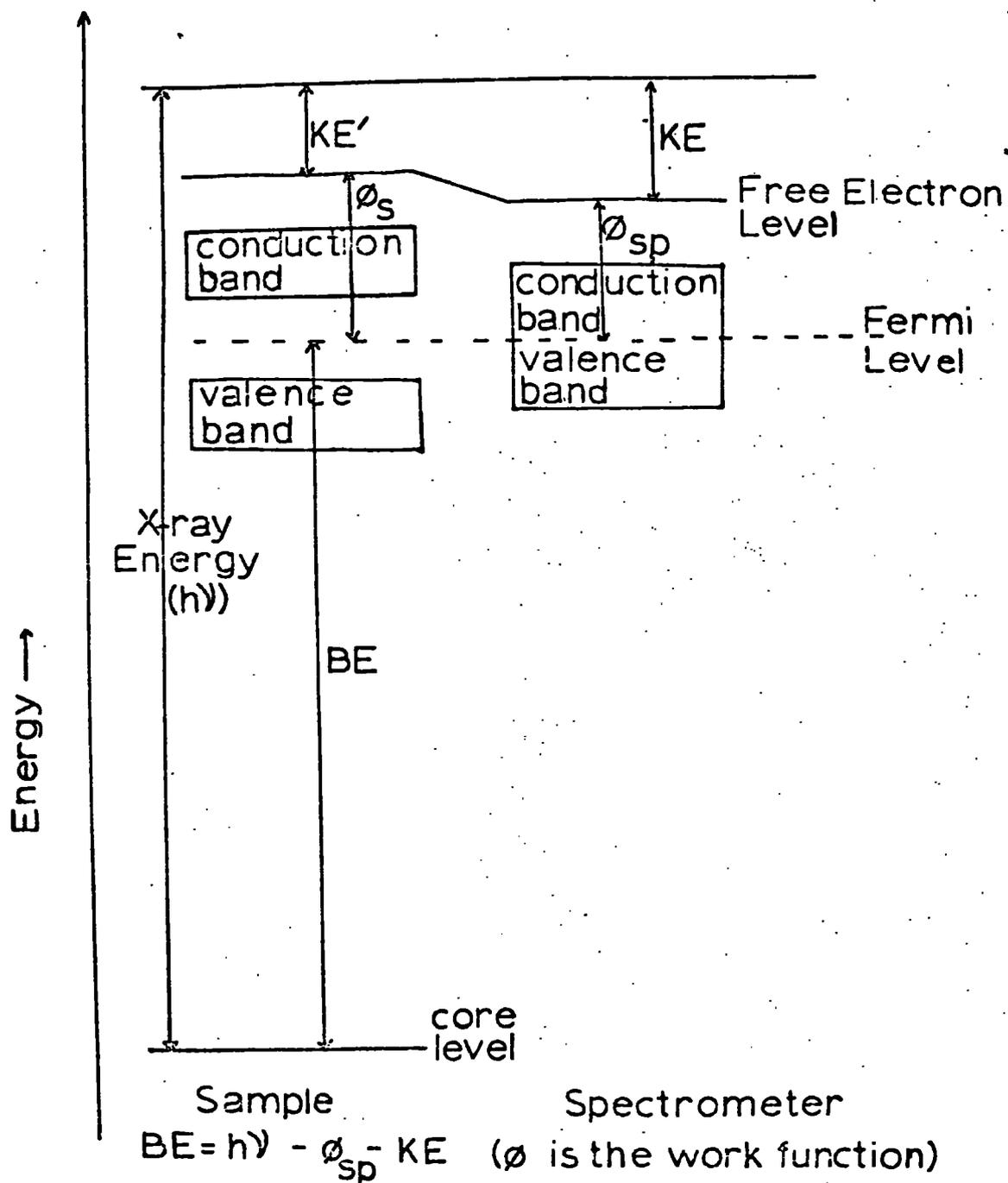
There are two fundamental means of determining the ionisation
potential. Firstly, application of Koopmans ' theorem gives from the
ground state wavefunction estimates of IP in the absence of any
electronic reorganisation. The latter may be taken into account
however by the computationally more espensive determination of the
difference in energies between the hole state ion and the ground
state [102]. Their relationship to the observed gas phase value and
the correctionsinvolved are shown in Fig.2.5. The hole state
calculation will give a good absolute value if

$$\Delta E_{corr} \simeq 0 \quad \text{and} \quad \Delta E_{rel} \simeq 0 \qquad (17)$$

and Koopmans' value (ϵ) will apply with the additional proviso that

$$\Delta E_{relax} \simeq 0 \qquad (18)$$

For shifts in core levels, Clark and Barber[103] and for the valence
levels, Richards[104], have indicated that only the differences in these
ΔE values need be considered and these are generally approximately
zero. For the valence levels due to the considerable variety in the
form of these orbitals, changes in the correlation and relaxation energies
can however drastically alter assignments based on Koopmans' theorem.
For the core levels evidence to date suggest shifts in core binding
energies are due to factors other than these. In charged species
relaxation energies are expected to vary considerably. This is indicated
by studies on the ground and hole state of the classical and bridged
protonated acetylene (Table.2.4.). Though an extreme case these
differences in energies are certainly not negligible. Schwartz[105]
from studies of first row hydrides obtained very good agreement with the

Figure 2.5

Relationship between Experimental and Theoretically Calculated Binding Energies.
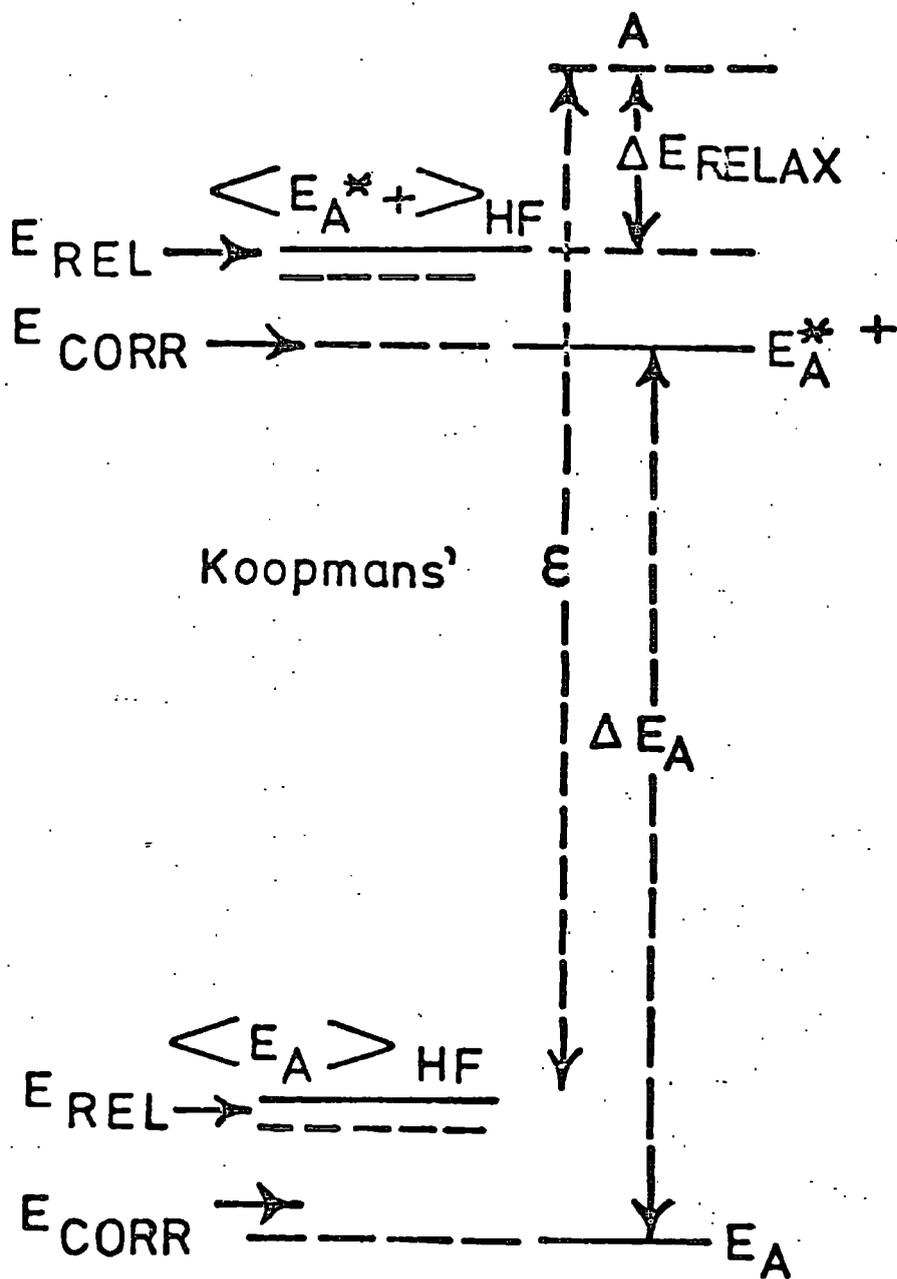
✱ INDICATES CORE HOLE

experimental values and seems to confirm Bagus' original contention[102] that the single determinant SCF wavefunction can provide practical, but not rigorous, upper bounds to the energies of the inner hole states. In general hole states calculations give IP's which are accurate to within a few tenths of eV of the gas phase measurement.

It is pertinent to mention other approaches to the problem here. Jolly and Hendrickson[106] developed an equivalent core method which states that

'When a core electron is removed from an atom in a molecule or ion, the valence electrons relax as if the nuclear charge on the atom had increased by one unit'.

As an example consider the following

$$CH_4 \longrightarrow {}^*CH_4^+ + e^- \qquad \Delta E = BE_{CH_4}$$

$${}^*CH_4^+ + N^{5+} \longrightarrow NH_4^+ + {}^*C^{5+} \qquad \Delta E = \delta_o$$

with $\delta_o \sim 0$

Summing :

$$CH_4 + N^{5+} \longrightarrow NH_4^+ + {}^*C^{5+} + e^- \qquad \Delta E = BE_{CH_4} + \delta_o$$

Similarly for CF_4

$$CF_4 + N^{5+} \longrightarrow NF_4^+ + {}^*C^{5+} + e^- \qquad \Delta E = BE_{CF_4} + \delta_1$$

Then:

$$CF_4 + NH_4^+ \longrightarrow NF_4^+ + CH_4 \qquad \Delta E = BE_{CF_4} - BE_{CH_4} + (\delta_1 - \delta_o)$$
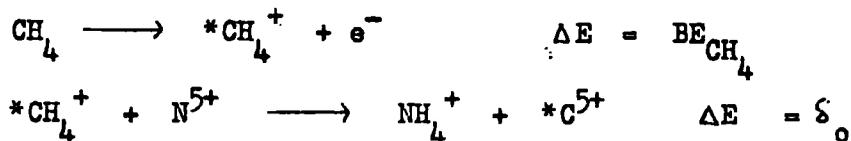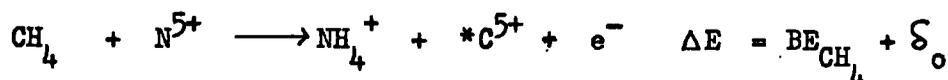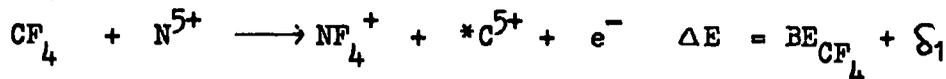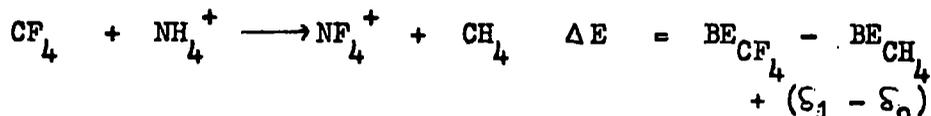
Energy data either calculated or thermodynamic is thus capable of giving shifts in core ionisation energies and has proved valuable in calculating shifts from isodesmic reactions (i.e. where the number and types of bonds or lone pairs remains constant in reactants and products: correlation changes will be minimised). These isodesmic heats of

reaction include the electronic relaxtion. Further with the consistency of bonding type in reactants and products calculated energies may augment the thermodynamic data with little loss in accuracy as has been illustrated by Clark and Adams[107]. A recently proposed alternative to hole state calculations directly calculates the ionisation energy by a perturbation treatment producing a 'transition Fock operator' over a MO basis[108]. The authors indicate that the value of this method lies in calculations of large molecules where convergence procedures may be difficult with the standard variation procedure.

At a lower level of rigor and sophistication the charge potential model[100] is extensively used in conjunction with empirical charge data according to the equation

$$BE = BE_o + kq_i + \sum_{j \neq i} q_i / r_{ij}$$ (19)

where BE_o is a reference level

q_i charge on atom i

r_{ij} is internuclear distance i,j.

k constant (approximating the average one centre core/valence integral) The formula may be derived from Koopmans' theorem and hence suffers from the same deficiencies. However as has been shown recently the relaxation energies neglected in Koopmans' theorem tend to follow a similar relationship[110], thus by treating k and BE_o as parameters this deficiency may be overcome.

c). Deficiencies of the Models.

A detailed study of the ionised states of the CH_4 molecule by Clementi and Popkie[111] with a basis set approaching the Hartree-Fock limit showed there was no change in correlation energy for the core hole state and neutral species. This is complemented by the more detailed work of Meyer[112] who analysed the correlation energy changes for the three ionisations of CH_4. He again reached the same conclusion for the core hole state but showed considerable differences in correlation energies for the $2a_1$ and $1f_2$ ionizations. This is a general feature that whereas correlation corrections for core hole states are small or negligible, corrections for valence states may be of the order of 1-2eV.

Estimates of the changes in correlation may be obtained by the use of equations 1.110 and 1.111. With no change in the geometry upon ionisation $\Delta E_{inter}(\Delta E_{AB})$ is anticipated to be as an initial approximation small. Application to the protonated acetylene system shows no appreciable change in correlation upon ionisation. Detailed analysis shows that while the 1s - 1s correlation energy is lost, contraction of the valence electronic cloud at this centre, with an increased population balances this change in qualitative agreement with the more extensive work of Meyer. That electronic relaxation arises solely from valence electrons may readily be demonstrated by calculation of the expectation value of the orbital radii for the Ne atom and 1s core hole states[113]. The 1s 0.1576(0.1545), 2s 0.8921(0.8171) and 2p .9652(.7993) radii indicate little charge in the core orbital but significant charge in the valence region, the values in parentheses referring to the hole state. For valence ionisation the changes are less.

It finally remains to indicate an interesting new feature of ESCA concerning the shape of the spectra. In UPS studies the lifetime of the hole state is quite long and greater than the nuclear vibration time ($\sim 10^{-13}$ sec.) but much shorter than the photoelectron process ($\sim 10^{-16}$ sec.) giving rise to vibrational fine structure. For ESCA the resolution is much lower so no fine structure is to be expected both on instrumentation grounds and also as a result of the Heisenberg Uncertainty principle[114].

$$\Delta E \Delta T \geq \hbar \qquad (20)$$

Of some interest then is the observation by Sieghahn and co-workers (employing a high resolution spectrometer based on a fine focus X-ray monochromatization scheme), that the C_{1s} spectra of CH_4 (in the gas phase) exhibits a marked degree of asymmetry[111]. With a large extended basis set calculations were performed on the ground state, the core hole state and the equivalent core species of CH_4 and are shown in Figure 2.6. The equivalent cores calculation was performed with the same orbital exponents as the neutral molecule for computational efficiency.

There are several points of interest. Firstly, the above approximation is seen to be small in so far as the shape of the curve is concerned. Both results give a shorter C-H bond length of $\sim$ 0.06A. In the sudden approximation of no nuclear relaxation a transition will thus occur to one of the vibrationally excited states of the ion. Indeed the observed spectral envelope is in qualitative agreement with that estimated from a separation of $\sim$3000cm^{-1} (0.38eV) of the vibrational levels; the most probable transition will not be $v_0' \leftarrow v_0''$

Figure 2.6

Variation in Total Energy with Internuclear Distances in CH_4, its Core Hole and Equivalent Core States
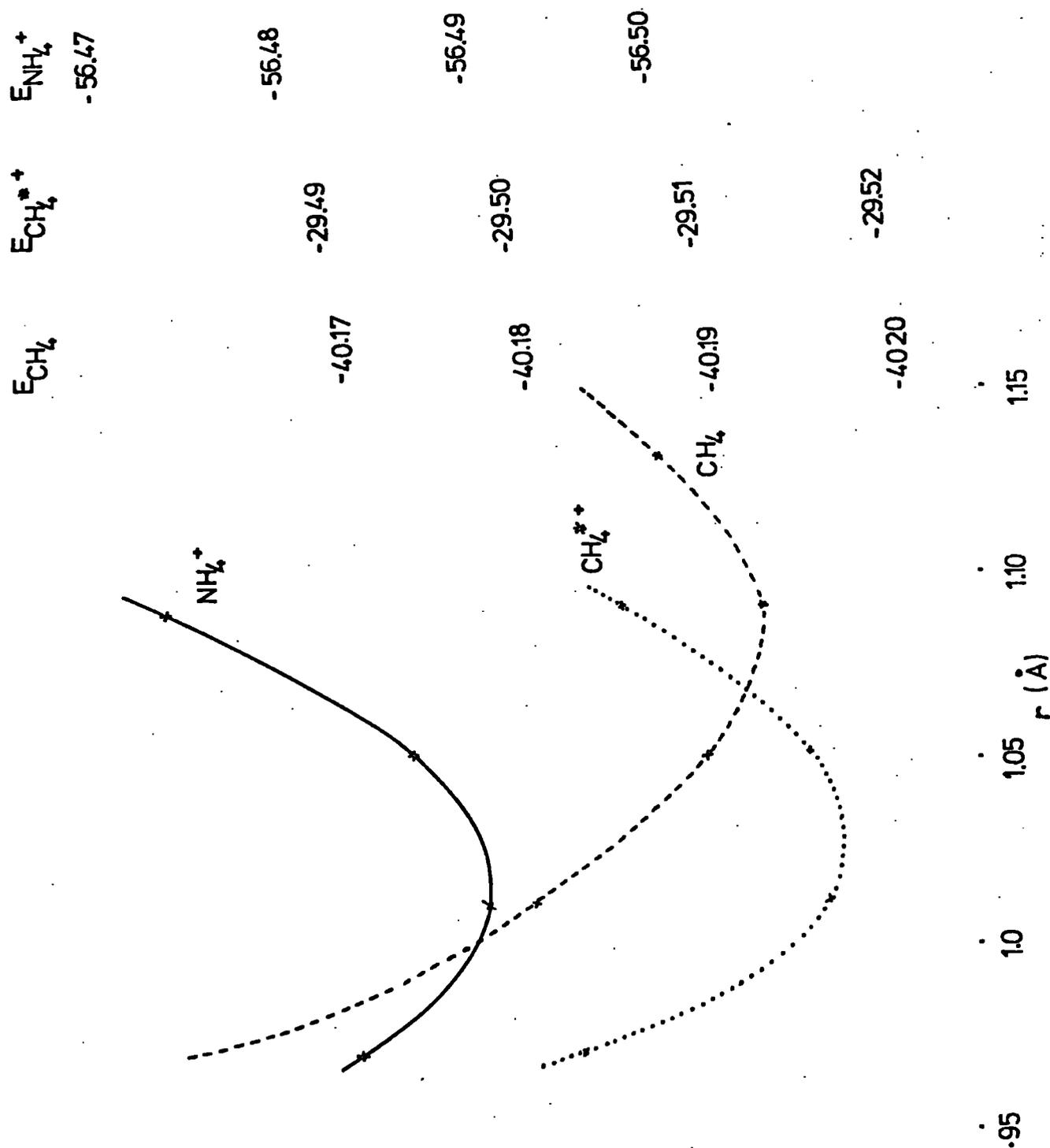
The important ramification of these remarks is that with high resolution spectrometers the line width can give further details concerning the bonding environments of particular centres (see. Chapter 5). Though assignments of experimental binding energies through the intensity maxima will be somewhat arbitrary (since this may correspond to the transition to a vibrationally excited state in the hole state) the anticipated errors should be generally of the order of 0.1 - 0.2 eV. Of more importance is that at higher resolution the approximation of a standard type gaussian for a particular core ionization (in deconvoluting a complex spectra) will no longer apply, though with the present commercially available ESCA spectrometers this criteria will only apply in extreme cases.

CHAPTER III.

Studies of some Three-Membered-Rings.

Introduction.

The interaction of a carbon-carbon double bond with an atom or group of atoms can result in the extreme in either of the structures of type I or II. These may vary from the simplest of cases where $X = H^+$, a straightforward
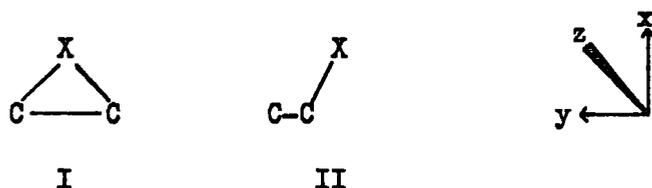
protonation, to an inorganic complex with X a transition metal with associated ligands. There are a number of basic points of interest common to all however which are itemised below:

(i) The relative energies of I and II.

(ii) The electronic structure of the small strained ring of I.

(iii) How substituents at C and/or X alter the chemistry of I and II.

In particular I can correspond to one of four positions on a potential energy manifold depending on the nature of X.

(i) A stable local minimum.

(ii) Unstable w.r.t. unimolecular decomposition via a metastable minima.

(iii) Reactive intermediate unstable w.r.t. external influences via bimolecular decomposition.

(iv) Energy maxima corresponding to a T/S.

The field of study is restricted in this chapter to the case where the C-C fragment is the acetylene unit. Not only then will there be an interaction in the plane of the ring of X with pxπ orbitals of acetylene but also a secondary interaction involving the pzπ orbitals of both X and the acetylene molecule, which can have a considerable influence on

the stability of I.

The basis sets used for the calculations were those of Dunning[36] and Siegbahn[37] (see appendix). For second row atoms this was augmented by the addition of d type functions with exponents as detailed below. The IBMOL V program[52] was employed for the majority of calculations supplemented by later work with the faster and more efficient ATMOL group of programs[53].

1). $X = H^+$, Protonated Acetylene.

As a first step a detailed study was made of structures I and II with $X = H^+$. With the addition of d type polarization functions to the sp basis on carbon the relative energy difference as detailed with the large basis in the preceding · chapter was reduced by approximately 9 kcal mole^{-1} in favour of I. Computational expense however does not generally allow calculations with such an extended basis at carbon. To a good approximation however this neglect will generally result in a similar underestimation of the stability of I with respect to II for a non-extended basis at carbon. With the specified basis in this chapter a difference in energy of 21.6 kcal.mole^{-1} was found for I and II compared with the lower estimate of ~5 kcal.mole^{-1} from chapter 2. It is thus anticipated that this basis will underestimate the ring stability by ~15 kcal.mole^{-1}.

Formation of the (bridged) protonated acetylene(also referred to as symmetrically bridged vinyl cation) involves bending of the C-H bonds which will split the degenerate π levels. With adjustment to the geometry in I the π orbital energy of 10.96 eV is lowered to 10.33 eV and 10.14 eV for the π_x and π_z orbitals respectively. The π_x orbital can then interact with the vacant s orbital of the proton with a subsequent lowering in energy. Thus substituents which can lower the π_x
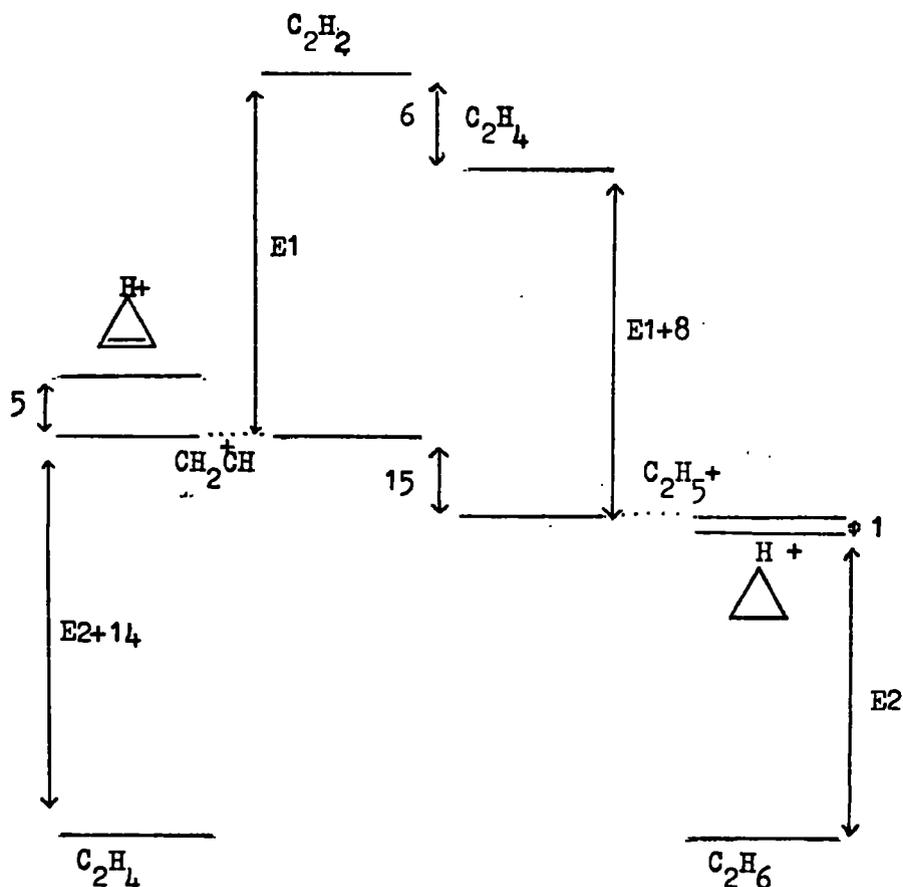
Figure 3.1. Relative energies for the C_2H_2/H^+ and C_2H_4/H^+ systems in kcal.mole^{-1} (not to scale).

orbital energy (π acceptors) will preferentially stabilise a protonated form.

Though explicit consideration will not be given to the corresponding olefin-X interactions it is pertinent to indicate here the relationship between the two. A wealth of evidence is now available which suggests that the classical and bridged ethyl cations are closely similar in energy.[87] This contrasting behaviour can be explained by either a preferential stabilising influence in the bridged protonated ethylene or in the classical vinyl cation. Considering the bridged ion the orbital of ethylene is acknowledged to be to higher energy than that in acetylene; the interaction with the vacant s orbital will be somewhat

reduced. The strain energy of the unsaturated ring will however counteract this. Estimates of the relative thermodynamic stability of the classical cations as related to hydride ion addition place the vinyl cation 14-15 kcal.mole^{-1} above the ethyl cation.[82,116] Further for the reaction:

$$CH_3\text{-}\overset{+}{C}H_2 + HC\equiv CH \longrightarrow CH_2\text{=}CH_2 + CH_2\text{=}\overset{+}{C}H$$
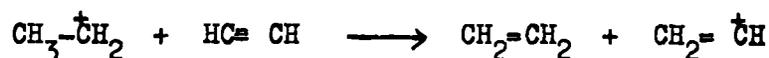
endothermic as written, the energy difference is determined from thermochemical data to be 6 kcal.mole^{-1}.[117,118] This gives relative energies between the two systems as shown schematically in Figure 3.1. Thus while acetylene is seen to be slightly less reactive to gas phase protonation the preference for a stable bridged structure is reduced. Comparative data for $X = CH_3^+$, CH_2 also substantiates these arguments.[116]

2). First and Second Row Bridging Atoms($X = O$, F^+, S, Cl^+).

With the gaussian basis (see Appendix) augmented by d type functions for sulphur ($\gamma = .25$) and chlorine ($\gamma = .8$) calculations were performed on the above four structures of type I. Geometric optimisation of the ring was only performed for $X = S$ as a check of that employed in later calculations. Energies were calculated for five points on this potential surface and fitted to the equation

$$E = E_0 + k_{C=C} (X_{cc}-C_{cc})^2 + k_{C-S} (X_{cs}-C_{cs})^2$$

where k and X are the force constant and equilibrium bond length respectively. This generated a geometry with C–C and C–S bond lengths of 1.290Å and 1.803Å respectively. The force constant for C–C was greater by a factor of $\sim$ X3 indicating the weakness of the C–S bond in the ring.

Estimates of the geometries for oxiirene and bridged fluoro- and

chloro-vinyl cations were obtained by comparison with corresponding optimised[119,120] and experimental[92] geometries from studies of bridged ethylenes. The final geometries are shown in Table 3.1.

The atomic charges from a Mulliken population analysis for the four bridged species together with those for the bridged vinyl cation are shown in Table 3.2. Considering firstly the ion, similar charges with $X = H^+$, F^+, Cl^+ of .53e are found on the vinylic hydrogens which account for the formal positive charge. The carbon-bridging atom bond is considerably polarized; for $X = H^+$, Cl^+ a positive charge of .33e on the bridging atom and for $X = F$ a negative charge of -.26e in accord with electronegativity considerations. Similar comparisons can be made for oxiirene and thiirene where now formal charges of -.55e and -.51e reside on the heteroatom. Though the magnitude of the charge separation is likely to be overestimated (as has already been commented upon) the trends are likely to be correctly reproduced. The population of the heteroatom shows an occupancy of ~2e. From the form of the molecular orbitals shown schematically in Figure 3.2. the highest π orbital is antibonding w.r.t. the C-X systems. This is a feature common to anti-aromatic systems to which formally all these systems (except $X=H^+$) belong, vis 4π valence electron in a 3 membered ring. A further prediction which might be made from a simple Huckel M.O. picture of bonding in the species would be a low 1st I.P. (since for the normal Huckel parameters the HOMO turns out to be approximately non-bonding[121]). Hence for oxiirene (8.93eV) and thiirene (7.7oeV) these first ionisation potentials as estimated from Koopmans' theorem are unusually low. These destabilising influences and the variations in the series can be interpreted by consideration of the valence pz orbital energies of X.

Table 3.1.

Geometries for ▷—X

X	C-C	CC-1rX	OCCH
H^+	1.214	1.15	177°
O	1.240	1.288	147.7°
F^+	1.240	1.260	177°
S^*	1.320(1.290)	1.664(1.660)	156°
Cl^+	1.240	1.680	177°

* Values in parenthesis refer to minimised geometry.

Table 3.2.

Orbital Energies and Populations in ▷—X

X=		H^+	O	F^+	S	Cl^+
		20.6($B\pi$)	8.9($B\pi$)	19.5($B\pi$)	7.7($B\pi$)	18.3($B\pi$)
		23.9($A\sigma$)	13.5($A\sigma$)	26.2($A\sigma$)	11.8($B\sigma$)	21.2($B\sigma$)
Orbital Energies. (eV)		27.5($A\sigma$)	14.7($B\sigma$)	26.4($B\sigma$)	13.0($A\sigma$)	22.9($A\sigma$)
		29.4($B\sigma$)	16.4($B\pi$)	28.7($A\sigma$)	13.6($B\pi$)	23.2($B\pi$)
		40.0($A\sigma$)	19.4($A\sigma$)	29.4($B\pi$)	19.1($A\sigma$)	27.5($A\sigma$)
Total	X	0.330	− 0.548	− 0.260	− 0.510	0.330
Charges	C	− 0.200	− 0.048	0.100	− 0.060	− 0.190
	H	0.540	0.321	0.531	0.320	0.530
Relative σ Overlap C-C		0.676	0.125	0.320	0.195	(0)
Total Energies(au)		−151.3476	−175.5636	−474.0960	−535.7049
Atom Energies		− 74.5774	− 98.5229	−397.3167	−458.8266

Figure 3.2. Highest 4 Occupied Orbitals in Thiirene.

SA(1)

SS(2)

AS(3)

SA(Highest)
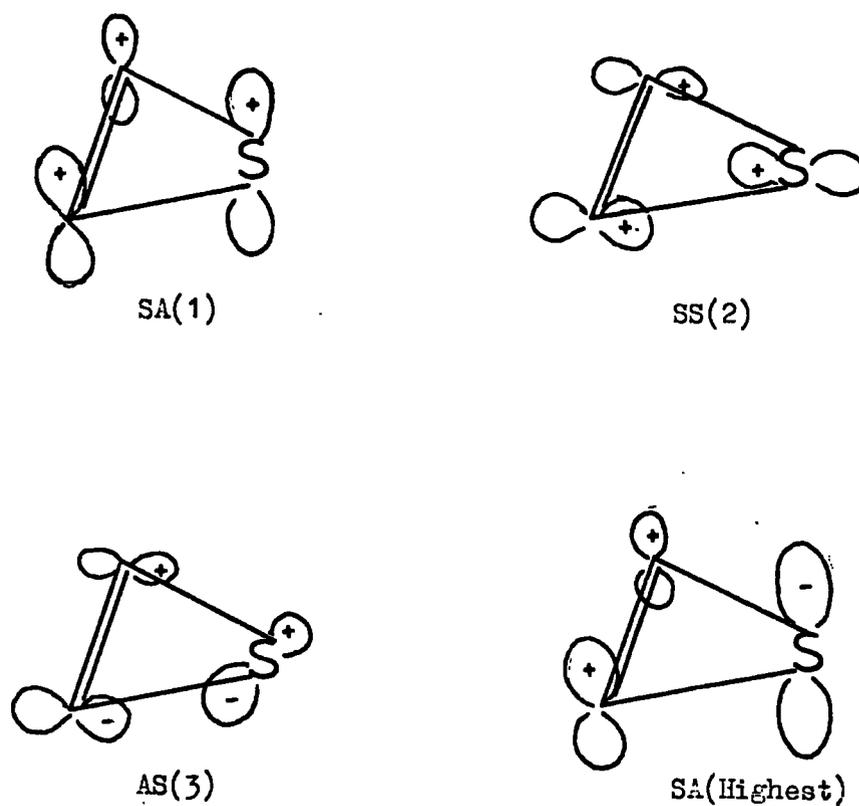
Figure 3.3. Orbital Interaction Diagram for X + C=C

p_y

p_x

C≡C

X
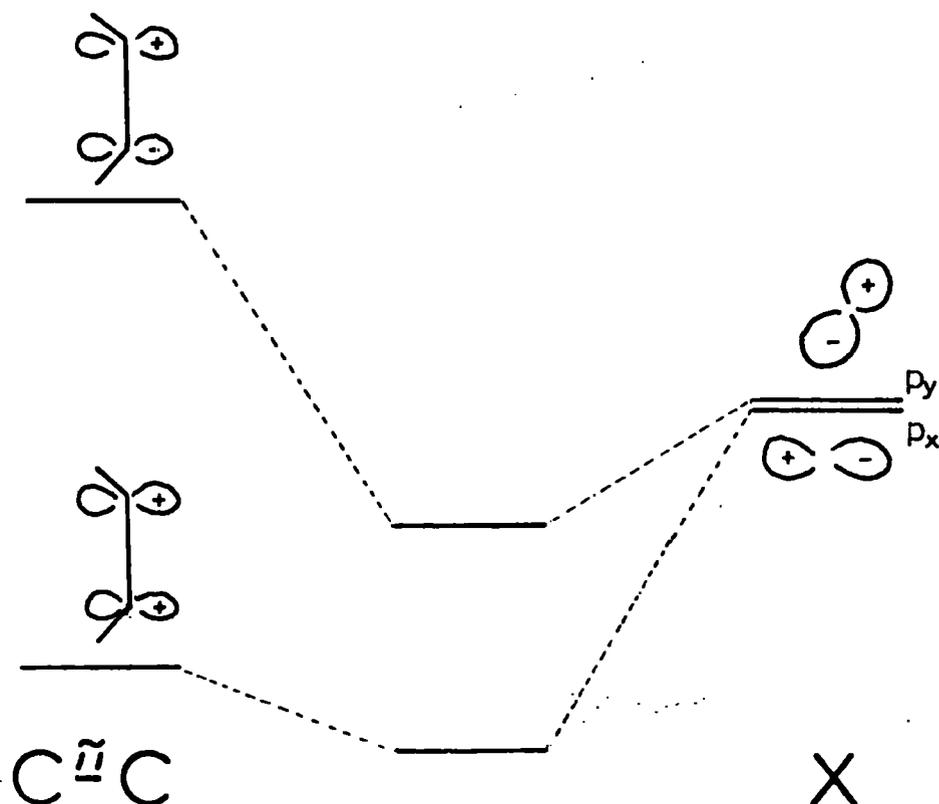
Thus as this energy decreases in the order $H(>)$ $F > Cl$ and $O > S$, the $b_2\pi$ level is destabilised as the repulsive interaction with the acetylene system increases.

Studies of the in-plane bonding in three membered rings had notable early contributions from Coulson and Moffitt,[122] who proposed the 'bent-bond' model for cyclopropane and Walsh[123] who employed an sp^2 hybridisation scheme for the same molecule. Latterly Kochanski and Lehn[124] have performed M.O. calculations on a number of ring systems and proposed a partially localised picture of the bonding. A study of some heteroatomic three membered rings has also been undertaken by Clark[125,126]. A more practical approach in this study however is to consider the interactions between the orbitals of the separated X and acetylene units with variation in X. The orbital interaction scheme for a typical monoatomic X is shown in Figure 3.3. This scheme is completely general. When X is a transition metal (e.g. Pt) the approach is very similar to the descriptions employed in metal-olefin complexes such as Zeise's salt as first presented by Dewar and Chatt and Duncanson.[127,128]

The orbital energies of the highest occupied sigma orbitals show significant variations (Table 3.2.) The $b_2\sigma$ orbital is formed mainly from the py a.o. of the heteroatom which interacts with the π_x^* orbital of the acetylene. As this interaction increases with decreasing valence py orbital energy of X, the antibonding contribution of the π_x^* orbital reduces the C–C σ bond overlap in the order $H^+ > F^+ > Cl^+$. Concurrent with this will be some strengthening of the acetylene heteroatom linkage. This bonding will also be dependent on the overlap in the $a_1\sigma$ orbitals involving the carbon and heteroatom valences and px orbitals.

A pictorial representation of the bonding in the xy and xz planes

is gained from constructing total electron density maps as shown in
Figure 3.4. for thiirene. There is high electron density outside the
ring, consistent with previous analyses, with a low net bonding
interaction of the π electrons.

Estimates of the stabilities of the rings can be made by
consideration of the reaction:

$$\triangleright\!\!-X + H^+ \longrightarrow \triangleright\!\!-H^+ + X(^1D)$$
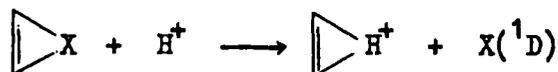
where the singlet state of the free atom X is taken (if the triplet
state is required an extra stabilisation of 45.2, 59.7, 26.4, 33.3
kcal.mole^{-1} for X = O, F$^+$, S, Cl$^+$ respectively will occur[129]). The
energy changes given in Table 3.3. indicate the marked lower stability
of thiirene and oxiirene due to the predicted π-π antiaromaticity of
the ring system. For the former an estimate of this has been made by
performing a calculation where non-interaction of the carbon and sulphur
pz is imposed by symmetry blocking the Fock matrix and iterating to self
consistency. The difference in energy between the two calculations
gives an 'antiaromaticity' of 103 kcal.mole^{-1}. This is seen to account
for the majority of the destabilisation.

For the halonium ions the order of stability of the bridged ions is
predicted to be X = F$^+$ > H$^+$ > Cl$^+$ with respect to the separate acetylene
and cation. It is more useful however to compare the relative stability
of the heteroatom in bridging and saturated environments. The energy
change for the hypothetical reaction

$$CH_4 + Y^+ \longrightarrow CH_3Y + H^+ \quad (Y = F, Cl)$$
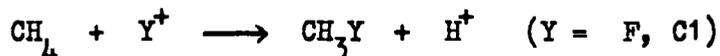
has been determined from thermochemical data,[130,131] (at $0^\circ K$ as reference
level). This allows the energetics of the reaction,

$$\triangleright\!\!-X^+ + CH_4 \longrightarrow CH_3X + \triangleright\!\!-H^+$$
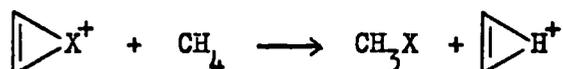
to be studied. Again a marked lower stability in the ring is observed,

Figure 3.4.   Total Electron Density Map in the two symmetry planes
of Thiirene(Contours 0.01,0.03,0.05,0.07,0.10,0.15,0.25).
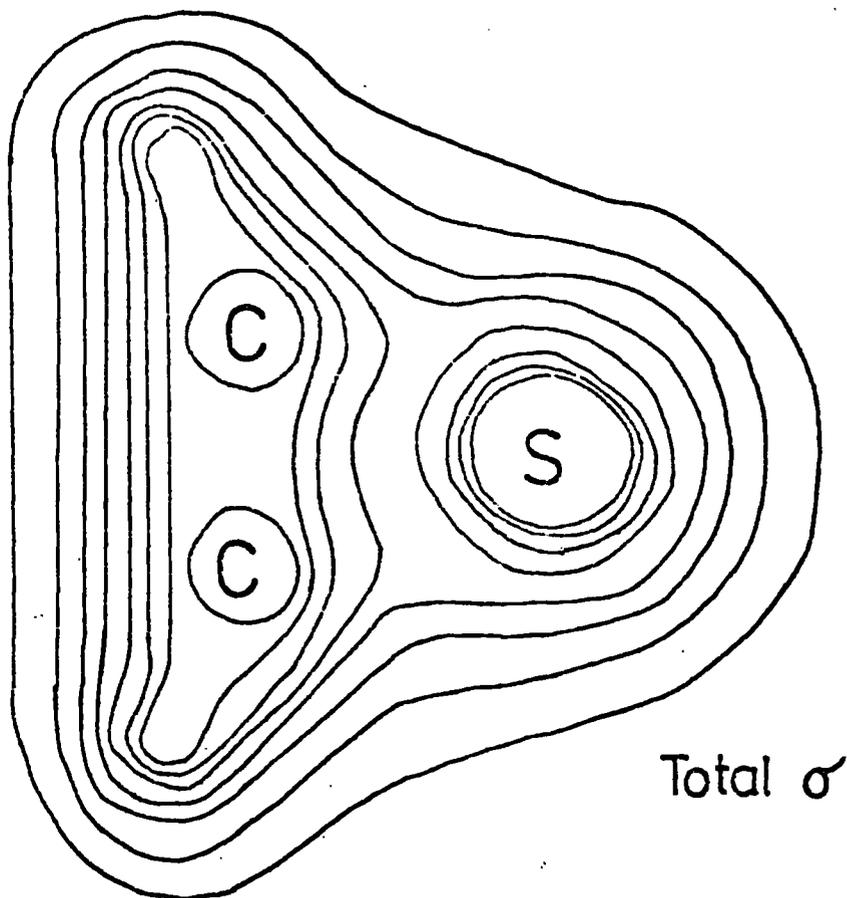
Total σ
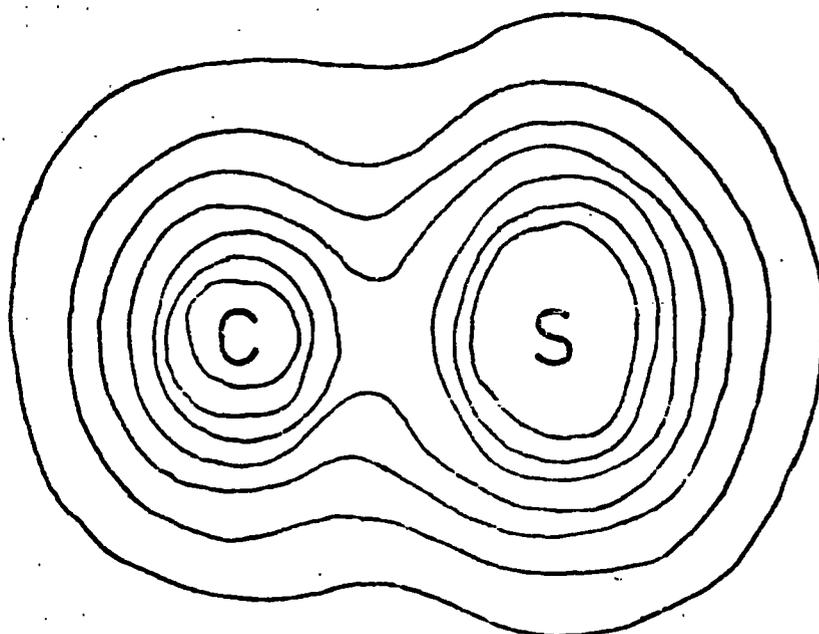
Total π

the order of bridged stabilities being $X = H^+ > Cl^+ > F^+$. Studies by

Clark and Lilley on the analogous saturated species[120] generated

similar relative stabilities as displayed in Table 3.3. Though their

original comparisons were referenced to the stability of the β

-substituted cation, employing thermochemical data with their

relative energies these have been referenced via the reaction

$$\triangleright\!\!Y^+ \quad + \quad CH_4 \quad \longrightarrow \quad CH_3Y \quad + \quad \triangleright\!\!H^+ \quad (Y = H, F, Cl)$$
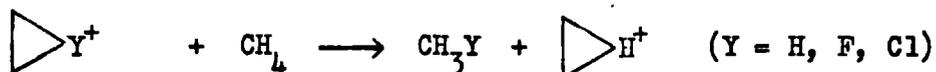
This allows an estimation of the energetics of the exchange reaction

$$\triangleright\!\!H^+ \quad + \quad \|\!\!\triangleright\!\!X \quad \longrightarrow \quad \triangleright\!\!X^+ \quad + \quad \|\!\!\triangleright\!\!H \quad (X = F^+, Cl^+)$$
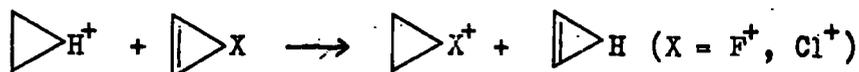
to be calculated and hence the relative stabilities of the bridged

acetylene as measured by hydrogenation. The high exothermicity is not

unexpected and is in qualitative agreement with the anticipated $\pi-\pi$

repulsions in the ring.

For the isoelectronic neutral species data may be obtained by

absolute calculations for $X = S$ from the thermodynamic cycle:

$$\|\!\!\triangleright\!\!S \quad + \quad \triangleright\!\!H \quad \xrightarrow{\Delta H} \quad \triangleright\!\!H \quad + \quad \triangleright\!\!S$$

$$\Big\downarrow D1 \qquad \Big\downarrow D2 \qquad \nearrow D4 \qquad \nearrow D3$$

$$C_2H_2 \qquad H^+$$

$$S(^1D) \qquad C_2H_4$$
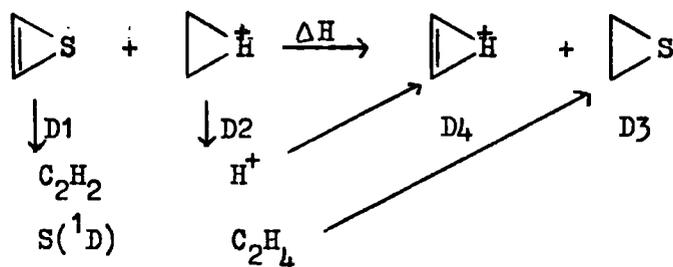
The energy D3 has been computed by Csizmadia et al.[132] with a

similar basis to be -66.2 kcal.mole^{-1} and from Figure 3.1. D4-D2 $\sim$13

kcal.mole^{-1}. The exothermicity (ΔH) of 26.3 kcal.mole^{-1} is

approximately 20 kcal.mole^{-1} lower than for bridging Cl^+.

An estimate for the analogous reaction with $O(^1D)$ can be made from

thermochemical data. To retain the same level of accuracy however, it

is necessary to relate the experimental thermochemical ΔH_f^o [129-131] for

the decomposition $(-D3)$ to $O(^3P)$ (83.09 kcal.mole^{-1}) and $S(^3P)$

Table 3.3.

Energy Changes for Exchange Reactions.

X	E1	E2	E3	E4	E5
H^+	(0)	(0)	(0)	(0)	(0)
$O(^1D)$	-121.9				-57.0*
$F^+(^1D)$	- 47.9	-44.6	8.8	2.9	-47.5
$S(^1D)$	-116.2				-26.3**
$Cl^+(^1D)$	- 54.0	-29.1	24.6	21.4	-50.5

E1 : [△X] + H^+ ⟶ [△H+] + X

E2 : [△Y] + CH_4 ⟶ [△H+] + CH_3Y

E3 : [△Y] + $CH_3CH_2^+$ ⟶ [△H+] + $CH_2YCH_2^+$

E4 : [△Y] + CH_4 ⟶ [△H+] + CH_3Y

E5 : [△H+] + [△X] ⟶ [△X] + [△H+]

* Employing thermodynamic tables, see also text.

** Employing thermodynamic tables.

Table 3.4.

Total Energies of some Thiirenes and their Decomposition Products (au)

Molecule	Energy	Molecule	Energy	Molecule	Energy
[△S]	-474.0960	[△SO]	-548.7655(.7753)	[△SO_2]	-623.4120(.4114)
[⟩S]	-476.5387	[⟩SO]	-551.1905	[⟩SO_2]	-625.8816
C_2H_2	- 76.7379	$S(^1D)$	-397.3167	$CH_2(^1A)$	- 38.8222
$SO(^1A)$	-472.0598	SO_2	-546.7849	C = S	-435.1757
[△S-H]	-474.2825(.4178)*				

Values in parenthesis refer to interpolated geometries.

* S-H 75° out of plane.

$(58.0 \text{ kcal.mole}^{-1})$ with the computed singlet reaction of Csizmadia.

There are two main points of interest which accrue from these results. Firstly the destabilisation is less for the larger second row elements where the valence π orbital is more diffuse. A similar dependence on the charge of the heteroatom is also observed. Secondly the unsaturated ring will be destabilised by upwards of 40 kcal.mole^{-1}, due to the antiaromaticity, with respect to its saturated analogue. This can conceivably be removed by a reduction in the $\pi - \pi$ repulsion with suitable substituents. This important ramification will be pursued in the next section.

The major cause of any error in these results will be due to inaccurate geometries for the bridged acetylene species. Estimates of these are not likely to be in error however by greater than .01 a.u. as indicated by the low force constant associated with the heteroatom in thiirene and opposing energy changes in the C=C and C-X bonds for displacement of X perpendicular to C-C. Subsequent analysis on thiirene and its S-oxides in widely differing geometries substantiated this assumption.

3). <u>S-substituted thiirenes.</u>

The studies of the three membered rings have been extended by a consideration of some S-substituted thiirenes, the reason for this being two fold. Firstly, and continuing the above line of approach, they represent molecules where the expansion of the valence shell at the heteroatom might be expected to be of some importance in a similar manner to that found for transition metals. Secondly such ring systems are of current interest since although thiirene itself is unknown, derivatives of this 1-oxide and 1,1-dioxide have recently been synthesised.[133-135]

A detailed consideration of the bonding pattern of these molecules at this time is thus particularly apposite. Comparative studies have thus been performed on thiirene and its derived S-protonated, 1-oxide and 1,1-dioxide.

Preliminary CNDO/2 studies showed from a consideration of PBO populations that in progressing along the series thiirene, thiirene-1-oxide, thiirene-1, 1-dioxide that the C-C bond should become progressively longer and the C-S progressively shorter. This will be discussed later.. For computational simplicity therefore a standard ring geometry for all three ring systems incorporating a slightly longer C-C bond than previously derived for the parent ring system was used. The geometries for the S-oxides were subsequently modified in light of a crystallographic determination of the structure of 2,3-diphenyl thiirene-1,1-dioxide.[136] This was employed as the cyclic sulphone geometry, that for the sulphoxide being interpolated using CNDO PBO data.

a) <u>Relative Stabilities and Bonding.</u>

The total energies for the substituted thiirenes with some of their decomposition fragments are shown in Table 3.4. To make a realistic assessment of the relative stabilities of the S-oxides two thermodynamic cycles were considered. Firstly the singlet decomposition reaction

$$\triangle X \longrightarrow C_2H_2 + X \text{ (singlet)}$$
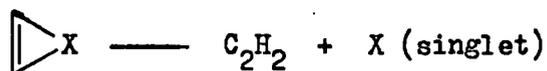
gave calculated energy changes of:

X = S (+25.99). X = SO (-20.90), X = SO$_2$ (-69.55 Kcal.mole^{-1})

This is not unexpected as it represents the increased stability of the S-oxide decomposition product. The ring stability may itself be investigated by comparison with saturated non-cyclic S-oxides.

Calculations were performed on dimethyl sulphide and the sulphone and

sulphoxide employing experimentally determined geometries.[92,137,138]

By evaluation of the energy change for the reaction

$$\triangleright\!\!\text{S} \ + \ \underset{Me}{\overset{Me}{>}}\!\!X \ \longrightarrow \ \triangleright\!\!X \ + \ \underset{Me}{\overset{Me}{>}}\!\!S \qquad (X = SO, SO_2)$$

and thermodynamic data for the saturated molecules the relative

stabilities were calculated and are shown as in Table 3.5.

Table 3.5.

Relative Heat of Formation of S-oxides (kcal.mole^{-1}) with standard/
experimental geometries and most stable conformer.
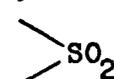
$\triangleright$S	(0)	$>$S	(0)
$\triangleright$SO	-36.4	$>$SO	-26.4
$\triangleright$SO$_2$	-62.3	$>$SO$_2$	-78.3

In view of the fact that the cyclic sulphoxide is stabilised

w.r.t. the dimethyl analogue by 10 kcal.mole^{-1} it is perhaps surprising

that the sulphone is destabilised by 16 kcal.mole^{-1}. With allowances

for the partial geometry optimisation these differences in energies are

reduced to 5 kcal.mole^{-1} and 5 kcal.mole^{-1} respectively, still in the

same direction. It appears then that if both ring systems exhibit

similar ring strain and σ bonding properties then relatively speaking

the sulphoxide removes a considerably greater portion of the antiaromaticity.

There is some available thermochemical evidence to support this result

from studies by Carpino and co-workers.[135]

To shed further light on this most unusual result the energy

levels and charge distributions have been closely investigated. The

interpretation is aided by considering the effect on the electronic

Figure 3.5a. <u>Orbital Interaction of HOMO's of Thiirene and Oxygen.</u>
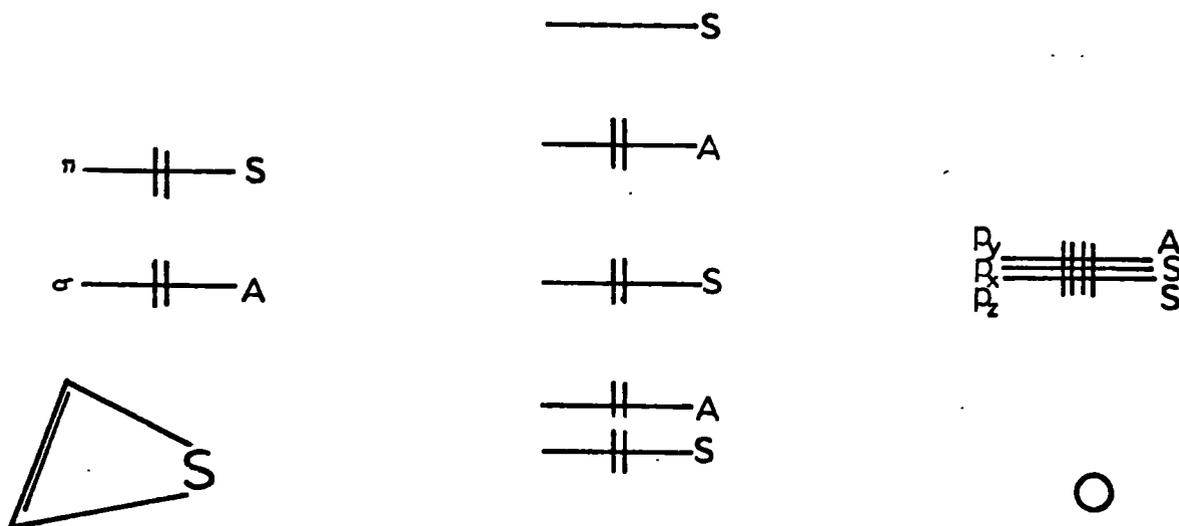
Figure 3.5b. <u>Relative Orbital Energies of C_2H_2, S, SO, SO_2.</u>
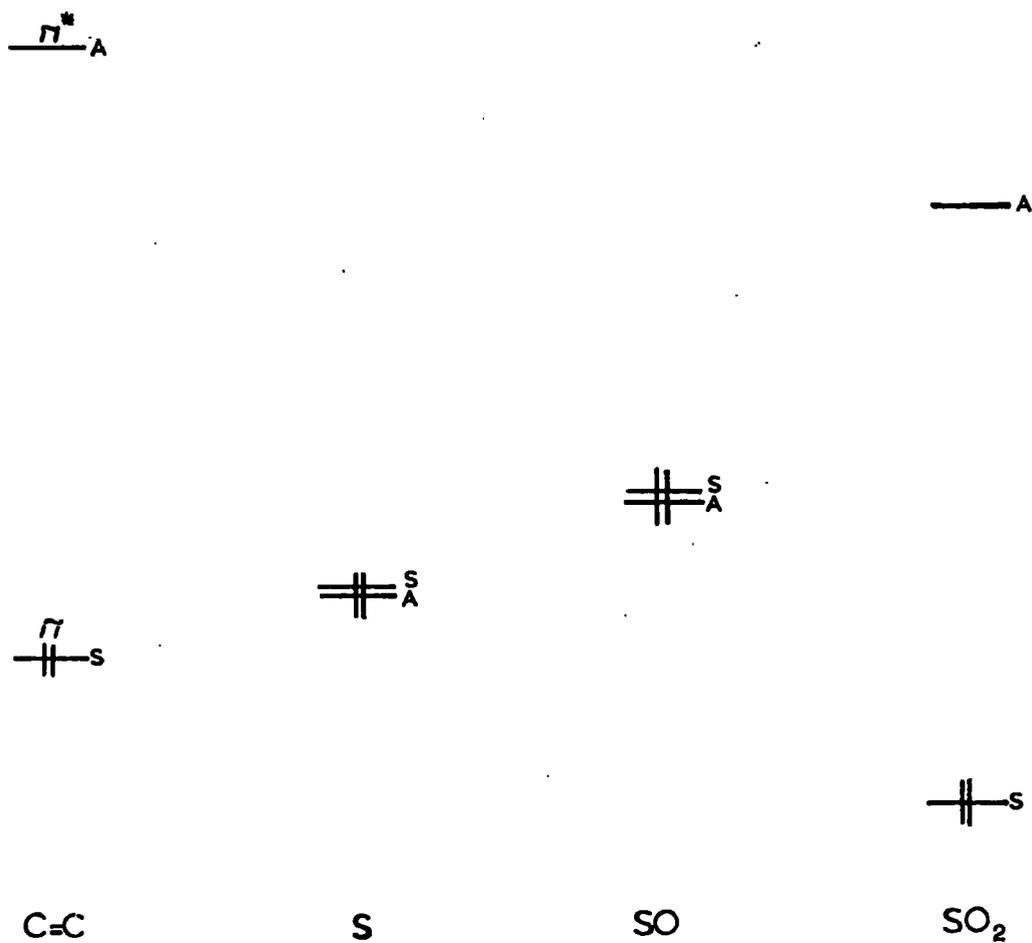
structure caused by addition of one or two oxygen atoms at sulphur in the geometry of the sulphoxide and sulphone. The orbital interaction diagram is shown schematically in Figure 3.5. Clearly the highest filled π orbital of thiirene will be markedly stabilised upon interaction with the O_{2px} orbitals.

For the sulphoxide and sulphone there is strictly no σ-π separability but the form of the orbitals indicates that this is a reasonable approximation. The intra-ring π-π repulsions will be reduced as indicated by the decreased S_{3pz} populations(X = S (4.011e), X = SO (3.069e), X = SO_2 (2.689e)), the former change in population being considerably more drastic than the latter. Comparison with their dimethyl analogues however shows this is not extraordinary;for Me_2X, X = S (3.959e), X = SO (3.083e), X = SO_2 (2.722e). The energy of this cyclic π orbital is however now lower than the highest occupied σ orbital in the sulphone and sulphoxide as is seen from Table 3.6 . These species should thus exhibit a decreasing facility for one electron oxidation.

Secondly,the ring structure will be determined essentially by the σ bonding between the acetylene and heteroatom. This in turn depends on the energies of the highest occupied symmetric and lowest unoccupied anti-symmetric σ orbitals of the heteroatom. (The latter is a consequence of the least-motion addition of singlet X to acetylene being symmetry-forbidden as is consistent with the general analysis of cheletropic reactions).[139] The energy of this virtual orbital (which is mainly due to S_{3py}) will be increased in the order X = S < SO < SO_2 as an antibonding combination of O_{2py} orbitals is added. Conversely the symmetric orbital will fall in energy. Though energies of virtual orbitals cannot readily be calculated estimates can be made from the

Fock matrix elements with the values adjusted from optical spectroscopy.[140]

The relative ordering·of the levels can then be reproduced and hence an

orbital interaction diagram constructed similar to Figure 3.5a.

The form of this diagram: (Figure 3.5b) is now capable of

explaining the considerable variation in calculated charge and bond

overlap populations (Table 3.6.). In going to the sulphone there is a

substantially increased donation into the π^* orbital of the acetylene.

This results in a weaker C-C bond as indicated by the overlap. Consistent

with this approach is an increased C-S bond overlap also in the same order.

This is in agreement with the recent crystallographic study of the

substituted sulphone where the C-C and the C-S bonds are respectively

longer and shorter than those calculated for thiirene.

If the total overlaps are split into contributions from orbitals

either symmetric or antisymmetric in a plane through sulphur and oxygen

it is seen that though the antisymmetric molecular orbitals are

responsible for the majority of the variation in overlap in the C-C bond,

the symmetric orbitals are significant in C-S overlap variations.

Within this analysis of the σ and π contributions, thiirene and its

dioxide show opposing effects: antibonding π overlap in thiirene is

reversed (X = S (-.069e), X = SO_2 (+.036e)) whereas the antibonding

situation increases in the σ system (X = S (-.033e), X = SO_2 (-.082e)).

The latter will result from the lowering in energy of the symmetric

sulphur orbitals and hence an increased repulsive interaction with the

occupied acetylene px + px orbital. For X = SO however the higher 3py

orbital energy of the sulphur will offset this to some extent with the

results that the repulsive situation will be less than anticipated.

Unfortunately the symmetry of the species does not allow separation of

the σ and π components to substantiate this, but qualitative comparisons

Table 3.6.

Orbital Energies of Thiirene and Dimethyl S-Oxides. (eV).

▷S	>S	▷SO	>SO	▷SO₂	>SO₂
7.7(SA)	8.75(SA)	10.1(A)	9.45(A)	10.4(AS)	11.4(AS)
11.8(AS)	11.35(SS)	10.1(B)	10.5(B)	11.95(SA)	11.8(SA)
13.0(SS)	13.65(AS)	11.6(A)	13.3(A)	13.5(AA)	12.45(SS)
13.6(SA)	15.25(SA)	15.6(A)	14.8(A)	13.5(SS)	12.7(AA)
19.1(SS)	15.65(AS)	15.6(B)	14.9(B)	13.5(AS)	15.3(SA)

Experimental :

>SO   9.01, 10.17 [142]
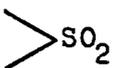
>SO₂   10.65(AS), 11.18(SA), 11.65(AA), 12.0(SS) [143]

Table 3.7.

Population Analysis of Thiirene and Dimethyl S-Oxides (Standard Geometries)

		▷S	>S	▷SO	>SO	▷SO₂	>SO₂
Total Charges	S	-0.510	-0.334	0.120	0.233	0.457	0.601
	CH	0.255	0.117	0.239	0.200	0.300	0.264
	O			-0.598	-0.632	-0.529	-0.564
μ (au)			0.678	1.706	1.632	2.109	2.184

Overlaps in Thiirenes.		C-C	C-S	C-C	C-S	C-C	C-S
Symmetric (SS) + (SA)	σ	.494	-.033	.723	-.043	.480	-.010
	π	.261	-.069			.225	-.036
Antisymmetric (AS) + (AA)		-.241	.150	-.331	.160	-.399	.171

between orbitals show this to be true.

The CNDO/2 partition bond overlaps from which the later ab initio geometries were calculated are essentially unchanged from these, as evident in the sulphoxide where change of geometry does not affect these conclusions. Though the total energy for this geometry was lower than that initially assumed there was a negligible change in energy employing the experimental geometry for the sulphone. From previous experience similar basis sets underestimate the C=C separation by 0.02Å. This is likely to be the cause of the apparent disparity.

It is pertinent to point out that such an analysis for the corresponding saturated series is in complete accord with these results. With the unsaturated molecules there is a much greater variation in overlap between thiirene and its 1-oxide than with the dioxide. Replacement of acetylene by ethylene will raise the orbital energies by ~1.0eV with a subsequent preference for overlap as indicated by Hoffmann.[141]

b). Electronic Structure

A comparison between the orbitals of the thiirene and dimethyl S-oxides raises a number of points of interest. Firstly the AS orbital (for classification see Figure 3.2.) is to lower energy for the dimethyl species. This orbital is composed mainly from S-O and the antisymmetric combination of the carbon orbitals: their repulsive interaction will be greater in the smaller angled CSC ring form. The highest occupied SA orbital, which is ~1.6eV less stable in thiirene than in dimethyl sulphide is. of comparable energy in the sulphones. The low value of this orbital in the sulphoxide reflects the mixing-in of lower energy ring σ molecular orbitals. A detailed analysis of the a.o.

contributions in corresponding orbitals displayed no great variations.

Comparison of the total charges on each centre again indicates the anomalous nature of the thiirene-1, 1-dioxide and dimethyl sulphone. Whilst the charge increases in the dimethyl species by .568e and .368e with addition of one and two oxygens the corresponding increases for the vinyl species are .630e and .337e. This is accompanied by a decrease in the expected charge at carbon in the cyclic sulphoxide. This reflects the relatively lower donation of charge to the S-O sulphur due to its higher px orbital energy. Contributions to the total population from the symmetric σ orbitals support this argument. The carbon populations for $X = S$ (3.069e) $X = SO$ (3.066e) and $X = SO_2$ (2.97e) display the decreased donation of charge to the sulphoxide sulphur (for $X = SO$ a σ/π division is assumed at the carbon which should not greatly affect the argument).

A useful intuitive guide to the bonding is often provided by the dipole moment. Experimentally determined values for the diphenyl thiirene-1,1-dioxide and dimethyl sulphone of 5.63D (soln.)[143] and 4.49 (gas)[144] respectively compare with that for dimethyl sulphoxide of 3.96D.[144] The calculated values (Table 3.7.) are in agreement for the first two members of the dimethyl series with the experimental, the divergence for the sulphone suggesting a low experimental value. Of greater significance however is the fact that the calculated dipole moments between the corresponding S-oxides are similar. For the analogous carbonyl system conjugative stabilisation is commonly invoked to account for the increased dipole in diphenylcyclopropenone (5.14D)[145] over acetone (2.88D)[144] Thus these results indicate considerably less, if any, such interaction in the cyclic S-oxides

4). ESCA Study of Some S-Oxides.

It would be convenient if these calculations could be checked

independently by an experimental technique to signify the similar

charge distributions. For this reason ESCA studies were performed on

some substituted thiirene-1-oxides and 1,1-dioxide and dimethyl sulphone

and sulphoxide. Liquid samples were expanded into a reservoir shaft and

diffused through a metrosil plug and condensed on gold as thin films.

It was convenient to mount the solids on scotch tape. Spectra were

recorded on an AEI ES100 spectrometer with $MgK\alpha_{1,2}$ as the X-ray course.

For the thin film samples energy referencing was accomplished by

monitoring the Au $4f_{7/2}$ level at a binding energy of 84.0 eV. For

solids sample charging was in no case greater than 1 eV. Referencing

was accomplished from the centroid of the C1s peak to 285.0 eV (BE).

An interesting observation was that over a period of time the diphenyl

thiirene 1-oxide peaks to lower BE were observed appropriate to a C-$\underline{S}$ or

$\underline{S}$-S type environment though sufficient information was not available to

produce any definite conclusion. There was also evidence for the

formation of a lower BE peak in dimethyl-1, 1-dioxide. For the S_{2p}

levels spectra are shown in Figure 3.6.a,b and the binding energies

collected in Table 3.8. As expected the $S_{2p_{3/2}}$ peak shifts to higher

BE in going from the sulphoxide to sulphone.

The binding energies may be discussed in terms of the charge

distribution via the charge potential model in which the binding energy

is related to the charge distribution though equation 2.19. Since

similar absolute binding-energies for the $S_{2p_{3/2}}$ level are observed for

both the substituted thiirene-1-oxide and dimethyl sulphoxide it can be

inferred that these related molecules possess a similar charge

Figure 3.6a.

S_{2p}

Binding
Energy e.v.   169   167   165   163

Figure 3.6b.

93.
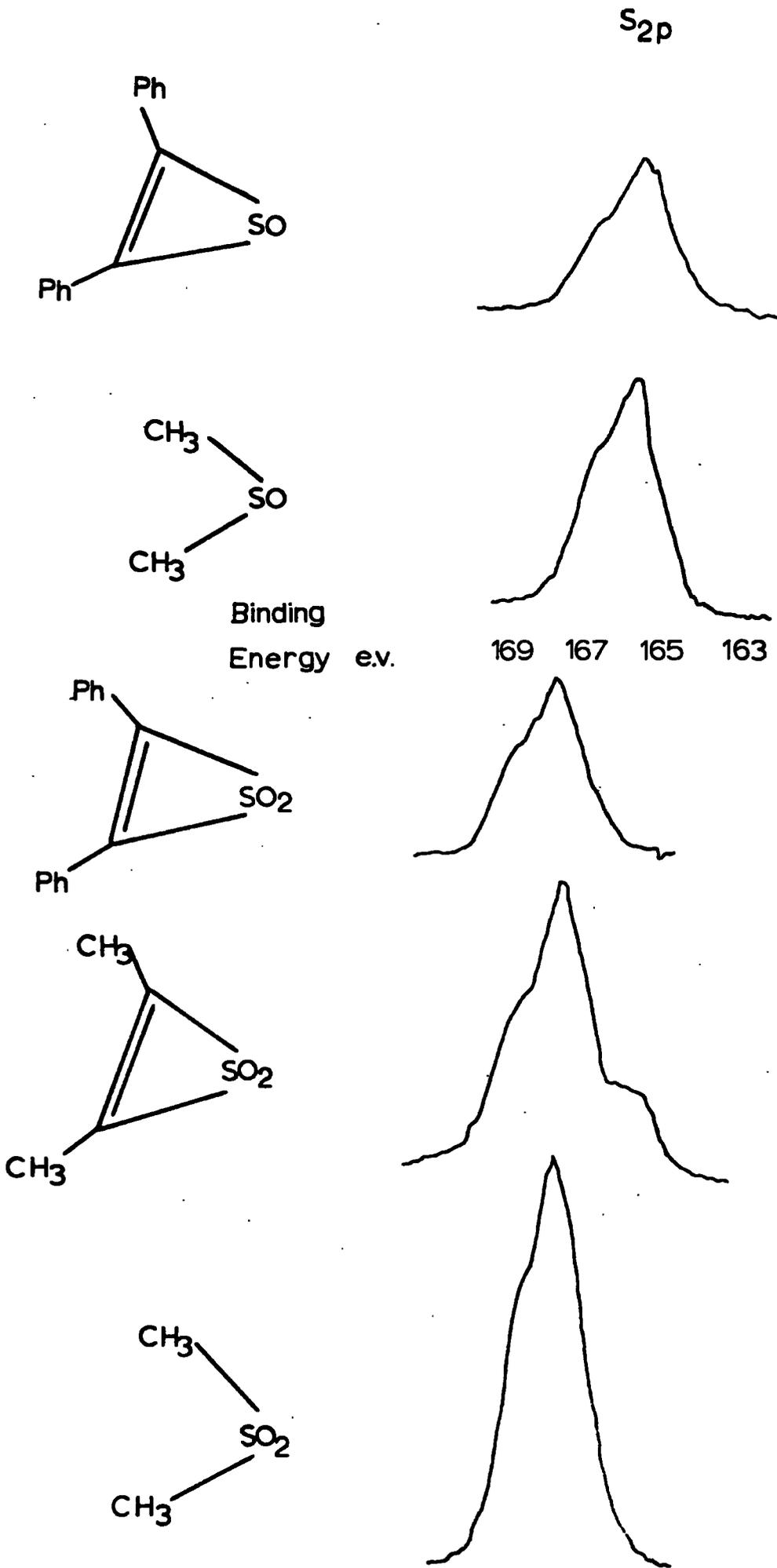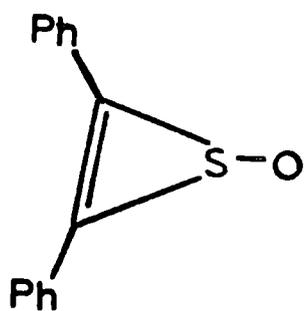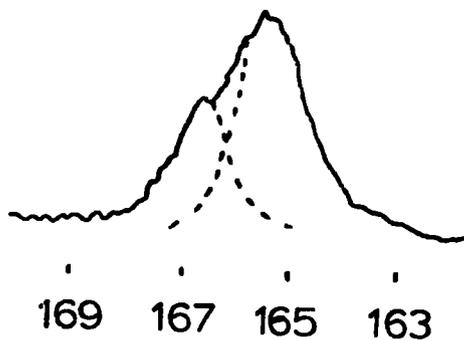
Time in
spectrometer
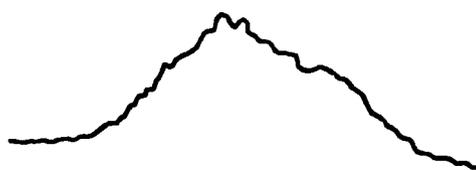
2 hrs.
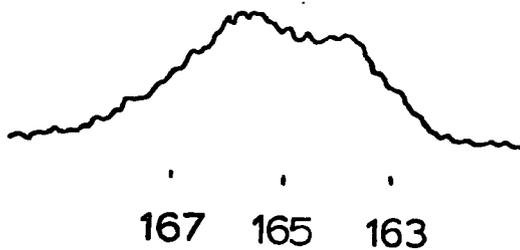
3 hrs.

12 hrs.

distribution in the vicinity of the sulphur atom. This conclusion

also holds for the analogous dioxides and provides further indication

that the charge distribution in the two S-oxide series are similar.

Koopmans' theorem was also applied to determine the BE's and

the theoretical shifts. Though the calculated shifts are

overestimated there is an almost linear relationship for the shifts

within the same series. This overestimation though merely reflects

the neglect of the electronic relaxation energy in the application of

Koopmans' theorem as will be discussed in more detail in the next

chapter.

5). <u>Contribution from 'd' type Orbitals in the Bonding Scheme.</u>

No explicit mention has been made above concerning participation

of d orbitals in the bonding scheme. It is important that when

discussing d orbital participation in the cyclic S-oxides a distinction

be made between that accepted to be observed in a non-cyclic S-oxide

and due to ring σ and π bonding. There can be no argument of the

former in the S-oxides; the total d populations substantiate this,

but the latter (ring contributions) are of some interest and have been

investigated.

Firstly in the sigma plane inclusion of $d_{x^2-y^2}$ and d_{xy} orbitals

will aid in formation of hybrids in the small angled rings. This is

indicated by the slightly larger d populations of the ring sulphur

(Table 3.9.). Secondly in the π system there is a considerable increase

in the S d_{xz} of $\sim$ .11e in the cyclic sulphone. This is a combination

of charge polarization and conjugation between the σ oxygen and

carbon π electrons which is aided by the symmetry of this orbital as is

shown below. There is no appreciable change in the dyz population.

Table 3.8.

ESCA Results for Thiirene and Dimethyl S-Oxides. (eV).

	$\triangleright S$	$>S$	Ph$\triangleright$SO	$>$SO	Ph$\triangleright$SO$_2$	$>$SO$_2$
Exp. $S_{2p3/2}$			165.9	165.6	167.8	167.7
Koopmans'	180.28	180.05	184.15	183.67	187.48	187.07

Table 3.9.

D Orbital Populations. (e)

	$\triangleright$S	$\triangleright$S	$\triangleright$SO$_2$	$\triangleright$SO$_2$
d_{xy}	.077	.102	.314	.314
d_{xz}	.043	.007	.295	.182
d_{yz}	.0	.004	.241	.246
$d_{x^2-y^2}$	.011	.015	.260	.072
d_{z^2}	-.018	.022	.228	.364
$\Sigma d\sigma$	.130	.140	.802	.750
$\Sigma d\pi$	.043	.011	.536	.428

Table 3.11.

Fourier Analysis of Inversion Barriers in some Thiirenes:

$$\Delta E = A\cos(1-2\theta) + B\cos(1-4\theta) \quad (\text{kcal.mole}^{-1})$$

	$\triangleright$S-H	$\triangleright$S-P	$\triangleright$S-O
A	42.1	34.5	52.7
B	10.0	7.5	26.4
θ_{min}	90°	90°	60°
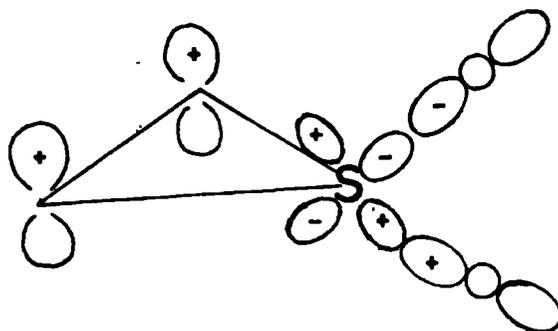
It can be seen then that the major role of the d orbitals in these species is involved with the S—O dπ—pπ bonding and this accounts for the majority of the d bonding in each series of S—oxides. Their inclusion in the basis has the effect however of a lowering in the sulphur orbital energies which will increase the symmetric interactions. On this basis d orbital participation in these rings is of secondary importance.

6).   Conformational Studies.

The out-of-plane angle in the sulphoxide was assumed to be $60°$, the approximate angle in the majority of similar molecules. This arises from a consideration of the valency of the sulphur with its preferred tetrahedral configuration. There will also be an additional destabilisation of any planar structure through the resulting antiaromaticity in the ring. To investigate this further the out-of-plane angle has been varied for the cyclic sulphoxide and the energy computed for the various conformations. Similar calculations were performed on the S—protonated species. For completeness both sets were performed with the optional exclusion of d orbitals on the heteroatom.

The results from Figures 3.7a,c give large barriers to inversion, 83 and 65 kcal.mole^{-1} for the protonated thiirene and 117.5 and 105 kcal.mole^{-1} for the sulphoxide, the barriers being calculated

Figure 3.7.   Inversion Barriers in Thiirenes.
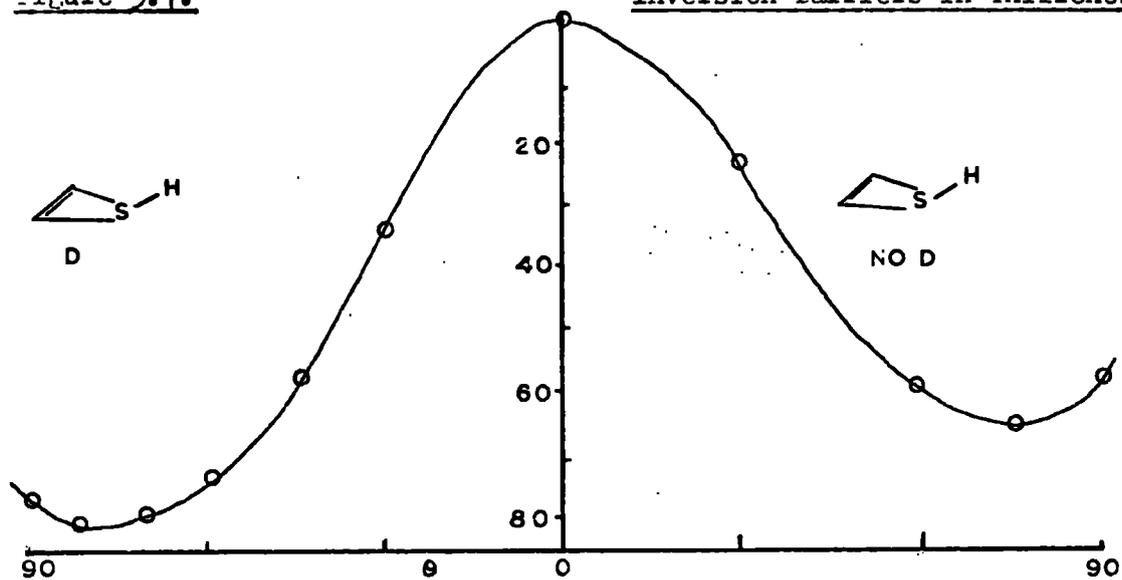
Fig.a.
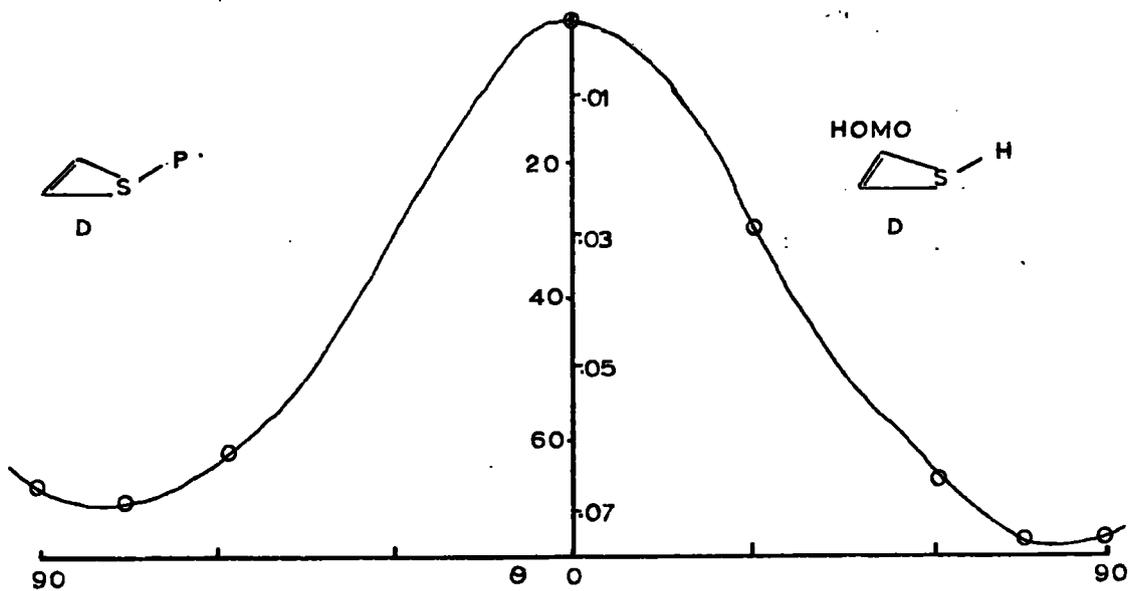
Fig.b.
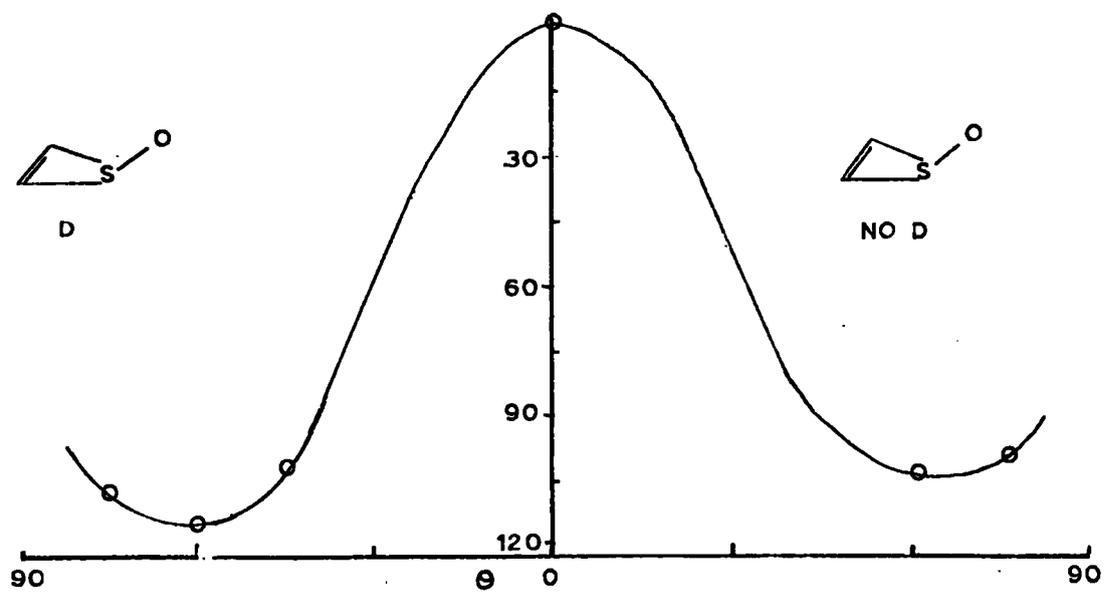
Fig.c.

respectively with and without d orbitals included in the basis. There are several ways in which this barrier can be viewed. A commonly employed technique is the decomposition of the total energy into attractive (V_{ATT}) and repulsive (V_{REP}) elements.[146] The total energy may then be written as

$$E = V_{ATT} + V_{REL}$$

$$V_{ATT} = V_{nn} + V_{ne} + T$$

$$V_{REP} = V_{ee}$$

with the nomenclature of the first chapter.

With the larger basis the barriers were found to be attractive in both cases (Table 3.10). It is of interest then that the computed antiaromaticity of protonated thiirene, calculated by localising the valence sulphur electron pair is 86.3 kcal.mole^{-1}, comparable to the inversion barrier. An alternative view of this situation can be taken by considering σ and π protonation at sulphur. The highest $a_1\sigma$ orbital has a substantial contribution from S_{3px} and this orbital is considerably reduced in energy upon protonation. In the π protonated conformer the highest π orbital is lowered in energy as the symmetry allows reduction of the C–S π-π repulsion. Further the variation in energy of this π' orbital qualitatively mirrors the total energy change on inversion. This though does not necessarily imply any special effect attributable to the ring as will be discussed below.

Closer analysis shows a significant lowering in energy of the highest $b_2\sigma$ orbital in going to the π protonated conformer. From the previous rationalisation of the bonding this should be reflected in an increased C–C overlap. This is strikingly apparent (Table 3.10); the

Table 3.10. Barriers to Inversion in some Thiirenes.

$\triangle$SH

	d in		d out	
	$\theta = 0^{\circ}$	$\theta = 75^{\circ}$	$\theta = 0^{\circ}$	$\theta = 75^{\circ}$
E_{TOT}.	-474.2825	-474.4178	-474.2554	-474.3603
E_{ATT}.	-737.5478	-737.8169	-737.4165	-737.4073
E_{REP}.	263.2653	263.3991	263.1610	263.0470

$\triangle$SO

	d in		d out	
	$\theta = 0^{\circ}$	$\theta = 60^{\circ}$	$\theta = 0^{\circ}$	$\theta = 60^{\circ}$
E_{TOT}.	-548.5785	-548.7655	-548.5080	-548.6784
E_{ATT}.	-904.6348	-906.9428	-904.4076	-906.6585
E_{REP}.	356.0563	358.1772	355.8997	357.9802

Mulliken Population Analysis of Protonated Thiirene (d in)

	$\theta = 0^{\circ}$	$\theta = 90^{\circ}$
Pop.^{n} S-H	16.537	16.406
Overlap.		
C-C (B)	0.724	0.728
C-C (A)	-0.315	-0.246
C-S	-0.038	-0.001

total change in the C-C overlap being due almost entirely to these b orbitals. Thus in going to the planar form the increased electron density on the sulphur raises the S_{3py} orbital energy, which is then capable of increased donation to the $p_{x}\pi^{*}$ orbital of acetylene. The change in bonding in this C-C unit will thus account for the larger attractive barrier. This behaviour and the high barriers for inversion will be expected to be quite general for all small rings, the main factor affecting the barrier being the energy of the $'S_{3py}$ orbital' in the bridging unit. Thus in the sulphone the inherently higher orbital energy will be expected to show a greater variation in overlap and a higher barrier is observed.

A dramatic illustration of this is that as the barrier is controlled by the potential at the sulphur, the motion of a unit charge should be effective in simulating the protonated thiirene barrier. Computations of the total energy with the ring in the same geometry were thus employed with the basis functions of the hydrogen deleted. The computed barrier is shown in Figure 3.7b. The barrier height of 68 kcal $mole^{-1}$ is in excellent agreement with the true calculated barrier. (In small ring systems this method should then be most effective in estimating the barrier to inversion and hence give information concerning the interactions involving the bridging atom. No two-electron integrals need be recalculated and starting vectors from previous converged runs may be employed to accelerate convergence).

A final analysis was performed by expressing the barriers as a truncated fourier series. With symmetry about $\theta = 0$ in the studied range $-90° < \theta < 90°$ the barrier may be expressed as (Table 3.11.)

$$V(\theta) = A(1-\cos2\theta) + B(1-\cos4\theta)$$

The A term with maxima and minima at $\theta = 0$ and $\theta = 90°$ respectively

will represent the tendency for σ/π protonation, the B term for a hybrid
(e.g. px + pz)as opposed to a trigonal sp^2 configuration. As a check
differentiating this equation for minimum θ gives

$$\cos 2\theta_{min} = -A/4B$$

The results are gratifyingly in accord with expectation. The
larger A value reflects the greater differential σ/π interactions of
the SO group as already discussed and similarly its larger B term the
tendency for hybrid formation. From such a limited expansion it is not
surprising that θ_{min} is in error for the protonated forms. Qualitatively
however the results are in good agreement though the accuracy for the
sulphoxide is fortuitous.

7). **Thermodynamic Cycles.**

Much mention has been made of the stability of these bridged
structures. Mainly these have been subjective analyses with comparisons
between different molecules. The theory does not allow accurate absolute
determinations of the heat of atomisation, and hence that involved in
dissociative reactions since correlation energy considerations are of
importance. It is however still of some importance to calculate these
quantities to shed light on their possible thermodynamic stabilities and
relative energies. Experimental geometries were employed where available
with additional data being derived from CNDO/2 studies. Geometries for
some of the larger molecules are given in the appendix. The reactions
themselves fall conveniently into 5 classes and are discussed below.

a). **Chelotropic Reactions.**

The energies for the reaction

$$\triangleright X \longrightarrow C_2H_2 + X(\text{Singlet}).$$
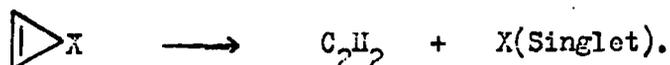
Table 3.12.

<u>Chelotropic Reactions.</u> *

▷X ⟶ C_2H_2 + X(singlet) kcal.mole^{-1}
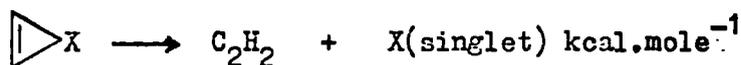
X	E	X	E	X	E
H^+	157.1	O	35.3	F^+	109.2
Cl^+	103.1	S	41.0	SO	− 5.2
SO_2	− 54.5	$SH^+(0°)$	− 0.8	$SH^+(75°)$	84.1

* Including 15 kcal.mole^{-1} ring correction.

Table 3.13.

<u>Estimated Heats of Reaction.</u> *   kcal.mole^{-1}

Reaction		kcal.mole^{-1}
▷S ⟶ CS + CH_2		76.6
▷SO ⟶ CS + CH_2 + O		134.4
SO + CH_2 + H		
▷SO_2 ⟶ CS + CH_2 + 2 O		177.7
▷S ⟶ ▷S		23.4
▷SO ⟶ ▷SO		27.8
▷SO_2 ⟶ ▷SO_2		35.0
▷S ⟶ S = C = CH_2		− 33.7
▷SH ⟶ H − C = CH(SH)		− 59.5(planar)
▷SH ⟶ H − C = CH(SH)		25.4(75°)
⟶ CH_2 + CS + H^+		278.5
▷SH ⟶ ▷S + H^+		117.0(planar)
▷SH ⟶ ▷S + H^+		201.9(75°)
2SO ⟶ SO_2 + S		− 24.7

* Including 15 kcal.mole^{-1} ring correction.

have been mentioned in detail above but for completion are grouped

together in Table 3.12. A correction factor of 15 kcal.mole^{-1} has been

applied to account for the relative deficiency of the basis for the

cyclic as compared with the non-cyclic reaction products. For the

deprotonation reaction (X = H$^+$) the calculated value (157.1 Kcal.mole^{-1})

is some 10 kcal.mole^{-1} higher than that obtained from thermodynamic data

and figure 3.1. (146 Kcal.mole^{-1}) but in reasonable agreement in view

of the considerations mentioned above. It is also of some interest that

for X = SH$^+$ in its stable conformer the bridged structure is quite stable

and shows no tendency to decompose in this manner. This is reasonable

from the above discussion of the out-of-plane stabilisation of this

molecule.

b). C-H Bending.

Though not strictly classified as a reaction the angular strain in

the C-H unit varies quite considerably with the bridging group from

Table 3.13.
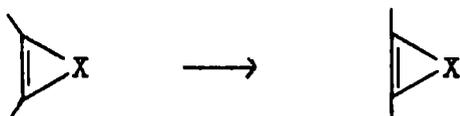
This serves as a hypothetical point on the chelotropic potential

energy surface. The barrier for this process should as a first

approximation correlate with the 'S$_{3px}$' orbital energy assuming a twisted

leaving group X for convenience and is in qualitative accord with these

results.

c). Ring Opening.

Three ring opening processes have been considered. With the

standard basis the open vinyl cation is favoured by 21.6 kcal., reduced

to 5 kcal.mole^{-1} however by a better bonding description of the ring.

Assuming a similar contribution to the bonding in the other rings, the conversion of thiirene to thiaketene is predicted to be exothermic by no more than 33 kcal.mole^{-1}. This still represents a ring destabilisation of ~30 kcals with respect to the bridged-protonated acetylene. Protonation at sulphur with a consequent out-of-plane bending produces a bridged structure which is now to lower energy however by 25 kcals than the β-thionyl cation. (A calculation of this process in the literature which gave results at variance to these has been checked and the author has since kindly informed that there was an unfortunate error in his work).[147] This is consistent with results from studies on the substituted fluoro-and chloroethyl cations. Indeed if the ring opening reaction of the bridged protonated acetylene is assumed to be ~6 kcals.mole^{-1} more exothermic than the analogous ethylene reaction and the isoelectronic Cl^+ and SH^+ exhibit a similar exothermicity again for the analogous reaction in the ethylene system (15.81 kcal.mole^{-1})[120] then the ring opening of the protonated thiirene is anticipated to be endothermic by ~22 kcals. in close agreement with the calculated. This again emphasizes the conventional behaviour of the small ringed protonated thiirene.

d). Decomposition.

Some feasible decomposition reactions are also shown in Table 3.13. These energy changes will be subject to considerable error in certain of the equations since the correlation energy of the products will often be considerably different from the reactants. This will be supplemented by the underestimation of the energy of the ring system. It is notable that the majority of the fragmentation reactions considered are highly endothermic. This is mainly attributable to the reactions considered

including the singlet states only of the products, which lie several

tens of kcals.mole^{-1} above the triplet electronic states.

e). Disproportionation.

The energetics for the isodesmic reaction

$$2 \, {>}SO \longrightarrow {>}S \, + \, {>}SO_2$$
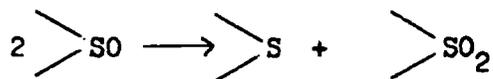
should be well described with the H.F. formalism. The energy change

has been computed for this reaction for both the thiirene and dimethyl

series. The exothermicity calculated for the latter (-24.7 kcal.mole^{-1})

is in excellent agreement with that calculated from their heats of

formation (-25.5 kcal.mole^{-1}) giving some foundation for the

qualitative energy changes calculated with this basis. For the ring

forms the reaction is now calculated to be endothermic by 10 kcal.mole^{-1}

using the partially optimised geometries, reflecting the relative

decreased stability of thiirene.

8). Studies of some Thiophenes.

Though not strictly within the limits defined for this chapter the

thiophenes make an interesting study in comparison with the thiirene as

aromatic and antiaromatic systems respectively. Calculations at the

CNDO level provided much background data for the above analyses and was

found to be qualitatively accurate in many cases. Notably the barrier to

inversion of the S-protonated thiirene was quite accurately reproduced

and the charge distributions were found to be in good qualitative

agreement with the non-empirical results and gave reasonable estimates

of shift in the core levels for the ESCA data. Two notable failures were

that in the planar S-protonated geometry the basis with d orbitals

converged to the wrong state and the barrier in the sulphoxide was

greatly underestimated. With this in mind calculations at the same level

Figure 3.8.

Energy Levels and Overlaps in Thiophen-S-Oxides.
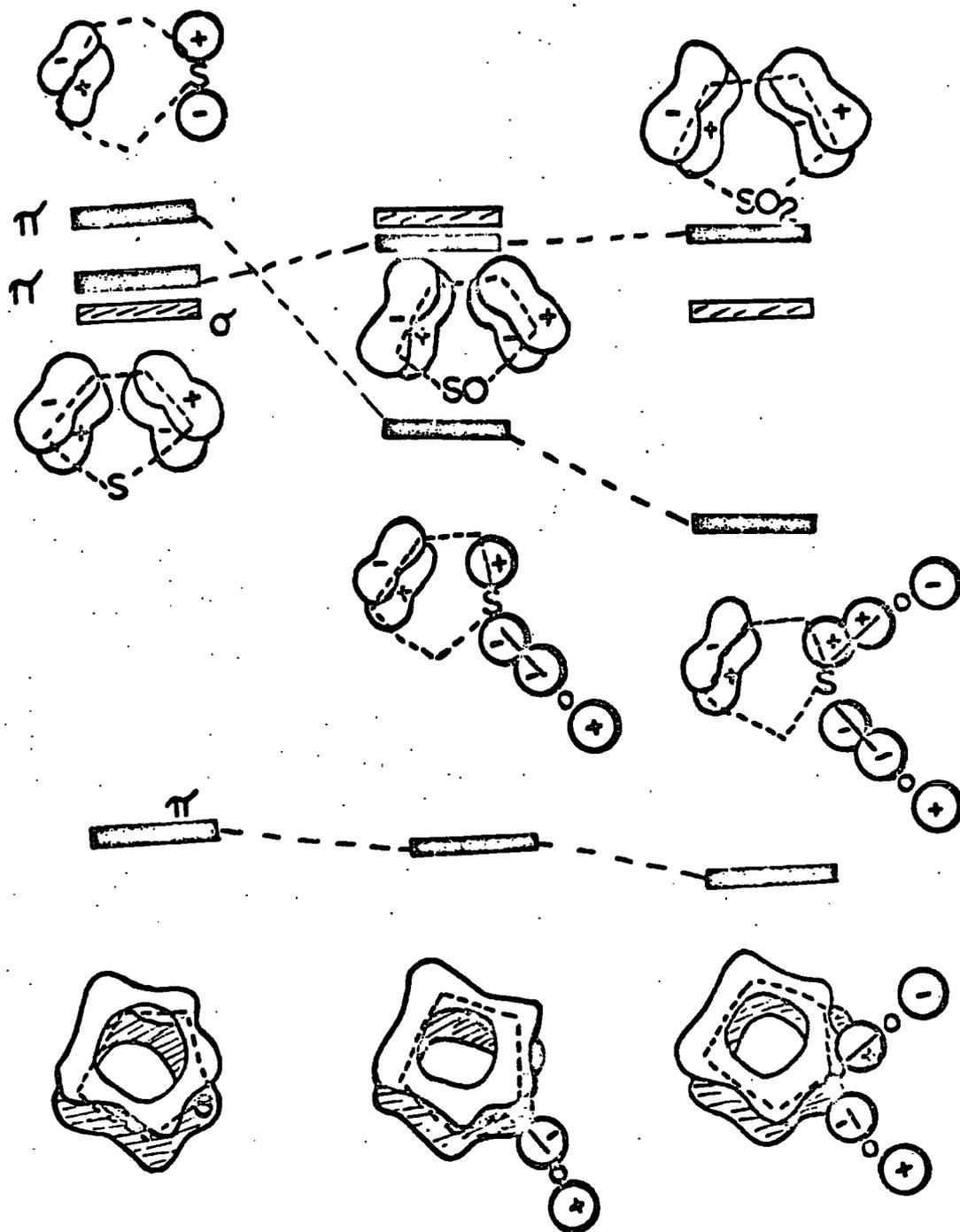
C_1-C_2	(0)	+0·017	+0·035	+0·062
C_2-C_3	(0)	-0·030	-0·035	-0·076

Scis butadiene

of accuracy were performed on thiophene and its S protonated and 1-and

1,1-dioxides. A standard geometry was taken for the ring derived from

thiophene and d orbitals were optionally removed from the basis,

convergence to the correct state being checked closely in each

calculation. The barriers for the S-protonated thiophene were

computed to be 37.7 kcal.mole^{-1} and 27.4 kcal.mole^{-1} with and without

d orbitals respectively. The out-of-plane angle (90°) was much larger

than has been reported from non-empirical studies (~70°).[148] For the

sulphoxide the barrier with d orbitals of 24.5 kcal.mole^{-1} is quite

reasonable.[149] the out-of-plane angle being ~55°.

The series thiophene, thiophene-1-oxide and its -1,1-dioxide can

be treated in a similar manner as the analogous thiienes. In figure

3.8. the variation in the higher orbital is shown schematically. Whilst

the $a_2\tilde{n}$ level remains approximately constant the $b_1\tilde{n}$ is lowered in energy

upon interaction with the oxygen 2p orbitals, with enhancement from the

large contribution from S_{3pz} orbital. This increases the localisation

in the ring as is seen from measurements of the partition bond overlap

where the values for butadiene are included for completeness. This is in

accord with the chemical properties of these molecules. viz the increased

diene character.

Two main conclusions can be drawn from these results in comparison

with those for the analogous thiirene series.

a). Whereas introduction of oxygen at sulphur stabilises the

thiirenes by reducing the $\tilde{n}$-$\tilde{n}$ repulsions (antiaromaticity) and lowering

the susceptibility to one electron oxidation the reactivity is increased

in the thiophene series as the diene nature is increased and the

aromaticity reduced.

b)   There is a natural tendency then to rationalise the large difference in the magnitude and direction of the barriers in the thiirene and thiophenes in terms of these two factors.   Though superficially this is correct it is important to recognise the contribution from the C-C bonding in the thiirenes is of comparable importance.

CHAPTER IV.

Studies of some Group V Heterocycles derived from Pyridine.

Introduction

The modification of the electronic structure and reactivity consequent on replacing a CH group by N in going from benzene to pyridine (I) is of considerable interest. Further, the recent synthesis of the corresponding phosphorus (II) and arsenic (III) analoges of pyridine[150] has raised additional points of interest, more particularly concerning the variation in energies of the outer valence levels. In this chapter these somewhat larger π systems have been examined with consideration to both the above mentioned points. The geometries employed in the calculation are shown in fig.4.1. and are derived from experimental data for pyridine[151] and 2,6-dimethyl-4-phenyl phosphabenzene[152]. The ring geometry for the latter differs insignificantly from that recently determined for phosphabenzene by microwave spectroscopy [153]. For arsabenzene a bond order-bond length relationship together with standard tables of bond lengths was used to estimate the carbon-arsenic bond length, the carbon hydrogen skeleton being derived from that for phosphabenzene. For comparative studies of the three ring systems STO 3G basis sets were employed, augmented by 3d (for P) and 4d (for As) functions for II and III respectively. Standard exponents were taken for carbon, nitrogen and phosphorus atoms appropriate to a molecular[154] environment together with an optimised value for hydrogen derived from studies of benzene[27] (ζ = 1.21) For arsenic, best atom exponents were employed. The valence d functions were chosen employing Burns' rules[155] and gave values for phosphorus ζ = 1.4 and arsenic ζ = 0.95. A more flexible STO 3-31G was also employed for the ground states of I and II , but was not economically or computationally feasible for III or the more detailed studies of the hole states of I. The calculations employed the ATMOL series of

Figure 4.1

Geometries of Pyridine (I), Phosphabenzene (II) and Arsabenzene (III).
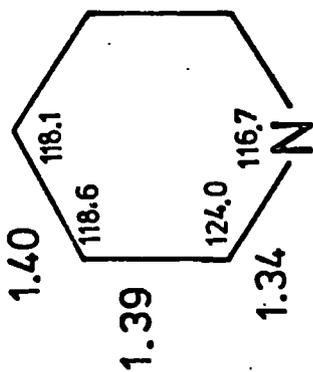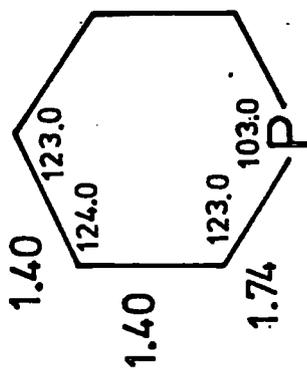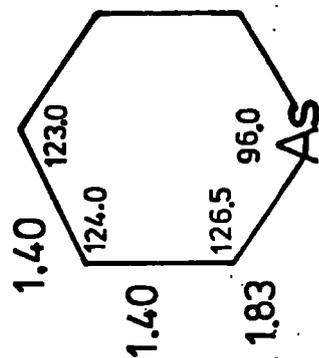
programs on both the ICL 1906a and IBM 370/195 computers.

1). Ground State Properties.

a) Pyridine.

The minimal basis set calculation (total energy - 243.591 au.) and the extended basis set calculation (total energy - 243.819 au.) give energies considerably higher than those reported in the literature due to Clementi[156], Petke[157] and Roos and co-workers[158]. This is due to the limited gaussian expansion of Slater orbitals inadequately describing the cusp regions of the 1s type core orbitals. First order energy considerations though will not be of importance in this section. For the valence electron distribution, the basis sets used here should be comparable to those of Clementi's and Roos's respectively.

As a rough guide to the overall electron distribution in I, II and III, Table 4.1. shows the results of Mulliken population analysis for the comparable STO 3G basis sets. For pyridine it is clear that the nitrogen is an overall electron acceptor for both σ and π systems. For the σ system this arises predominantly from electron migration from the adjacent (ortho) CH groups whilst the build up of π density at nitrogen is accompanied by a decrease at the C_γ (para) and C_α (ortho) carbon atoms. It is notable that the decrease in π density at C_γ is more than double that at C_α and this may be attributed to the larger density at the former.

The populations for the hydrogens are essentially the same. It may naively be argued therefore that (α) substituents should produce a substantial perturbation to the σ system whilst substituents at the γ positions should influence the π system rather more. This receives

Table 4.1.   Mulliken Population Analysis of I, II, III.

	I	II	III
X	6.97	11.788	23.735
(=N,P,As)	1.055	3.034	9.459
	7.252	14.822	33.195
d. Population	–	.350	10.306
C	4.943	5.106	5.189
	.990	1.015	.870
	5.933	6.130	6.061
C	5.042	5.077	5.067
	1.001	.929	.922
	6.043	6.006	5.989
C	5.059	4.999	5.058
	.963	1.058	.952
	6.022	6.057	6.009
H1	.954	.974	.928
H2	.955	.966	.945
H3	.955	.970	.946
overlap densities			
X–C	.257	.282	.316
C –C	.254	.241	.227
C –C	.254	.249	.240

some support from recent low energy photoelectron studies of chloro[159]

and fluoro[160] substituted pyridines but further discussion of the

orbital energies will be deferred till later.

To reinforce an earlier comment concerning the delocalised nature

of the natural orbitals a density contour plot for the 'lone pair'

orbital is shown in Figure 4.2. This clearly indicates that although

there is a considerable degree of localisation of the 'lone pair' there

are significant contributions from other atoms.

b).Phosphabenzene and Arsabenzene.

The calculations on II were performed using three different basis

sets and the results are shown in Table 4.2. There are several features

of interest. Firstly, addition of the 3d functions on the heteroatom

(basis set 2) lowers the energy by a relatively small amount

(0.07 au in 526 au.), especially when compared with the further

lowering in energy of ~ 0.03 au upon addition of the s(d) function.

This suggests that these functions merely serve to increase variational

freedom of the basis set. That these d orbitals are mainly acting as

polarization functions for the valence sp basis set is clearly

demonstrated by an analysis of the electron distribution on phosphorus.

The d orbital population on phosphorus for basis set 3 (Table 4.2.)

(.567e) contrasts with the increased total population compared with basis

set 1 (Table 4.2.) (.25e). Similar considerations are expected to apply

to III. These findings are contrary to those of Schweig and co-workers[161]

though the semi-empirical CNDO/2 calculations are now known to

overestimate the contribution of d orbitals at this level of approximation.

The results of the population analysis for I, II and III (Table 4.1.)

show a decreasing σ electron density at the heteratom in the order

Figure 4.2

Density plot of the $a_1\sigma$ 'lone pair' orbital of pyridine in the molecule plane. Contours are ·001, ·005, ·01, ·03, ·06, ·10, · 15 a.u.
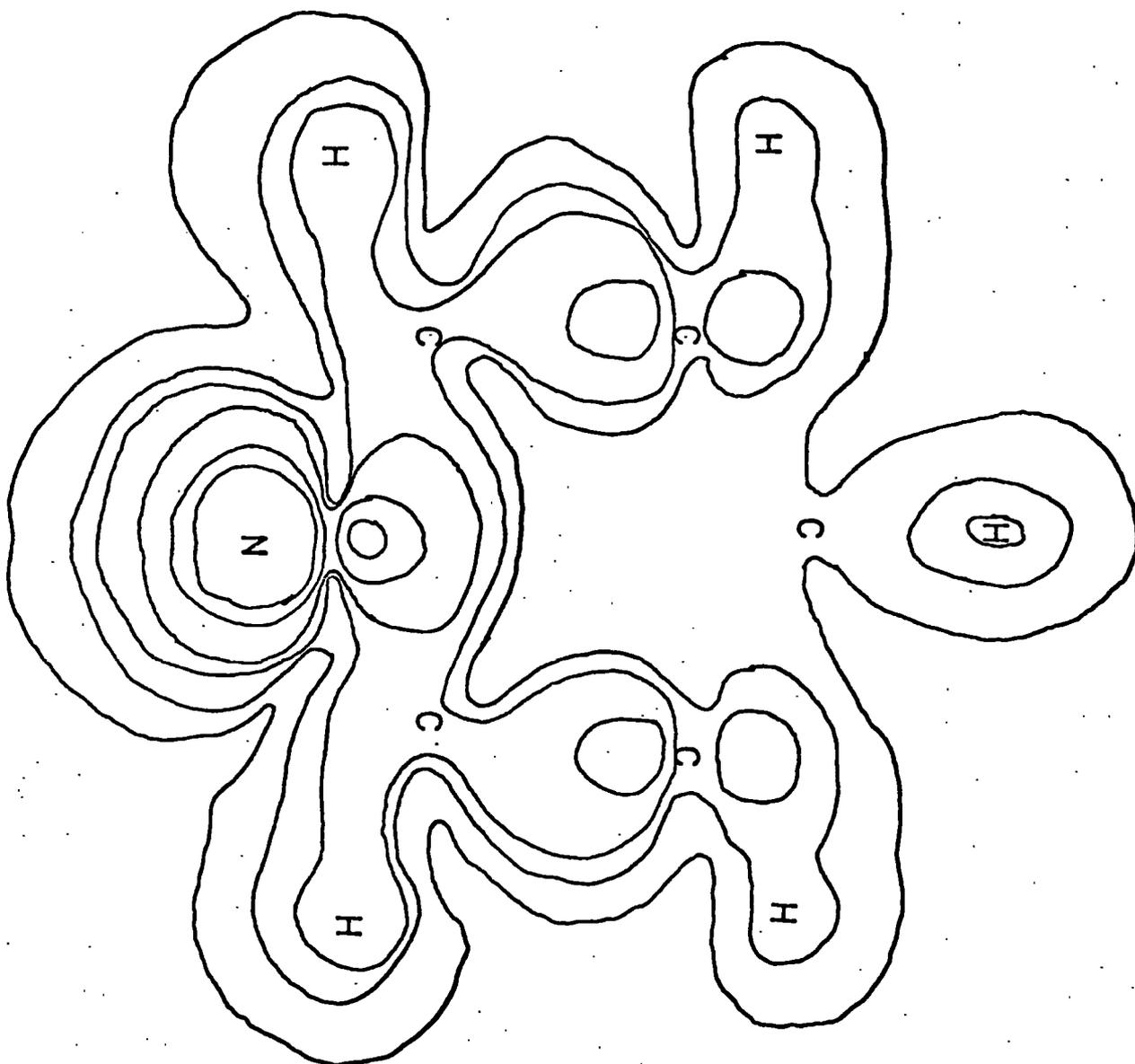
I > II > III; thus for pyridine the overall N σ charge is negative whilst for phosphabenzene and arsabenzene the heteroatoms are now overall σ electron donors to the adjacent CH groups. Quantitatively it can be seen that the changes in population in going from I to II are greater than for II to III. This is reasonable in the light of simple electronegativity considerations (N 3.04, P 2.19, As 2.18)[162].

The valence π electron densities at the heteroatom follow the unexpected order As>N>P . This is probably an artifact of the Mulliken analysis. The radial maxima for the relevant valence orbitals are for I, II and III (e.g. for 2s, 3s and 4s 1.10, 1.70 and 1.78 au respectively for N, P, As) This increase of size has two probable consequences concerning the analysis. Firstly, there will be increasingly arbitrary division of overlap densities between the atoms with increasing 'size' differential between the orbital involved. Secondly, and probably of more importance, as the location of the radial maxima moves further away from the nucleus the concept of apportioning charges to atoms in a molecule becomes more tenuous in absolute terms. For this reason more reliance was placed here on relative populations within each molecule rather than between similar sites in different molecules.

With the above consideration it is probably quite significant that the electron populations on carbon in II and III follow the order C_β(meta) < C_γ(para) < C_α(ortho) which is the exact opposite of that calculated for I. The π electrons themselves exhibit a similar though somewhat less precise order. A clearer indication is given by the π overlap population. The increased bond localisation in the series I to III is clearly evident. For example, the C_α-C_β bond overlap decreases

Table 4.2.   Energies and d Populations for II and III.

	Basis Set	(1) Minimal	(2) +5D	(3) +6D	(4) STO3-31G + 6D
Total Energy II (a.u.)		-526.5450	-526.6154	-526.6450	-526.9732
Total Energy III(a.u.)			-2401.7099		
Total Popn. at P in II		14.590	14.822	14.841	
d Popn. at P in II		-	0.350	0.567	

Table 4.3.   Valence Orbital Energies and Ionization Potentials for the Highest Molecular Orbital of each Symmetry of I,II,III.

Orb.	El. reorg I α	π	I Exp.	ϵ	Hole	II Exp.	ϵ	Hole	III Exp.	ϵ
a_2	1.58	0.04	9.8	8.15(9.09)	7.52	9.8	7.89(8.21)	8.57	9.6	8.66
b_1	1.28	0.39	10.5	8.69(9.80)	7.98	9.2	6.41(9.20)	7.74	8.8	7.41
a_1	1.21	0.75	9.7	9.09(10.40)	6.58	10.0	8.37(9.79)	-	9.9	8.78
b_2	1.02	0.35	12.5	12.54(13.53)	12.09	11.5	10.84(12.35)	12.0	11.0	11.21

ϵ ≠ Koopmans' Values

with respect to the C_β- C_γ and C_α-heteroatom bond overlap in the series. Though the chemistry of II and III are still relatively unexplored experimental evidence indicates an increase in the diene -like character in the same order (I < II < III)[163].

The computed dipole moments for I and II with the split basis sets are 2.14D and 1.75D respectively. These are in excellent agreement with the experimentally determined values of 2.2D[164] and 1.55D[165] both in magnitude and direction. The single zeta basis though gave less satisfactory values of 2.0D for I, 0.54D for II and 3.18D for III, the latter value again being an artifact of the basis with regard to arsenic.

The computed decrease in the s:p ratio in the lone pair orbital not only affects the dipole but will also have a profound effect on the basicity. The point charge model was thus employed (including electronic relaxation) to shed further light on this field. Two reaction paths were taken in which a unit positive charge, simulating the proton, approached the heteroatom, either in the σ plane along the C_2 axis or along the p_z axis of the heteroatom. The variation in energies for these two approaches are shown in Figure 4.3.

There are two main factors affecting the energy profile. Firstly, in the σ plane the approach of the unit charge is 'steeper' in I due to the less polarisable 'harder' lone pair of nitrogen compared with II. At shorter distances a greater relative interaction occurs at N: thus protonation in the σ plane is more favourable for I. Secondly, the smaller loss of aromaticity and the polarizability of the p_z orbital renders II more favourable to π attack than I.

From the position of the energy minima an estimate can be made of the relative aromaticity of II. This should be related to the difference

Figure 4.3.   Approach of Point Charge to Heteroatom in Pyridene and Phosphabenzene.

Point Charge — Heteroatom Distance.
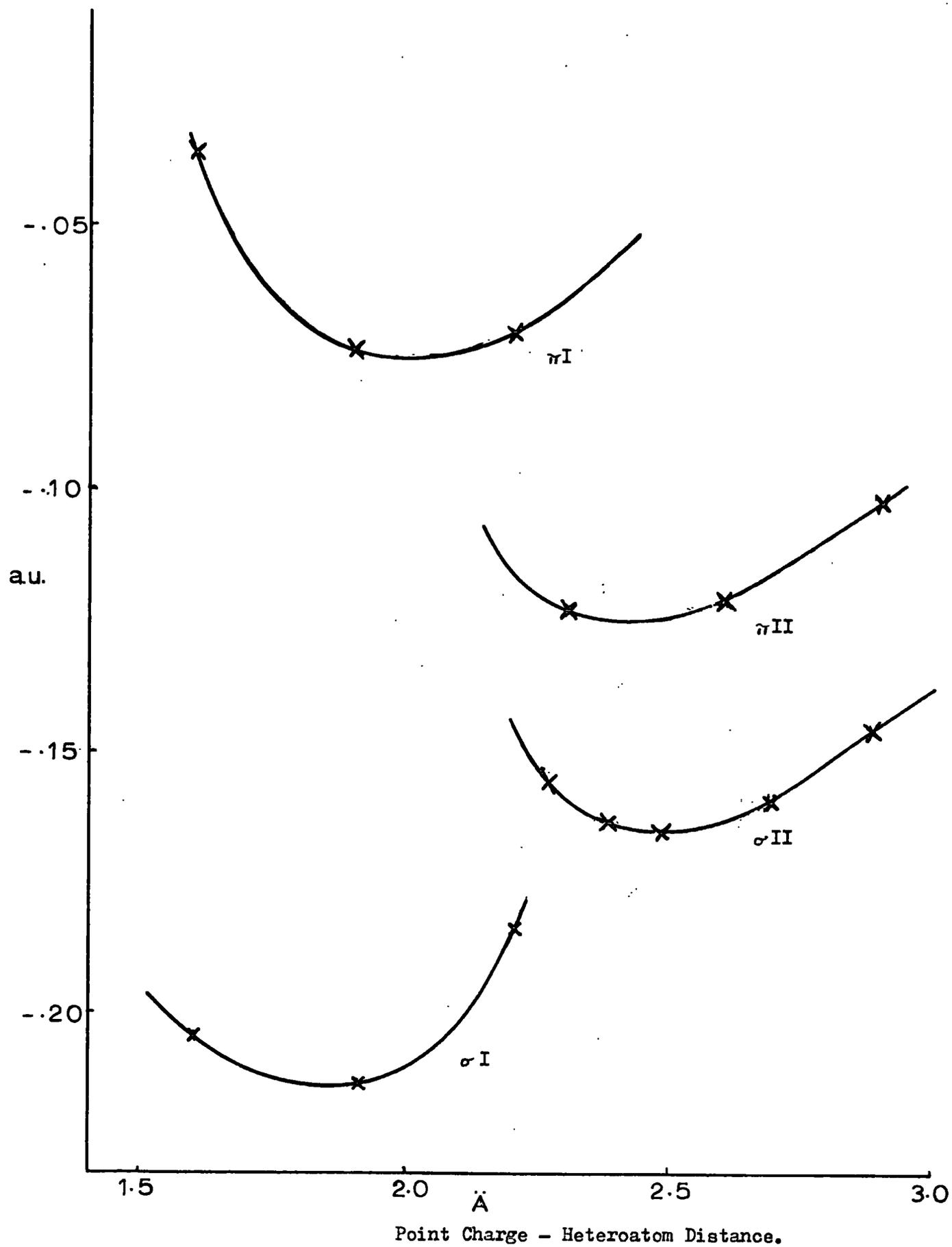
in energy between the minima for σ and π protonation. The value for

I ($\sim$85 Kcal mole^{-1}) is considerably reduced in II ($\sim$25 Kcal mole^{-1}) and

is hence anticipated to be less than for III.

c). Electrophilic Attack.

The point charge model was employed to simulate the approach of an

electrophile (H^{+}) to the three trigonal carbon sites in pyridine. The

result of this addition was anticipated to lead to a structure related

to the 'Wheland Intermediate'[166]. A hypothetical reaction path for this

formation is the approach of the unit charge along the 'Wheland axis' of

one of the C-H bonds with the out-of-plane bending of the other hydrogen.
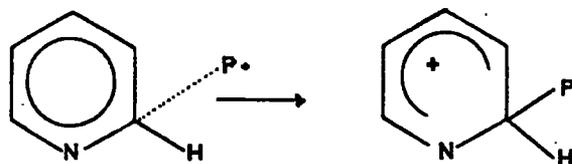
At long range this out-of-plane bending is expected to be small. Points

on the reaction surface for approach of the point charge to the α, β

and γ carbons of planar pyridine were thus computed and the energy

profiles are shown in Figure 4.4. There is a slight activation energy of

the order of 1.2 Kcals at large internuclear separation. The energy drops

quite rapidly as shorter range interactions become dominant and the order

$\alpha > \beta > \gamma$ is inferred from the minima. At these distances however ($\sim$1.4A)

the model will not be valid as both out-of-plane bending and the

contribution from the point charge '1s ao' will not be insignificant.

In the classical model of protonation the positive charge is assumed

to be delocalised over the ortho and para ring positions as indicated below.
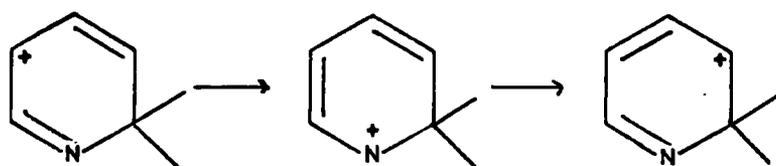
Figure 4.4.   Approach of Point Charge along Wheland Axis to Pyridene.

Point charge – Carbon Distance (along Wheland Axis)
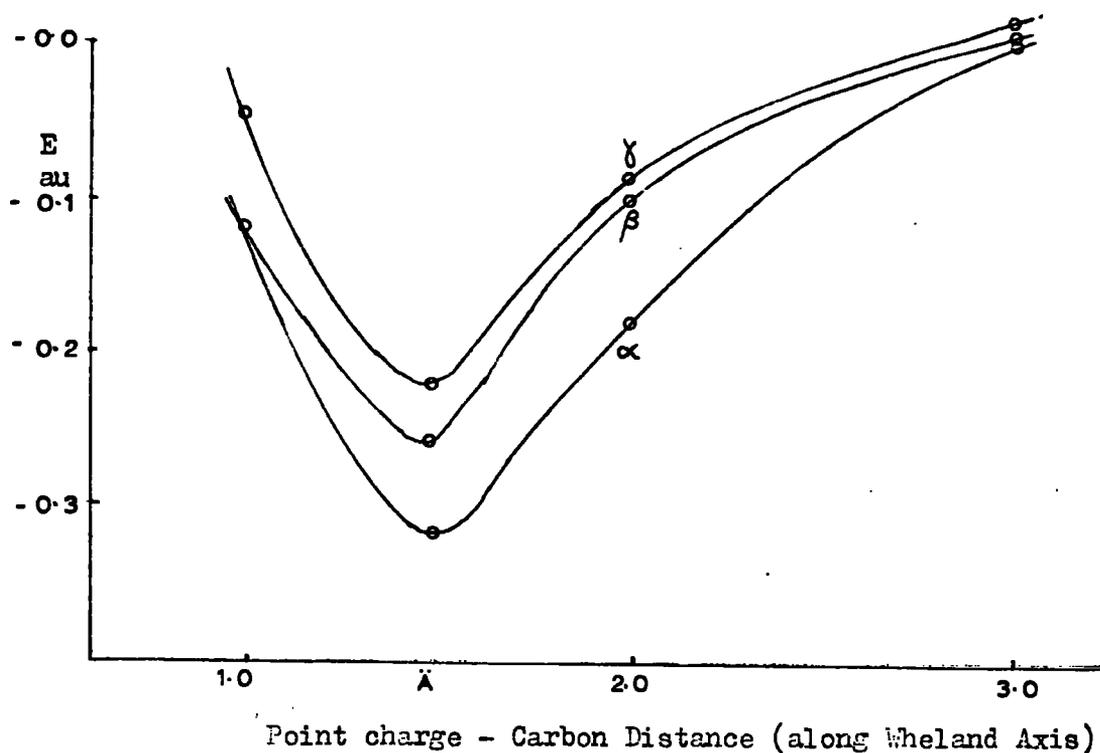
Figure 4.5.   Change in Electron Density (σ/π) with Point Charge
2.0Å from α, β, γ C of I (–ve indicates loss e.)
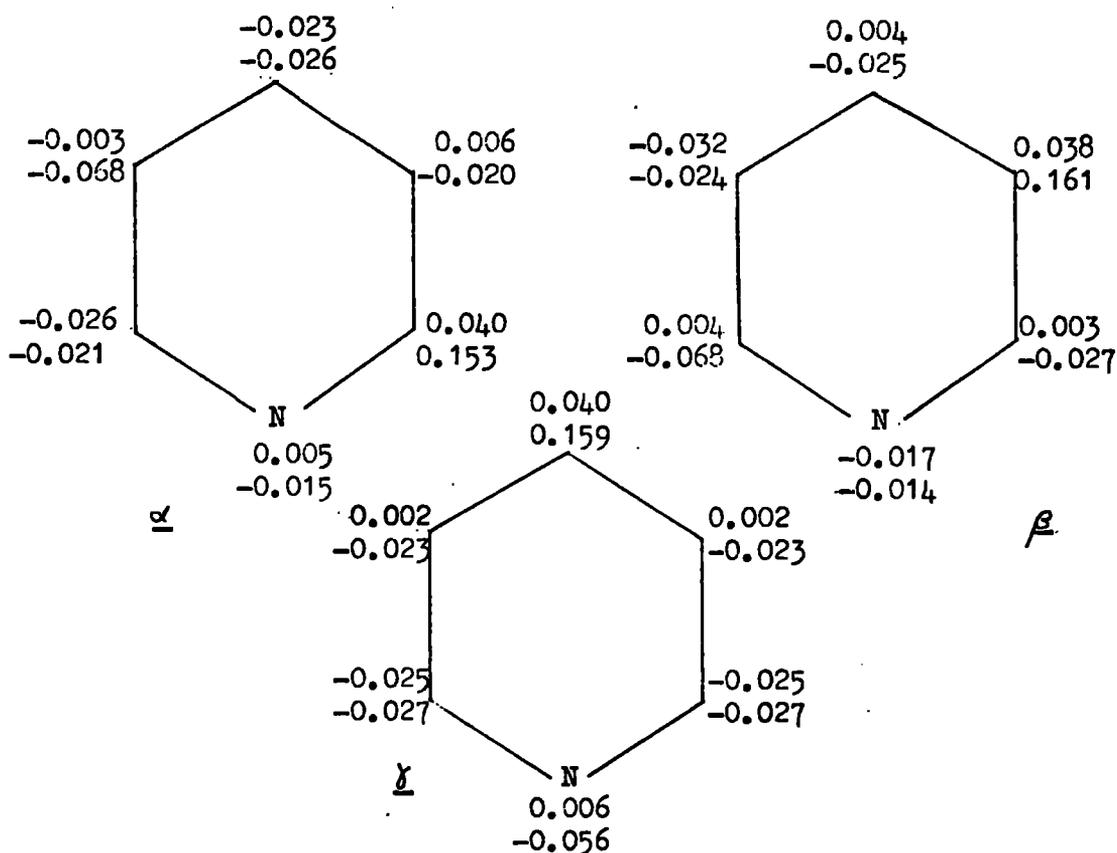
Figure 4.6a. Density Difference Map Point Charge 2.0A from
X C in I (in Molecular Plane).
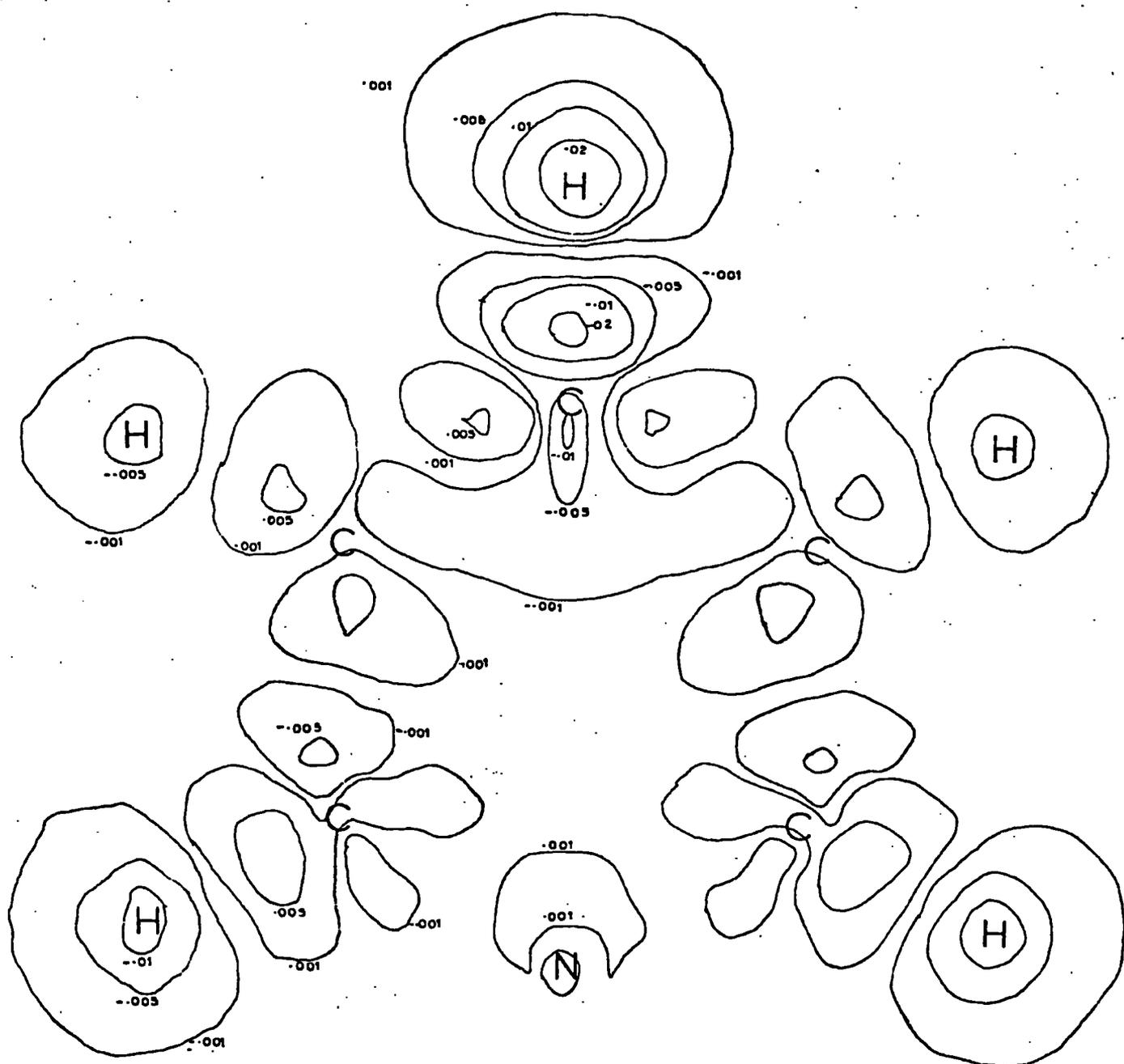
Figure 4.6b.   Density Difference Map Point Charge 2.0Å from
δ C in I (1.15Å above Molecular Plane).
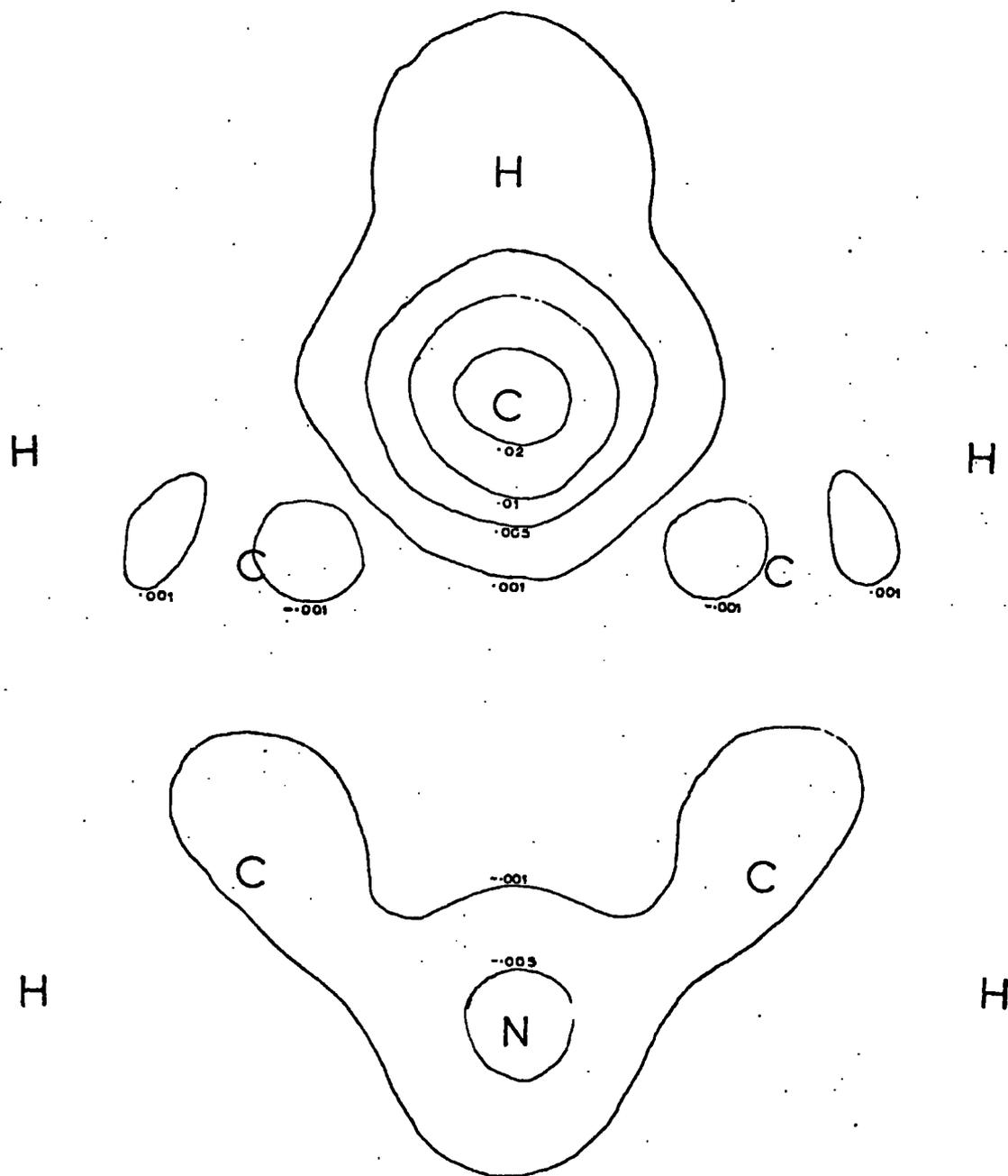
The movement of charge in the substrate with a point charge carbon separation of 2.0Å was taken to investigate this electron rearrangement. Though this will be somewhat deficient in representing the Wheland structure it should give an indication of the type and degree of electronic rearrangement consistent with the approach of an electrophile. The change in σ and π charge is shown in Figure 4.5. There are a number of points of interest. Firstly the approach of the unit charge to the β position gives the greatest increase in p_z electron density compared with the α and γ attack. In the ground state the β carbon also has the largest p_z electron density; overlap in forming the new bond will be largest at the β carbon.

The increase of π density at the site of attack is accompanied by a decrease in π density at the other sites in the order para $\gg$ meta$\sim$ortho. Clearly, substituents in the para position, where the chnage in π density is greatest will thus have a profound effect on the π electron distribution. This is in agreement with the properties of para substituents in phenyl ligands in for example transition metal complexes. The relatively small change in π density at the ortho sites can be readily understood in terms of this polarization of the π cloud by the point charge. Thus the atoms remote from the perturbation, but still directly conjugated to it show the largest changes in electron density. This is well illustrated in Figure 4.6. by plotting density difference maps in the molecular plane and at a distance above it (1.15Å) (corresponding to the radial maxima of a carbon 2p ao) for a point charge – carbon distance of 2.0Å at the carbon para to nitrogen.

An alternative view of this study is to examine the changes in electronic structure which occur for α, β, γ position of the nitrogen in

the point charge-ring.   With N in the γ position to the point charge

the flow of π electrons is accentuated with respect to C due to the

greater electronegativity of nitrogen.   The β position to the site of

attack by the point charge however gives the largest loss in σ

electron density, the σ electron flow to the adjacent atoms aiding the

movement of π charge to the site of attack.   This interplay of σ/π

charge will also be apparant in the next section in ionisation of

valence π levels.

2).   <u>Core and Valence Energy Levels.</u>

Both high energy (ESCA) and low energy (UPS) photoelectron

spectroscopy provide powerful tools for investigating structure and

bonding.   Conversely the data arising from these investigations

provide a critical test of theoretical treatments.   These quite large

systems exhibit some most interesting properties and a detailed

analysis was thus undertaken to shed further light on the ionizations

of I, II and III.

a).   <u>Valence Ionization.</u>

A confirmation of previous assignments of the UPS spectra of I,[9,167-8]

II, III has been obtained[169] from correlations with ionization potential

data for the free heteroatoms and their hydrides[170].   The ionization

potential of the top $b_1\pi$ occupied orbital of I, II, III should correlate

with the ionization potential of the free atoms X = N, P, As, Sb ($^4S_{3/2} \rightarrow\ ^3P_0$)

N,14.53; P,11.0; As,9.81; Sb,8.64eV respectively, the data for antimony

complementing that for I, II, III.   A linear least squares fit yielded

the relationship

$$IP\ (b_1\pi)\ =\ 5.24\ eV\ +\ 0.362\ IP(X) \qquad r\ =\ .9998$$

As indicated by the correlation coefficient (r) the regression is

almost perfect. Further for IP (C) = 11.26[159] a value of 9.32 eV is obtained for the corresponding (first) ionization potential of benzene (experimental 9.24[171]). Similarly by employing the ionization of the lone pair orbitals of NH_3, 10.9; PH_3, 10.6; AsH_3, 10.5; SbH_3, 10.0 eV, these may be correlated with the corresponding $a_1\sigma$ 'lone pair' orbital in I, II and III. A semi-empirical study by Schweig and co-workers is also consistent with this interpretation[172]. It is of considerable interest however to determine the basis for the variation in these valence orbital energies of I, II and III.

As a first step in the theoretical study, the four highest valence ionization potentials of I, II and III were computed from the ground state calculations employing Koopmans' theorem. From the results (Table 4.3.) a reversal in the ordering of the $a_2\pi$ and $b_1\pi$ orbitals is observed in going from I to II and III. This is consistent with much of the character of the heteroatom discussed above, the increased size and decreased electronegativity will tend to destabalise the $b_1\pi$ orbital.

The $a_2\pi$ orbital has a node passing through the heteroatom. Its orbital energy should not vary therefore, at least to first order, upon change of the heteroatom (with different basis sets this will not necessarily be reflected). If this orbital is taken as a standard then the $a_2\pi$ $-a_1\sigma$ separation derived from Koopmans' theorem is seen to decrease from 1eV for I to .1eV for III. Experimentally there is very little difference in separation (~.2eV) in going from I to III with the $A_1^2\sigma$ being the lowest energy state in I. With the double zeta

basis and from other studies in the literature[156-158] the 'lone pair'

orbital of nitrogen ($a_1\sigma$) is of lower orbital energy than either the

$a_1\pi$ or $b_1\pi$. This consistency for all of these calculations

shows that the result is not basis set dependent. This suggests

therefore that there may well be large differences in the re-organisation

and/or correlation energies for ionizations from the highest σ and π

orbitals.

In the particular case of I and II, this was investigated

by performing calculations on the valence ionized states. This proved

to be a very intricate process unlike the core hole state calculation

discussed in the next section. Convergence to the required state was

not always guaranteed, especially when another state of the same

symmetry and similar energy to that required existed. Starting vectors

from the ground state were employed and convergence was accentuated by

judiciously chosen values of the missing coefficients between the three

classes of orbitals (doubly and singly occupied and virtual) employing

the SCF method , Hillier and Saunders[15]. For the first ($^2A_2\pi$)

state of pyridine a convergence limit of 10^{-5} in energy was reached in

91 cycles.

Considering firstly the results for pyridine, for the $a_2\pi$, $b_1\pi$

and the $b_2\sigma$ ionizations there is relatively little change in energy.

The ionization from the $a_1\sigma$ orbital is however appreciably lowered in

energy and the order is now in accordance , - though somewhat

overestimated, with that experimentally observed. Clearly there must

be considerable electronic re-organisation to account for this charge.

Further insight into this re-organisation was gained by comparing

the deviations in the atomic orbital populations at each centre for the

the unrelaxed and relaxed cationic species.   With the nomenclature
of equation 2.5.

$$q_\mu = P_{\mu\mu} + \mu \sum_{\mu \neq \nu} P_{\mu\nu} S_{\mu\nu}$$

If an electron is removed from orbital k the expression becomes

$$q_\mu = 2 \sum_{i \neq k} c_{\mu i}^2 + 2 \sum_{\nu \neq \mu} \sum_{i=k} c_{\mu i} c_{\nu i} S_{\mu\nu} + c_{\mu k}^2 + \sum_{\nu \neq \mu} c_{\mu k} c_{\nu k} S_{\mu\nu}$$

For the unrelaxed ion the wavefunction for the neutral molecule
was taken and the analysis carried out with a single occupancy of
orbital k .   Similarly for the relaxed ion the valence hole state
wavefunction was employed.   The electronic re-organisation was then
given by (Table 4.3.).

$$\text{El.reorg.} = \sum (q_\mu(\text{relaxed}) - q_\mu(\text{unrelaxed}))$$

There is an approximate correlation between the energy of
re-organisation (E.reorg) and El.reorg. during relaxation.   This
relationship will be complex however as a greater energy charge will
be involved for variations in the populations of nitrogen than at
carbon as indicated for the $^2A_1 \sigma$ and $^2B_2 \sigma$ states.   The relative
magnitudes do however indicate the important re-organisation from
electrons in symmetries other than those undergoing ionization.   This
is strikingly so for the $^2A_2 \pi$ state where almost the whole of the
charge is due to the σ electrons.   Closer examination reveals that this
is composed of a considerable (50%) drift of σ electron density from
the C_α and C_β hydrogens to the carbon atoms to relieve the loss of
electron density: σ donation aiding π ionization.

Figure 4.7a.   Density Difference Map (Hole State -Ground State) in
            Molecular Plane for $^2b_1$ Ionisation I (Contours 1-6
            -0.03, -0.02, -0.01, 0.01, 0.02, 0.03).

Figure 4.7b.   Density Difference Map (Hole State – Ground State) in
Molecular Plane for $^2a_1$ Ionization I (Contours 1-6
–0.03, –0.02, –0.01, 0.01, 0.02, 0.03).
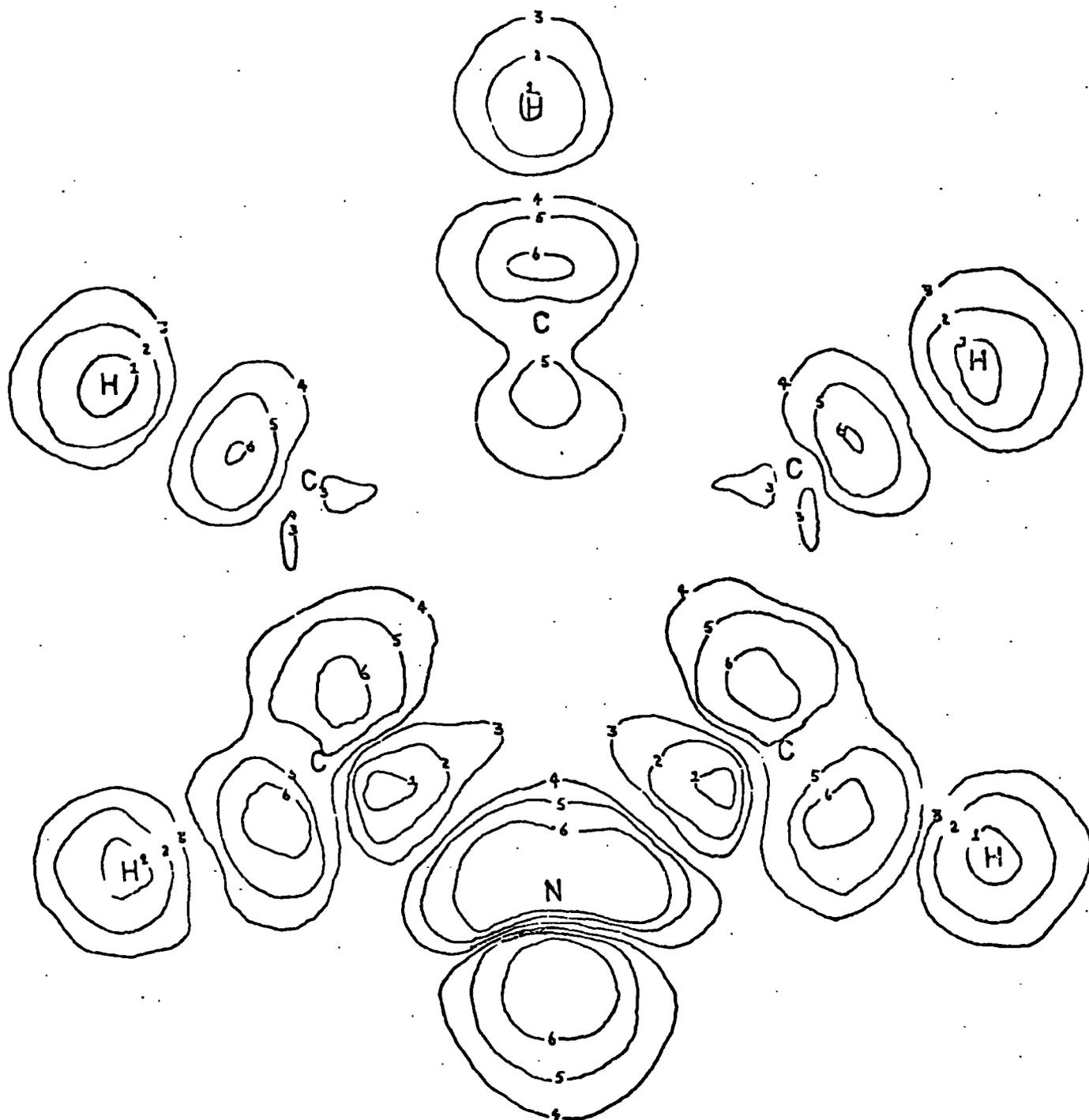
A clearer indication of the manner of this re-organisation is given by plotting the density difference maps between the unrelaxed and relaxed species. Thus for the $^2B_1\pi$ and $^2A_2\pi$ states this σ drift (.458e and .472e respectively) is seen to be considerable (Figure 4.7.) The $^2A_1\sigma$ state displays considerable re-organisation at the nitrogen. There is a net loss from the N_{2py} orbital of .640e but this is partly offset by an increase for the 2pz orbital of .380e . There is also a considerable change in the electronic structure in the rest of the molecule.

For II the hole state calculations give higher energies for the relaxed ion than that anticipated from the orbital energies. These values for the single zeta calculation are however quite low in absolute terms as a result of the minimal basis. The ordering and relative separation are in good agreement with the UPS results.

Though the Koopmans' theorem for valence ionization has been seen to be defficient in the strong form i.e. no re-organisation, it can be employed with most encouraging results in a weak form where studies are made of related molecules. This can be well illustrated by considering the divergence of the double zeta orbital energies from those of spectroscopic studies. The agreement is good except for the $^2A_1\sigma$ state where different re-organisation energy for the N and P 'lone pairs' are expected.

b)   Core Ionization.

When a more localised electron is ionised a considerable amount of electronic re-organisation is anticipated to result. To qualify this,

for core ionization, binding energies were computed from Koopmans'
theorem and hole state calculations for I. These have been compared
with solid state ESCA measurements in this laboratory where
assignments were made in terms of Koopmans' theorem and the charge
potential model viz: ground state models[173]. The results are
displayed in Table 4.4. with due account taken of the difference in
reference levels.

The relaxation energies for the C_{1s} levels though quite substantial
(10.7eV) are essentially constant at the different sites within the
molecule. Further, the absolute binding energies from the hole state
calculations are in excellent agreement with experiment. In a similar
manner to the above, the valence electronic relaxation accompanying core
ionization was computed. This is now much larger (~3.6e) than the
re-organisation from valence ionization. It is more convenient and
conceptionally useful to display this relaxation in terms of movement of
σ and π charge as shown in Figure 4.8. The striking feature is the
large net migration of electron density in both the σ and π systems to
the atom on which the core hole is localised. The most interesting
result is a considerably greater population at this site due to the
greater potential field of the now less efficiently screened nuclear
charge. Further, the π electron redistribution for σ core ionization
constitutes 40% of the total change.

Intermediate between the localised core holes and the delocalised
valence hole states are the hypothetical delocalised holes. These
were investigated by delocalising the singly occupied molecular
orbital over the $\alpha(\alpha')$ and $\beta(\beta')$ C_{1s} orbitals to represent the C_α and C_β

132.

Figure 4.8. Change in Electron Density (σ/π) for Core Ionization of I (-ve indicates increase e density).
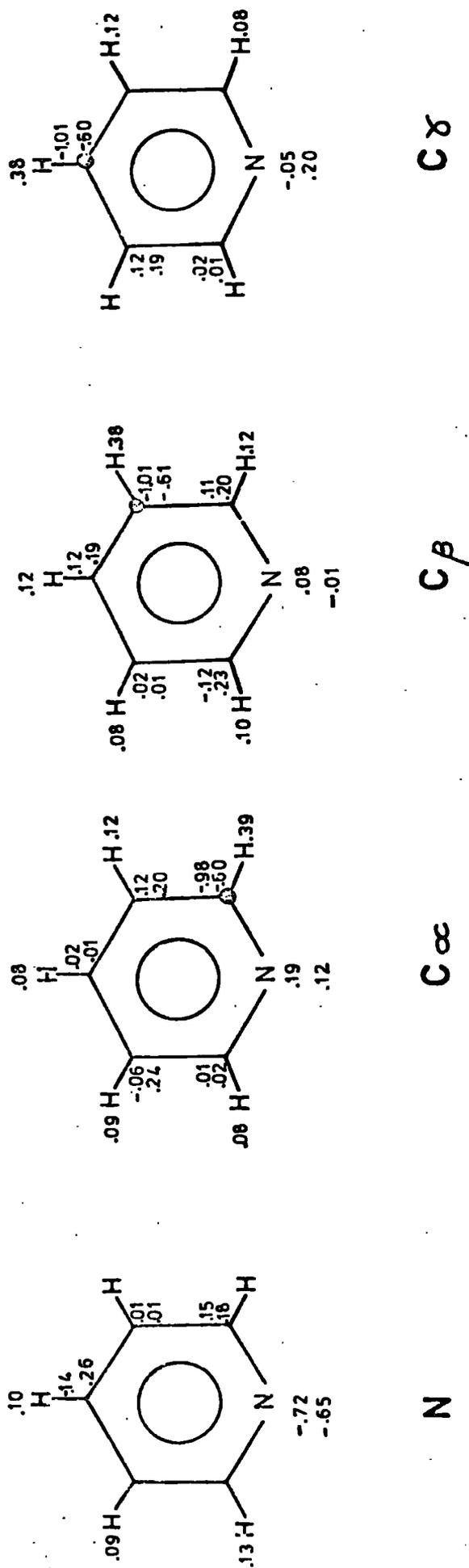
Table 4.4. Core Orbital Energies & Ionization Potentials of 1s Orbital
for I, II, III.

Core Hole	exp.[b]	I(eV) $-\epsilon_j$	Hole	II[a](eV) $-\epsilon_j$	III(eV) $-\epsilon_j$
N	404.2	417.21	405.31		
C	290.3	301.16	290.48 (296.15)[c]	298.75	301.08
C	289.5	300.33	289.47 (295.22)[c]	300.22	301.48
C	289.9	300.62	289.79	299.51	301.25

a   Basis Set (2) Table 4.2

b   Values taken from Ref. 173 with solid state correction of 4 eV.

c   Values in parenthesis refer to delocalised hole state
calculations.

delocalised holes respectively. The results from Table 4.4. clearly
show that energetically localised holes are preferred. This is in
agreement with the results from similar studies of smaller systems.
There is also quantitative support for the proposal that delocalised
holes over t centres will produce a hole charge of $1/t$ for that of a
localised hole with a corresponding decrease of $1/t$ in the total
re-organisation energy[174].

In light of the success of Koopmans' theorem for I it may be
reasonable expected that such an approach extends to II and III. The
ordering of the core binding energies is now inverted with respect to
I and the separation becomes less distinct. The reduction in
electronegativity of the heteroatom thus influences not only the
valence electronic structure but also reflects in the relative energies
of the core levels of I, II and III.

c).Correlation Energy Considerations.

For the core levels considered above the close agreement between theory and experiment tends to indicate that correlation energy differences between the neutral molecule and core hole states must be quite small. For valence levels there is still considerable divergence between theory and experiment. The different spatial distribution of the electrons between different valence orbitals will lead to differences in correlation energy changes upon ionization. An attempt was made to estimate this contribution by means of the pair population method.

From equation 1.111.

$$E_{corr}^{intra} = \sum_i \frac{1}{2} \rho_i \varepsilon_{ii} + \sum_{i<j} \varepsilon_{ij} \rho_i \rho_j$$

This expression however, applies strictly to closed shell systems. An estimate for the hole state correlation energy was obtained by taking ρ_i as the total ao electron density in the expression

$$\Delta E_{corr}^{intra}(\text{hole state}) = \sum_i \frac{1}{2} \rho_i \varepsilon_{ii} + \sum_{i<j} \rho_i \rho_j \varepsilon_{ij} - \sum_i \frac{1}{2} \rho_{ki} \varepsilon_{ii}$$

where ρ_{ki} is the electron density of the singly occupied molecular orbital k . The last term will compensate to some extent for the hypothetical correlation of the $\frac{1}{2}\alpha$ and $\frac{1}{2}\beta$ electrons in the singly occupied MO being absorbed into the first terms. The atomic pair correlation energies (ε) are taken from Snyder and Basch[66].

The results (Table 4.5.) for the STO-3G basis indicate that electron correlation changes are likely to be considerably smaller for core as opposed to valence ionizations. Though the number of electron pairs is reduced upon ionization, the large increase in electron density in the vicinity of a core ionized atom is more than sufficient to

TABLE.4.5. Comparison of Calculated and Experimental Core and Valence Ionization Potentials of I Corrected for Correlation Effects.

Hole	E_{corr}(eV)	$(E_{hole} + E_{corr})$(eV)	E_{exp}(eV)	*(eV)
a_2	1.45	8.97	9.8	0.8
b_1	1.53	9.51	10.5	1.0
a_1	1.49	8.01	9.7	1.6
b_2	1.30	13.39	12.5	-0.9
N	.11	405.44	404.2	1.2
C	.27	290.75	290.3	0.5
C	.19	289.66	289.5	0.2
C	.27	290.06	289.9	0.2

compensate for this loss in E_{corr}^{intra} .

With the above corrections the agreement between the calculated and experimental valence ionization potentials is improved. A more flexible basis would however account for some of the discrepancy as spatially similar orbitals appear to exhibit a similar divergence.

CHAPTER V.

Studies of Thiathiophthen.

In this chapter the most interesting thiathiophthen system is considered. These molecules, though first prepared in the 1920's [175] were only structurally characterised in the late 1950's [176], and have since provoked considerable interest in the formulation of the bonding of the S-S-S system where the S-S distances (~2.4A) are considerably shorter than the sum of their Van de Vaal radii (~3.1A). This bonding pattern in the neutral molecule, radical anion and dianion and effect of change of geometry in the triatomic sulphur unit have been investigated together with comparison via Koopmans' theorem with ESCA data for the neutral molecule. Substituent effects have also been simulated to determine their likely effect on the electronic structure. It is pertinent to indicate that these studies exhibit an interesting comparison with the above studies of the thiirenes and thiophenes. Whereas for the former little is known of both the chemistry and bonding, the reverse applies to thiophene. For the thiathiophthen system however, though there is a considerable amount of experimental data now available there has been little study of the bonding.

The calculations in this chapter employed the STO-3G basis set optionally augmented by d orbital of exponent 1.2 on sulphur. This basis lacks the flexibility of the basis of Chapter 3 for these very large molecules due to computational expense (integral evaluation on the ICL1906a for thiathiophthen was ~12 hours). The main interest is however in interpreting trends in bonding properties for which this basis has previously been proved adequate.

1)   Introduction

The 6a -thiathiophthen system was only recently discovered in 1958 by Bezzi et al[176] through an X-ray crystallographic study of the 2,5 - dimethyl derivative which had previously been assumed to be a 1,2 dithiepine structure resulting from the reaction of diacetylacetone and P_2S_5 [175]. The sulphur sequence was found to be linear with S-S bond of 2.36Å as compared with the value of 2.10A for the length of a S-S . single bond in a cis-planar disulphide group.   Subsequent experimental investigations on a number of derivatives[177] have indicated an aromatic 10π system and S-S bond lengths which vary greatly with the substituent pattern.   This has most conveniently been rationalised in terms of a σ skeleton comprising C-C and C-S bonds and delocalised S-S σ bonds with a 10π system delocalised over the whole molecule.   The three sulphur sequence is assumed equivalent to that in the trihalide ions and is referred to as a three-centre four-electron bond[178].   This sulphur sequence is then, though both σ and π in character, weak and more liable to change when either the σ or π system is perturbed.

There have been a number of limited theoretical studies on the symmetry of the triatomic sulphur system.   A great wealth of crystallographic data now indicates a linear or almost linear sulphur system and the investigations have either considered displacement of the central sulphur along this line of the centres of the three sulphur atoms (CNDO)[179,180], or by pivoting the central sulphur about C3a(EHT)[181], the latter study by Gleiter being complimented by electronic polarization studies[182].   Though the results are mutually contradictory, the former predicting a broad potential minimum, the latter an unsymmetrical structure with a double minimum, it appears that there is relatively

little difference in energy between these two structures. A

non-empirical study has been reported by Palmer and Findlay[183].

It has proved possible to differentiate between these two

structures by ESCA studies[115,184-186] of the sulphur molecular core

binding energies and these studies of Siegbahn, Clark, Lindholm, Davis,

have yielded valuable information concerning the electronic structure

of substituted thiathiophthen. Studies of the valence energy levels by

UPS where interatomic interactions are at a minimum have also proved

useful[184].

Much is now known of the chemistry of these species. In general

they undergo attack by nucleophiles at C2,C5 and electrophiles at C3,C4.

Reactions involving attack at, or replacement of, a sulphur atom lead to

a variety of products depending on the substrate and provide a method for

the preparation of a wide variety of similar species[177].

Table 5.1.
Total Energies of I, II, III as a function of Basis Set.

Structure	Basis Set*		Energy(au)
I	Minimal	(1)	1368.0253
I	Minimal + 5 d on S	(2)	1368.2207
I	Minimal + 6 d on S	(3)	1368.3092
I	Minimal + 6 d on S6a only	(4)	1368.1093
II	Minimal + 5 d on S	(2)	1368.2207
III	Minimal + 5 d on S	(2)	1368.2196

* Basis Set type in parenthesis.

2). <u>Molecular Structure.</u>

For the symmetrical ring system (I) the geometry established for the 2,5 - dimethylthiathiophthen[176] was employed. To simplify the calculation a prototype unsymmetrical structure (II) was generated by displacing the central sulphur 0.1Å towards S6 along the line of the three sulphur atomic centres. This difference of 0.2Å between the S6a–S6 and S6a–S1 bond lengths corresponded quite closely to that found in 3,4 diphenylthiathiophthen[187]. An extreme distortion of the central sulphur of 0.2Å was also considered (III).

The results (Table 5.1.) emphasize the very small energies that are likely to be involved in distortion of the central sulphur. Further comment cannot be made on the basis of the energies however as the geometry for the remainder of the molecule is unoptimised. Displacement of the central sulphur will certainly result in second order charges, noticably in the C3a–S6a bond length. This result, taken in conjunction with the semi-empirical data mentioned above indicates that not only intra-molecular perturbations but also intermolecular forces in the crystal lattice may produce non-symmetrical structures. The X-ray crystallographic results, together with the majority of ESCA data refer to bulk properties and as such can only measure the combined effect of these two forces. Spectroscopic studies in the gas plane, where intermolecular interactions are greatly reduced, are therefore required to experimentally determine the structures of the free molecules. At present the accuracy required is difficult to attain.

To elucidate the molecular structure from calculations for substituted thiathiophthens there are two established courses of action which may be taken.

a). A complete calculation for the symmetric and unsymmetric substituted ring system. This will be computationally very expensive.

b). Considering only the symmetric ring calculation the S6a-S6 and S6a-S1 overlaps may be compared, the greater overlap would then be expected to produce the shorter bond. This still involves recalculations of a large number of new integrals involving the substituent group.

For molecules of this size therefore an alternative approach was required. This was based on approximating an effective potential at the atom in the substituent which is bonded to the ring. For example methyl and phenyl substituents are bonded to the ring through sp_3 and sp_2 hybrid orbitals respectively, the latter will in general be lower in energy than the former. The approximation is then to consider only this ring bonding atom and represent its potential by means of an s-type function. By varying either the exponent or the nuclear charge the electronegativity of the substituents as compared with hydrogen may be considered. If the nuclear charge is varied however only the 1 centre integrals require recomputation. An SCF calculation then produces the wavefunction of a model substituted thiathiophthen. This method was therefore adopted. Nuclear charges of 1.03 and 0.97 were taken to represent substituent of greater and lesser electronegativity than hydrogen. Calculations were performed on both the symmetrical and 0.1Å unsymmetrical ring structures for the model substituents C(5). The two structures in each model of I and II are now separated in energy, but only by a very small amount ($\sim$.1 kcal.) These models though predict different structures in accord with position of the central sulphur to

minimise the nuclear repulsion but further investigation of the energy was not considered in view of the comment above.

Attention was focused therefore on the overlaps of the sulphur atoms in the symmetric ring structure. An overlap analysis (Table 5.2.) supports the above energy analysis, the main difference in density occurring in the p_σ-p_σ overlap. With the greater nuclear charge at the H5 site there is a slight decrease ($\sim 0.001e$) at S6 compared with S1. The π. density is however increased by a similar amount. The overall effect then is to replace some σ bond character with π density and thus reduce the overlap. The converse applied with a nuclear charge of .97 at H5 . With this interchange in σ/π bonding it is perhaps not surprising that for 2-phenyl substituents the S-S-S geometry is a critical function of the orientation of the phenyl ring with respect to the molecular plane of the thiathiophthen[180].

3). <u>Electronic Structure</u>

It has been previously mentioned (Chapter 3) , that the structure and bonding in cases where sulphur is formally dicovalent can be well understood without invoking 3d orbital participation. The same analysis for d orbital participation was applied to the symmetric thiathiophthen and results are shown in (Table 5.1.). Addition of the contracted five d basis to the minimal basis set produced a significant energy lowering of .1953 a.u. This is mainly due however to the increased variational freedom of the sp basis set as is shown by the further lowering in energy of .0885a.u. upon addition of the three further s(d) functions. The results from a Mulliken population analysis (Table 5.3.) indicate however a considerably greater d orbital contribution from the central

Figure 5.1.   Total Electron Density Map in Molecular Plane Thiathiophthen
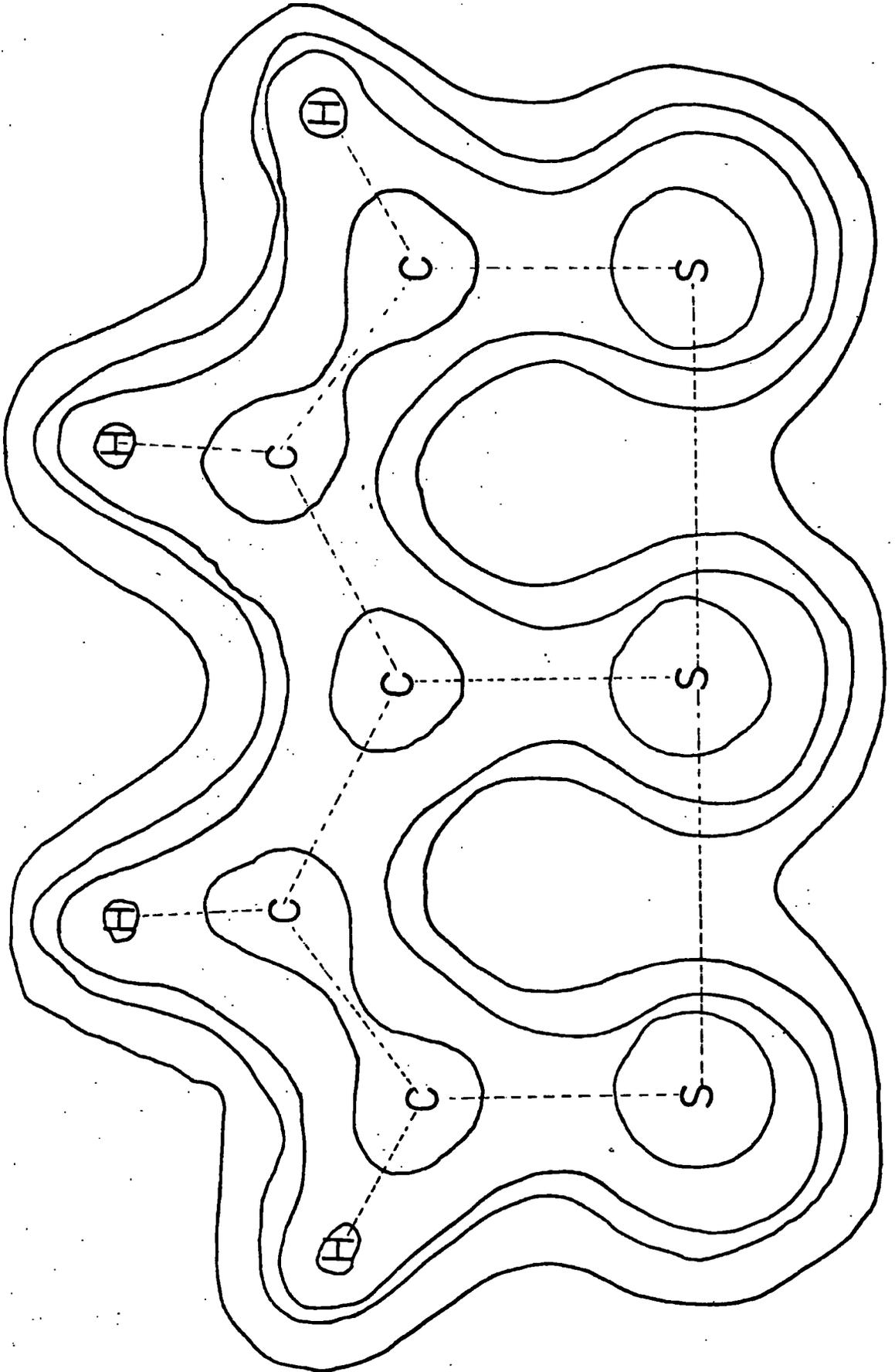
Figure 5.2. Orbital Interaction Diagram for S – S – S 3 Centre Bond.
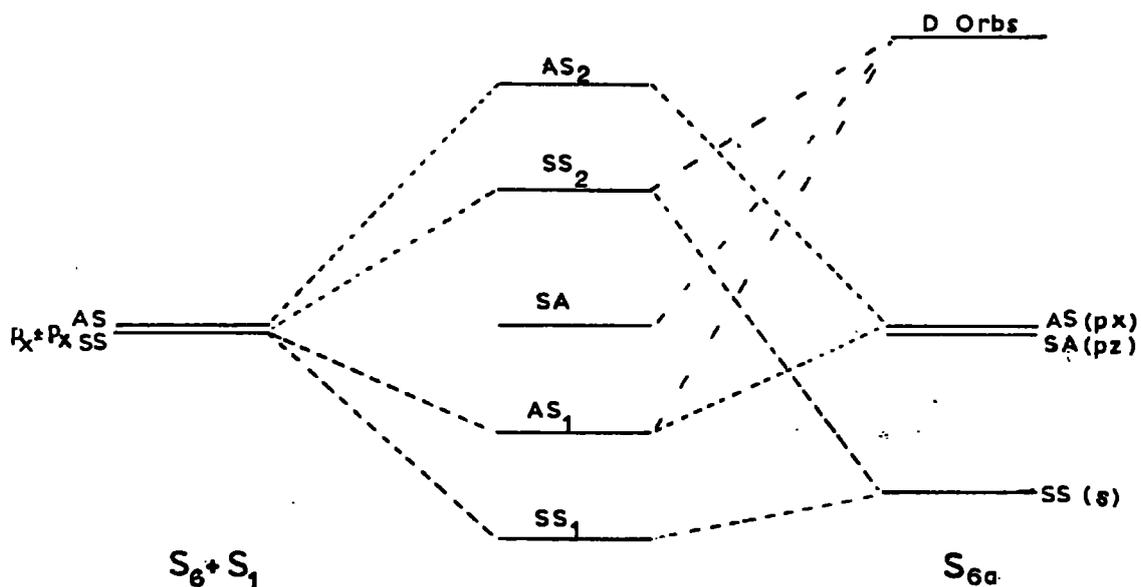
Table 5.2.

Sulphur-Sulphur PBO with variation of Nuclear Charge at H5

Nuc. Charge:	0.97		1.0	1.03	
S6a–S6	S6a–S1	S6a–S6(1)	S6a–S6	S6a–S1
0.1756	0.1747	0.1745	0.1735	0.1748
0.0840	0.0839	0.0839	0.0839	0.0840
0.1178	0.1164	0.1171	0.1164	0.1178

Table 5.3.

Milliken Population Analysis with Basis Set (2) for I and II.

Centre	I		II	
	σ	π	σ	π
S6a	12.307	3.870	12.303	3.873
S6	12.406	3.756	12.311	3.817
S1	12.406	3.756	12.527	3.683
C3a	5.039	0.786	5.033	0.793
C2	5.093	0.822	5.111	0.800
C5	5.093	0.822	5.069	0.854
C3	4.954	1.094	4.969	1.068
C4	4.954	1.094	4.969	1.068

Table 5.4.

Orbital Energies of I and II with Basis Set (2) (4 in parenthesis)

Orbital	I(eV)	II(eV)	Orbital	I(eV)	II(eV)
	6.27(5.87)	6.27		6.39(6.41)	6.28
	8.58(8.40)	8.57		9.24(9.17)	9.29
	11.00(10.67)	11.00		11.60(11.39)	11.59
$S6a_{2p}$	176.41(175.41)	176.39	$S6_{2p}$	173.25(172.52)	174.21
$S1_{2p}$	173.25(172.52)	172.35			

Table 5.5.

Sulphur 2p Core Binding Energies with Basis Set (2) for I and II.

	I		II	
Centre	Exp.	Calc.	Exp.	Calc.
S1	(0)	(0)	-0.7	-0.43
S6	(0)	(0)	0.7	0.48
S6a	1.5	1.55	1.5	1.55

sulphur.   A calculation with a minimal + 6 d type functions on the
central sulphur indicated no great effect above and beyond that of
increased variation in the basis set.

The results of Mulliken population analysis(I and II)reveal quite
strikingly the transfer of σ charge density from S6 to S1 as the
S6a-S6 bond length is decreased.   This is accompanied by a drift of
π electrons from S1 to S6, thus though the differences in total
population at the two terminal sulphur is only 0.08e the net difference
in σ electron density is more than twice this, thus supporting the
concept of the longer bonded terminal sulphur being much more
nucleophilic than in the symmetrical species[188].   The electron
distribution in the rest of the ring and especially at S6a remains
essentially unchanged in going from I to II.   The striking feature is
then that geometrical changes of the central sulphur may be expected in
general, to have only a small effect on the chemistry of the molecule.

The electronic structure for I is well described by a density contour
map (Figure 5.1.)   The weak S-S bonds are well reproduced in comparison
with the C-C and C-S bonds apparent.   The bond, no bond reasonance theories
which have been applied with much vigour to these compounds are not easily
rationalised by these results.   It is perhaps better to consider the
central sulphur residing in a two dimensional potential well bonded by the
terminal sulphurs.   An extension of the three centre 4 electron bond
model is then capable of explaining the nature of the electronic structure
in a more realistic manner.

An interaction scheme for the highest occupied molecular orbitals of
I is shown schematically in (Figure 5.2.).   The orbital SS_2 is
destabilised due to interaction with the 3s orbital of the central

sulphur. Further support that no d orbital participation operates here
to lower this energy is as given by comparing the differences in the
$a_1\sigma$ and $a_2\pi$ orbital energies of I for basis sets (1) and (2) (Table 5.4.)
The values of 0.55 and 0.61eV respectively indicate no appreciable
stabilisation by d orbitals at this level. The highest π orbital (AS)
is shown below SS_2 in accordance with calculated orbital energies, (see
below). If this scheme is applied to structure II then their antibonding
interaction will cause a priori a drift of electron density in this orbital
to S1. A flow of electrons to the S6a p_2 orbital in the orbital (AA)
(not shown) formed from the two terminal sulphur pz orbitals will then
account for the increased π density of S6a.

There is a most important corollary to this approach, namely, that
coupled with the charge density data the triatomic sulphur system may be
considered as an almost separable entity in so far as deformations in the
structure are concerned. This was dramatically illustrated by a
calculation of the dipole moment along the x and y axes in I and II.
As expected the x dipole in II of 1.18D is directed along the axis in a
manner in accord with the population analysis data. The striking feature
was the almost constancy of the y component (3.541D in I, 3.543D in II).
Further, the model substituted species of I displayed no appreciable
changes in the differences in total populations at the sulphur atoms,
beyond that of the carbohydron skeleton acting as overall electron
attractors or donors. Changes in overlap do occur however and this may
result in some change of geometry which will depend on the nature of the
substituent.

4). **Core and Valence Energy levels.**

The core & valence energy levels of I and II are shown in Table 5.4. The notable feature is that there is little overall difference in the energies for either structure. This is not surprising however as the majority of the higher levels are either weak or non-bonding in the sulphur unit. The results correlate well with He 548Å photoelectron spectra but indicate that an analysis of UPS spectra is unlikely to aid in the elucidation of the molecular structure in contrast to some observations from correlation with Huckel calculations[184]. Indeed this is not surprising since the Huckel scheme will be in error due to the large calculated changes in both σ and π populations.

It is of some interest then that there are quite large differences in the core 2p levels for the terminal sulphurs. Previous experience has shown that with this small basis a scaling factor is required to interpret the shifts in binding energy to accommodate for the fact that the basis is a considerable way from the Hartree-Fock limit. With this correction the shift in binding energy for the $S_{2p3/2}$ core levels in Table 5.5. between the central and terminal sulphur for I obtained from the S_{2p} core level eigenvalues is determined to be ~ 1.55eV. This is in good agreement with previously reported measurements in this laboratory[185]. For the model unsymmetrical structure (II) there is a marked change in the core level eigenvalues of the terminal sulphur, that at S6 moving to higher energy. These theoretical results for the shifts are again in good agreement with results taken from 3, 4 - diphenylthiathiophthen. For this and other substituted unsymmetrical structures, analysis by the charge potential model has indicated that substituent effects are small

as far as the S core levels are concerned. The model structure II is thus likely to be a very good approximation of the changes in the core energy levels. To examine this further and with the usual notation

$$\Delta E_i = kq_i + \sum_j q_j/r_{ij}$$

an analysis employing the charge potential model was undertaken.

A population analysis showed negligible change in total population on S6a but a corresponding increase at S1 and decrease at S6 in going from I to II. The S6a core orbitals will thus remain essentially unchanged in energy from equation (1) though there will be an approximate corresponding increase and decrease in the S6 and S1 binding energies respectively.

The bonding scheme above therefore accounts for the remarkable result that distortion of the symmetrical thiathiophthen ring system produces a far greater effect on the core levels, which are not involved in bonding, than on the valence levels which are.

It is also of interest to note that in a recent study by Siegbahn[115] using a high resolution ESCA instrument the observed S_{2p} lines were extremely broad. This has been rationalised in an analogus manner to those of CH_4 in chapter 2 and the conclusion of a very broad potential minimum in the ground state is in complete accord with the finding above.

5). Radical Anion

There were two main points of interest in a study of the radical anion. Firstly, the lowest unoccupied molecular orbital of thiathiophthen is anti-bonding in the triatomic sulphur unit. This change in bonding may drastically alter the shape of the potential energy curve for the motion

Table 5.6.

Spin Densities in I and III with Basis Set(2)

Centre	Spin(I)	Spin(III)	Centre	Spin(I)	Spin(III)
S6a	0.106	0.098	S6	0.068	0.064
S1	0.068	0.086	C3a	0.423	0.406
C2	0.119	0.107	C5	0.119	0.132
C3	0.001	0.011	C4	0.001	0.001

Total Energy I — −1368.1480au. Total Energy III −1368.1454au.

Table 5.7.

Mulliken Population Analysis with Basis Set (2) of I and II(Dianion)

	I		II	
Centre	α	π	α	π
S6a	12.455	4.170	12.364	4.151
S6	12.491	4.087	12.340	4.173
S1	12.491	4.087	12.647	4.013
S6a–S6	0.200	0.074	0.240	0.036
S6a–S1	0.200	0.074	0.144	0.024

Total Energy (au) − 1367.8391   − 1367.8382

of the central sulphur. Secondly, the actual distribution of the unpaired electron is of interest as ESR studies are unable to give a direct measurement.

The results indicated from Table 5.6. that there is a slight lowering in energy of the symmetrical radical structure and this is supported by the observation of the symmetric 2,5-diphenylthiathiophthen radical anion compared with the slightly unsymmetrical parent[189].

The unpaired electron distribution displays a much larger density at C2 and C5 than C3, C4 and is in qualitative agreement with results for the 2,5-diphenylthiathiophthens. The largest density is at C3a with ~.25e in the triatomic sulphur sequence.

6). **Dianion**

Single or double electron additions do not in general play an important role in the chemistry of a molecule. It was of some interest then to examine the feasibility of a proposed scheme for the rearrangement of thiathiophthens by attack from sulphide nucleophile[190]. The proposed mechanism:-

involves uptake of 2 electrons producing a transient intermediate before rearrangement and loss of sulphur to form the six membered ring structure. The critical feature was the stability of the dianion which has now been demonstrated to be quite stable by polarographic studies. Calculations
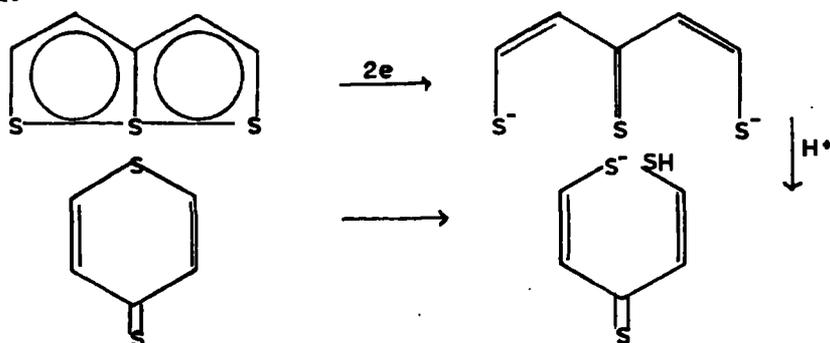
were performed on I, II and III with the lowest unoccupied π orbital
of the thiathiophthen doubly occupied. The striking feature
(Table 5.7) was the increased stability of the S-S-S 3 centre bond
even though the π orbital is antibonding in the triatomic sulphur
system. Though this π overlap is indeed reduced, the rearrangement
in the σ system concomitent with uptake of two electrons strengthens
the σ S-S bonds. Of the increase in σ electron density at the
central and terminal sulphurs in the dianion, no more than 20% can be
attributed to d orbital participation. Protonation at either the
central or terminal sulphurs will weaken the σ bond and the ring
structure is anticipated to result. Again it is interesting to note
that the unsymmetrical dianion structure is of comparable energy to
the symmetrical species. There is however, a considerable difference
in the overlap and hence the bonding between S6a - S6 and S6a - S1.
For highly unsymmetrical thiathiophthens the reaction may not be
general.

CHAPTER VI.

The Interaction of a Radical with an Unsaturated Centre.

Introduction

The interaction of a electrophile with an olefinic centre has received considerable experimental study. In contrast however the corresponding radical addition has received relatively little theoretical study and the models so far developed to account for the experimental observables have derived in general from qualitative arguments. There are definite advantages in a detailed study of this process in that theoretically calculated values can be related to the experimentally determined gas phase values of generally both $\Delta H^\dagger$ and $\Delta S^\dagger$ which correspond to the isolated molecules. Despite this fact however, the theoretical treatment is more difficult requiring a somewhat greater computational expense than that for the analogous cation species.

Both INDO and non-empirical calculations have been performed in this chapter in an attempt to produce better qualitative and where possible quantitative arguments to rationalise this body of experimental data.

1). Experimental & Theoretical Background.

The pioneering work of Mayo and Walling[191] was mainly confined to a study of the thermodynamic stability of various radical-olefin products and lead to the anti-Markovnikov rationalisation of orientation of attack in unsymmetrical olefins. Although there has been much subsequent qualitative work on radical addition reactions, notably in the field of polymer chemistry[192], there have been few kinetic studies until quite recently. The previously employed gas phase radical techniques for studying radical abstractions were modified initially by Szwarc and co-workers[193], who applied comparative rate studies in the determination of the rate of attack of methyl radical to a number of olefins and aromatics.[194,195] Cvetanovic has also undertaken similar studies with a number of radicals.[196] With the advent of coupled gas chromatographic/mass spectrometry methods, accurate detailed studies have since enabled not only the overall rate of addition to an olefin but the individual rates at each centre to be determined. The radicals employed have ranged from the very electrophilic $F \cdot$[197] and $O(^3P)$[198] to the more 'nucleophilic' $CH_3 \cdot$ Notable in this field of study with substituted methyl radicals has been the work of Tedder and co-workers who have indicated the activation energy to be largely responsible for the orientations in radical addition.[199]

Despite the increasing wealth of experimental data there have been few satisfactory theoretical studies to account for the rates and orientation of radical addition. Much consideration has been given to the properties of the reactants. The chemical reactivity index, free valence, was derived by Coulson[200] as a measure of the reactivity of a site in a conjugated molecule. Szwarc et al. later developed in a series of papers a treatment relating the π localisation energy to the methyl

affinities of the olefin[195,201]. The repulsive influence of the potential energy surface was also considered and a considerable body of experimental data was rationalised. Fukui has also applied his frontier orbital theory to this class of reactions[202,203] and studies have demonstrated the importance of the carbon π electron density in the olefin in orientation of attack.[204] In a novel approach Haselbach has applied UPS data from some olefin studies in a rationalisation of this problem[205].

Recently attempts have been made to depart from these isolated molecule approximations to determine the nature of the transition state. At the ab initio level Buenker[206] and co-workers considered the reaction in terms of a repulsive and attractive surface for the amino radical-ethylene system which is known to have a high activation energy and found an approximate 60% change in the hybridisation at the reactant centre. Studies by Basilevsky and Chlenov[207] and Hoyland[208], who calculated the geometry of the methyl radical-ethylene transition state at the MINDO level, have demonstrated the reactant nature of the T/S. An interesting analysis by Yamabe et al. employing this geometry considered the orbital interaction in a CI analysis where the wavefunction was constructed from that of the isolated reactant molecules[209].

2). <u>Some Studies of Typical Radical - Olefin Addition.</u>

a). <u>Method</u>

A systematic study of the potential energy surface, even at the INDO level, for a series of olefin radical reactions to investigate the importance of olefin substituents and the nature of the radical was deemed likely to prove computationally impractical. The INDO calculations

were found to yield an incorrect surface as has been reported in other studies[210] and a more detailed investigation at the ab initio level would have to, for computational reasons at this time, be very limited. Further, activation energies between sites are likely to differ by the order of only 5 Kcal mole^{-1},[211] and should generally be relied upon only in closely related structures. The study has thus been approached in two ways.

    i). Static Study. This included investigations of the frontier orbitals, charge distributions and stabilities of the reactants. Consideration to similar properties of the radical products is also included in this section together with the relative stabilities of the radical conformers in comparison with the analogus cationic and anionic species.

    ii). A dynamic study of the interaction of a radical with a double bond in both the RHF and UHF formalisations by computation of a P.E. surface for attack.

The more sensitive properties viz; densities and overlaps of the two extremes on the P.E. surface (products and reactants) which reflect more clearly the variation in bonding with substituent changes were therefore employed initially to develop a model for the transition state. This was then employed to try to rationalise data relating to rate and orientation of radical attack. In the main fluorethylenes were taken as the substrates with hydrogen, methyl and fluorine radicals for which a reasonable amount of experimental data is available. This series was later extended to consider a wider range of substituent effects in the radical and olefin in the INDO studies. The calculations were performed at both the semi-empirical INDO level[63] (to enable a wide study with little computational expense per calculation) and the non-empirical level

(detailed analysis) employing a HF 4,31G basis[28],(see appendix) in the RHF and UHF formalisms. Though the single excited states can interact directly with the ground state doublet (compared with doubly excited states for closed shell species), the single determinantal wavefunction becoming therefore less precise, RHF and, especially in spin density studies, UHF calculations have however been previously employed with a sufficient accuracy to encourage their use in this study without any CI analysis. This is certainly a considerable deficiency however in some of the later studies quoted here but in view of the lack of study in this most important field, it was deemed justifiable in a first investigation to obtain a better qualitative if not quantitative description. In the non-empirical studies the ATMOL series of programs were employed, implemented on IBM 370/195 machines. The difficulties encountered in convergence (especially in ii) necessitated considerable user monitoring. The restart facilities of the ATMOL SCF routines enabled a GEC 2050 work station to be used in a semi-interactive mode with the 370/195; this was especially important in the first ten cycles of the SCF to ensure the correct electronic configuration.

b). The Olefin (X)

In Table 6.1. is shown the variation in the highest occupied σ and π orbital energies and charge densities for fluorine and methyl substituted ethylenes. In the plane of the molecule the fluorine acts to stabilise the σ MO's whilst the π orbital is destabilised. This perfluoro effect has been observed experimentally in the UV photoelectron spectra of C_2H_4 and C_2F_4 [212]. There is an accummulation of charge at the least heavily fluorinated carbon in accord with simple π electron theory . The methyl group acts in an analogous manner except

Table 6.1.   Ground State Properties of some Olefins.

	$CH_2 = CH_2$	$CH_2 = CHF$	$CH_2 = CF_2$	$CHF = CF_2$	$CF_2 = CF_2$	$CH_2 = CHMe$
HOσMO	-0.562	-0.594	-0.668	-0.634	-0.673	-0.560
HOπMO	-0.582	-0.538	-0.529	-0.503	-0.496	-0.505
LUπMO	0.225	0.204	0.186	0.161	0.139	0.197
q_e 2pπ	1.0	1.076 0.972	1.158 0.941	1.125 1.008	1.086 1.086	1.035 0.978
HOπMO Ceff.	0.707	0.672 0.523	0.704 0.462	0.596 0.496	0.535 0.535	0.667 0.557
LUπMO	0.707 0.707	0.680 0.717	0.649 0.728	0.661 0.704	0.676 0.676	0.665 0.625
π Overlap	1.0	0.975	0.944	0.932	0.914	0.971

	$CH_2 = CH_2$	$CH_2 = CHF$	$CH_2 = CF_2$
q_e^{*} 2pπ	0.744	0.792 0.775	0.853 0.830
Overlap	0.069 0.061	0.077 0.065	0.088 0.070
Matrix**	0.061 0.064	0.059 0.060	0.053 0.053
Total	0.256	0.261	0.265

* Refers to non-empirical calculations with split valence basis(see text).

** Elements of overlap matrix between 2pz double zeta basis functions.

that the greater proximity in energy of the methyl pseudo- π orbitals raises the highest π mo by a greater amount; $\Delta\varepsilon_\pi C_2H_3F/C_2H_4$ 0.67eV. $\Delta\varepsilon_\pi C_2H_3Me/C_2H_4$ 1.34eV. The LUMO is also lowered in energy.

As will become apparent later the form of the localised HOMO and LUMO are of considerable importance in a discussion of these reactions. Also included then in Table 6.1. are the C_{2pz} coefficients of these two orbitals which will be important in determining the magnitude of the overlap with orbitals of the radical. An estimation of the relative energies of these pz orbitals at each carbon may be obtained from the HOMO α and β spin orbitals of the product radical. Taking a number of substituted ethyl radicals (see below and Table 6.4.) these orbitals were found to be essentially localised on the trigonal C sp^2 centre; their energies should thus represent the localised orbital energies at each site. With increased α fluorination the SOMO is increased in energy. On the other hand β fluorine substitution results in a greater lowering in energy. Though the eigenvalue of the SOMO is not directly related to orbital energies it is seen that for the same number of fluorine substituents there is little appreciable change in their eigenvalues. Quantitatively these results reflect the interaction of the fluorine lone pairs with a half closed shell orbital and mirror in many aspects the previously mentioned experimentally observed perfluoro effect from the UV photoelectron studies.

It is of some importance to note that the INDO results generate charge distribution from a normalised basis assuming no overlap between centres. The relative π charge distribution at the different sites within the molecules studied should be however quite reasonable and consistent with results from non-empirical valence double zeta calculations on the olefins. In this context it is possible to separate the

contribution to the π population at each carbon from the overlap in the Mulliken population of the double zeta results and to investigate the relative π overlaps, size and populations of the localised 2pz orbitals of carbon. The results from Table 6.1. indicate that whilst the general conclusion of the INDO results still holds the INDO basis does not show the variations in the total π density of a C_{2pz} ao as a function of fluorination. Thus in going from ethylene to 1,1 difluoroethylene the C_{2pz} population at both carbons is increased (that at the CH_2 carbon still being greater); the relative occupancies of the two components in the double zeta C_{2pz} basis indicate that the C_{2pz} atomic orbital has undergone contract whilst the radial maxima of the atomic CH_2 C_{2pz} orbital increases. This is not unreasonable on the basis of the inductive power of fluorine. Further evidence is provided from studies of the acetylenes in Chapter 2 when $\langle 1/r \rangle$ indicated the contraction of the $\equiv C-F$ and $\equiv C-Cl$ carbon charge cloud. The important ramification of this is that with fluorine substitution at the α carbon the repulsive interaction with an approaching radical will be less at long internuclear distances; at the other carbon centre the overlap will be however somewhat greater. Consistent with this approach is the increase in overlap population with increasing fluorine substitution (the INDO results giving the incorrect order due to the decrease in the magnitudes of the C_{2pz} ao with F substitution.). Analysis of the cross terms from the double zeta 2pz basis again indicate the somewhat larger contribution from the CH_2 carbon function of larger radical maxima.

c). Radical Intermediate (RX)

The production of the radical intermediate (RX) results in the formation of a new sigma bond. The strength of this new C-R bond as

Table 6.2.

Overlaps and Spin Densities in Product Radicals.

Radical	R-X PBO $\alpha \times 10^4$	R-X PBO $\beta \times 10^4$	Energies (au)	Spin Density on R $\alpha \times 10^4$	Spin Density on R $\beta \times 10^4$
H – $CH_2 = CH_2$	(0)	(0)		(0)	(0)
H – $CH_2 = CHF$	5	30	(0)	-12	5
H – $CHF = CH_2$	-7	2	0.0230	9	18
H – $CH_2 = CF_2$	4	47	(0)	-22	5
H – $CF_2 = CH_2$	-6	5	0.0393	13	36
H – $CHF = CF_2$	3	53	(0)	-11	24
H – $CF_2 = CHF$	7	38	0.0154	1	43
H – $CF_2 = CF_2$	7	58		-7	42
H – $CH_2 = CH_2$	(0)	(0)			
$CH_3 – CH_2 = CH_2$	372	273			
$NH_2 – CH_2 = CH_2$	-936	-899			
F – $CH_2 = CH_2$	-804	-657			
$CH_3 – CH_2=CH_2$	(0)	(0)			
$CF_3 – CH_2=CH_2$	-4	28			
$(CH_3)_2CH – CH_2=CH_2$	-17	-124		9.541	9.435
$(CH_3)_2CF – CH_2=CH_2$	-109	-110		12.524	12.438
$(CF_3)_2CH – CH_2=CH_2$	-70	-90			

Geometry.

C–C 1.43A C–H 1.08A C–F 1.33A

CH_2 10° out of plane. HCH 122°

Tetrahedral at attacked centre, staggered conformer.

reflected in the α and β P.B.O. has been determined for a number of R and X and is shown in Table 6.2. (Inall these calculations a staggered geometry is assumed for RX). In general the changes in the structure of X do not greatly change the αPBO but do result in some change in the βPBO; changes in the nature, both in size and electronegativity of R cause large variations both in α and β PBO. An interesting feature is that increase of the electron withdrawing powers of R actually increase the βPBO whilst decreasing the PBO. This is also apparent if the differences in α & β overlaps are considered with change of the bonding atom in R: ΔPBO($\beta-\alpha$) CH_3(-0.002),F(0.012). For the substituted ethylenes with R=H the α and β overlaps are greater at the methylene site as a result of the greater π density. The similarity in total overlap at both sites in the trifluoroethylene however is due largely to the increased βPBO at CF_2.

The spin densities are also included in Table 6.2. The main point of interest here is that whilst the α spin density of R remains approximately constant with increased fluorination of X due to a balancing of inductive and delocalising effects there is a marked increase in β spin density. A similar observation with increased fluorination is observed for R.

The relative stabilities of the radical products is often used as a guide to give the preference in addition to olefins. In Table 6.3. the addition of H and F to a number of fluoroolefins has been considered where the geometry for the product assumes no rotation of the methylene function (i.e. staggered). In the case of R=H the results are in accord with classical ideas concerning the stabilising influence of F - α to an unpaired electron. For R = F however there is a much smaller

Table 6.3.

SOMO Energies of some Radicals.(au.)

Radical	ε SOMO	ε SUMO
CH_3	-0.528(-0.438)	0.109(0.142)
CH_2F	-0.492(-0.443)	0.092(0.138)
CHF_2	-0.486(-0.421)	0.068(0.133)
CF_3	-0.509(-0.411)	0.034(0.128)

	SOMO	SUMO		SOMO	SUMO		SOMO	SUMO
CH_3 $-CH_2$	-0.405	0.121	$-CHF$	-0.384	0.121	$-CF_2$	-0.373	0.119
CH_2F $-CH_2$	-0.438	0.088	$-CHF$	-0.418	0.088	$-CF_2$	-0.404	0.088
CHF_2 $-CH_2$	-0.479	0.059	$-CHF$	-0.449	0.061	$-CF_2$	-0.434	0.061

Values in parenthesis refer to planar geometry, otherwise tetrahedral or as Table 6.2.

Table 6.4.

Rotational Barriers in some Substituted Ethyl Radicals.

'Radical'	θ	E	θ	E	θ	E	E
F CH_2-CH_2	0	(0)	45	0.005	90	0.009	0.009
F CH_2-CF_2	0	(0)	45	0.0	90	0.001	0.001
CH_3 $CHF-CF_2$	0	(0)	30	0.001	90	0.001	0.001
CH_3 CF_2-CHF	0	(0)	60	-0.003	90	-0.004	-0.004
	120	-0.003	180	0.0			
F CH_2-CF_2+	0	(0)	90	0.022			0.022
F CH_2-CH_2+	0	(0)	90	0.046			0.046
F CH_2-CF_2-	0	(0)	90	-0.008			-0.008
F CH_2-CH_2-	0	(0)	90	-0.002			-0.002

Geometries as Table 6.2. except planar sp^2 employed.

preference and in the opposite direction. This is in accord however to the preference for fluorine saturation of a carbon atom where thermochemical data indicates a relative stability of CF_3-CH_3 over CF_2H-CFH_2 of some 1.3 kcal.mole^{-1}. Further limited investigations employing CH_3 and CF_3 as the radical indicated these to give preferences in an analogous manner to H. This is particularly interesting in the case of CH_3/C_2HF_3 where experimental study indicates a preference for attack at the CF_2 carbon: the product radical $CH_3-CHF-\overset{\bullet}{C}F_2$ is however calculated to be considerably more stable than its isomer[213].

d). **The Reactant Radical.**

It is relevant merely to state three important points concerning the radical.

i) Increase in substitution will decrease the spin density at the attacking radical atom. The coefficient at this atom of the SOMO will also be decreased.

ii) Increase in size will increase the repulsion (nuclear and electronic) with the olefin.

iii) In the series $CH_3 - CF_3$ the SOMO, largely localised on the carbon will be altered in energy less than that for the SUMO ($=LUMO\,\beta$) (Table 6.3.).

e). _Discussion._

From the data discussed above a model was developed within which the addition of R to one of the sites in X could be studied. This is shown in Figure 6.1. where the α and β spin electrons are considered separately. For example in the reactant ethylene there will be equal contributions of $\frac{1}{2}$e to the pz population in carbon from electrons of

Figure 6.1. Orbital Interaction Diagram of SOMO(R) with $\tilde{n}$, $\tilde{n}^*$(X).

α (anion type)

β (cation type)

R   X   R   R   X

Attractive   Repulsive   Attractive

R.(1) +   →   R   1   R( ) +   →   R
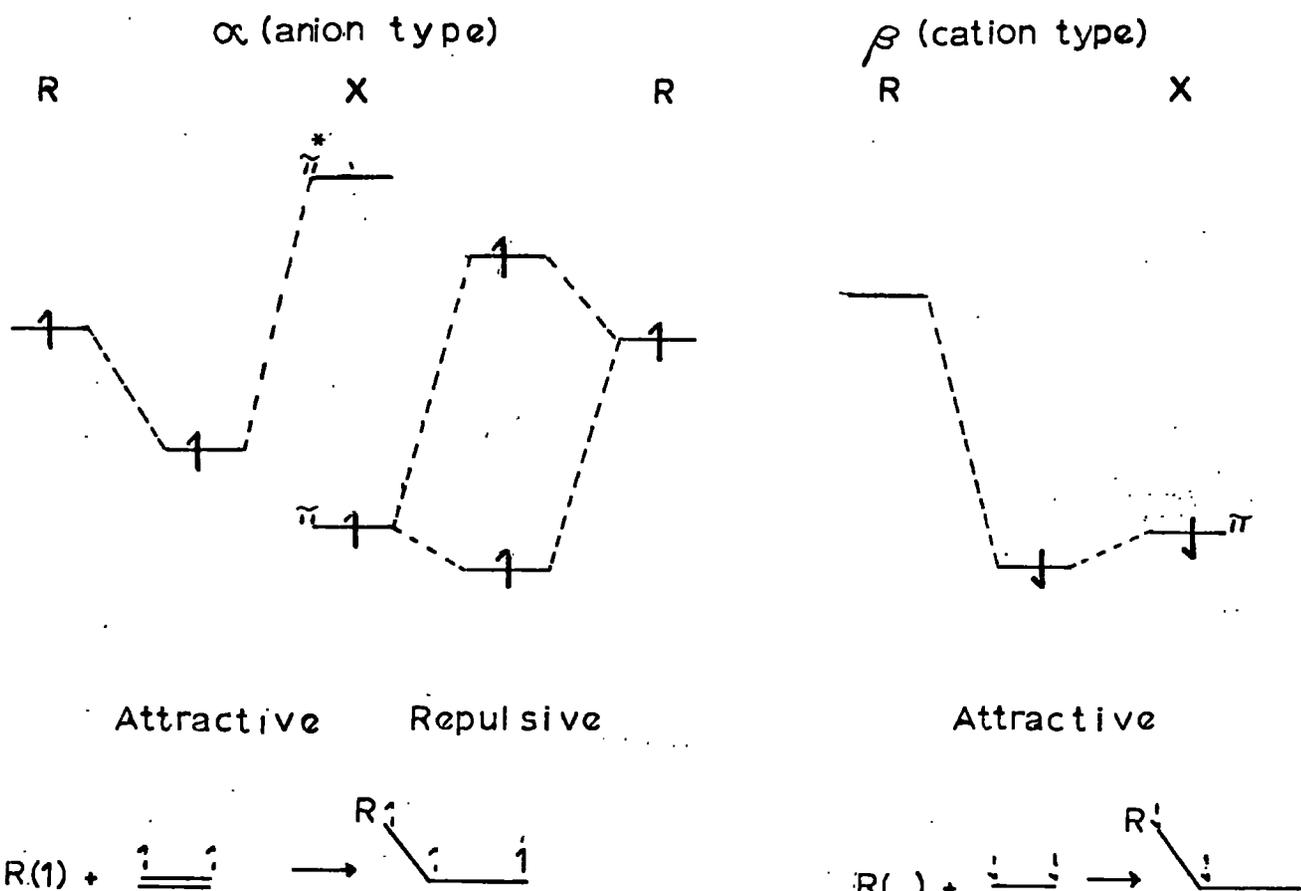
Figure 6.2. Relative Orbital Energies and Coefficients R + $CH_2=CF_2$.

0.728 CF_2
0.649 CH_2

CH_3

F

CH_3

F

0.462 CF_2
0.704 CH_2

ORBITAL ENERGY

α (R)   X β (R)
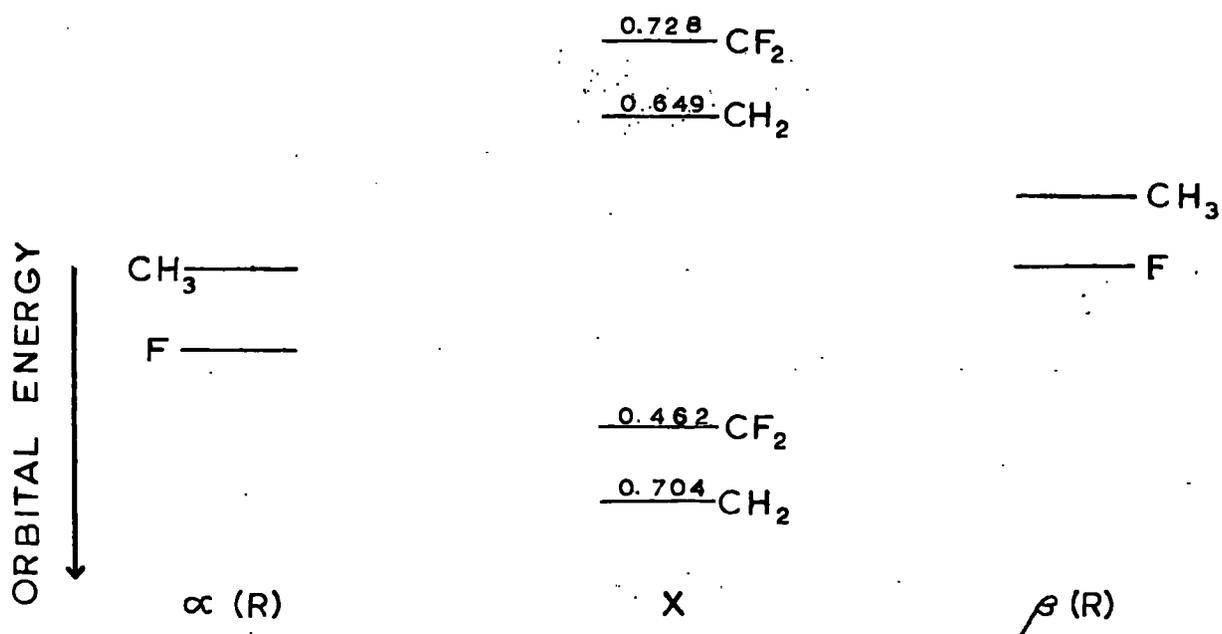
both α and β spin. In the product radical one centre will have almost exclusively α spin; the T/S will lie in a region somewhere between these two extremes.

If the formation of the radical product is considered in terms of attractive and repulsive surfaces then considering the change in bonding only the main contributions will arise from the energy of the new C - R bond with a decrease in energy due to the weakening of the C-C bond of X in the transition from a sp^2 to an sp^3 hybridisation at the centre of attack. These reactions are thus in general very exothermic and the T/S may be expected to occur early in the reaction in accord with the general proposition for the form of P.E. surfaces of Polyani. Both reactant and product properties were however included in the model to develop a more detailed picture of the T/S.

In the initial stages from Figure 6.1. the α electrons may be thought of as acting repulsively in the R-X interaction whilst the β electrons give an attractive interaction. The electronic repulsive curve will follow an approximate $1/r^n$ dependence at large internuclear distance (i.e. a sensitive function of r) and will be greatest at the site with the largest density. Conversely the LUMO β spin orbital of Rwill also gives the greatest attractive overlap with this site.

Employing this model then it is possible to rationlise many of the subtleties of the data presented above. This has the effect of building a picture of the various contributing factors which may be evident in the T/S and hence discerning how the nature of the reactant may alter electronic structure and stability of such a proposed species.

Considering firstly the β electrons. The lower the energy of the

SUMO of R the greater will be the overlap with the HOMO of the olefin.

This is reflected in the increase of the β PBO from Table 6.2. in

going from $(CH_3)_2CH$ to $(CF_3)_2CF$. Again this overlap will be

greatest in unsymmetrical olefins at the site with highest π

density (Table 6.1.) as seen from the fluoro substituted ethyl radicals.

It is of some importance that in this series there is comparatively

little change in the α PBO across the series compared with the β PBO

Change in R however produces a comparable change in both the α and β

PBO. Thus if the product radical represented the T/S then differentially

it appears that the bonding as indicated by the β PBO of the new radical-

olefin bond will be of greater importance in determining the orientation

of addition. This proposition has been tested previously in a

different presentation by Tedder and co-workers who related the

activation energy of the addition to the bonding possibilities of the

olefin.[199,214]

$$E_{obs} = A(L_\mu + Bq_e)$$

where E_{obs} is the activation energy, L_μ the π localisation energy,

q_e the π electron density at the site of addition and A and B are

constant, the theoretical quantities being derived from Huckel

calculations. If overlap is the dominant factor in the T/S there

should be a direct relationship between the activation energy and the

C_{2pz} coefficient of the highest occupied π MO of the olefin for addition

of the same R. Tedder's experimental values for C_3F_7[214] and CCl_3[204]

gave good correlations for the expression

$$E_{obs} = Const. - k.coeff.C_{2pz}$$

Radical	Const.	k	r
CH_3	3.0	−8.9	.47
C_3F_7	20.1	22.7	.86
CCl_3	14.4	15.0	.85

(where the coeff. C_{2pz} refers to the INDO results) though in the case of $CH_3 \cdot ^{213}$ the correlation was unsatisfactory. This result is not unreasonable as the LUMOβ orbital of $CH_3^{\cdot}$ is relatively higher in energy with the new bond C–C somewhat weaker than in $-CCl_3$ or $-C_3F_7$ and hence overlap with HOMO of the ethylenes will be comparatively less. Other factors may thus be of some importance.

The α electron of the radical as shown in this scheme will be involved in both attractive and repulsive interactions. If for example an unsymmetrical X is taken (e.g. $CF_2 = CH_2$) then from Figure 6.2. the picture is more complicated. Firstly considering overlap as reflected in the magnitudes of the coefficients of the π orbitals of X with a standard R there will be a marked preference for a stabilising interaction with the CF_2 function where coefficients of the HOMO and LUMO π orbitals are respectively lower and higher than at the CH_2 carbon. The opposite conclusion is reached however if the dependence upon the relative energies of the orbital is involved, there now being a preference for the CH_2 carbon. Similarly for the β electrons the coefficients and overlap arguments give conflicting orientations at the CH_2 and CF_2 sites respectively. Since however the overlap is approximately proportional to the product of the coefficients but only inversely related to the separation of the energy levels, the variations in the former are anticipated to have a greater effect on the activation energies. Further, available experimental evidence together with these studies indicate addition to the CH_2 carbon. It appears then that the α electrons in the majority of cases effectively play little part in determining the orientation of attack.

For radicals where the electron repulsive surface is anticipated

to be more important (e.g. CH_3) the changes in π density at each site in the ethylene must now be considered as affecting both attractive and repulsive surfaces and generally in opposite senses. As this becomes more important so departures from product stability and T/S bonding methods will increase. If this repulsive surface is major it should be possible to correlate the activation energy now with the repulsion as reflected by the π charge densities at the carbons. Unfortunately no satisfactory correlation was found with the INDO results though different size of the localised C_{2pz} ao makes any correlations tenuous.

The total C-R overlaps for similar radicals is seen to decrease as R becomes less electronegative. Indeed for CH_3 and CF_3 this change is comparable with that at the CH_2 and CHF sites in C_2HF_3 It has already been established that for CH_3 no correlation is obtained between the activation energy and the bonding properties. Thus if the transition state, which will have a weak R-X bond, exhibit comparable changes in this overlap the entropy of this weak complex should show considerable changes. This will be reflected in the variation in the A factor. A decrease in bonding in the T/S will result in an increase in the entropy of activation and hence the A factor will also be increased ($A \propto e^{\Delta S/R}$). The much larger A factor encountered for methyl radical attack compared with perfluoroisopropyl and trichloromethyl radical mitigate for some factor other than the energy of the repulsive interactions. There is also evidence from these A factors for methyl radical addition that this term is of greater importance in determining the orientation in certain of the fluoroethylenes than with the other radicals.[214] For the present it is pertinent to comment briefly upon the observation of attack at the CFH site in trifluoroethylene

by methyl radicals. Indeed from the comments concerning the size and electron distribution from the non-empirical studies of the olefins the propensity for attack by a nucleophilic type radical at the site where the charge cloud has undergone the greatest contraction is not unreasonable. An explanation based on these entropy arguments is also entirely reasonable. It is apparent from the above that the lack of correlation with the HOMO of the olefin by implication also indicates an increased interaction with the LUMO. With the available data indicating the coefficents as opposed to separation between the energy levels being of greater importance in determining the orientation the predicted attack at the CF_2 site is in accord with the experimental findings.

3). Rotational Barriers in Radicals (Cations and Anions)

    a). Semi-Empirical Study.

The previous analysis was in terms of a separation of components arising from α and β spins conforming to anionic and cationic half shell electronic species respectively. This naive approach proved an effective method of analysis of the addition reaction. It was thus decided to investigate this method further by the consideration of rotational barriers in some radicals. The characteristic feature of these barriers is that they are low compared with their charged counterparts but there exists in general a slight preference for the eclipsed conformer in substituted ethyl radicals.[215] Physically this is not surprising in view of the relatively larger calculated barriers for the cation from studies by Pople and co-workers.[96] Barrier to rotation in some substituted ethyl systems have been calculated and are shown in Table 6.5. With the orbital interaction scheme employed

in the second chapter introduction of fluorine at a cationic carbon
will serve to raise the energy of this $2p\pi$ ao with the result that
the barrier to rotation for the cation is reduced. The barrier is
somewhat overestimated due to the standard geometries employed. The
opposite situation is found in the anions though now the difference
is considerably less. In the radical then the behaviour is as
expected indicating the power of this approach. The quite complex
barrier in the fluorine substituted propene radicals also exhibits this
underlying trend in fluorination at the radical centre.

It may be argued that repulsive interactions across the C-C
bond between the atoms rather than the interaction with the $'C_{2p\pi}'$
orbital are responsible for these barriers. To eliminate this
possibility calculations were performed on a number of 2-propene
radicals where any atom-atom interactions are expected to be small.
The results are shown in Table 6.5. The barriers are again small and
in qualitative agreement with the above. It is of interest now that
introduction of the fluorine at the terminal CH_2 carbon increases the
barrier. There are two reasons for this. Firstly the SOMO, now one
carbon unit remote from the two fluorines, is lowered in energy
($CH_3-\dot{C} = CH_2$ $\epsilon = 0.330au$, $CH_3-\dot{C} = CF_2$ $\epsilon = 0.422au$)
Secondly the fluorines now in the same plane as the p orbital can
reduce the repulsive (α) interaction by withdrawing electrons from this
a.o. (eclipsed $FCH_2-\dot{C} = CX_2$: $X = H$ 1.027, $X = F$ 0.972)

In going to the eclipsed from the staggered form in $XCH_2-\dot{C} = CH_2$
a considerable increase in α spin density is observed on X accompanied
by a similar decrease in β density. (This has been used as a probe for
determination of the conformer in substituted ethyl radicals by

Table 6.5.

Rotational Barriers and Overlaps[*] in some
Substituted Propyl Radicals.

			Staggered		Eclipsed	
Compound		E	α	β	α	β
H $-$ CH_2 $-$ C $-$ CH_2		0.0	0.336	0.335	0.331	0.330
F $-$ CH_2 $-$ C $-$ CH_2		0.0020	0.243	0.240	0.232	0.244
H $-$ CF_2 $-$ C $-$ CH_2		-0.0019	0.336	0.335	0.333	0.331
F $-$ CF_2 $-$ C $-$ CH_2		0.0	0.243	0.242	0.246	0.245
H $-$ CH_2 $-$ C $-$ CF_2		0.0	0.336	0.335	0.332	0.325
F $-$ CH_2 $-$ C $-$ CF_2		0.0082	0.243	0.231	0.233	0.243

* PBO Overlaps in X $-$ C Radical.

Figure 6.3.   Energy Components for Rotational Barriers in Ethyl Species.

$$\Delta_E = (E_{stog} - E_{eclip})_{a.u.}$$

$$CH_2F \ \text{---} \ CH_2 \cdot$$
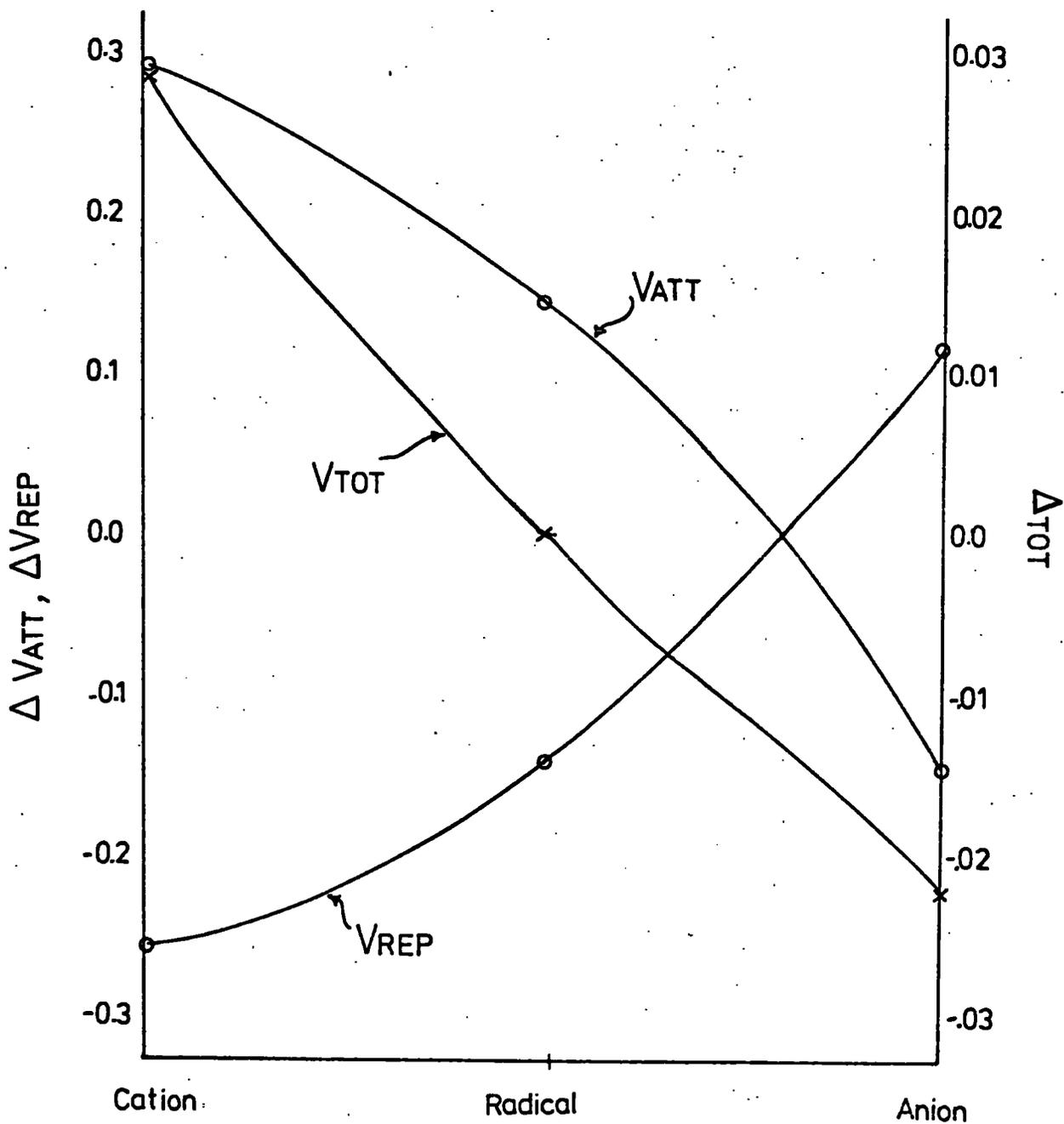
calculation of β hyperfine coupling constants).[216,217] With X = F this is accompanied by changes in α and β bond overlaps according to the scheme

which will be reduced by electronegative goups (CF_2) in the same plane.

b). Non-Empirical Study.

The rotational-barriers in the β- fluoroethyl species were further investigated by a non-empirical study. The 4-31G Hartree-Fock basis was employed and a standard geometry for the radical taken. The CH_2 centre was assumed planar with a HCH angle of 110°. The total energies for the cation, anion and radical (both RHF and UHF) together with the component energies are given in Table 6.6. Due to the short C-C bond the cation and anion barriers are again overestimated: the barriers for the radical is similar in both calculations and in accord with experiment (0.46 kcal.mole^{-1}) . These variations in energy are quite nicely represented in Figure 6.3 where the changes in total, attractive (defined as Vne) and repulsive energies in the cation, anion and radical in the staggered and eclipsed conformer have been plotted. The addition of one and two electrons to the cation results in the expected relatively smaller attractive and repulsive energies in the eclipsed conformer; the total energy is seen however to mirror the changes of the attractive energy component; viz. the barriers are attractive in all three species. This is a most interesting observation since repulsive effects in the anion might 'a priori' be anticipated to be dominant.

A number of points of interest arise from an analysis of the

Table 6.6. Non-Empirical Energies for Staggered and Eclipsed 2-F Ethyl Cation, Anion and Radical.

	Staggered	Eclipsed	Δ	Staggered	Eclipsed	Δ	Staggered	Eclipsed	Δ
Total E	-176.2973	-176.3255	0.0282	-176.6490	-176.6503	0.0013	-176.6047	-176.5827	-0.0220
				(-176.6457)	(-176.6468)	(0.0011)			
V_{REP}	380.2320	380.4886	-0.2566	387.6793	387.8230	-0.1437	394.3373	394.2196	0.1177
				(387.6709)	(387.8132)	(0.1423)			
V_{ATT}	-556.5293	-556.8141	0.2848	-564.3283	-564.4733	0.1450	-570.9420	-570.8023	-0.1397
				(-564.3166)	(-564.4600)	(0.1434)			
ϵ_i HOMO	-0.777	-0.800		-0.409	-0.377		-0.013	0.013	
				(0.131)	(0.150)				
Pop. C $2p\pi$ at CH_2	0.058	0.134		0.996	1.018		1.886	1.980	

Values in parenthesis refer to RHF Calculations on the Radical.

Δ = $E_{STAGGERED} - E_{ECLIPSED}$

Geometry: C-C 1.43Å   C-F 1.33Å CH_2F Tetrahedral θHCH 116° (Planar.)

175.

Figure 6.4. Density Difference Map (Eclipsed − Staggered) in Plane 4.4au. behind C of CH_2F.
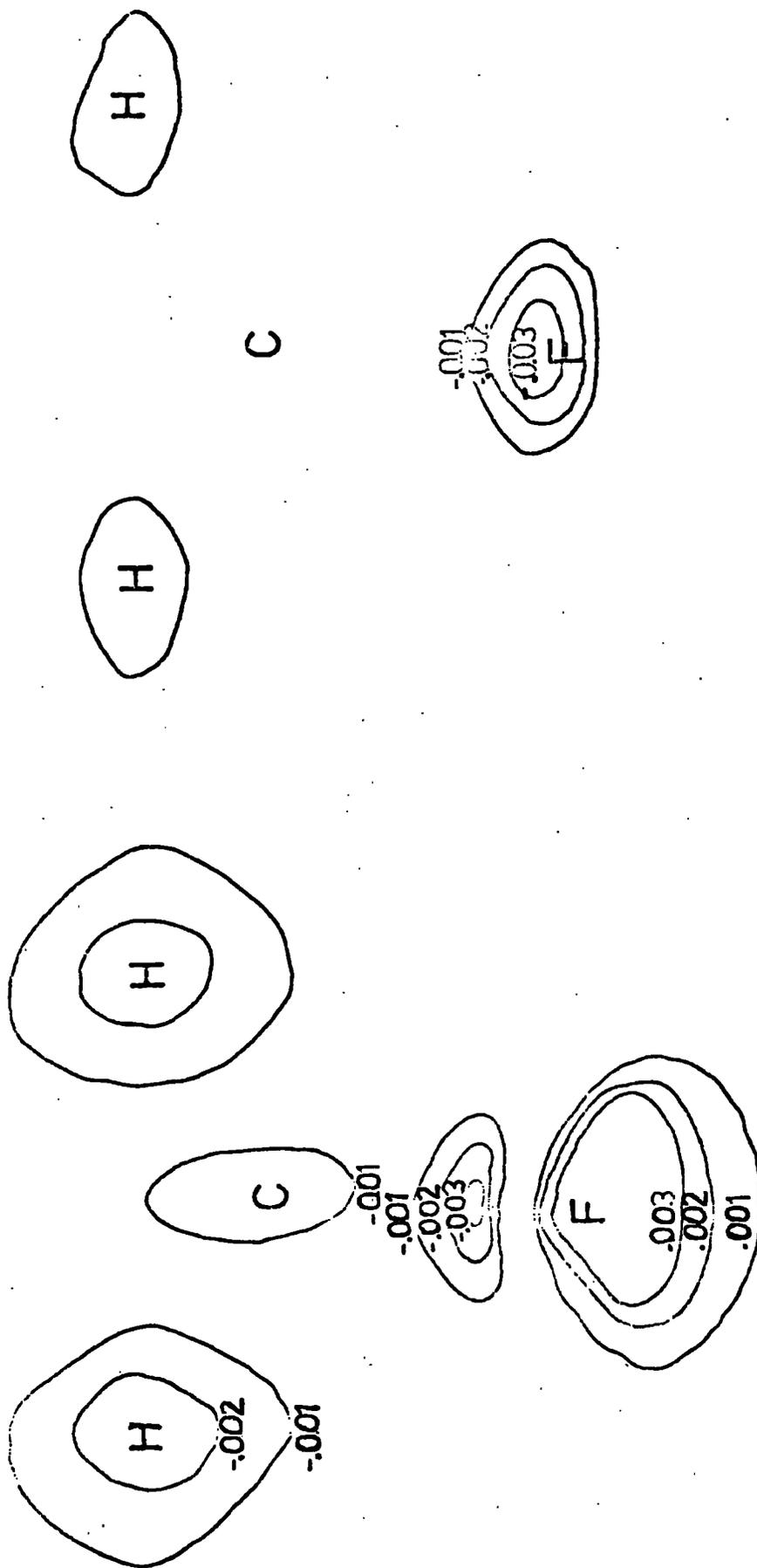
orbitals and electron distributions in the cation and anion. Firstly
the barriers and calculated lowest energy conformer are consistent
with the analysis in terms of overlap of the carbon 2p a.o. with the
pseudo η orbitals of the fluoromethyl group. The magnitudes of the
V_{ATT} and V_{REP} terms though are much smaller in the anion. A further
indication that the electronic changes in the anion are smaller than
in the cation is given by plotting the density difference map for
the two conformers in a plane 4.4 a.u. behind the methyl carbon
(Figure 6.4). Both qualitatively and quantitively there is a smaller
variation in the anion.

Similar examination of the radical shows its energies and
electronic structure to be composed of unequal components of the cation
and anion with, considering solely the total energies, a larger
contribution from the latter. This is a result of the repulsive
interactions in the anion being overestimated if interpolation to the
radical is employed. Though fortuitous the interpolated V_{ATT} employing
the cation and anion energy data is in excellent agreement with that
calculated in the radical. Recourse to the orbital interation diagram
shows that while these π attractive interations are different in cation
and anion the repulsive interaction is only found in the anion. A
reduction in this repulsion by delocalising the negative charge in the
anion (and hence radical) will tend to produce a staggered conformer.
This provides an alternative rationalisation of the preference for the
staggered anion in $FCH_2-\overset{\bullet}{C}F_2$ as calculated above where the fluorine now
delocalises this negative charge.

In conclusion it has recently been reported that the βCl ethyl
radical exists in a form approaching a bridged structure.[215,216] From

studies of the bridged cations, both F^+ and Cl^+ are known to be

favoured in bridging environments as opposed to the β position in the

cation.[120,217,218] Calculations at the INDO level on the corresponding

2-F ethyl radical where all geometric parameters were varied gave

however no tendency to bridge. This is in accord with partially

optimised studies by Hudson and Biddles.[219] Though semi-empirical

calculations tend to overestimate the stability of bridged structures a

preference for a geometry approaching a bridging form has been reported

from an INDO study of β chloroethyl radical.[220] This evidence suggests,

together with data available concerning the stereoselectivity of radical

addition to olefins (e.g. Br_2),[221] that the bridging capabilities in the

radical might parallel those calculated for the cation.

4). <u>Radical Addition to Allenes.</u>

    a). <u>Method.</u>

As a subject of some interest calculations at the INDO level were

also performed to investigate the reaction of free radical addition to

allenes. There is relatively little documentation in the literature on

this subject but the available data may be conveniently rationalised by

the following scheme[222]

Central attack proceeds with a rapid rotation to give a resonance

stabilised intermediate whilst terminal attack proceeds reversibly, there

being no similar stabilising influence. For allene itself terminal

attack is invariably preferred whilst substitution at the terminal

carbons greatly increases the preference for central attack.[222]

Fluorine atoms also appear to have a slight preference for central

attack.[223]

The procedure for investigation was similar to that employed

for the olefin. The allenes themselves were studied for overlap and

charge distribution and the product radicals for the stability and

bonding trends in the T/S. This was augmented by limited studies of

the potential energy surfaces.

b). The Allenes.

In Table 6.7. are shown the π populations for a number of simple

allenes. The picture is complicated somewhat due to the two

orthogonal π systems and both π repulsion and σ inductive effects are

seen to be important. The features evident in the ethylenes are still

retained. For allene itself the π population is considerably higher

at the terminal carbons. Introduction of a methyl group results in an

increase in the population of the $p\pi$ orbital of the C=CHMe group which

isless than that observed for fluorine substitution; both in accord

with the findings for ethylene. The introduction of two fluorine atoms

at the same site results in a markedly higher $p\pi$ population on the

central carbon compared with either terminal carbon.

Introduction of the F and Me groups also affects the π overlap

populations. For allene the π overlap (.947e) is increased slightly in

the CH_2= C unit to .958e with substitution of F and by .950e with Me.

The changes in the other fragment are opposite and considerably larger

(.924e C=CHMe, .928e C=CHF) in qualitative agreement with the energies

Table 6.7. <u>Ground State Properties of some Allenes.</u>

		CH$_2$ = C = CH$_2$		CH$_2$ = C = CHMe		CH$_2$ = C = CHF		CH$_2$ = C = CF$_2$	
Orbital Energies	HO	-0.49	-0.49	-0.48	-0.45	-0.54	-0.47	-0.58	-0.46
	LU	0.19	0.19	0.20	0.18	0.17	0.18	0.15	0.16
p pops.		1.083	0.945	1.098	0.940	1.003	0.989	0.941	1.017
		0.945	1.083	0.969	1.062	1.020	1.042	1.091	1.007
Overlaps		0.947	0.947	0.950	0.924	0.958	0.928	0.961	0.905
Coefficients: HO MO		0.67	0.49	0.61	0.48	0.64	0.54	0.65	0.63
		0.49	0.67	0.51	0.59	0.53	0.56	0.57	0.51
LU MO		0.47	0.57	0.61	0.58	0.67	0.57	0.69	0.56
		0.57	0.46	0.57	0.58	0.55	0.65	0.53	0.66

Figure 6.5. INDO Minimised Geometries of some Substituted Allyl and Propyl Radicals.
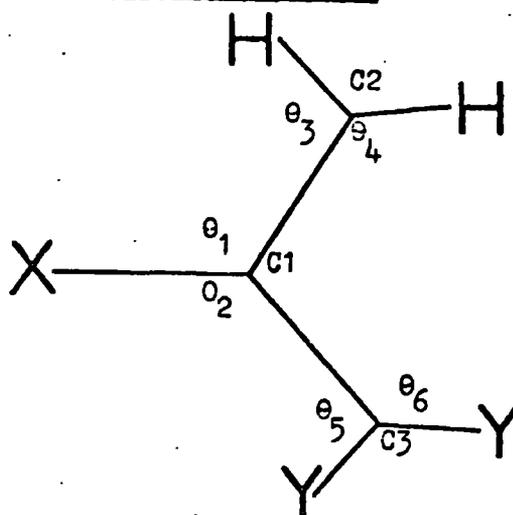
X	Y	X-C1	C1-C2	C1-C3	θ_1	θ_2	θ_3	θ_4	θ_5	θ_6
H	H	1·08 +	1·371	1·371	117·8	117·8	124·3	123·2	124·3	123·2
H	F	1·08 +	1·364	1·379	119·4	119·2	124·6	123·3	130·1	124·3
F	H	1·355	1·375	1·375	116·0	116·0	124·8	121·2	124·8	121·2
F	F	1·37 +	1·363	1·390	119·8	113·7	176·7	119·7	128·9	123·7

+ Assumed
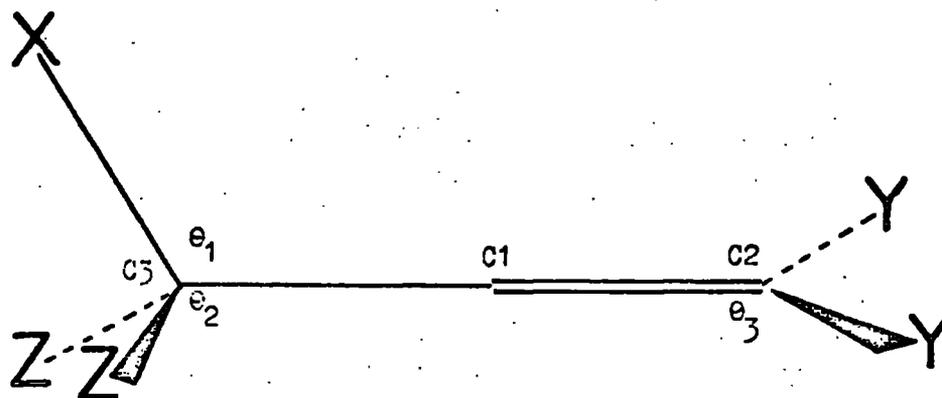
X	Y	Z	X-C3	C3-C1	C1-C2	θ_1	θ_2	θ_2'	θ_3
H	H	H	1·08 +	1·417	1·287	112·5	111·2	119·1	125·4
H	H	F	1·08 +	1·428	1·282	114·2	112·8	117·5	125·3
H	F	H	1·08 +	1·412	1·304	111·3	111·8	118·8	127·4
F	H	H	1·37 +	1·423	1·284	112·8	111·4	119·7	125·2
F	H	F	1·37 +	1·424	1·281	118·1	113·1	120·6	125·2
F	F	H	1·37 +	1·423	1·302	112·2	111·6	119·5	127·2

+ Assumed θ' dihedral angle

of these π orbitals. The conclusion is then that increased substitution will increase the appropriate π density at the central carbon with a reduction in the π bonding from the substituted group to the central carbon. Further in attack at the central carbon atom it is this weaker C-C bond which undergoes rotation to give the planar radical.

c). Product Radicals.

The minimised geometries ($\div$ 0.1 $kcal.mole^{-1}$) and energies for a number of product radicals are shown in Figure 6.5. and Table 6.8. Considering firstly the addition of H to allene and 1,1-difluoroallene there is a slight preference for the product from central attack. Introduction of two fluorines now increases this preference. The bond lengths and angles are qualitatively reasonable, fluorine tending to lengthen the adjacent C-C bonds. The analogous products from fluorine addition give the opposite preference for central attack, difluorination now giving rise to a preference for attack at the CF_2 group due to the stability of the CF_3 function.

The consistency of these calculations is indicated by the similar geometry of the C = CH_2 group in the radical products and the results for difluoroallene with H and F are in reasonable agreement with the less flexible study of Kispert, Pittman and co-workers.[224]

The charge and overlap population for the terminal radicals has been mentioned above and follow closely the trends in the ethyl radicals. The allyl radicals show most interesting variation in the α and β spin overlaps with the new C-H or C-F bond as seen in Figure 6.5. The α and β overlaps for C-H are both increased with difluorination; the C-F α and β overlaps show opposing variations, the increased β overlap being

Table 6.8.

Relative Product Stabilites of Allenes with various Radicals(kcal.mole^{-1})

Allene + H	Terminal(C3)	Central	Terminal(C2)
$CH_2 = C = CH_2$	0.3	(0)	0.3
$CH_2 = C = CF_2$	20.6	(0)	21.8
$CH_2 = C = CHMe$	12.1	(0)	15.9
Allene + F			
$CH_2 = C = CH_2$	8.0	(0)	8.0
$CH_2 = C = CF_2$	17.6	(0)	− 2.9
$CH_2 = C = CHMe$	5.0	(0)	8.2
Allene + Me*			
$CH_2 = C = CH_2$	0.3	(0)	0.3

(−ve indicates more stable product radical)

* For partially minimised geometry only,all others fully minimised geometries.

larger however.

Employing non-minimised standard geometries a methyl substituent
is seen to favour the central attack of both H and F radicals
(Table 6.8.). Limited calculations also indicated that there was
little difference in the relative stabilities for central or teminal
attack with methyl radical. Thus in general the product stability
indicates then that for the radicals H·, CH₃· with allene there is
little preference for central or terminal attack but with substitution
central attack becomes more favourable over the unsubstituted carbon as
the substituent delocalises the unpaired electron.

d). Reaction Surface for Attack of H· and F· to Allenes.

The reaction scheme as proposed imbodies two important steps.

i) Terminal attack will be thermodynamically controlled
i.e. product stabilities will be of considerable importance.

ii) The formation of the allyl radical involves a crossing
of energy surfaces and poses the question at which stage of the reaction
does the rotation occur.

The former has already been partially answered with a general
favouring for attack at the unsubstituted end. To investigate the
latter the two PE curves for approach to planar and perpendicular allenes
have been calculated to determine the crossover point. In this region
the barriers were then calculated. With increasing substitution the
crossover occurred at larger internuclear distance, the rotational
barrier being very small ($\sim$1 kcal.mole^{-1}).

Though it is not possible at the INDO level to calculate the
position of this rotation (w.r.t. the energy maxima) on the potential
energy surface it is reasonable to suppose that this increased
internuclear crossover distance with substitution will result in an

increased contribution of the lower planar allyl radical energy surface
in the T/S. With the attacking radical now locked onto this lower
energy surface there will hence be less tendency for attack at the
terminal carbons.

5). Non-Empirical Reaction Surfaces for Addition of Radicals
to Olefin.

a). Method.

To test the validity of the previously developed models,
calculations at a non-empirical level have been performed on structures
representing the transition state arising from methyl radical and
fluorine atom addition to ethylene. These represent two extremes of a
nucleophilic and electrophilic radical respectively. Though a MINDO
optimised geometry is available for the former[208] no investigation has
been reported for the latter.

It has been already stated that the Hartree-Fock single
determinant method is generally incapable of obtaining a reliable
description of the potential energy surface of a bound system. In this
particular case the number of closed shells remains the same and
correlation corrections should be of minor importance.[225] An RHF
approach should thus in this context be of reasonable quality. A
criticism of this approach is however that the closed shell α and β
spin charge distribution will be equivalent. To introduce maximum
flexibility, geometry optimisation for the fluorine-ethylene system
employed the UHF formalism. This serves to introduce higher doublet
states into the wavefunction but suffers from the deficiency of
quartet, octet etc., contamination.[18].

The basis set employed was of double zeta quality for the valence

atomic orbitals. Though this greatly increases the computational time the considerable degree of charge polarization necessitates a flexible basis. This has been vividly illustrated by Buenker and co-workers[206] in a study of the amino radical ethylene system. The previously employed 4,31G fit to the H.F. functions was employed in all the subsequent calculations.

b). F· and CH$_3$ Addition to Ethylene.

Despite the considerable symmetry a full geometry optimisation to determine the energy maxima on the minimum energy PE surface for the reaction was computationally not feasible. The following assumptions were thus employed.

i). The C-C bond length and the sp^2-sp^3 conformation at the site of attack change in a linear manner.

ii). The trigonal unattacked site retains the same geometry

iii). No change in the C-H bond lengths.

iv). Attack by the fluorine atom proceeds along the tetrahedral axis with a fixed CH$_2$F 'tetrahedral' angle. Fluorine in bridging environments gave energies considerably higher, (4.3 kcal.mole^{-1} at a distance of 2.4Å from each carbon) and this structure will thus not be on the minimum energy PE surface. This is in accord with previous studies in this laboratory on β fluoroethyl cation and fluoronium ion where the LUMO eigenvalues of the cation species were employed to estimate the relative stabilities of the radical.

The problem is now reduced to only two variables, namely the change in hybridisation of the ethylene and the C-F separation. Limits of 1.34Å and 1.44Å were employed on the C-C separation for fluorine at infinite separation from the ethylene and in staggered fluoroethyl radical. A

Figure 6.6. Non-empirical Potential Energy Surface for Addition of F to C_2H_4.

Energies in a.u. w.r.t. isolated F and C_2H_4

Table 6.9. Population Analysis for Me· and F· + C_2H_4 T/S's.
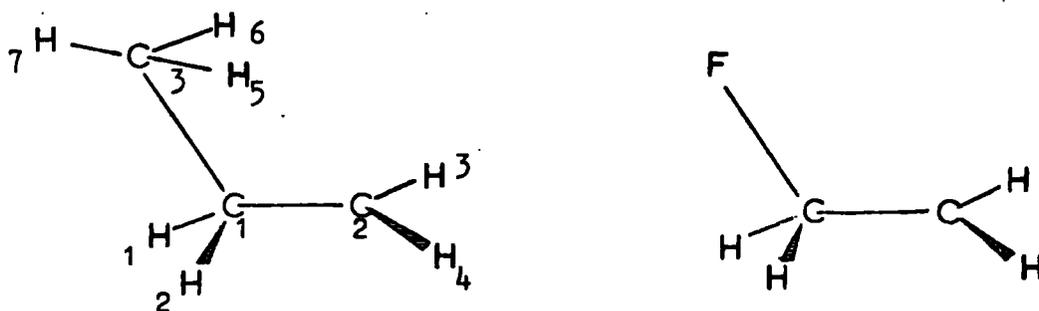
| | Total Density | | | Spin Density | | |
Centre	α	β	Σ	RHF	UHF($\alpha-\beta$)	RHF SOMO
C1	2.832	3.547	6.379	6.431	-0.715	0.018
C2	3.669	2.771	6.440	6.447	0.898	0.056
H1(H2)	0.409	0.349	0.758	0.760	0.060	0.0
H3(H4)	0.343	0.418	0.761	0.761	-0.075	0.002
F	4.994	4.149	9.143	9.078	0.845	0.921
F-C1	-0.043	0.007	-0.036			
C1-C2	0.210	0.189	0.399			

Me + C_2H_4

	α	β	Σ	RHF	UHF($\alpha-\beta$)	RHF SOMO
C1	2.811	3.594	6.405	6.409	-0.783	-0.019
C2	3.669	2.818	6.487	6.501	0.851	0.044
H1(H2)	0.418	0.357	0.775	0.774	0.061	0.0
H3(H4)	0.353	0.424	0.777	0.772	-0.071	-0.001
C3	3.957	2.721	6.678	6.678	1.236	0.971
H5(H6)	0.337	0.431	0.768	0.765	-0.094	0.001
H7	0.346	0.444	0.790	0.739	-0.098	0.002
(CH_3)	4.977	4.027	9.004	8.997	0.950	0.975
C3-C1	-0.042	-0.020	-0.062	-0.119		
C1-C2	0.223	0.224	0.447	0.550		

bond correlate with a 'product T/S'. If this observation is general
the explanation of the correlations of activation energies with product
stability, the formation of the stronger C-X bond and also localisation
energies of the olefin substrate etc., as observed for a number of
previously investigated systems follow. immediately.

From the above the correlation with localisation energies in the
olefin has been quantitatively successful for a large number of
radicals.[212,226] A notable failure is however in the case of the
methyl radical. The results of Hoyland indicated a reactant geometry
for the transition state but no charge distributions were quoted. To
investigate this further, calculations were performed on a model methyl
radical-ethylene transition state employing the C_2H_4 geometry of the
F + C_2H_4 T/S with a H_3C-C separation of 2.5A. The resultant UHF
charge distributions are also shown in Table 6.9. For the α spin
electrons this distribution is very similar; there is little transfer
of an α electron to ethylene but considerable and similar polarization
of the α spin electrons. The β spin electrons exhibit however a quite
considerable difference there being now only a very small net transfer
of β electrons to the methyl group with the C_1-C_2 β bond overlap
comparable to the α bond overlap. This is in accord with the LUMO
spin orbital being of higher energy in methyl radical: hence less
overlap and charge transfer. Though the polarization in the ethylene
is still quite significant ($\sim 2/3e$) the new C-C bond will be quite
weak. As a result though the activation energy should show some
dependence on the localisation energy of the π system. Any charge
dependent or density dependent term involving bonding of the attacking
methyl radical will be very slight. For a similar but more electrophilic

radical (e.g. CF_3) however, a stronger bond is anticipated and a better correlation.

There are a number of further points of interest in comparison of the methyl radical and fluorine atom results. Firstly the actual magnitudes of the activation energies as calculated are in qualitative agreement with the experimental. Though no data is available for fluorine the energy (3.07 kcal.mole^{-1}) compares favourably with the results of Rowlands and co-workers[197] and is considerably less than that for methyl radical (7.09 kcal.mole^{-1}) the latter in good agreement with the experimental ($\sim$8 kcal.mole^{-1}).[214,227] Zero point energy corrections may be of some importance due to low barriers and have been estimated to be of the order of 1 kcal.mole^{-1}.[207] In light of the weakness of the new bond this should be considered as an upper limit and it is anticipated that for the same radical, differences in these corrections will be small. The activation energies as calculated by the RHF method are considerably higher 10.98 and 11.99 kcal.mole^{-1} respectively for F and CH_3. Qualitatively the results are in good agreement with the total charge distribution for the UHF procedure, the UHF single determinantal procedure appears thus adequate in rationalising the total electronic charge. (This is fortunate as considerable difficulty is experienced in UHF convergence whilst that for the RHF procedure though requiring considerable monitoring did not suffer from the same limitations). Finally the overall distributions between radical and ethylene from these calculations are consistent with the model proposed and embodies the previous proposition of Szwarc that a methyl radical adds to olefin centres in a nucleophilic fashion.[194]

c). $CH_3 \cdot$ Addition to Trifluoroethylene.

An experimental result of some interest is the reversed orientation to that expected for CH_3 additions to C_2HF_3.[213] Whilst the normal mode of radical attack is at the CHF centre there is a preference with methyl radicals of $\sim 7:1$ for the CF_2 centre. To investigate this, calculations were performed on the CH_3 / C_2HF_3 system with a 25% conversion to the product radical of the ethylene substrate as a model for the T/S. Unfortunately the UHF procedure did not lead to any converging situation. The RHF method was operable however and the results are displayed in Table 6.10. The activation energies as calculated for attack at the CFH and CF_2 sites of 9.04 and 8.22 Kcal.mole^{-1} are qualitatively in accord with those of Tedder (8.6, 6.2 Kcal.mole^{-1} respectively) and reflect the inverted orientation pattern.

The results of a Mulliken population analysis again indicate little transference of the unpaired electron to the olefin. It is of interest that whilst the unpaired electron density on the methyl is similar for both sites there is a slightly higher total density for addition at CF_2. This is again in agreement with the observed higher β spin INDO densities for the substituent at the most fluorinated site observed in the product radicals. The magnitude of the difference (.007e) is however very much smaller than in the product radicals.

There is an increasing amount of data becoming available that repulsive interactions are of great importance in determining the rate of reaction at a centre. In this particular case the total energy has been separated into attractive (V_{NE}) and repulsive components. The changes in both components are large between the two sites, the V_{ATT}

Table 6.10.   Me· + C$_2$HF$_3$ T/S Energies and Population Analysis.
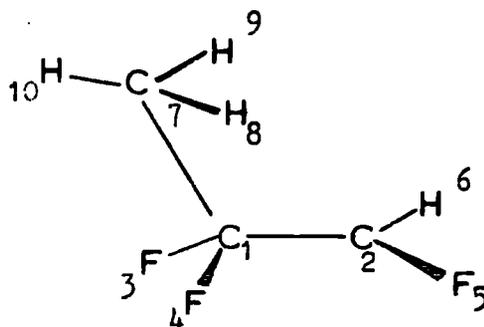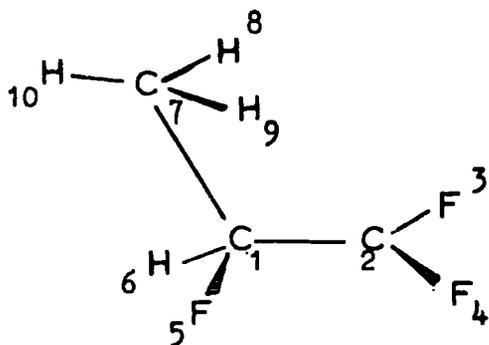
	Me at CFH	RHF	Me at CF$_2$
	−412.2295	E$_{TOT}$	−412.2308
	−651.6659	E$_{Elec.}$	−655.5854
	239.4365	E$_{Nuc.}$	243.3547
	−1044.7263	1 Elec.	−1052.5851
	409.8151	KE	409.8072
	−1454.5414	V$_{ATT}$	−1462.3923
	1042.3119	V$_{REP}$	1050.1615

Total	Spin	Centre	Total	Spin
5.963	−0.009	C1	5.295	0.004
5.330	0.028	C2	5.959	0.015
9.363	0.002	F3	9.369	−0.001
9.363	−0.003	F4	9.369	−0.001
9.362	0.002	F5	9.364	0.001
0.628	−0.003	H6	0.646	0.0
6.705	0.976	C7	6.717	0.975
0.749	0.002	H8	0.755	0.002
0.765	0.002	H9	0.765	0.002
0.771	0.002	H10	0.760	0.003
8.990	0.982	Me	8.997	0.982
−0.085		C1−C7	−0.047	
0.469		C1−C2	0.473	

term is however dominant indicating the greater attractive interaction at the CF_2 site. This is stubstantiated by the bond overlap populations of the new C-C bond (though these are negative in each instance). This is contrary to the findings for the product radical where greater overlap was found at the CFH site for a number of radicals. (An INDO calculation for attacking methyl radical also substantiates this). One possible conclusion is that changes in overlap density are due to the interactions of the radical SOMO with the LUMO of the olefin and follows the dependence established above on the coefficients. Indeed this overlap is reduced (employing the RHF data) in the order $CF_2 > CFH > CH_2$. This interaction with the LUMO of the ethylenes is consistent with the interpretation of Yamabe and co-workers.[209] Concerning this overlap in the new bond it is of interest to compare in the UHF procedure the α and β overlaps of the substrate with Me and F radicals. It is evident that for ethylene substrate the β overlap is increased with respect to the α overlap for the fluorine T/S in accord with the lower energy LUMOβ spin orbital of F.

To complement this study by now changing the ethylene substrate a final calculation was performed on the model T/S (25% conversion) for fluorine atom addition to CF_2 carbon in trifluoroethylene in the UHF formalism and the α and β spin overlap populations in the new bond computed (with the same C-F bond length as in $F./C_2H_4$). With comparison to the ethylene substrate the α overlap (-0.028e) is now increased whilst a decrease is observed in the β overlap population (-0.048e). From Table 6.10. the energies of the localised CHF and CF_2 carbon .pz orbitals are seen to be closely similar in these environments. However

the π charge cloud in the vicinity of the CF_2 carbon is anticipated to be somewhat contracted as compared with the CH_2 carbon in ethylene thus reducing the repulsive and attractive interactions in the C-F bond. This alternative suggestion will also account for the observed order in the computed CH_3-C RHF overlaps. It is probable that both schemes play an important role indetermining the orientation of addition in $CHF=CF_2$. It should be appreciated however that only in such cases where the π cloud in the olefin is drastically altered will (which can generally be regarded as second order effect) the 'size' of the localised π orbital in the olefin become of importance.

APPENDIX.

Co-ordinates, Basis Sets,
Thermochemical Data, Programs Employed.
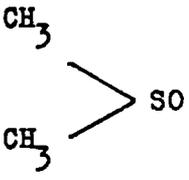
Molecule	Atom	X	Y	Z
CH_3 ⟩SO CH_3	S	1.889763	0.0	0.0
	C	4.139425	2.581567	0.0
	C	4.139425	-2.581567	0.0
	O	1.067741	0.0	-2.65552
	H	3.172717	4.389765	0.0
	N	5.340305	2.500857	-1.659962
	H	5.340305	·2.500857	1.659962
	H	3.172717	-4.389765	0.0
	H	5.340305	-2.500859	-1.659962
	H	5.340305	-2.500859	+1.659962
▷SO_2	C	3.144477	1.246894	0.0
	C	3.144477	-1.246894	0.0
	S	0.0	0.0	0.0
	O	-1.353070	0.0	2.343517
	O	-1.353070	0.0	2.343517
	H	3.959229	3.076860	0.0
	H	3.959229	-3.076860	0.0
CS	C	0.0	0.0	0.0
	S	2.900410	0.0	0.0
$S = C = CH_2$	S	-2.947840	0.0	0.0
	C	0.0	0.0	0.0
	C	2.482990	0.0	0.0
	H	3.466300	1.794692	0.0
	H	3.466300	1.794692	0.0
$H - C - C\overset{H}{\underset{H}{\langle}}S$	C	0.0	0.0	0.0
	C	2.607870	0.0	0.0
	S	4.395060	2.916428	0.0
	H	2.498494	4.594367	0.0
	H	-2.012596	0.0	0.0
	H	3.626450	1.764235	0.0
▷SO_2	C	2.905460	1.266068	0.0
	H	4.134008	2.956941	0.0
	S	0.0	0.0	0.0
	O	-1.453091	0.0	2.329283
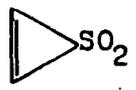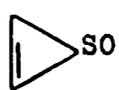
Molecule	Atom	X	Y	Z
▷SO	C	3.102127	1.235900	0.0
	H	4.330674	2.923677	0.0
	S	0.0	0.0	0.0
	O	1.253787	0.0	2.501057
CH_3 ... SO_2	S	1.889763	0.0	0.0
	C	3.995525	2.647311	0.0
	C	3.995525	-2.647311	0.0
	O	0.456935	0.0	-2.379917
	O	0.456935	0.0	2.379917
	H	2.948708	4.410341	0.0
	H	5.198817	2.620530	-1.659962
	H	5.198817	2.620530	1.659962
	H	5.198817	-2.620530	1.659962
	H	5.198817	-2.620530	-1.659962
	H	2.948708	-4.410341	0.0
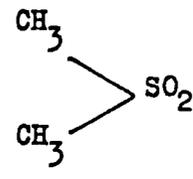
Coordinates of some Acetylenes (as employed in Chapter 2) a.u.

Molecule	Z Coordinates (Molecule aligned along this axis).
HCCH	0.0, 2.002, 4.283, 6.285.
FCCH	0.0, 2.417, 4.6809, 6.6708.
ClCCH	0.0, 3.084, 5.3725, 7.3605.
NCCCH	0.0, 2.1864, 4.7980, 7.0714, 9.0688.

Coordinates of 6a-thiathiophthen (as employed in Chapter 5) a.u.
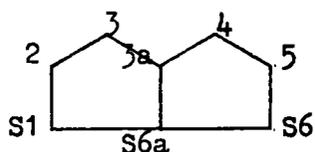
S6a	0.0	0.0	0.0
S6	4.440942	0.0	0.0
S1	-4.440942	0.0	0.0
C3a	0.0	3.310076	0.0
C5	4.551276	3.159645	0.0
C2	-4.551276	3.159645	0.0
C4	2.425286	4.593639	0.0
C3	-2.425286	4.593639	0.0
H5	6.344892	4.133497	0.0
H2	-6.344892	4.133497	0.0
H4	2.603163	6.626815	0.0
H3	-2.603163	6.626815	0.0

Coordinates of some Radical - Olefin T/S and Intermediates(as employed in Chapter 6.) a.u.

Molecule	Atom	X	Y	Z
	F	3.587900	2.432900	0.0
	C	2.702400	0.0	0.0
	C	0.0	0.0	0.0
FCH$_2$-CH$_2$	H	3.400500	-0.958900	1.660900
	H	3.400500	-0.958900	-1.660900
staggered	H	-1.081500	1.730900	0.0
and eclipsed	H	-1.081500	-1.730900	0.0
	H	-1.081500	0.0	1.730900
	H	-1.081500	0.0	-1.730900
	C	0.0	0.0	0.0
T/S for Me·	C	2.570076	0.0	0.0
and F· to	H	3.651608	1.730818	0.0
	H	3.651608	-1.730818	0.0
C$_2$H$_4$	H	-0.989468	1.769777	-0.232994
	H	-0.989468	-1.769777	-0.232994
	C	-1.551206	0.0	4.461966
	H	-0.773879	-1.722206	5.033409
	H	-0.773879	1.722206	5.033409
	H	-3.576934	0.0	4.013181
	F	-1.357305	0.0	3.729171
	C	0.0	0.0	0.0
	C	2.570080	0.0	0.0
	H	3.758154	1.659493	0.0
	F	3.890737	-2.138414	0.0
	F	-1.331839	-2.113236	-0.278211
C$_2$HF$_3$ in T/S	F	-1.331839	2.113236	-0.278211
Geometries.	C	0.0	0.0	0.0
	C	2.570080	0.0	0.0
	H	-1.081534	-1.716011	-0.225916
	F	-1.218512	2.179448	-0.286932
	F	4.047405	-2.033370	0.0
	F	4.047405	2.033370	0.0

Basis Sets Employed

Gaussian Basis Sets (as employed in Chapter 3).

Exponent	Coefficient	Exponent	Coefficient
Carbon S		**Oxygen S**	
994.7	0.032628	2200.0	0.0267586
160.0	0.214349	332.2	0.195756
39.91	0.824315	76.93	0.846397
11.82	1.0	21.74	1.0
3.698	1.0	6.773	1.0
0.6026	1.0	1.103	1.0
0.1817	1.0	0.3342	1.0
Carbon P		**Oxygen P**	
4.279	0.209524	8.356	0.221139
0.8699	0.881228	1.719	0.872694
0.2036	1.0	0.3814	1.0

Exponent	Coefficient	Exponent	Coefficient
Sulphur S		**Sulphur P**	
25506.3	0.005916	129.088	0.029069
3812.82	0.045815	29.6305	0.179893
860.556	0.229375	8.84715	0.478170
242.94	0.794115	2.85576	0.496736
79.0448	1.0	0.626108	1.0
27.5705	1.0	0.175223	1.0
6.49476	1.0		
2.42078	1.0	**Sulphur D**	
0.469815	1.0	0.25	1.0
0.173396	1.0		

Exponent	Coefficient
Hydrogen S	
6.48055	0.156319
0.981039	0.904665
0.217979	1.0

Basis Sets Employed. (contd.)

Acetylenes (Slater Orbitals)

	Type.	Single	Double	
H	1s	1.000	0.9716	1.2321
	2p		1.375,0.79	
C	1s	5.6727	5.2309	7.9690
	2s	1.6083	1.1678	1.8203
	2p	1.5679	1.2557	2.7263
	3d		1.895,1.429	
N	1s	6.6651	6.1186	8.9384
	2s	1.9327	1.3933	2.2216
	2p	1.9170	1.5059	3.2674
	3d		1.935,2.437	
F	1s	8.6501	7.9179	11.0110
	2s	2.5638	1.9467	3.0960
	2p	2.550	1.8454	4.1710
	3d		2.186,3414	
Cl	1s	16.5239	12.0587	17.6501
	2s	5.7152	4.9261	6.9833
	2p	6.4966	5.3574	9.5674
	3s	2.3561	2.0091	3.3416
	3p	2.0387	1.6092	2.8587
	3d		2.022,2.103	

Pyridine, Phosphabenzene, Arsabenzene, 6a-thiathiophthen(STO 3G)

H 1s	1.21
C 1s:2s:2p	5.67,1.73,1.73
N 1s:2s:2p	6.67,1.95,1.95
P 1s:2s:2p:3s:3p:3d	14.50,5.31,5.31,1.90,1.90,1.40
S 1s:2s:2p:3s:3p:3d	15.47,5.79,5.79,1.95,1.95,1.20
As 1s:2s:2p:3s:3p:3d:	32.28,12.06,14.54,6.20,5.95,5.79,
4s:4p:4d	2.24,1.86,0.95

Basis Sets Employed (contd.)

Radical-Olefin HF Basis (as employed Chapter 6).

Exponent	Coefficient	Exponent	Coefficient	Exponent	Coefficient
	Carbon 1s		Carbon 2s		Carbon 2p
158.79200	0.0648888	32.165900	−0.0874263	4.620170	0.0997425
28.86820	0.2815200	5.550890	−0.2444120	1.057310	0.3559750
7.82464	0.5338980	0.425297	0.6464920	0.311279	0.5258960
2.49060	0.2707320	1.0	1.0	0.0988179	1.0
	Fluorine 1s		Fluorines 2s		Fluorine 2p
361.73200	0.0651740	79.444500	−0.0889846	10.907700	0.1225110
65.87110	0.2850680	13.987600	−0.2592360	2.515680	0.3950710
17.96720	0.5385960	1.069980	0.6603240	0.708224	0.5037310
5.70045	0.2609610	0.326013	1.0	0.208634	1.0
	Hydrogen 1s				
5.216845	0.0567254				
0.945618	0.2601414				
0.265203	0.5328461				
0.088019	1.0				

Themochemical Data

Values refer to $0°K$ (or from non-empirical studies) except where otherwise stated.

Molecule		Molecule		Molecule	
O	- 9.589	S	22.562	C_2H_4	14.515
$O_g(^3P)$	58.98	$S_g(^3P)$	66.1	C_2H_2	54.32
F^+	419.57	Cl^+	327.47	CH_4	- 15.991
CH_3F	- 54.08	CH_3Cl	- 18.764	H^+	365.14
C_2H_5Cl	- 23.331	C_2H_6	- 16.523	$C_2H_3^+$	269.[*]
$C_2H_5^+$	219.[**]	$(CH_3)_2S$	- 5.033	$(CH_3)_2SO$	- 31.427
$(CH_3)_2SO_2$	- 83.3				

$$CH_3CH_3 \longrightarrow CH_3CH_2^+ \qquad (0)^{***}$$

$$CH_3CH_2F \longrightarrow FCH_2CH_2^+ \qquad 9.9$$

$$CH_3CH_2Cl \longrightarrow ClCH_2CH_2^+ \qquad 7.2$$

[*]   Reference 118.

[**]   Reference 117.

[***]   References 119,120,217,218.

Programs Employed

Many of the programs employed in this thesis are versions of the program packages discussed in Chapters 1 and 2. These were adapted where required to comprise an efficient and compact system. This work entialed production of:-

a) Geometry Minimisation Routine attached to the CNINDO program. Modification also allowed CNDO and INDO calculations with optional inclusion of d orbitals, variable convergence facilities, partition bond overlap calculation and convergence monitoring.

b) Interconversion of ATMOL-IBMOL input decks. Libraries were constructed for the easier formulation of IBMOL decks in Chapter 3. An improved version of POPAN 3 of VEILLARD and co-workers was employed for all the contour maps enclosed from both IBMOL and ATMOL calculations.

c) Applications Programs. Several programs for internal use have been developed. Of particular importance to this work are the following;

i) Correlation Energy estimates for molecules comprised of first row atoms.

ii) Line Printer Plotter for rapid production of contour maps.

Detailed below are three of the main programs employed; for geometry minimisation (Subroutine Main) contour mapping and for correlation energies. All are in FORTRAN IV.

```
1        PLOTTER PROGRAM FOR DENSITY CONTOUR MAPS
2
3           DIMENSION A(210,10),B(210,10),NDAT(10),P(120,120)
4           DIMENSION Z(10)
5           DIMENSION TITLE(20)
6           READ(5,27) (TITLE(I),I=1,20)
7        27 FORMAT(20A4)
8           WRITE(6,27)(TITLE(I),I=1,20)
9           READ(5,10)NJTYPE,AMAX,AMIN,BMAX,BMIN,DCT
10  C        NJTYPE IS 1 THEN ONE CONTOUR PER PAPER
11       10 FORMAT(I2,4F7.4,A1)
12          READ(5,53) (Z(I),I=1,10),ICHOIC
13  C     READ IN FORMAT A1. CAN BE A B C D E...OR X X X X X ETC.
14       53 FORMAT(10A1,I1)
15          DIMENSION TCP(120)
16          DO 16 I=1,120
17       16 TCP(I)=DCT
18          DO 26 J=1,12
19          K=10*J
20       26 TCP(K)=Z(1)
21          READ(5,11)NCONT,NTYPE,(NDAT(I),I=1,NCONT)
22  C     NCONT NO OF CONTOURS   NTYPE ANYTHING   NDAT NO OF DATA IN EACH CONT
23       11 FORMAT(I2,I2,10I4)
24  C        CARDS HERE FOR DATA READING
25          DO 21 K=1,NCONT
26          IF(ICHOIC.EQ.0) READ(5,721) NDAT(K)
27      721 FORMAT(I3)
28          IL=NDAT(K)
29          DO 22 L=1,IL,4
30       22 READ(5,13) A(L,K),B(L,K),A(L+1,K),B(L+1,K),A(L+2,K),B(L+2,K),
31         1A(L+3,K),B(L+3,K)
32       13 FORMAT(4(1X,F6.3,1X,F6.3,3X))
33  C        INSERT HERE
34       21 CONTINUE
35          ADIF=AMAX-AMIN
36          BDIF=BMAX-BMIN
37          IF(NJTYPE)40,40,41
38       40 CONTINUE
39          DO 92 I=1,120
40          DO 92 J=1,120
41       92 P(J,I)=0.0
42          DO 51 I=1,NCONT
43          IL=NDAT(I)
44          X=Z(I)
45          IF(NTYPE) 60,60,61
46       60 CONTINUE
47          DO 52 J=1,IL
48          II=A(J,I)*120/ADIF
49          JJ=B(J,I)*120/BDIF
50       52 P(JJ,II)=X
51          GO TO 62
52       61 CONTINUE
53          DO 152 J=1,IL
54          II=A(J,I)*120/ADIF
55          JJ=B(J,I)*120/BDIF
56      152 P(II,JJ)=X
57       62 CONTINUE
58       51 CONTINUE
59          WRITE(6,73)
60          WRITE(6,72)TCP
61          DO 45 I=1,120
62          P(I,120)=TCP(I)
63       45 WRITE(6,72) (P(I,J),J=1,120)
64          GO TO 80
65       41 CONTINUE
66          DO 64 I=1,NCONT
67          DO 91 IM=1,120
68          DO 91 JM=1,120
69       91 P(JM,IM)=0.0
70          WRITE(6,73)
71       73 FORMAT(1H )
72          WRITE(6,72)TCP
73          IL=NDAT(I)
74          X=Z(I)
75          IF(NTYPE)206,206,207
```

```
76       206 CONTINUE
77           DO 65 J=1,IL
78           II=A(J,I)*120/ADIF
79           JJ=E(J,I)*120/BDIF
80           P(JJ,II)=X
81        72 FORMAT(1H5,120A1)
82        65 CONTINUE
83           GO TO 208
84       207 CONTINUE
85           DO 241 J=1,IL
86           II=A(J,I)*120/ADIF
87           JJ=E(J,I)*120/BDIF
88       241 P(II,JJ)=X
89       208 CONTINUE
90           DO 32 IK=1,120
91           P(IK,120)=TCP(IK)
92        32 WRITE(6,72) (P(IK,J),J=1,120)
93        64 CONTINUE
94        80 CONTINUE
95           STOP
96           END
97
98
99           CORRELATION ENERGY PROGRAM
100
101.         DIMENSION AC(7),AN(7),AC(7),AF(7)
102      C    CORRELATION ENERGY PROGRAM
103           COMMON/BLK1/AH,AC,AN,AC,AF
104           DIMENSION PCP(5,20),ITYPE(20),AP(5,5) ,CCR(5,5),CR(5)
105           DIMENSION TITLE(20)
106      500 CONTINUE
107           WRITE(6,125)
108      125 FORMAT(1H1)
109      105 FORMAT(25A3)
110      C   READ IN DATA
111           READ(5,105) (TITLE(I),I=1,20)
112      C  OPTION CARD FOR FURTHER RUNS
113           WRITE(6,105) TITLE
114           READ(5,10) NATOMS
115       10 FORMAT(I4)
116      C   READ FCPS FOR EACH ATOM
117           READ(5,11)(ITYPE(I),(PCP(K,I),K=1,5),I=1,NATOMS)
118       11 FORMAT(I4,6X,5F10.6)
119      C    SET UP INTRACORREL MATRIX FOR EACH ATOM
120           TOTAL=0
121           WRITE(6,23)
122           CHARGE=0
123           DO 12 M=1,NATOMS
124           II=ITYPE(M)
125           GO TO (70,20,20,20,20,30,40,50,60,20,20), II
126       30 DO 31 I=1,7
127       31 CR(I)=AC(I)
128           GO TO 80
129       40 DO 41 I=1,7
130       41 CR(I)=AN(I)
131           GO TO 80
132       50 DO 51 I=1,7
133       51 CR(I)=AC(I)
134           GO TO 80
135       60 DO 61 I=1,7
136       61 CR(I)=AF(I)
137           GO TO 80
138       70 DO 71 I=1,7
139       71 CR(I)=0
140           CR(I)=AH
141       80 CONTINUE
142      C SET UP DENSTY MATRIX
143           DO 13 K=1,5
144           DO 13 L=1,5
145           AP(K,L)=PCP(K,M)*PCP(L,M)
146       13 CONTINUE
147      C
148      C  SET UP CORREL MATRIX
149           CCR(1,1)=CR(1)
150           CCR(2,2)=CR(4)
```

```
151          DC 16 I=3,5
152          CCR(1,I)=CR(6)
153          CCR(1,I)=CR(3)
154          CCR(2,I)=CR(5)
155       16 CCNTINUE
156          CCR(1,2)=CR(2)
157          CCR(3,4)=CR(7)
158          CCR(3,5)=CR(7)
159          CCR(4,5)=CR(7)
160          DC 17 L=1,5
161          DC 17 K=1,5
162       17 CCR(K,L)=CCR(L,K)
163    C
164    C     MULTIPLY CUT TO FIND E CCRREL FCR EACH CENTRE
165          S=C.C
166          CIAG=C.
167          SUM=C.C
168          DC 48 K=1,5
169          DC 18 L=1,K
170       18 SUM=SUM+CCR(L,K)*AP(L,K)
171          S=S+CCR(K,K)*AP(K,K)
172          CHARGE=CHARGE+PCP(K,M)
173       48 CIAG=CIAG+CCR(K,K)*PCP(K,M)*.5
174          SUM=SUM-S+CIAG
175          WRITE(6,19) M,ITYPE(M),SUM,(PCP(K,M),K=1,5)
176       19 FCRMAT(1H ,5X,I2,15X,I2,1CX,F7.4,1CX,5(F7.4,3X),//)
177       23 FCRMAT(1H ,'CENTRE NC.',5X,'CENTRE TYPE',5X,'  E CCRREL A.U.',
178       1'        1S          2S          PX          PY          PZ     ',/)
179          TCTAL=TCTAL+SUM
180          GC TO 5C
181       20 CCNTINUE
182       21 FCRMAT(1H ,'INVALIC DATA FCR CENTRE ',I2)
183          WRITE(6,21) M
184       50 CCNTINUE
185       12 CCNTINUE
186          WRITE(6,25) TCTAL
187       25 FCRMAT(1H ,'  TCTAL INTRAMCLECULAR CCRRELATICN ENERGY = ',F7.4)
188          WRITE(6,135) CHARGE
189      135 FCRMAT(1H ,40X,'CHECK.......TCTAL CHARGE = ',F7.4)
190          GC TC 5CO
191       63 CALL EXIT
192          END
193          BLCCK CATA
194          CCMMCN/BLK1/AH,AC,AN,AC,AF
195          DIMENSICN AC(7),AN(7),AC(7),AF(7)
196          CATA AH/-.C4C9/,
197       1    AC/-.C4C2,-.CC14,-.CC12,-.C12S,-.C118,-.C25E,-.C123/,
198       1          AF/-.C35E,-.CC14,-.CC16,-.C11S,-.CC64,-.C25E,-.C123/,
199       1          AC/-.C4C9,-.CC15,-.CC15,-.C284,-.C139,-.C25E,-.C123/,
200       1          AN/-.C4C9,-.CC13,-.CC14,-.C136,-.C13S,-.C25E,-.C123/
201          END
```

```
1                 GEOMETRY MINIMISATION PROGRAM  SUBROUTINE MAIN
2
3           BLOCK DATA
4           COMMON/CRB/CRB%S<
5           COMMON/PERTPL/EL%1P<
6           COMMON/CPTICN/CPTICN,CPNCLC,HUCKEL,CNDC,INCC,CLCSEC,CPEN
7           INTEGER CPTICN,CPNCLC,HUCKEL,CNDO,INDC,CLCSED,CPEN
8           INTEGER CPB,EL
9           DATA CNDC/äCNDCä/
10          DATA INCC/äINDCä/
11          DATA CPEN/äCPENä/
12          DATA CLCSEC/äCLSDä/
13          DATA CRB/ä    Sä,ä  PXä,ä  PYä,ä  PZä,ä DZZä,ä CXZä,ä CYZä,äCX-Yä,
14        1 ä DXYä/
15          DATA EL/ä   Fä,ä  HEä,ä  LIä,ä  BEä,ä   Bä,ä   Cä,ä   Nä,ä   Cä,
16        1 ä   Fä,ä  NEä,ä  NAä,ä  MGä,ä  ALä,ä  SIä,ä   Pä,ä   Sä,ä  CLä,
17        2 ä  ARä/
18          END
19          IMPLICIT REAL*8(A-H,C-Z)
20          COMMON/ARRAYS/APC%1S2CC<
21          COMMON/INFC/NATCMS,CHARGE,MULTIP,AN%35<,C%35,3<,N
22          COMMON/PEPTBL/EL%1E<
23          COMMON/CRB/CRB%S<
24          COMMON/GAB/XYZ%2CCC<
25          COMMON/INFC1/CZ%35<,U%8C<,ULIM%35<,LLI%35<,NELECS,CCCA,CCCB
26          COMMON/CPTICN/CPTICN,CPNCLC,HUCKEL,CNDC,INCC,CLCSEC,CPEN
27          COMMON/AUXINT/A%17<,B%17<
28          COMMON/DAH/DCRB
29          INTEGER DCRB
30          INTEGER  CPTICN,CPNCLC,HUCKEL,CNDC,INDC,CLCSED,CPEN
31          INTEGER CRP,EL,AN,CHARGE,CZ,U,ULIM,CCCA,CCCB
32          DIMENSION XP(6C),YP(6C),ZP(6C),R(6C,6C),IZAT(6C),NAME(9)
33          DIMENSION NAP(6C),NBP(6C),ACP(6C),NDP(6C),ILAZYP(6C)
34          DIMENSION THPCDP(6C),FHCP(6C),RCDP(6C)
35          COMMON/FLK/SCEMZ(2,3),PSCUN,IENSC
36          INTEGER IENSC,RSCUN,IPZR
37          DIMENSION MTP(20),NTP(2C)
38          COMMON/HEL/WP(2C),IPZR
39          WRITE%7,98C<
40      98C FORMAT%4H   <
41       45 READ%5,9CC<ICHG,%NAME%I<,I%1,9<
42      9CC FORMAT%I2,9A4<
43          IF%ICHG.EC.99<GC TC 99
44          WRITE%6,95C<%NAME%I<,I%1,9<,ICHG
45      95C FORMAT%1H1,9A4,7HCHARGE#,I3<
46          WRITE%7,981<ICHG,%NAME%I<,I%1,9<
47      981 FORMAT%I2,8X,9A4<
48          READ(5,4C)CPTICN,CPNCLC
49          WRITE(8,245)CPTICN,CPNCLC
50    C     MCDIFIED READ STATEMENT
51          READ(5,25C)NATCMS,CHARGE,MULTIP,DCRB
52          IF(DCRB.EC.C) WRITE(9,1453)
53          IF(DCRB.EC.1) WRITE(9,1454)
54     1453 FORMAT(5X,'C CRBITALS IN')
55     1454 FORMAT(5X,'C CRBITALS CUT')
56          WRITE(8,6C)NATCMS,CHARGE,MULTIP
57          READ(5,9C1)NCAT,(IZAT(I),I=1,3),KWIK,R12,R23,THETAP
58      901 FORMAT%412,I1,2F7.4,F14.7<
59          WRITE%6,951<NCAT,%IZAT%I<,I%1,3<,KWIK
60      951 FORMAT %8HCNCAT # I2, 14H    IZAT%1< # I2, 14H    IZAT%2< # I2,
61        1 14H    IZAT%3< # I2, 11H    KWIK # I1<
62    C     CHANGE IN PARAMATER N TCM AS A CCL AN H F7.4  VARIABLE
63          RSCUN=1
64      967 WRITE(7,964)RSCUN
65          IENSC=1
66          READ(5,317)IPZR
67      317 FORMAT(I2)
68          DC 963 I=1,IPZR
69          READ(5,96C)MTP(I),NTP(I),WP(I)
70      963 CONTINUE
71      476 DC 474 I=1,IPZR
72          MT=MTP(I)
73          NT=NTP(I)
74          W=WP(I)
75      96C FORMAT(2I2,F7.4)
```

```
76      C       TEST FCR ENC CARC   IF M=SS STCP
77              IF(MT.EC.SS) GO TC SS
78      C       TEST FCR M  IF M = C FIRST PUN AND W=C  M=2.3 FULL RUN
79              IF(MT.EC.C) GO TC S73
80              IF(MT-3)S61,S61,S62
81          S61 IF(NT-7)712,713,714
82          712 R12=R12+h
83              BCW=R12
84              GC TC 474
85          713 R23=R23+W
86              BCW=R23
87              GC TC 474
88          714 THETAP=THETAP+h
89              BCW=THETAP
90              GC TC 474
91          S62 IF(NT-8)722,723,724
92          722 RCCP(MT)=RCCP(MT)+h
93              BCW=RCDP(MT)
94              GO TC 474
95          723 THBCCP(MT)=THBCCP(MT)+h
96              BCW=THBCDP(MT)
97              GC TC 474
98          724 PHCP(MT)=PHCP(MT)+h
99              BCW=PHDP(MT)
100     C       IN ALL CASES MT WILL BE ECUIVALENT TC IZAT(NC).
101         474 CCNTINUE
102             SCENZ(2,IENSC)=BCW
103             RSCUN=MT
104
105         973 WRITE(6,952)R12,R23,THETAP
106         952 FCRMAT %7H R12 # F7.4, 1CH     R23 # F7.4, 12H     THETA # E14.7<
107             IF %KWIK - 1< 1, 2, 3
108           1 CCCS#-1./3.
109             SSIN#%2./3.<*SQRT%2.<
110             GO TO 4
111           2 CCCS#-C.5
112             SSIN#C.5*SCRT%3.<
113             GC TC 4
114           3 THETA=THETAP*3.1415S26536/18C.
115             CCCS=CCCS(THETA)
116             SSIN=CSIN(THETA)
117           4 DC 51 I#1,3
118             XP(I)=C.C
119             YP(I)=0.C
120          51 ZP(I)=3.0
121             XP(2)=R12
122             XP(3)=R12-R23*CCCS
123             YP(3)=R23*SSIN
124             DO 5 I # 4, NCAT
125           5 XP(I)=10CCC.C
126             WRITE%6,953<
127         953 FCRMAT %8BHC  NA    NB    NC    ND    IZAT%NC<    ILAZY        RCD
128           1             THBCD            PHABCD/<
129             DC 52 I#4,NCAT
130     C
131             WRITE(6,964)RSCUN
132         964 FCRMAT(I2)
133     C       TC DC LCCP WITH NEW PARAMETER TEST FCR VALUE CF M
134             IF(MT.CE.1) GC TC 6S
135         965 READ(5,9C2)NAP(I),NBP(I),NCP(I),NDP(I),IZAT(I),ILAZYP(I),
136           1PCCP(I),THBCCP(I),PHDP(I)
137          66 NA=NAP(I)
138             NB=NBP(I)
139             NC=NCP(I)
140             ND=NDP(I)
141
142             ILAZY=ILAZYP(I)
143             RCC=RCDP(I)
144             THBCC=THBCCP(I)
145             PHABCC=PHCP(I)
146
147         9C2 FCRMAT%5I2,I1,F7.4,2F14.7<
148     C       CHECK THAT CCCRCINATES CF ATCMS NA, NB, NC HAVE BEEN CALCULATED
149     C
150           7 IF(XP(NA) & XP(NC) & XP(NB) -7CCC.C)S,5C,5C
```

/

```
151          8 WRITE?6,S54<NA,NB,NC,NC,IZAT?ND<,ILAZY,RCD,THRCD,PHARCC
152        954 FCRMAT %3X,I2,3X,I2,3X,I2,3X,I2,6X,I2,1OX,I1,7X,F7.4,8X,E14.7,4X,
153            1E14.7<
154            IF ?ILAZY - E< 7S, 7E, 7S
155         7E RBC=CSCRT((XP(NC)-XP(NB))**2+(YP(NC)-YP(NC))**2+(ZP(NC)-ZP(NB
156            1<<**2<
157            XP?NC<*XP?NC< + ?XP?NC< -XP?NB<<*RCC/RBC
158            YP?NC< = YP?NC< + ?YP?NC< - YP?NB<<*RCC/RBC
159            ZP?NC< = ZP?NC< + ?ZP?NC< - ZP?NB<<*RCC/RBC
16C            GC TC 52
161   C
162   C        MCVE ATCM C TC CRIGIN
163   C
164         7S XA = XP?NA< -XP?NC<
165            YA = YP?NA< -YP?NC<
166            ZA = ZP?NA< - ZP?NC<
167            XB = XP?NB< - XP?NC<
168            YB = YP?NB< - YP?NC<
169            ZB = ZP?NB< - ZP?NC<
17C   C
171   C        RCTATE ABCUT Z-AXIS TC MAKE YB # 0, XP &VE. IF XYB TCC SMALL,
172   C        RCTATE FIRST 90 CEGREES ABCUT Y AXIS
173   C
174            XYB=CSQRT(XB**2+YB**2)
175            K # 1
176            IF ?XYB - C.1< 9, 1C, 10
177          9 K # C
178            XPA # ZA
179            ZPA # -XA
180            XA # XPA
181            ZA # ZPA
182            XPB # ZB
183            ZPB # -XB
184            XB # XPB
185            ZB # ZPB
186            XYB=CSCRT(XB**2+YB**2)
187         1C CCSTH # XB/XYB
188            SINTH # YB/XYB
189            XPA # XA*CCSTH & YA*SINTH
19C            YPA # YA*CCSTH - XA*SINTH
191   C
192   C        RCTATE ABCUT Y AXIS TC MAKE ZB VANISH
193   C
194         11 RBC=CSCRT(XB**2+YB**2+ZB**2)
195            SINFH # ZB/RBC
196            COSPH=CSQRT(1.-SINPH**2)
197            XCA # XPA*CCSPH & ZA*SINPH
198            ZCA # ZA*CCSPH - XPA*SINPH
199   C
2CC   C        RCTATE ABCUT X AXIS TC MAKE ZA # C, YA &VE
2C1   C
202         12 YZA=CSCRT(YPA**2+ZCA**2)
2C?            CCSKH # YPA/YZA
204            SINKH # ZCA/YZA
205   C
206   C        CCCRCINATES A, ?XCA,YZA,C<, B, ?RBC,C,C<, C, %C,C,C<, NCNE -VE
207   C        CCCRCINATES CF C NCW CALCULATED IN NEW FRAME
208   C
2C9            IF ?ILAZY - 1< 13, 14, 15
21C         13 CCSC # 1.C
211            SIND # C
212            GC TC 21
213         14 CCSC # C.5
214            SIND#C.5*SCRT?3.<
215            GC TC 21
216         15 IF ?ILA7Y - ?< 16, 17, 18
217         16 CCSC # -C.5
218            SINC#C.5*SCRT?3.<
219            GC TC 21
22C         17 CCSC # -1.C
221            SINC # 0
222            GC TO 21
223         18 IF ?ILAZY - 5< 1S, 2C, 22
224         1S CCSC # -C.5
225            SINC#-0.5*SCRT?3.<
```

```
226        20 CCSD # C.5
227           SINC#-C.5*SCRT#3.<
228        21 CCSA # -1.C/3.C
229           SINA#%2./3.<*SQRT#2.<
230           GC TC 29
231        22 IF #ILAZY - 7< 23, 24, 2€
232        23 CCSC # 1.0
233           SINC # 0
234           GC TC 25
235        24 CCSC # -1.C
236           SINC # 0
237        25 CCSA # -C.5
238           SINA#C.5*SCRT#3.<
239           GC TC 29
240        26 IF #ILAZY - S< 27, 28, 28
241        27 CCNTINUE
242           GC TC 29
243        28 THBCC#THBCD*3.1415926536/1EC.
244           PHABCC#PHABCC*3.1415926536/180.
245           SINA=CSIN(THBCC)
246           CCSA=CCCS(THBCC)
247           SINC=CSIN(PHABCC)
248           CCSC=CCCS(PHABCC)
249        29 CCNTINUE
250           XD # RCD*CCSA
251           YD # PCD*SINA*CGSC
252           ZD # RCD*SINA*SINC
253    C
254    C     .TRANSFCRM CCCRCINATES CF D BACK TC CRIGINAL SYSTEM
255    C
256        30 YPC # YC*CCSKH - ZC*SINKH
257           7PC # 7C*CCSKH & YC*SINKH
258           XPC # XC*CCSPH - 7PC*SINPH
259           ZCD # 7PD*CCSPH & XC*SINPH
260           XCC # XPC*CCSTH - YPC*SINTH
261           YCC # YPD*CCSTH & XPD*SINTH
262           IF #K - 1< 31, 32, 31
263        31 XRD # -ZCD
264           ZRC # XQD
265           XCC # XPC
266           ZCD # ZRD
267        32 XP(NC)=XQD + XP(NC)
268           YP#NC< = YCC + YP#NC<
269           ZP#NC< = ZCC + ZP#NC<
270        52 CCNTINUE
271           WRITE#6,95C<#NAME#I<,I#1.9<,ICHG
272           WRITE#6,955<
273       955 FCRMAT #78HCNO. CF ATCM        X-CCCRCINATE          Y-CCCRDINAT
274          1E          Z-CCCRCINATE/<
275           DC 41 I#1,NCAT
276           WRITE(6,956)I,XP(I),YP(I),ZP(I)
277       956 FCRMAT#1H ,5X,I2,15X,F1C.7,11X,F10.7,11X,F10.7<
278           IF#IZAT#I<.EC.99<GC TC 41
279           WRITE(7,982)IZAT(I),YP(I),YP(I),ZP(I)
280       982 FCRMAT(I4,3(3X,F12.7))
281        41 CCNTINUE
282           WRITE#7,98C<
283        5C WRITE#6,958<
284       958 FCRMAT#1H0,38HCCCRDS.CF 1 REFERENCE ATCM UNAVAILABLE<
285           K=1
286           DC 634 I=1,NCAT
287           IF(IZAT(I).EC.98)GC TC 634
288           AN(K)=IZAT(I)
289           C(K,1)=XP(I)
290           C(K,2)=YP(I)
291           C(K,3)=ZP(I)
292
293    C     CCNVERSICN CF CCCRCINATES FRCM ANGSTRCMS TC ATCMIC UNITS
294           DC 229 J=1,3
295       229 C(K,J)=C(K,J)/.5291670C
296           K=K+1
297       634 CCNTINUE
298           IF(CPTICN.EC.CHCC) GC TC 226
299       211 DC 225 I=1,NATCMS
300           IF(AN(I).LE.9) GC TC 224
```

```
301        222 WRITE(6,223)
302        223 FCRMAT(5X,46HTHIS PROGRAM DOES NOT DC CALCS. FOR,
303          1    51H MOLECULES CONTAINING ELEMENTS HIGHER THAN FLUORINE<
304            STOP
305        224 CONTINUE
306        225 CONTINUE
307        226 CONTINUE
308            WRITE(6,964)RSCUN
309            CALL CCEFFT
310            CALL INTGRL
311            IF (RCPNCLC.FC.OPEN< GC TC SC
312         8C CALL HUCKCL
313            CALL SCFCLC
314            WRITE(6,964)RSCUN
315            CALL CPRINT
316            GC TC 1CC
317         SC CALL HUCKCP
318            CALL SCFCPN
319            CALL CPRINT
320        1CC CONTINUE
321            IENSC=IENSC+1
322            IF(IENSC.GE.4) GC TC 254
323            WRITE(6,964)RSCUN
324            IF(RSCUN.LE.1) GC TC 967
325        220 FCRMAT(2CA4)
326        230 FCRMAT(1F1.5X,2CA4)
327         4C FCRMAT%A4,1X,A4<
328        245 FCRMAT(5X,A4,1X,A4)
329        250 FCRMAT(3I4,11X,I1)
330         6C FCRMAT%/5X,I4,18H ATOMS    CHARGE  #,I4,18H   MULTIPLICITY #,I4/<
331         7C FOPMAT%I4,3%3X,F12.7<<
332            GC TC 476
333        254 CONTINUE
334                    DIMENSICN PG(5),RG(5),SG(5),TG(5),DEN(3),DAN(3),
335          1         DIN(3),FIN(3),CIN(3)
336            DC 64 I=1,2
337            RG(I)=SCENZ(2,I+1)-SCENZ(2,I)
338         64 SG(I)=SCENZ(1,I+1)-SCENZ(1,I)
339            RG(3)=SCENZ(2,1)-SCENZ(2,3)
340            SG(3)=SCENZ(1,1)-SCENZ(1,3)
341            DC 623 I=1,3
342                TG(I)=SCENZ(1,I)
343        623 PG(I)=SCENZ(2,I)**2
344                DC 517 I=1,2
345                RG(I+3)=RG(I)
346                SG(I+3)=SG(I)
347                PG(I+3)=PG(I)
348        517    TG(I+3)=TG(I)
349            DC 3C1 I=1,3
350            DEN(I)=TG(I)*RG(I+1)+TG(I+1)*RG(I+2)+TG(I+2)*RG(I)
351
352            DAN(I)=PG(I)*RG(I+1)+PG(I+1)*RG(I+2)+PG(I+2)*RG(I)
353            DIN(I)=PG(I)*SG(I+1)+PG(I+1)*SG(I+2)+PG(I+2)*SG(I)
354            FIN(I)=DEN(I)/DAN(I)
355        3C1    CIN(I)=DIN(I)/(DEN(I)*(-2.DC))
356            WRITE(6,743)
357        743 FCRMAT(//32H     MT    NT    COORDINATE CHANGE)
358            DC 744 I=1,IPZR
359            WRITE(8,745)NTP(I),NTP(I),WP(I)
360        745 FCRMAT(/1H ,2X,I2,4X,I2,7X,F9.4)
361        744 CONTINUE
362            DC 748 I=1,3
363        749 FCRMAT(/1H ,5X,F16.1C,4X,F9.4,4X,1PD14.7,4X,-1PF9.4)
364        748 WRITE(8,749)SCENZ(1,I),SCENZ(2,I),FIN(I),CIN(I)
365            FC=(FIN(1)+FIN(2)+FIN(3))/3
366             CMIN=(CIN(1)+CIN(2)+CIN(3))/3
367            WRITE(8,747)CMIN,FC
368        747 FCRMAT(/1H ,1CX,1CHMINIMUM = ,F9.4,5X,5HFC = ,1PD14.7)
369            MT=MTP(IPZR)
370            NT=NTP(IPZR)
371            IF(MT-3)441,441,442
372        441 IF(NT-7)443,444,445
373        443 GAR=CMIN-R12
374            GC TC 449
375        444 GAR=CMIN-R23
```

```
376              GO TO 449
377          445 GAR=CMIN-THETAP
378              GC TC 449
379          442 IF(NT-6)446,447,448
380          446 GAR=CMIN-FCCP(MT)
381              GG TC 449
382          447 GAR=CMIN-THBCOP(MT)
383              GC TC 449
384          448 GAR=CMIN-PHCP(MT)
385          449 DC 351 I=1,IPZR
386              MT=MTP(I)
387              NT=NTP(I)
388              W=WF(I)
389              IF(MT-2)461,461,462
390          461 IF(NT-7)412,413,414
391          412 R12=R12+GAR*W/WP(IPZR)
392              GC TC 351
393          413 R23=R23+GAR*W/WP(IPZR)
394              GC TC 351
395          414 THETAP=THETAP+GAR*W/WP(IPZR)
396              GC TC 351
397          462 IF(NT-8)422,423,424
398          422 RCCP(MT)=FCCP(MT)+GAR*W/WP(IPZR)
399              GC TC 351
400          423 THPCOP(MT)=THBCOP(MT)+GAR*W/WP(IPZR)
401              GC TC 351
402          424 PHDP(MT)=PHCP(MT)+GAR*W/WP(IPZR)
403          351 CCNTINUE
404              GC TC 967
405           99 STGP
406              END
```

References

1.   D.T. Clark, Ann. Report Chem. Soc. (B), 1971, 68, 43.

2.   E. Schrödinger, Ann. Physik., 1926, 79, 361, 489, 734, 81, 109;

      Phys. Rev., 1926, 28, 1049.

3.   M. Born and J.R. Oppenheimer, Ann. Physik., 1927, 84, 457.

4.   D.R. Hartree, Proc. Camb. Phil. Soc., 1928, 24, 89; 1928, 24, 111;

      1928, 24, 426.

5.   V. Fock, Z. Physik., 1930, 126, 61.

6.   J.C. Slater, Phys. Rev., 1930, 35, 210.

7.   C.C.J. Roothaan, Rev. Mod. Phys., 1951, 23, 69.

8.   K. Siegbahn, C. Nordling, A. Fahlman, R. Nordberg, K. Hamrin, J. Hedman,

      G. Johansson, T. Bergmark, S.E. Karlsson, I. Lidgren and B. Lindberg,

      ESCA 'Atomic, Molecular and Solid State Structure Studied by Means of

      Electron Spectroscopy', Almquist and Wiksells, Upsala, 1967.

9.   D.W. Turner, C. Baker, A.D. Baker and C.R. Brundle, 'Molecular

      Photoelectron Spectroscopy', John Wiley and Sons Ltd., 1970.

10.   T.A. Koopmans, Physica, 1933, 1, 104.

11.   C. Edmiston and K. Ruedenberg, Rev. Mod. Phys., 1963, 35, 457.

12.   S.F. Boys, Rev. Mod. Phys., 1960, 32, 296.

13.   R.K. Nesbet, J. Math. Phys., 1961, 2, 701.

14.   C.C.J. Roothaan, Rev. Mod. Phys., 1960, 32, 179.

15.   I.H. Hillier, V.R. Saunders, Int. J. Quantum Chemistry, 1970, 4, 503;

      Proc. Roy. Soc. A, 1970, 320, 161.

16.   W.J. Hunt, P.J. Hay and W.A. Goddard, III, J. Amer. Chem. Soc., 1972, 94,

      638.

17.   J.A. Pople and R.K. Nesbet, J. Chem. Phys., 1954, 22, 571.

18.   A.J. Freeman and R.E. Watson, 'Magnetism', Ed. G.T. Rado and H. Suhl,

      (Academic Press, New York, 1965).

19. P.S. Bagus and B. Liu, Phys. Rev., 1966, 148, 79.

20. J.C. Slater, Phys. Rev., 1930, 36, 57.

21. S.F. Boys, Proc. Roy. Soc. (London), 1950, A200, 542.

22. C. Zener, Phys. Rev., 1930, 36, 51.

23. I. Shavitt, Methods in Computation Physics, 1963, 2, 1.

24. H.B. Jansen and P. Ros, Theoret. chim. Acta, 1972, 27, 95.

25. E. Clementi and D.L. Raimondi, J. Chem. Phys., 1963, 38, 2686.

26. J.M. Foster and S.F. Boys, Rev. Mod. Phys., 1960, 32, 303.

27. W.J. Hehre, R.F. Stewart and J.A. Pople, J. Chem. Phys., 1969, 51, 2657.

28. R.F. Stewart, J. Chem. Phys., 1969, 50, 2485.

29. R. Ditchfield, W.J. Hehre and J.A. Pople, J. Chem. Phys., 1971, 54, 724.

30. E. Clementi, D.L. Raimondi and W.P. Reinhardt, J. Chem. Phys., 1967, 47, 1300.

31. E. Clementi, J. Chem. Phys., 1964, 40, 1944.

32. E. Clementi, R. Matcha and A. Veillard, J. Chem. Phys., 1967, 47, 1865.

33. E. Clementi, 'Tables of Atomic Wave Functions', a supplement to IBM J. Res. Develop., 1965, 9, 2.

34. J.L. Whitten, J. Chem. Phys., 1966, 44, 359.

35. E. Clementi and R. Davis, J. Comput. Phys., 1967, 2, 223.

36. T. H. Dunning, J. Chem. Phys., 1970, 53, 2823.

37. P. Siegbahn and B. Roos in Proceeding Computational Problems in Quantum Chemistry, Strasburg, 1969, 53.

38. D.R. Whitman and C.J. Hornback, J. Chem. Phys., 1969, 51, 398.

39. R.K. Nesbet, Rev. Mod. Phys., 1960, 32, 272.

40. R.K. Nesbet, J. Chem. Phys., 1964, 40, 3619.

41. A.A. Frost, J. Chem. Phys., 1967, 47, 3707.

42. R.E. Christoffersen, J. Amer. Chem. Soc., 1971, 93, 4104.

43. H. Preuss, Z. Naturforsch, 1956, 11, 823.

44. J.L. Whitten, J. Chem. Phys., 1966, 44, 395.

45. I.G. Csizmadia, M.G. Harrison, J.W. Moscowitz, S.S. Seung, B.T. Sutcliffe and M.P. Burnett, 'The Polyatom System', Q.C.P.E. No.47A.

46. E. Clementi, J. Mehl and W. von Niessen, J. Chem. Phys., 1971, 54, 508.

47. V.R. Saunders, I.H. Hillier, M.F. Guest and M.F. Chiu, ATMOL, Atlas Computing Laboratories, 1973.

48. J.E. Eilers and D.R. Whitman, J. Amer. Chem. Soc., 1973, 95, 2067.

49. M. Yoshimine, Technical Report RJ-555, IBM Corp., 1969.

50. R.C. Raffenetti, Chem. Phys. Lett., 1973, 20, 335.

51. R. McWeeny, Proc. Roy. Soc., 1956, A235, 496.

52. E. Clementi and J. Mehl, 'IBM System 360 IBMOL 5 Program, Quantum Mechanical Concepts and Algorithms', IBM Research Laboratory, San Jose, June 1971.

53. V.R. Saunders, M.F. Guest and M.F. Chiu, ATMOL 2, Atlas Computer Laboratories, 1973.

54. A.D. McLean, Proceedings of Conference on Potential Energy Surfaces in Chemistry, Ed. W.A. Lester, IBM Research Laboratory, San Jose, 1971.

55. E. Clementi, J. Mehl and W. von Niessens, J. Chem. Phys., 1971, 54, 508.

56. J.A. Pople and D.L. Beveridge, 'Approximate Molecular Orbital Theory', McGraw-Hill, 1970.

57. J.A. Pople, D.P. Santry and G.A. Segal, J. Chem. Phys., 1965, 43, S129.

58. J.A. Pople and G.A. Segal, J. Chem. Phys., 1967, 47, 158.

59. J.A. Pople, D.L. Beveridge and P.A. Dobosh, J. Chem. Phys., 1967, 47, 2026.

60. J.A. Pople and G.A. Segal, J. Chem. Phys., 1965, 43, 5136.

61. C.C.J. Roothaan, J. Chem. Phys., 1951, 19, 1445.

62. D.P. Santry and G.A. Segal, J. Chem. Phys., 1967, 47, 158.

63. J.A. Pople and P.A. Dobosh, CNINDO, QCPE, 91, 141, 142, 144.

64. J.W. McIver, Jnr. and A. Komornicki, Chem. Phys. Lett., 1971, 10, 373.

65. W.L. Bloemer and B.L. Bruner, Chem. Phys. Lett., 1972, 17, 452.

66. L.C. Snyder and H. Basch, J. Amer. Chem. Soc., 1969, 91, 2189.

67. R. Ditchfield, W.J. Hehre, J.A. Pople and L. Radom, Chem. Phys. Lett., 1970, 5, 13.

68. W.J. Hehre, R. Ditchfield, L. Radom and J.A. Pople, J. Amer. Chem. Soc., 1970, 92, 4796.

69. P.O. Löwdin, Advan. Chem. Phys., 1959, 2, 207.

70. R.K. Nesbet, Advan. Chem. Phys., 1969, 14, 1.

71. D. Sinanoğlu, Advan. Chem. Phys., 1969, 14, 237.

72. H. Önder Pamuk, Theoret. chim. Acta, 1972, 28, 85.

73. L.C. Snyder, Robert A. Welch Foundation Research Bulletin, 1971.

74. E.A. Hylleras, Z. Physik., 1928, 48, 569.

75. E. Clementi, J. Chem. Phys., 1967, 46, 284.

76. A.C. Wahl, J. Chem. Phys., 1964, 41, 2600.

77. W.A. Goddard, III and R.C. Ladner, J. Amer. Chem. Soc., 1971, 93, 6750.

78. R.S. Mulliken, J. Chem. Phys., 1955, 23, 1883, 1841, 2338, 2343.

79. L. Ch. Cusachs and P. Politzer, Chem. Phys. Lett., 1968, 1, 529.

80. P.O. Löwdin, J. Chem. Phys., 1950, 18, 365.

81. P. Politzer and R.R. Harris, J. Amer. Chem. Soc., 1970, 92, 6451.

82. G. Richards in Atlas Computing Laboratory Symposia, 1971.

83. R.L. Flurry, D. Breen and D.L. Howland, Theor. chim. Acta, 1971, 20, 371.

84. E.A. Laws and W.N. Lipscomb, Israel J. Chem., 1972, 10, 77.

85. L.C. Snyder and T. Amos, J. Chem. Phys., 1965, 42, 3670.

86. D.T. Clark, Specialist Periodical Report J.C.S., 'Organic Compounds of Sulphur, Selenium and Tellurium, 1969, 1.

87. P.C. Hariharan, W.A. Lathan and J.A. Pople, Chem. Phys. Lett., 1972, 14, 385.

88. P.C. Hariharan and J.A. Pople, Theoret. chim. Acta, 1973, 28, 213.

89. M.S.B. Munson, J. Amer. Chem. Soc., 1965, 87, 2332.

90. W.J. Hehre, L. Radom and J.A. Pople, J. Amer. Chem. Soc., 1972, 94, 1496.

91. E. Hückel, Z. Physik., 1931, 70, 204.

92. Tables of Interatomic Distances, Ed. L.E. Sutton, Chemical Society Special Publication, Nos.11 (1958) and No.18 (1965).

93. A.D. McLean and M. Yoshminie, IBM J. Res. Devel., 1968, 206.

94. R. Hoffmann, Accounts of Chemical Research, 1971, 4, 1.

95. R.S. Mulliken, J. Chem. Phys., 1939, 7, 339.

96. R. Hoffmann, L. Radom, J.A. Pople, P. von R. Schleyer, W.J. Hehre and L. Salem, J. Amer. Chem. Soc., 1972, 94, 6220.

97. R. Bonaccorsi, E. Scrocco and J. Tomasi, J. Chem. Phys., 1970, 52, 5270.

98. D.T. Clark and D.B. Adams, Tetrahedron, 1973, 29, 1887.

99. P. Auger, J. Phys. Radium, 1925, 6, 205; Comput. Rend., 1925, 180, 65.

100. K. Siegbahn, C. Nordling, G. Johansson, J. Hedman, P.F. Heden, K. Hamrin, U. Gelius, T. Bergmark, L.O. Werme, R. Manne and Y. Baer, 'ESCA Applied to Free Molecules', North Holland, 1969.

101. J.S. Levinger, Phys. Rev., 1953, 90, 11.

102. P.S. Bagus, Phys. Rev. A, 1965, 139, 619.

103. M. Barber and D.T. Clark, Chem. Comm., 1970, 22.

104. W.G. Richards, Int. J. Mass Spec. Ion Phys., 1969, 2, 419.

105. M.E. Schwartz, Chem. Phys. Lett., 1970, 5, 50.

106. W.L. Jolly and D.N. Hendrickson, J. Amer. Chem. Soc., 1970, 92, 1863.

107. D.T. Clark and D.B. Adams, J. Chem. Soc. Faraday Trans. II, 1972, 68, 1819.

108. O. Goscinski, B.T. Pickup and G. Purvis, Chem. Phys. Lett., 1973, 22, 167.

109. D.T. Clark, 'Chemical Aspects of ESCA', pp. 373-507, Electron Emission Spectroscopy, Ed. W. Dekeyser, D. Reidel Publishing Co., 1973, Dordrecht, Holland.

110. D.T. Clark, I.W. Scanlan and J. Muller, Theoret. chim. Acta, (submitted for publication).

111. E. Clementi and W. Popkie, J. Amer. Chem. Soc., 1972, 94, 4057.

112. W. Meyer, J. Chem. Phys., 1973, 58, 1017.

113. J.A. Pople and G.A. Segal, J. Chem. Phys., 1966, 44, 3289.

114. W. Heisenberg, Z. Physik., 1926, 31, 617.

115. U. Gelius, E. Basilier, S. Svensson, T. Bergmark and K. Siegbahn, J. Elec. Spec., 1974, 2, 405.

116. L. Radom, P.C. Hariharan, J.A. Pople and P. von R. Schleyer, J. Amer. Chem. Soc., 1973, 95, 6531.

117. F.P. Lossing and G.P. Semeluk, Can. J. Chem., 1970, 48, 955.

118. F.P. Lossing, Can. J. Chem., 1971, 49, 357; 1972, 50, 3973.

119. D.T. Clark and D.M.J. Lilley, J. Chem. Soc. (D), 1970, 1042.

120. D.T. Clark and D.M.J. Lilley, Tetrahedron, 1973, 29, 845.

121. C.A. Coulson and A. Streitweiser Jnr., Dictionary of π-Electron Calculations, Pergamon Press, Oxford, 1965.

122. C.A. Coulson and W.E. Moffitt, Philos. Mag., 1949, 40, 1.

123. A.D. Walsh, Trans. Faraday Soc., 1949, 45, 179; Nature, 1947, 159, 165, 172.

124. E. Kochanski and J-M. Lehn, Theoret. chim. Acta, 1969, 14, 281.

125. D.T. Clark, Proc. Israel Academy of Science and Humanities, 1970, 238.

126. D.T. Clark, Theoret. chim. Acta, 1969, 15, 225.

127. M.J.S. Dewar, Bull Soc. Chim. Fr., 1951, 18C, 79.

128. J. Chatt and L.A. Duncanson, J. Chem. Soc., 1953, 2939.

129. C.E. More, N.B.S. Atomic Energy Levels 1949.

130. JANAF Thermochemical Tables, 1965.

131. N.B.S. Technical Note 270-4, 'Selected Values of Thermodynamic Properties', 1969.

132. P.O. Strauz, R.K. Gosavi, A.S. Denes and I.G. Csizmadia, Theoret. chim. Acta, in press.

133. L.A. Carpino and L.V. McAdams, III, J. Amer. Chem. Soc., 1965, 87, 5804.

134. L.A. Carpino, L.V. McAdams, III, R.H. Rynbrandt and J.W. Spiewak, J. Amer. Chem. Soc., 1971, 93, 476.

135. L.A. Carpino and H-Wn. Chen, J. Amer. Chem. Soc., 1971, 93, 785.

136. L.A. Carpino and H.L. Ammon, personal communication.

137. M.S. Viswamitsa and K.K. Kannas, Nature, 1966, 209, 1016.

138. D.E. Sands, Z. Krist., 1963, 119, 245.

139. R.B. Woodward and R. Hoffmann, 'The Conservation of Orbital Symmetry', Weinheim, 1970.

140. G. Herzberg, 'Molecular Spectra and Molecular Structure', Vol. 3, Princeton, N.J., 1966.

141. R. Hoffmann, H. Fujimoto, J.R. Svenson and C-C. Wan, J. Amer. Chem. Soc., in press.

142. H. Bock and B. Solouki, Angew. Chemie, 1973, 11, 436.

143. B. Solouki, H. Bock and R. Appel, Angew Chemie, 1973, 11, 927.

144. Handbook of Chemistry and Physics, Ed. R.C. Weast, The Chemical Rubber Co., 1970.

145. R. Breslow, T. Eicher, A. Krebs, R.A. Peterson and J. Posner, J. Amer. Chem. Soc., 1958, 80, 5991.

146. L.C. Allen, Chem. Phys. Lett., 1968, 2, 597.

147. I.G. Csizmadia, A.S. Denes and G. Modena, J. Chem. Soc. (D), 1972, 8.

148. D.T. Clark, Int. J. Sulphur Chem., 1972, C7, 11.

149. K. Mislow, A. Rank, J.D. Andose and R. Tang, Int. J. Sulphur Chem., 1971, A1, 66.

150. A.J. Ashe, III, J. Amer. Chem. Soc., 1971, 93, 3293.

151. B. Bak, L. Hansen-Nygaard and J. Rastrup-Andersen, J. Mol. Spectrosc.,
     1958, 2, 361.

152. J.C.J. Bart and J.J. Daly, Angew Chem., International Edn., 1968, 7, 811.

153. R.L. Kuczkowski and A.J. Ashe, III, J. Mol. Spectrosc., 1972, 42, 457.

154. W.J. Hehre, R. Ditchfield, R.F. Stewart and J.A. Pople, J. Chem. Phys.,
     1970, 52, 2769.

155. G. Burns, J. Chem. Phys., 1964, 41, 1521.

156. E. Clementi, Chem. Rev., 1968, 68, 341; J. Chem. Phys., 1967, 46, 4731.

157. J.D. Petke, J.L. Whitten and J.A. Ryan, J. Chem. Phys., 1968, 48, 953.

158. T. Almlof, B. Roos, U. Wahlgren and H. Johansen, J. Elec. Spectrosc.,
     1973, 2, 51.

159. J.N. Murrell and R.J. Suffolk, J. Elec. Spectrosc., 1972, 1, 471.

160. G.H. King, J.N. Murrell and R.J. Suffolk, J.C.S. Dalton, 1972, 1, 564.

161. H. Oehling and A. Schweig, Tetrahedron Lett., 1970, 4941.

162. A.L. Allred, J. Inorg. Nucl. Chem., 1961, 17, 215.

163. A.J. Ashe, III, and M.D. Gordon, J. Amer. Chem. Soc., 1972, 94, 7596.

164. A.L. McClellon, Table of Dipole Moments, W.H. Freeman and Co.,
     San Francisco, 1963.

165. K. Dimroth and W. Stade, Angew Chem., 1968, 80, 966.

166. G.W. Wheland, J. Amer. Chem. Soc., 1942, 64, 900.

167. R. Gleiter, E. Heilbronner and V. Hornung, Angew Chem., International
     Edn., Engl., 1970, 9, 901.

168. A.D. Baker, D. Betteridge, N.R. Kemp and R.E. Kirby, Chem. Commun.,
     1970, 286.

169. C. Batich, E. Heilbronner, V. Hornung, A.J. Ashe, III, D.T. Clark,
     D. Kilcast, I. Scanlan and U.T. Cobley, J. Amer. Chem. Soc., 1973,
     95, 928.

170. A.W. Potts and W.C. Price, Proc. Roy. Soc. London, 1972, 326A, 181.

171. L. Ashrink, E. Lindholm and O. Edquist, Chem. Phys. Lett., 1970, 5, 609.

172. H.L. Hare, A. Schweig, H. Hahn and J. Radloff, Tetrahedron, 1973, 29, 475.

173. D.T. Clark, R.D. Chambers, D. Kilcast and W.K.R. Musgrave, J. Chem. Soc. Faraday II, 1972, 68, 309.

174. L.C. Snyder, J. Chem. Phys., 1971, 55, 95.

175. F. Arndt, P. Nachtwey and J. Pusch, Ber., 1925, 58, 1633.

176. S. Bezzi, M. Mammi and G. Garbuglio, Nature, 1958, 182, 247.

177. D.H. Reid, Specialist periodical Report, J.C.S., 1969, Organic Compound of Sulphur, Selenium and Tellurium, p.321.

178. R. Gleiter and R. Hoffmann, Tetrahedron, 1968, 24, 5899.

179. D.T. Clark and D. Kilcast, Tetrahedron, 1971, 27, 4367.

180. A. Hordvik, L.K. Hansen and L.J. Soethre, J. Chem. Soc. (D), 1972, 222.

181. R. Gleiter, V. Hornung, B. Lindberg, S. Hogberg and N. Lozac'h, Chem. Phys. Lett., 1971, 11, 401.

182. R. Gleiter, D. Schmidt and H. Behringer, Chem. Commun., 1971, 525.

183. M.H. Palmer and R.H. Findley, Tetrahedron Lett., 1972, 41, 4165.

184. B.J. Lindberg, S. Hogburg, G. Malmston, J.E. Bergmark, O. Nilsson, S.-E. Karlsson, A. Fahlman, U. Gelius, R. Pinel, M. Stavaux, Y. Mollier and N. Lozac'h, Chem. Scr., 1971, 1, 183.

185. D.T. Clark. D. Kilcast and D.H. Reid, J. Chem. Soc. (D), 1971, 638.

186. R.E. Davis and M.D. Coffey, J. Amer. Chem. Soc., (in press).

187. P.L. Johnson and I.C. Paul, Chem. Commun., 1969, 1014.

189. F. Gerson, R. Gleiter, J. Heinzer and H. Behringer, Angew Chemie, International Edn., 1970, 9, 306.

190. D.H. Reid and I. Ritchie, private communication.

191. F.R. Mayo and C. Walling, Chem. Reviews, 1970, 27, 351.

192. G.M. Burnett, Quarterly Reviews, 1950, 4, 292.

193. P.S. Stefani and M. Szwarc, J. Amer. Chem. Soc., 1962, 84, 3661.

194. M. Szwarc, Proc. Roy. Soc., 1959, A251, 394.

195. J.H. Binks and H. Szwarc, J. Chem. Phys., 1959, 30, 1494.

196. R.J. Cvetanovic and R.S. Irwin, J. Chem. Phys., 1967, 46, 1694.

197. T. Smail, R. Subramonia Iyer and F.S. Rowland, J. Amer. Chem. Soc., 1972, 94, 1041.

198. R.J. Cvetanovic, J. Chem. Phys., 1960, 33, 1063.

199. J.M. Tedder and J.C. Walton, Trans. Faraday Soc., 1964, 60, 1769.

200. C.A. Coulson, Discuss. Faraday Soc., 1947, 2, 9.

201. M. Szwarc, J. Phys. Chem., 1957, 61, 40.

202. K. Fukui in 'Molecular Orbitals in Chemistry, Physics and Biology', P-O. Löwdin and B. Pullman, Ed., Academic Press, New York, N.Y., 1964, p.513.

203. K. Fukui, H. Kato and T. Yonezawa, Bull. Chem. Soc. Jap., 1961, 34, 1111.

204. J.M. Tedder and J.C. Walton, Trans. Faraday Soc., 1966, 62, 1859.

205. H.R. Pfaedler, H. Tanida and E. Haselbach, Helvetica Chimica Acta, 1974, 57, 383.

206. S. Shih, R.J. Buenker, S.D. Peyerimhoff and C.J. Michejda, J. Amer. Chem. Soc., 1972, 94, 7620.

207. M.V. Basilevsky and I.E. Chlenov, Theoret. chim. Acta, 1969, 15, 174.

208. J.R. Hoyland, Theoret. chim. Acta, 1971, 22, 229.

209. H. Fujimoto, S. Yamabe, T. Minato and K. Fukui, J. Amer. Chem. Soc., 1972, 94, 9205.

210. J.J. Kaufman and R. Predny, Int. J. Quantum Chem., 1971, 5, 235.

211. J.M. Tedder and J.C. Walton, Progress in Reaction Kinetics, 1967, 4, 37.

212. C.R. Brundle, M.B. Robin, N.A. Kuebler and H. Basch, J. Amer. Chem. Soc., 1972, 94, 1451.

213. J.M. Tedder, J.C. Walton and K.D.R. Winton, J.C.S Faraday I, 1972, 68, 1866.

214. J.M. Tedder, J.C. Walton and K.D.R. Winton, J.C.S. Faraday I, 1972, 68, 160.

215. A.J. Bowles, A. Hudson and R.A. Jackson, Chem. Phys. Lett., 1970, 5, 552.

216. I.H. Elson, K.S. Chen and J.K. Kochi, Chem. Phys. Lett., 1973, 21, 72; J. Amer. Chem. Soc., 1973, 95, 5341.

217. D.T. Clark and D.M.J. Lilley, J. Chem. Soc. (D), 1970, 603.

218. D.T. Clark and D.M.J. Lilley, J. Chem. Soc. (D), 1970, 549.

219. I. Biddles, J. Cooper. A. Hudson, R.A. Jackson and J.F. Wiffen, Mol. Phys., 1973, 25, 225.

220. I. Biddles and A. Hudson, Chem. Phys. Lett., 1973, 18, 45.

221. P.S. Skeil, R.R. Pavlis, D.C. Lewis and K.J. Shea, J. Amer. Chem. Soc., 1973, 95, 6735.

222. L.R. Byrd and M.C. Caserio, J. Amer. Chem. Soc., 1970, 92, 5422.

223. F.S. Rowland, 10th International Fluorine Symphosia, Santa Cruz, 1973.

224. L.D. Kispert, C.U. Pittman, Jnr., D.L. Allison, T.B. Patterson, Jnr., C.W. Gilbert, Jnr., C.F. Haines and J. Prather, J. Amer. Chem. Soc., 1972, 94, 5979.

225. S. Peyerimhoff, J. Chem. Phys., 1965, 43, 998.

226. J.P. Sloan, J.M. Tedder and J.C. Walton, J.C.S. Faraday I, 1973, 69, 1143.

227. J.M. Sangster and J.C.J. Thynne, Trans. Faraday Soc., 1969, 2110.